

FINAL REPORT

Alternative for Perchlorates in Incendiary and Pyrotechnic Formulations for Projectiles

SERDP Project WP-1424

AUGUST 2009

Dr. Trevor T. Griffiths
QinetiQ Ltd.

This document has been approved for public release.



Strategic Environmental Research and
Development Program

This report was prepared under contract to the Department of Defense Strategic Environmental Research and Development Program (SERDP). The publication of this report does not indicate endorsement by the Department of Defense, nor should the contents be construed as reflecting the official policy or position of the Department of Defense. Reference herein to any specific commercial product, process, or service by trade name, trademark, manufacturer, or otherwise, does not necessarily constitute or imply its endorsement, recommendation, or favoring by the Department of Defense.

REPORT DOCUMENTATION PAGE			Form Approved OMB No. 0704-0188		
Public reporting burden for this collection of information is estimated to average 1 hour per response, including the time for reviewing instructions, searching existing data sources, gathering and maintaining the data needed, and completing and reviewing this collection of information. Send comments regarding this burden estimate or any other aspect of this collection of information, including suggestions for reducing this burden to Department of Defense, Washington Headquarters Services, Directorate for Information Operations and Reports (0704-0188), 1215 Jefferson Davis Highway, Suite 1204, Arlington, VA 22202-4302. Respondents should be aware that notwithstanding any other provision of law, no person shall be subject to any penalty for failing to comply with a collection of information if it does not display a currently valid OMB control number. PLEASE DO NOT RETURN YOUR FORM TO THE ABOVE ADDRESS.					
1. REPORT DATE (DD-MM-YYYY) 06-08-2009		2. REPORT TYPE Final		3. DATES COVERED (From - To) October 2005 – March 2009	
4. TITLE AND SUBTITLE Alternative for Perchlorates in Incendiary and Pyrotechnic Formulations for Projectiles			5a. CONTRACT NUMBER W912HQ-04-C-0031		
			5b. GRANT NUMBER -		
			5c. PROGRAM ELEMENT NUMBER -		
6. AUTHOR(S) T T Griffiths			5d. PROJECT NUMBER WP-1424		
			5e. TASK NUMBER -		
			5f. WORK UNIT NUMBER -		
7. PERFORMING ORGANIZATION NAME(S) AND ADDRESS(ES) QinetiQ, Fort Halstead, Sevenoaks, Kent, TN14 7BP, UK			8. PERFORMING ORGANIZATION REPORT NUMBER QINETIQ/09/00368		
9. SPONSORING / MONITORING AGENCY NAME(S) AND ADDRESS(ES) Bruce D. Sartwell Program Manager Weapons Systems & Platforms SERDP and ESTCP Program Offices 901 N. Stuart Street, Suite 303 Arlington, VA 22203-185			10. SPONSOR/MONITOR'S ACRONYM(S)		
			11. SPONSOR/MONITOR'S REPORT NUMBER(S) WP-1424		
12. DISTRIBUTION / AVAILABILITY STATEMENT Approved for Public Release, Distribution is Unlimited					
13. SUPPLEMENTARY NOTES					
14. ABSTRACT Pyrotechnic compositions containing potassium perchlorate are used in incendiary ammunition to mark an impact point or to act as ignition sources. Perchlorates inhibit iodide uptake by the thyroid gland and their level in drinking water is controlled. Research has been undertaken to find alternative perchlorate-free pyrotechnic incendiary compositions. The proposed ingredients were screened for their human toxicology, ecological toxicology and environmental mobility (aquatic and terrestrial) prior to the formulation studies. The thermal and pyrotechnic properties of control and novel replacement pyrotechnic compositions were examined. The combustion products predicted through a modeling study were also screened for their toxicity and environmental effects. The performance of selected compositions was assessed through gun firing trials. This combined with the environmental screening studies and an investigation into the aging characteristics of the formulations allowed down selection to a composition containing magnesium/aluminum alloy, sodium nitrate and calcium resinate. This material was found to have acceptable hazard characteristics.					
15. SUBJECT TERMS Ammunition, incendiary, pyrotechnics, perchlorate free					
16. SECURITY CLASSIFICATION OF:			17. LIMITATION OF ABSTRACT None	18. NUMBER OF PAGES xvi + 160	19a. NAME OF RESPONSIBLE PERSON Dr Trevor T Griffiths
a. REPORT Unclassified	b. ABSTRACT Unclassified	c. THIS PAGE Unclassified			19b. TELEPHONE NUMBER (include area code) 44 1959 515347

Standard Form 298 (Rev. 8-98)
Prescribed by ANSI Std. Z39.18

Table of contents

Table of contents	iv
List of acronyms and symbols	vi
List of figures	viii
List of tables	xiv
Acknowledgements	xvi
Executive summary	1
Objectives	4
Background	5
Introduction	5
Materials and methods	7
Environmental screening	7
Combustion modeling	8
Formulation studies	9
Pyrotechnic burning rate	14
Exothermicity measurements	14
Thermogravimetry	15
DSC studies under ignition conditions	15
Time to Ignition	15
DSC studies under non-ignition conditions	15
Bullet firing trials	15
Results and discussion	17
Ingredient environmental screening study	17
Pyrotechnic fuels	17
Pyrotechnic oxidants	21
Pyrotechnic binders and other ingredients	26
Combustion modeling	28
Combustion products environmental screening study	30
Formulation and performance studies	36
Magnesium/aluminum alloy based compositions	36

Combustion studies	36
Exothermicity measurements	38
Thermal analysis studies	39
Thermal studies on the ingredients	39
Magnesium/aluminum alloy	39
Oxidants	39
DSC experiments	40
Non-ignition DSC	44
Time to ignition studies	44
Magnesium based compositions	48
Combustion studies	48
Exothermicity measurements	48
Ignition DSC	49
Non-ignition DSC	50
Time to ignition	50
Magnesium-barium nitrate-potassium perchlorate	50
Aluminum based compositions	52
Combustion studies	52
Exothermicity measurements	53
DSC studies under ignition conditions	53
Gun firing trials	54
Ageing studies	61
Hazard assessment	63
Additional pyrotechnic and thermal studies	64
Conclusions and implications for future research/implementation	65
Literature cited	67
Figures	68
List of technical publications:	158
Technical reports	158
Conference/symposium proceedings	159
Published technical abstracts	159

List of acronyms and symbols

AD	Alzheimer's disease
B	Bioaccumulation
BAF	Bioaccumulation factor
BCF	Bioconcentration factor
CEA	Chemical Equilibrium with Applications
CEH	Centre for Ecology and Hydrology
DNA	Deoxyribonucleic acid
DoD	Department of Defense
DSC	Differential Scanning Calorimetry
DTA	Differential Thermal Analysis
GAP	Glycidyl azide polymer
GUI	Graphical Users Interface
HE	High Explosive
HSDB	Hazardous Substances Data Bank
IRIS	Integrated Risk Information System
LD	Lethal Dose
[L(E)C]	Lethal (Effect) Concentration
LOEC	Lowest-observed-effect concentrations
Log K _{ow}	Log octanol water partition coefficient
NOAEL	No-observed-adverse-effect level
NOEC	No observable effect concentration
P	Persistence
P, B & T	Persistence, Bioaccumulation and Toxicity
TG	Thermogravimetry
PolyGlyN	Polyglycidyl nitrate
PolyNIMMO	Poly(3-nitratomethyl-3-methyloxetane)
PTFE	Polytetrafluoroethylene

PVC	Polyvinylchloride
T	Toxicity
TG	Thermogravimetry
T _e	Extrapolated onset temperature
T _p	Peak temperature
TOXONLINE	Toxicology Literature Online
WHO	World Health Organization

List of figures

Figure 1; Main reaction products for 50% magnesium/aluminum alloy-barium nitrate-potassium nitrate.	68
Figure 2; Main reaction products for 50% magnesium/aluminum alloy-barium nitrate-sodium nitrate.	68
Figure 3; Main reaction products for 50% magnesium/aluminum alloy-barium nitrate-strontium nitrate.	69
Figure 4; Main reaction products for 50% magnesium/aluminum alloy-barium nitrate-barium sulfate.	69
Figure 5; Main reaction products for 50% magnesium/aluminum alloy-barium nitrate-calcium sulfate.	70
Figure 6; Main reaction products for 50% magnesium/aluminum alloy-barium nitrate-potassium sulfate.	70
Figure 7; Main reaction products for 50% magnesium/aluminum alloy-barium nitrate-sodium sulfate.	71
Figure 8; Main reaction products for 50% magnesium/aluminum alloy-barium nitrate-strontium sulfate.	71
Figure 9; Main reaction products for 50% magnesium-barium nitrate-potassium nitrate.	72
Figure 10; Main reaction products for 50% magnesium-barium nitrate-sodium nitrate.	72
Figure 11; Main reaction products for 50% magnesium-barium nitrate-strontium nitrate.	73
Figure 12; Main reaction products for 50% magnesium-barium nitrate-barium sulfate.	73
Figure 13; Main reaction products for 50% magnesium-barium nitrate-calcium sulfate.	74
Figure 14; Main reaction products for 50% magnesium-barium nitrate-potassium sulfate.	74
Figure 15; Main reaction products for 50% magnesium-barium nitrate-sodium sulfate.	75
Figure 16; Main reaction products for magnesium-barium nitrate-strontium sulfate.	75
Figure 17; Main reaction products for aluminum-barium nitrate-potassium nitrate.	76
Figure 18; Main reaction products for 50% aluminum-barium nitrate-sodium nitrate.	76
Figure 19; Main reaction products for 50% aluminum-barium nitrate-strontium nitrate.	77
Figure 20; Main reaction products for 50% aluminum-barium nitrate-barium sulfate.	77
Figure 21; Main reaction products for 50% aluminum-barium nitrate-calcium sulfate.	78
Figure 22; Main reaction products for 50% aluminum-barium nitrate-potassium sulfate.	78
Figure 23; Main reaction products for 50% aluminum-barium nitrate-sodium sulfate.	79
Figure 24; Main reaction products for 50% aluminum-barium nitrate-strontium sulfate.	79
Figure 25; Burning rate curve for magnesium/aluminum alloy-barium nitrate-potassium perchlorate.	80
Figure 26; Burning rate curve for magnesium/aluminum alloy-potassium perchlorate-2% calcium resinate compositions.	80
Figure 27; Burning rate curve for magnesium/aluminum alloy-potassium perchlorate-calcium resinate compositions with constant fuel:oxidant ratio and increasing calcium resinate content.	81
Figure 28; Burning rate curve for magnesium/aluminum alloy-barium nitrate compositions.	81

Figure 29; Burning rate curves for magnesium/aluminum alloy-barium nitrate-nitrate compositions.	82
Figure 30; Burning rate curve for magnesium/aluminum alloy-barium nitrate-sulfate compositions.	82
Figure 31; Burning rate curve for magnesium/aluminum alloy-strontium nitrate-potassium nitrate compositions.	83
Figure 32; Burning rate curve for magnesium/aluminum alloy-strontium nitrate-sodium nitrate compositions.	83
Figure 33; Burning rate curve for magnesium/aluminum alloy-barium nitrate-GAP compositions.	84
Figure 34; Burning rate curve for magnesium/aluminum alloy-barium nitrate-strontium nitrate-GAP compositions.	84
Figure 35; Burning rate curve for magnesium/aluminum alloy-barium nitrate-polyGlyN compositions.	85
Figure 36; Burning rate curve for magnesium/aluminum alloy-barium nitrate-strontium nitrate-polyGlyN compositions.	85
Figure 37; Burning rate curve for magnesium/aluminum alloy-barium nitrate-polyNIMMO compositions.	86
Figure 38; Burning rate curve for magnesium/aluminum alloy-barium nitrate-strontium nitrate-polyNIMMO compositions.	86
Figure 39; Exothermicity curve for magnesium/aluminum alloy-barium nitrate-potassium perchlorate.	87
Figure 40; Exothermicity curve for magnesium/aluminum alloy-potassium perchlorate-2% calcium resinate.	87
Figure 41; Exothermicity curve for magnesium/aluminum alloy-potassium perchlorate-calcium resinate compositions with constant fuel:oxidant ratio and increasing calcium resinate content.	88
Figure 42; Exothermicity curve for magnesium/aluminum alloy-barium nitrate compositions.	88
Figure 43; Exothermicity curve for magnesium/aluminum alloy-barium nitrate-nitrates.	89
Figure 44; Exothermicity curve for magnesium/aluminum alloy-barium nitrate-sulfates.	89
Figure 45; DSC Curve for a magnesium/aluminum alloy.	90
Figure 46; Simultaneous thermogravimetry-DSC curves for the oxidation of magnesium/aluminum alloy.	90
Figure 47; DSC curves for potassium perchlorate, barium nitrate and mixtures of these oxidants.	91
Figure 48; TG curves for barium nitrate and potassium perchlorate.	92
Figure 49; TG curves for barium nitrate potassium perchlorate mixtures.	92
Figure 50; Initial mass loss stage against potassium perchlorate content for a range of barium nitrate-potassium perchlorate mixtures.	93
Figure 51; TG-mass spectrometry curves for the decomposition of a 50% barium nitrate-50% potassium perchlorate mixture.	93
Figure 52; Ignition DSC curves for a range of magnesium/aluminum alloy-barium nitrate-potassium perchlorate compositions.	94
Figure 53; Ignition DSC curves for a range of magnesium/aluminum alloy-potassium perchlorate-calcium resinate compositions containing equal masses of magnesium/aluminum alloy and potassium perchlorate.	95

Figure 54; Ignition DSC curves for a range of magnesium/aluminum alloy-potassium perchlorate-2% calcium resinate compositions.	96
Figure 55; DSC curves for a range of mixtures of calcium resinate with magnesium/aluminum alloy and potassium perchlorate.	97
Figure 56; DSC curves for a 78.6% potassium perchlorate-21.4% calcium resinate mixture.	98
Figure 57; DSC curves for a 78.6% potassium perchlorate-21.4% calcium resinate mixture.	98
Figure 58; Simultaneous thermogravimetry-mass spectrometry curves for a 78.6% potassium perchlorate-21.4% calcium resinate mixture.	99
Figure 59; Infra red heating-mass spectrometry heating curves for a 78.6% potassium perchlorate-21.4% calcium resinate mixture.	100
Figure 60; Ignition DSC curves for a range of magnesium/aluminum alloy-barium nitrate compositions.	101
Figure 61 Ignition DSC; curves for a range of magnesium/aluminum alloy-barium nitrate-potassium nitrate compositions.	102
Figure 62; Ignition DSC curves for a range of magnesium/aluminum alloy-barium nitrate-sodium nitrate compositions.	103
Figure 63; Ignition DSC curves for a range of magnesium/aluminum alloy-barium nitrate-strontium nitrate compositions.	104
Figure 64; Ignition DSC curves for compositions containing 50% magnesium/aluminum alloy and 50% of the nitrates.	105
Figure 65; Ignition DSC curves for binary and ternary compositions containing 50% magnesium/aluminum alloy-50% sulfate.	106
Figure 66; Ignition DSC curves for ternary compositions containing 50% magnesium/aluminum alloy-35% barium nitrate and 15% sulfate.	107
Figure 67; DSC curves at different heating rates for a binary composition containing 50% magnesium/aluminum alloy-50% potassium perchlorate.	108
Figure 68; Plot of extrapolated onset temperature against heating rate for magnesium/aluminum alloy fusion and the exothermic reaction in 50% magnesium/aluminum alloy-50% potassium perchlorate.	109
Figure 69; DSC curves at different heating rates for a binary composition containing 48% magnesium/aluminum alloy-48% potassium perchlorate-2% calcium resinate.	110
Figure 70; Plot of extrapolated onset temperature against heating rate for magnesium/aluminum alloy fusion and the exothermic reactions in 48% magnesium/aluminum alloy-48% potassium perchlorate-2% calcium resinate.	111
Figure 71; DSC curves for ternary compositions containing 50% magnesium aluminum-50% metal sulfate.	112
Figure 72; DSC curves for ternary compositions containing 50% magnesium aluminum-35% barium nitrate and 15% metal sulfate.	113
Figure 73; Time to Ignition for a range of magnesium/aluminum alloy-potassium perchlorate-calcium resinate compositions containing equal masses of magnesium/aluminum alloy and potassium perchlorate.	114
Figure 74; Burning rate curve for magnesium-barium nitrate-potassium perchlorate.	114
Figure 75; Burning rate curve for magnesium-barium nitrate compositions.	115
Figure 76; Burning rate curve for magnesium-barium nitrate-nitrates compositions.	115
Figure 77; Burning rate curve for magnesium-barium nitrate-sulfate compositions.	116

Figure 78; Exothermicity curve for magnesium-barium nitrate-potassium perchlorate compositions.	116
Figure 79; Exothermicity curves for magnesium-barium nitrate-nitrate compositions.	117
Figure 80; Exothermicity curves for magnesium-barium nitrate-sulfate compositions.	117
Figure 81; DSC Curves for a range of 50% magnesium-barium nitrate-potassium perchlorate compositions.	118
Figure 82; Ignition DSC curves for a range of magnesium-barium nitrate-potassium nitrate compositions.	119
Figure 83; Ignition DSC curves for a range of magnesium-barium nitrate-sodium nitrate compositions.	120
Figure 84; DSC curves for a range of magnesium-sulfate compositions.	121
Figure 85; DSC curves for a range of ternary magnesium-barium nitrate-sulfate compositions.	122
Figure 86; DSC curves for a range of ternary 50% magnesium-35% barium nitrate-15% metal sulfate compositions.	123
Figure 87; Burning rate curve for aluminum-barium nitrate-potassium perchlorate compositions.	124
Figure 88; Burning rate curve for aluminum-barium nitrate compositions.	124
Figure 89; Burning rate curves for aluminum-barium nitrate-nitrate compositions.	125
Figure 90; Burning rate curve for aluminum-barium nitrate-sulfate compositions.	125
Figure 91; Exothermicity curve for aluminum-barium nitrate compositions.	126
Figure 92; DSC curves for a range of aluminum-barium nitrate compositions.	127
Figure 93; DSC curves for a range of aluminum-barium nitrate-potassium nitrate compositions.	128
Figure 94; DSC curves for a range of aluminum-barium nitrate-sodium nitrate compositions.	128
Figure 95; DSC curves for a range of aluminum-barium nitrate-strontium nitrate compositions.	129
Figure 96; Trial 1, stills for gun firing of bullet containing wax against steel target.	130
Figure 97; Trial 1, stills for gun firing of bullet containing wax against aluminum alloy target.	130
Figure 98; Trial 1, stills for gun firing of bullet containing 50% magnesium/aluminum alloy-40% barium nitrate-10% potassium perchlorate.	131
Figure 99; Trial 1, stills for gun firing of bullet containing pellets of 50% magnesium/aluminum alloy-40% barium nitrate-10% potassium perchlorate.	131
Figure 100; Trial 1, stills for gun firing of bullet containing 50% magnesium/aluminum alloy-35% barium nitrate-15% potassium nitrate.	132
Figure 101; Trial 1, stills for gun firing of bullet containing 50% magnesium/aluminum alloy-35% barium nitrate-15% sodium nitrate.	132
Figure 102; Trial 1, stills for gun firing of bullet containing 50% magnesium/aluminum alloy-35% barium nitrate-15% strontium nitrate.	133
Figure 103; Trial 1, stills showing the frame with the largest output from a range of compositions.	134
Figure 104; Trial 2, stills for gun firing of bullet containing 49% magnesium/aluminum alloy-49% potassium perchlorate and 2% calcium resinate.	135

Figure 105; Trial 2, stills showing the frame with the largest output from a range of compositions.	136
Figure 106; Trial 2, stills showing the frame with the largest output from a range of compositions Phantom camera on narrow field.	136
Figure 107; Trial 3, stills showing the frame with the largest output from a range of compositions.	138
Figure 108; Trial 4, stills for gun firing of bullet containing magnesium/aluminum alloy-sodium nitrate and either 2% or 4% binder.	139
Figure 109; Trial 4, stills for gun firing of bullet containing magnesium/aluminum alloy-potassium nitrate and either 2% or 4% binder.	140
Figure 110; Trial 5, stills for gun firing of bullet containing magnesium/aluminum alloy-potassium nitrate and either 2% or 4% calcium resinate or control compositions based on potassium perchlorate.	141
Figure 111; Microcalorimetry heat flow curves for magnesium/aluminum alloy.	142
Figure 112; Microcalorimetry heat flow curves magnesium/aluminum alloy.	142
Figure 113; Microcalorimetry heat flow curves for potassium perchlorate.	143
Figure 114; Microcalorimetry heat flow curves for calcium resinate.	143
Figure 115; Microcalorimetry heat flow curves for a 50% magnesium/aluminum alloy-50% potassium perchlorate composition.	144
Figure 116; Microcalorimetry heat flow curves for a 49% magnesium/aluminum alloy-49% potassium perchlorate-2% calcium resinate composition.	144
Figure 117; Microcalorimetry heat flow curves for a 44% magnesium/aluminum alloy-44% potassium perchlorate-12% calcium resinate composition.	145
Figure 118; DSC curves for 50% magnesium/aluminum alloy-50% potassium perchlorate composition unaged and aged for 7 days at 50°C and 65% RH.	145
Figure 119; DSC curves for 49% magnesium/aluminum alloy-49% potassium perchlorate-2% calcium resinate composition unaged and aged for 7 days at 50°C and 65% RH.	146
Figure 120; DSC curves for 44% magnesium/aluminum alloy-44% potassium perchlorate-12% calcium resinate composition unaged and aged for 7 days at 50°C and 65% RH.	146
Figure 121; Microcalorimetry heat flow curves for a 50% magnesium/aluminum alloy-40% potassium perchlorate-10% potassium perchlorate composition.	147
Figure 122; Microcalorimetry heat flow curves for a 50% magnesium/aluminum alloy-50% barium nitrate composition.	147
Figure 123; DSC curves for 50% magnesium/aluminum alloy-40% barium nitrate-10% potassium perchlorate composition unaged and aged for 7 days at 50°C and 65% RH.	148
Figure 124; DSC curves for 50% magnesium/aluminum alloy-50% barium nitrate composition unaged and aged for 7 days at 50°C and 65% RH.	148
Figure 125; Microcalorimetry heat flow curves for a 50% magnesium/aluminum alloy-50% sodium nitrate composition.	149
Figure 126; DSC curves for 50% magnesium/aluminum alloy-50% sodium nitrate composition unaged and aged for 7 days at 50°C and 65% RH.	149
Figure 127; Microcalorimetry heat flow curves for a 50% magnesium/aluminum alloy-50% potassium nitrate composition.	150
Figure 128; DSC curves for 50% magnesium/aluminum alloy-50% potassium nitrate composition unaged and aged for 7 days at 50°C and 65% RH.	150

Figure 129; Microcalorimetry heat flow curves for 48% magnesium/aluminum alloy-48% sodium nitrate-4% calcium resinate composition.	151
Figure 130; Microcalorimetry heat flow curves for 48% magnesium/aluminum alloy-48% sodium nitrate-4% lithographic varnish composition.	151
Figure 131; Microcalorimetry heat flow curves for 48% magnesium/aluminum alloy-48% sodium nitrate-4% GAP composition.	152
Figure 132; Microcalorimetry heat flow curves for a 50% magnesium/aluminum alloy-50% sodium nitrate composition.	152
Figure 133; Microcalorimetry heat flow curves for a 50% magnesium/aluminum alloy-50% sodium nitrate composition.	153
Figure 134; Microcalorimetry heat flow curves for 49% magnesium/aluminum alloy-49% sodium nitrate-2% calcium resinate composition.	153
Figure 135; Microcalorimetry heat flow curves for 49% magnesium/aluminum alloy-49% sodium nitrate-2% calcium resinate composition.	154
Figure 136; Microcalorimetry heat flow curves for 48% magnesium/aluminum alloy-48% sodium nitrate-4% calcium resinate composition.	154
Figure 137; Microcalorimetry heat flow curves for 48% magnesium/aluminum alloy-48% sodium nitrate-4% calcium resinate composition.	155
Figure 138; Burning rate curve for magnesium/aluminum alloy-sodium nitrate-calcium esinate.	155
Figure 139; Ignition DSC curves for a range of magnesium/aluminum alloy-sodium nitrate-calcium resinate compositions.	156
Figure 140; Plot of ignition temperature against calcium resinate content for a range of magnesium/aluminum alloy-sodium nitrate-calcium resinate compositions.	157

List of tables

Table 1; Formulation details for the IM-28 type control compositions.	10
Table 2; Formulation details for the RS-41 type control compositions.	10
Table 3; Formulation details for the binary compositions containing a fuel and barium nitrate.	11
Table 4; Formulation details for the replacement compositions containing barium nitrate and a second oxidant.	11
Table 5; Formulation details for the binary compositions containing magnesium/aluminum alloy, strontium nitrate and either sodium or potassium nitrate.	12
Table 6; Formulation details for ternary compositions containing magnesium/aluminum alloy, barium nitrate and an energetic binder.	12
Table 7; Formulation details for the binary compositions containing magnesium/aluminum alloy, barium nitrate, strontium nitrate and an energetic binder.	13
Table 8; Formulation details for the binary compositions containing metal-metal or metal-metal oxide combinations.	13
Table 9; Formulation details for the binary compositions containing magnesium/aluminum alloy, sodium or potassium nitrate and a binder.	14
Table 10; Formulation details for the binary compositions containing magnesium/aluminum alloy, sodium nitrate and calcium resinate.	14
Table 11; Gun firing trials.	15
Table 12; Environmental screening results for the pyrotechnic fuels.	17
Table 13; Environmental screening results for the pyrotechnic oxidants.	21
Table 14; Environmental screening results for the pyrotechnic binders.	26
Table 15; Predicted species after combustion and further reaction.	29
Table 16; Environmental screening results for the products of combustion.	30
Table 17; DSC temperatures for a 50% magnesium/aluminum alloy-50% potassium perchlorate composition at different heating rates.	43
Table 18; DSC Temperatures for a 49% magnesium/aluminum alloy-49% potassium perchlorate-2% calcium resinate composition at different heating rates.	44
Table 19; Time to ignition experiments on the range of magnesium/aluminum alloy-potassium perchlorate-calcium resinate compositions.	45
Table 20; Time to ignition experiments on the range of magnesium/aluminum alloy-potassium perchlorate-calcium resinate system.	46
Table 21; Times to Ignition for magnesium aluminum-barium nitrate-sodium nitrate composition.	47
Table 22; Times to Ignition for magnesium/aluminum alloy-barium nitrate-potassium nitrate compositions.	47
Table 23; Times to ignition for magnesium-barium nitrate-potassium nitrate compositions.	51
Table 24; Times to ignition for magnesium-barium nitrate-sodium nitrate compositions.	51
Table 25; Times to ignition for magnesium-barium nitrate-strontium nitrate compositions.	52
Table 26; Trial 1, Aluminum alloy target placed 10 m from muzzle.	55
Table 27; Trial 2, Aluminum alloy target placed 6 m from muzzle.	56
Table 28; Trial 3, Aluminum alloy target placed 6 m from muzzle.	58

Table 29; Trial 4, Aluminum alloy target placed 5.8 m from muzzle.	60
Table 30; Trial 5, Aluminum alloy target placed 6 m from muzzle.	61
Table 31; Heat flow and cumulative heat values after 28 day at 50 °C and 65% RH	63
Table 32; Hazard data for magnesium/aluminum alloy, sodium nitrate and 4% calcium resinate.	64

Acknowledgements

The financial support of the Strategic Environmental Research and Development Program (SERDP), under the direction of Dr. Jeffrey Marqusee, is gratefully acknowledged.

The author would also like to thank Paul D. Howe, Stuart Dobson, and Heath Malcolm, at the Centre for Ecology and Hydrology, for their assistance in preparing the Environmental Screening Study. Professor Ted Charsley, Jim Rooney and Hayley Markham, at the Centre for Thermal Studies, Huddersfield University, for carry out the thermal studies. The QinetiQ staff at Fort Halstead, Leslie Cox, Catherine Fisher, David Belsham and Peter Henning, who undertook the composition preparation, burning rate studies and bullet firing trials.

Executive summary

This report details studies undertaken in collaboration with SERDP in response to SON Number: PPSON-05-02, issued by the Department of Defense (DoD) in November 2003, with the goal of eliminating perchlorate based oxidizing material from incendiary and flash/smoke pyrotechnic formulations.

The replacement formulations need to meet or exceed current DoD-required safety and performance criteria which includes toxicity, stability, sensitivity, ignitability, hygroscopicity and have the ability to match the performance of the existing compositions which are used as incendiary mix or flash compositions in a range of projectiles.

Perchlorates are high energy oxidizers that have good thermal and chemical stability; they are used in a wide range of military applications including rocket propellants and pyrotechnics. When used in ammunition incendiary systems, compositions containing potassium perchlorate and metal fuels are formulated to produce both an incandescent flash and smoke to mark an impact point or act as ignition sources for flammable liquids. In some munitions the compositions are used to initiate an explosive train.

Potassium perchlorate has a high solubility in water which results in very low retardation in aquifers. Consequently, any groundwater plumes can be extensive and pose severe remediation problems. Potassium perchlorate can be released into the environment as a result of spillages during manufacture, demilitarization, or when ammunition fails to function correctly. The presence of potassium perchlorate in drinking water is a cause for concern as all perchlorates are recognized as a potential hazard to human health. In particular, their ingestion is known to inhibit iodide uptake by the thyroid gland.

The DoD requires the development of environmentally benign, perchlorate-free incendiary and pyrotechnic compositions for use within projectiles. QinetiQ was tasked to produce and assess perchlorate-free pyrotechnic formulations based on novel chlorine-free oxidizers and fuels that will be environmentally benign but meet safety and performance criteria.

To ensure that these new formulations are more environmentally benign than current perchlorate-based formulations, QinetiQ contracted the Centre for Ecology and Hydrology to review the literature and produce toxicity, mobility and environmental impact reports on candidate ingredients. Each of the fuels, oxidizers and binders were rated high, low or moderate against persistence, bioaccumulation and toxicity (P, B & T) criteria to ascertain their environmental impact.

The fuels selected were magnesium/aluminum alloy, magnesium, aluminum and boron. All of these showed high persistence but low values for bioaccumulation, toxicity and ecotoxicology and were therefore suitable for the formulation studies.

The oxidants selected were potassium dinitramide, barium, potassium, sodium and strontium nitrates, barium, calcium, potassium, sodium and strontium sulfates, copper, iron, molybdenum and tungsten oxides, and these generally showed high persistence. Potassium dinitramide, copper oxide and manganese oxide were found to have either a high bioaccumulation or toxicity rating. Copper oxide also showed high ecotoxicity. As a result of these ratings; these three materials were not used for the formulation studies.

The five binders selected were hexafluoropropylene vinylidene fluoride polymer, polyglycidyl nitrate (polyGlyN), poly(3-methyl-3-nitratomethyloxetane (PolyNIMMO), glycidyl azide polymer (GAP) and polyvinyl chloride (PVC). They all showed high persistence but low values for bioaccumulation, toxicity and ecotoxicity. In addition, the binder calcium resinate was investigated; this showed low persistence, bioaccumulation, toxicity and ecotoxicity. All of the binders were therefore suitable for formulation studies.

The NASA computer program CEA2 (Chemical Equilibrium with Applications) was used to determine the combustion products for a range of pyrotechnic compositions. Formulations containing 50% magnesium/aluminum alloy, magnesium or aluminum were examined. The oxidants used in the study were barium, potassium, sodium and strontium nitrate, and barium, calcium, potassium, sodium and strontium sulfate; the ternary compositions all contained barium nitrate. The predicted species were determined as a function of changing oxidant ratio. As the program only considers combustion, the effects of cooling, oxidation or hydrolysis on the species predicted had to be considered separately.

To ensure that the predicted products of combustion were environmentally benign, a review was conducted for QinetiQ by the Centre for Ecology and Hydrology at Monks Wood in the UK. The review indicated that ammonia, hydrogen sulfide and sulfur dioxide have high acute toxicity but low chronic toxicity and that many of the hydroxides have moderate acute toxicity but low chronic toxicity. The compounds of aluminum including magnesium aluminate can be moderately toxic to aquatic organisms; however, this is very much dependent on the hydrogen ion concentration. The sulfides tend to have moderate acute toxicity and high acute ecotoxicity and this is related to the release of hydrogen sulfide. Similarly, the nitrides may show acute toxic effects because of the release of ammonia on contact with water.

Laboratory scale formulation and manufacture of pyrotechnic compositions was conducted. Over 350 formulations containing magnesium/aluminum alloy, magnesium or aluminum as the fuel were prepared for pyrotechnic and thermal studies. Most of the formulation studies concentrated on the magnesium/aluminum alloy compositions; this was because the manufacturer of the ammunition would prefer the minimum of changes in the formulation so that the physical properties including flow and bulk density are minimized. These compositions are also likely to be more readily ignitable by impact on a target than those containing magnesium or aluminum as the fuel.

Burning rate and thermal data showed many of the formulations have potential as replacements for perchlorate-containing incendiary compositions. An assessment of their performance when they were gun fired was also undertaken. Many of the formulations showed promise as replacement materials and gave a light output and flash duration which matched or exceeded that of the control compositions containing potassium perchlorate.

Following discussions with SERDP, the technical requirement was changed so that the compositions would provide the lowest possible environmental impact, this would be achieved by avoiding the use of barium nitrate in the formulations. A series of gun firing and ageing studies were completed on formulations containing sodium and potassium nitrate and selected binders. A significantly lower rate of ageing was observed for the compositions based on sodium nitrate, and the ageing was further reduced by the addition of a binder particularly calcium resinate.

A further gun firing trial confirmed that the formulations containing magnesium/aluminum alloy-sodium nitrate and either 2% or 4% calcium resinate gave a performance that matched that of the control compositions containing potassium perchlorate in terms of flash size and duration. When subjected to longer term ageing at 50 °C and 65% RH, the composition containing 4% calcium resinate was found to have the lower heat flow. Ignition DSC showed that the ignition temperature for this formulation was also lower and hazard assessment confirmed that this formulation had acceptable safety characteristics.

It is therefore recommended that the formulation magnesium/aluminum alloy-sodium nitrate-4% calcium resinate is examined further as a replacement incendiary composition. The ingredients used in this formulation can be readily obtained and their cost is comparable with those presently used for the incendiary compositions.

Further work is needed to investigate the incendiary properties of this formulation and assess the flash brightness and duration at longer ranges. This work would involve filling ammunition and conducting the Incendiary Flash and Incendiary Ignition Tests [4]. Once the performance of the composition has been confirmed, it will be necessary to obtain additional data including Hazard Classification, Health Hazard and a Lifecycle Environmental Analysis before transition of the formulation into ammunition filling.

Objectives

The main aims of the project are to formulate and assess perchlorate-free incendiary and pyrotechnic formulations based on novel oxidizers and fuels which will be environmentally acceptable, and that will meet the guidelines of PPSON-05-02. They must be capable of meeting or exceeding current DoD-required safety and performance criteria which includes toxicity, stability, sensitivity, ignitability, hygroscopicity and an ability to match the performance of the existing compositions when used as an incendiary mix or flash composition used in a range of projectiles. A secondary objective is to reduce the formation of hot spots and brush fires on training ranges possibly through a reduction in the formulations heat of combustion.

In addition, the research will address the following criteria:

- The development of pyrotechnic formulations that are more environmentally benign than current perchlorate-based formulations.
- Any unburned residues from the functioned formulations should be more environmentally benign than current perchlorate-based formulations.
- Combustion products from functioning of the pyrotechnic formulations must be environmentally benign.
- Anticipated future manufacturing costs should be competitive with current systems

The program comprised an in-depth environmental and toxicity screening of the ingredients proposed for the formulation development. The materials that were examined included alkali metal dinitramide salts, alkali metal and alkaline earth nitrates and sulfates, metallic and metal oxides and energetic binders.

Initial laboratory scale formulation and manufacture of pyrotechnic compositions were followed by evaluation, with subsequent transition to technical demonstrator level. The program focused principally on the following technical objectives:

- Formulation studies;
- Assessment of formulations;
- Characterization by thermal analysis studies;
- Hazard assessment and compatibility studies;
- Determination of combustion products and unburned residues;
- An environmental assessment of the combustion products and unburned residues;
- Aging studies.

Background

Introduction

Perchlorates are high energy oxidizers that have good thermal and chemical stability and are used in a wide range of military applications including rocket propellants and pyrotechnics. When used in ammunition incendiary systems, compositions containing potassium perchlorate and metal fuels are formulated to produce both an incandescent flash and smoke to mark an impact point or act as ignition sources for flammable liquids. In some munitions the compositions are used to initiate an explosive train.

Potassium perchlorate has a high solubility in water which results in very low retardation in aquifers. As a result, any groundwater plumes can be extensive and pose severe remediation problems [1]. It can be released into the environment as a result of spillages during manufacture, demilitarization, or when ammunition fails to function correctly. The presence of potassium perchlorates in drinking water is a cause for concern as all perchlorates are recognized as a potential hazard to human health. In particular, their ingestion is known to inhibit iodide uptake by the thyroid gland.

The DoD requires the development of environmentally benign, perchlorate-free incendiary and pyrotechnic compositions for use within projectiles. QinetiQ was tasked to produce and assess perchlorate-free pyrotechnic formulations based on novel chlorine-free oxidizers and fuels that will be environmentally benign but meet safety and performance criteria.

Examples given of the more commonly used mixes which need to be replaced include:

- a) IM-28 incendiary flash composition is used in the 0.50" caliber ammunition. The heat produced from the crushing of the metal nose by impact initiates the composition which is:
 - magnesium/aluminum alloy (50%),
 - barium nitrate (40%)
 - potassium perchlorate (10%)
- b) RS-41 nose incendiary composition is used to initiate the explosive train in the 20mm PGU 28/B and the PGU-28A/B Semi-Armor-Piercing High Explosive Incendiary ammunition. It contains:
 - magnesium/aluminum alloy (49%)
 - potassium perchlorate (49%)
 - calcium resinate binder (2%)
- c) 40mm flash composition is initiated by a stab detonator upon projectile impact with the target and emits flash and smoke to simulate high explosive (HE) function. It contains:
 - potassium perchlorate (69%)
 - aluminum (22.5%)
 - sulfur (10%)
 - antimony sulfide (3.5%)

The choice of fuels, oxidants and binders used in pyrotechnic formulations was governed by the known systems. It is unlikely that it will be possible to directly substitute replacement oxidizing agents for the perchlorates used in pyrotechnic formulations and produce compositions with the necessary properties. Substitute oxidizers may not be as energetic or as efficient as the perchlorates and as a result, it was therefore necessary to re-formulate the compositions.

To ensure that these new formulations were more environmentally benign than current perchlorate-based formulations, QinetiQ contracted the Centre for Ecology and Hydrology (CEH), the UK's leading land and freshwater science institution based at Monks Wood in the UK, to review the literature and produce toxicity, mobility and environmental impact reports on candidate ingredients and their combustion products. The Centre for Thermal Studies at the University of Huddersfield investigated the thermal properties of the compositions.

Materials and methods

Environmental screening

A range of information sources were utilized to compile the toxicity and environmental screening report on several new ingredients and the products of combustion; the most pertinent of which are listed below.

- IPCS INCHEM
- TOXNET
- Hazardous Substances Data Bank (HSDB)
- Toxicology Literature Online (TOXONLINE)
- Integrated Risk Information System (IRIS)
- ISI Web of Knowledge: Web of Science
- Google Scholar

Each of the predicted products of combustion was rated high, low or moderate against persistence, bioaccumulation and toxicity (P, B & T) criteria to ascertain their environmental impact. The environmental persistence (P) of a substance is determined by its half-life in surface waters, groundwater, sediments and soils. In the case of an element, the persistence of likely compounds that may be formed is also considered. Bioaccumulation (B) of a substance is the uptake by organisms to a higher concentration than the medium in which they live. This is measured in the following ways:

Bioconcentration factor (BCF), the ratio of substance concentration in organism to substance concentration in medium.

- Bioaccumulation factor (BAF) – the ratio of substance concentration in organism to substance concentration in food.
- Log octanol water partition coefficient (Log K_{ow}) – the measure of the equilibrium concentration of a substance between octanol and water indicates the potential for partitioning into organic matter. A high Log K_{ow} indicates a substance that will preferentially partition into organic matter rather than water. Log K_{ow} is inversely proportional to the solubility of a substance in water.
- Human and ecological toxicity (T) ratings are determined. Information on human toxicology includes acute and chronic studies on laboratory mammals and humans. Where applicable, information on reproductive toxicity, teratogenicity, mutagenicity and carcinogenicity has also been summarized. Methods for quantifying toxicity include:
 - Lethal (Effect) Concentration (L(E)C₅₀) – the concentration at which 50% of the population are likely to demonstrate lethality.
 - No observable effect concentration (NOEC).

The criteria for high, moderate and low ratings are detailed below. Where information was not available, expert judgment was used to produce the ratings.

High:

P = Degradation half life: fresh water >40 days; freshwater sediment/soil >120 days.

B = $\text{Log } K_{ow} > 4.5$ or $\text{BCF} > 2000$ where data are available. If experimental BCF <2000, $\text{Log } K_{ow}$ does not apply.

T (Toxicity) = category 1 or 2 carcinogen or mutagen, and category 2 reprotoxins or evidence of endocrine disrupting effects.

T (Ecotoxicity) = Acute lethal (effect) concentration for aquatic organisms $L(E)C_{50} \leq 0.1 \text{ mg dm}^{-3}$ or long term NOEC $\leq 0.01 \text{ mg dm}^{-3}$.

Moderate:

P = Degradation half life: freshwater <40 days; freshwater sediment/soil <120 days.

B = $\text{Log } K_{ow} > 4$ or $\text{BCF} > 500$ where data are available. If experimental BCF is <500, $\text{Log } K_{ow}$ does not apply.

T (Toxicity) = category 2 carcinogen and category 3 mutagens or reprotoxins or evidence of endocrine disrupting effects.

T (Ecotoxicity) = Acute $L(E)C_{50} > 0.1 \text{ mg dm}^{-3}$ to $\leq 1 \text{ mg dm}^{-3}$ or long term NOEC $> 0.01 \text{ mg dm}^{-3}$ to $\leq 0.1 \text{ mg dm}^{-3}$.

Low:

P = Readily biodegradable (mineralization in <28 days).

B = $\text{Log } K_{ow} < 4$ or Bioconcentration Factor < 500.

T (Toxicity) = Non-carcinogenic, mutagenic or reprotoxic.

T (Ecotoxicity) = Acute $L(E)C_{50} > 1 \text{ mg dm}^{-3}$ or long term NOEC $> 0.1 \text{ mg dm}^{-3}$.

All metal-containing inorganic compounds were treated as inherently persistent. Bioaccumulation potential ratings were established using expert judgment. The Toxicity ratings for inorganic compounds are the same as those presented for organic compounds.

Combustion modeling

The NASA computer program CEA2 (Chemical Equilibrium with Applications) which calculates chemical equilibrium compositions and properties of complex mixtures was used to determine the combustion products for a range of compositions. This program, which uses a thermodynamic database containing over 2000 species, was executed under Windows XP through a Java Graphical Users Interface (GUI). The GUI allows the input file for the program to be modified and the output file to be viewed.

The problem selected for the task was the theoretical rocket performance during expansion from infinite area combustor, the pressure was fixed at 101.325 kPa and ions were used in the calculations. A reaction starting temperature of 2500 K was generally selected, and different

condensed species were included to assist with obtaining convergence; neither of these parameters affects the equilibrium values obtained or species predicted.

Binary, ternary and quaternary compositions containing either 50% magnesium/aluminum alloy, magnesium or aluminum were examined. The oxidants used in the study were barium, potassium, sodium and strontium nitrate, and barium, calcium, potassium, sodium and strontium sulfate; the ternary compositions all contained barium nitrate. The predicted species were determined as a function of changing oxidant ratio.

As the program only considers combustion, the effects of cooling, oxidation or hydrolysis on the species predicted had to be considered separately.

Formulation studies

Two methods of composition preparation were used. Formulations containing powdered ingredients were prepared by blending the ingredients together in a Turbula mixer. For the other compositions, the liquid binder was first coated onto the fuel. When an even coating had been achieved, the oxidants were added and stirred into the mixture. The homogeneous mix was achieved by sieving the composition three times through a 600 μ m sieve.

Before use, the liquid binders were dried in an oven at 60°C for 24 hours and the oxidants were oven dried for a minimum of 3 hours at 95 °C, and sieved through a 125 μ m sieve.

Three fuels were examined:

- magnesium/aluminum alloy (to JAN-M-454),
- magnesium (to Defence Standard 13-130/1 Grade 4, cut),
- aluminum.

Grade 4, cut magnesium is similar to that of Type 1 to MIL-DTI-382 granulation number 6. Grade 4 is specified to have nil retained on a 212 μ m sieve which is same as magnesium to granulation number 6 and 85% retained on a 63 μ m sieve rather than 90% retained on 125 μ m sieve (magnesium to granulation number 6).

The aluminum was atomized powder with a mean particle size of 5 μ m.

Control samples based on IM-28 type were prepared by mixing each of the fuels with barium nitrate (to MIL-B-162D) and potassium perchlorate (to MIL-P-217A). The ratios of each ingredient used in the compositions are shown in Table 1. A series of control samples based on RS-41 were also prepared; the formulation details are given in Table 2.

Fuel (%)	Barium nitrate (%)	Potassium perchlorate (%)
50	50	0
	45	5
	40	10
	35	15
	30	20
	25	25
	20	30
	15	35
	10	40
	5	45
	0	50

Table 1; Formulation details for the IM-28 type control compositions.

Magnesium/aluminum alloy (%)	Potassium perchlorate (%)	Calcium resinate (%)
63	35	2
58	40	2
53	45	2
49	49	2
45	53	2
40	58	2
35	63	2
48	48	4
47	47	6
46	46	8
45	45	10
44	44	12

Table 2; Formulation details for the RS-41 type control compositions.

A range of binary compositions containing each of the fuels and barium nitrate were prepared; the ratios examined are shown in Table 3.

A number of different replacement compositions containing 50% of a fuel, barium nitrate and a second oxidant were prepared. The ratios of the ingredients used in each mix are shown in Table 4. The second oxidant was potassium nitrate, sodium nitrate, strontium nitrate, barium sulfate, calcium sulfate, potassium sulfate, sodium sulfate or strontium sulfate.

Fuel (%)	Barium nitrate (%)
70	30
60	40
55	45
45	55
40	60
30	70

Table 3; Formulation details for the binary compositions containing a fuel and barium nitrate.

Fuel (%)	Barium nitrate (%)	Second oxidant (%)
50	50	0
	45	5
	40	10
	35	15
	30	20
	20	30
	10	40
	0	50

Table 4; Formulation details for the replacement compositions containing barium nitrate and a second oxidant.

Two other sets of formulations based on magnesium/aluminum alloy, strontium nitrate and either sodium or potassium nitrate were examined. Details of the formulations are given in Table 5.

Magnesium/aluminum alloy (%)	Strontium nitrate (%)	Sodium or potassium nitrate (%)
50	50	-
50	45	5
50	40	10
50	35	15
50	30	20
50	25	25
50	20	30
50	15	35
50	10	40
50	5	45
50	-	50

Table 5; Formulation details for the binary compositions containing magnesium/aluminum alloy, strontium nitrate and either sodium or potassium nitrate.

Ternary compositions containing equal parts by mass of magnesium/aluminum alloy and barium nitrate and from 0 to 10% binder were prepared; the binders examined were either GAP, PolyGlyN or PolyNIMMO (Table 6).

Magnesium/aluminum alloy (%)	Barium nitrate (%)	Binder (%)
50.0	50.0	0
49.5	49.5	1
49.0	49.0	2
48.5	48.5	3
48.0	48.0	4
47.5	47.5	5
47.0	47.0	6
46.5	46.5	7
46.0	46.0	8
45.5	45.5	9
45.0	45.0	10

Table 6; Formulation details for ternary compositions containing magnesium/aluminum alloy, barium nitrate and an energetic binder.

A similar set of compositions (Table 7) where equal parts by mass of barium nitrate and strontium nitrate were used in place of barium nitrate.

Magnesium/aluminum alloy (%)	Barium nitrate (%)	Strontium nitrate (%)	Binder (%)
50.0	25.00	25.00	0
49.5	24.75	24.75	1
49.0	24.50	24.50	2
48.5	24.25	24.25	3
48.0	24.00	24.00	4
47.5	23.75	23.75	5
47.0	23.50	23.50	6
46.5	23.25	23.25	7
46.0	23.00	23.00	8
45.5	22.75	22.75	9
45.0	22.50	22.50	10

Table 7; Formulation details for the binary compositions containing magnesium/aluminum alloy, barium nitrate, strontium nitrate and an energetic binder.

For the third gun firing trial a small number of binary metal-metal or metal-metal oxide formulations were prepared by sieve mixing the ingredients together. Formulation details are given in Table 8.

Material	Percentage	Material	Percentage
Aluminum	19	Tungsten	81
Magnesium/aluminum alloy	27	Ferric oxide(Fe_2O_3)	73
Aluminum	27	Ferric oxide (Fe_2O_3)	73
Nanometric aluminum-boron	27	Ferric oxide (Fe_2O_3)	73

Table 8; Formulation details for the binary compositions containing metal-metal or metal-metal oxide combinations.

The final formulation studies examined compositions based on magnesium/aluminum alloy, potassium or sodium nitrate and a number of binders (Table 9). The binders examined were calcium resinate, boiled linseed oil, lithographic varnish, PVC powder and GAP. These compositions were only subjected to gun firing and ageing studies.

Magnesium/aluminum alloy (%)	Potassium or sodium nitrate (%)	Binder (%)
49	49	2
48	48	4

Table 9; Formulation details for the binary compositions containing magnesium/aluminum alloy, sodium or potassium nitrate and a binder.

Following the results of the gunfiring trials and ageing studies a range of formulations based on magnesium/aluminum alloy, sodium nitrate and calcium resinate were prepared for thermal analysis studies (Table 10).

Magnesium/aluminum alloy (%)	Sodium nitrate (%)	Calcium resinate (%)
49	49	2
48	48	4
47	47	6
46	46	8
45	45	10
44	44	12

Table 10; Formulation details for the binary compositions containing magnesium/aluminum alloy, sodium nitrate and calcium resinate.

Pyrotechnic burning rate

Flares were prepared by pressing four 3 g increments of each composition into 12 mm diameter cardboard tubes at 6.7 kN. The column length of the pressed composition was determined and the flare burning time measured.

Exothermicity measurements

Exothermicity measurements were performed using a Parr Model 1425 semi-micro combustion calorimeter. Duplicate experiments were carried out on 100 mg powder samples in an argon atmosphere under pressure of 1 atmosphere. The samples were ignited in quartz dishes using a hot wire.

Thermogravimetry

Thermogravimetry (TG) was carried out using a Du Pont TG951 thermo balance; the 5 mg samples were heated under an argon atmosphere in alumina crucibles at $10\text{ }^{\circ}\text{C min}^{-1}$.

DSC studies under ignition conditions

Differential scanning calorimetry (DSC) experiments were performed on the compositions using a high temperature DSC developed for pyrotechnic studies. The measurements were made on 20 mg samples which were heated at $50\text{ }^{\circ}\text{C min}^{-1}$ in 2 cm tall quartz crucibles in an upward flowing argon atmosphere.

Time to Ignition

Time to ignition (TTI) experiments were carried out using a pre-heated furnace on 20 or 50 mg samples in 2 cm quartz crucibles in an argon atmosphere. Two inconel crucibles containing titanium powder were placed on the upper plate of the TTI head to reduce any oxygen impurities in the gas stream. An integral photo-detector was used to detect an ignition reaction.

DSC studies under non-ignition conditions

DSC studies were also performed under non-ignition conditions. Samples (10 mg) were examined in 2 cm tall quartz crucibles, at a heating rate of $10\text{ }^{\circ}\text{C min}^{-1}$ in an upward flowing argon atmosphere.

Bullet firing trials

Five gun-firing trials have been performed as part of the composition assessment. The target range and the number of bullets tested is given in Table 11.

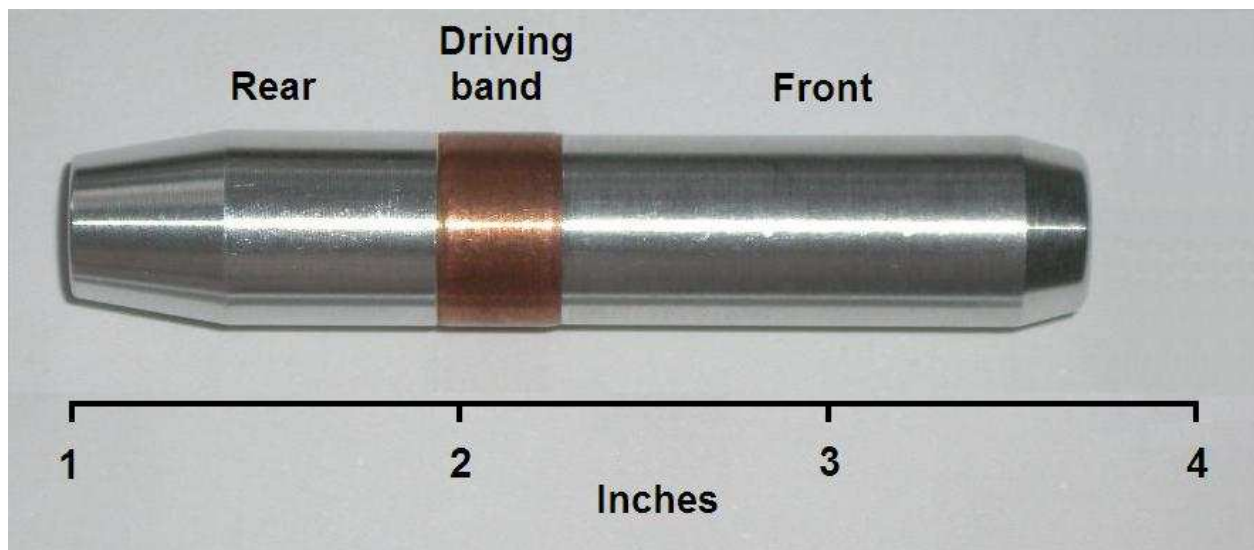
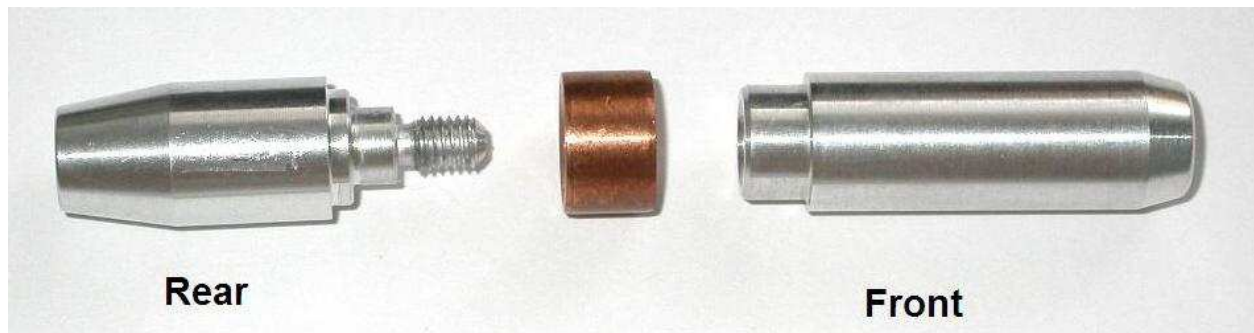
Trial number	Target range (m)	Bullet numbers
1	10	1-15
2	6	16-39
3	6	40-73
4	5.8	74-93
5	6	94-105

Table 11; Gun firing trials.

The compositions were filled into 0.5” caliber experimental rounds. These consist of front and rear sections which screw together and a copper driving band. Photographs of the individual components, an assembled round and the ammunition are shown below.

Approximately 0.7 g of loose composition or two 0.7 g pellets were filled into the cavity in the front section and retained using a self adhesive disc of aluminum foil. A cartridge case containing a reduced charge of propellant was crimped onto the rear section. The target was initially positioned 10 m from the muzzle of the gun but this was reduced to around 6 m for subsequent trials. The charge adjustment allowed the velocity of the ammunition at the short range to be matched to that normally observed at full range.

A Phantom high speed video camera was used to record the impact of the projectile at the aluminum alloy target. The framing rate was set to 3800 frames s^{-1} with a 10 μs exposure. Rounds filled with wax were also examined to establish the light output from the impact of the round alone.



Results and discussion

Ingredient environmental screening study

The results of the environmental screening studies of the ingredients are summarized in Table 12 to Table 14. The results are color coded with red denoting high, yellow for medium and green for low. Summaries of the information obtained by CEH during the literature review for the fuels, oxidants and binders are detailed below each table.

Pyrotechnic fuels

The results in Table 12 show that all of the pyrotechnic fuels showed high persistence but low values for bioaccumulation, toxicity and ecotoxicology. All of the fuels are therefore suitable for formulation studies.

	Persistence	Bioaccumulation	Toxicity	Ecotoxicity
Aluminum	Red	Green	Green	Green
Boron	Red	Green	Green	Green
Magnesium	Red	Green	Green	Green
Magnesium/aluminum alloy	Red	Green	Green	Green

Table 12; Environmental screening results for the pyrotechnic fuels.

Aluminum

Aluminum is not found as a free metal because of its reactivity. When aluminum powder comes into contact with air and/or water it releases flammable hydrogen gas and forms aluminum oxide. It has only one oxidation state (+3) in nature.

At pH values greater than 5.5, naturally occurring aluminum compounds exist predominantly in an undissolved form such as gibbsite ($\text{Al}(\text{OH})_3$) or as aluminosilicates, except in the presence of high amounts of dissolved organic material, which binds with aluminum and can lead to increased concentrations of dissolved aluminum in streams and lakes.

Several factors influence aluminum mobility and subsequent transport within the environment. These include chemical speciation, hydrological flow paths, soil-water interactions, and the composition of the underlying geological materials. The solubility of aluminum in equilibrium with solid phase $\text{Al}(\text{OH})_3$ is highly dependent on pH and on complexing agents such as fluoride, silicate, phosphate and organic matter.

Upon acidification of soils, aluminum can be released into solution for transport to streams. Mobilization of aluminum by acid precipitation results in more aluminum being available for plant uptake.

Aquatic unicellular algae showed an increased toxic effect at low pH, where bioavailability of aluminum is increased. For aquatic organisms, L(E)C₅₀ values range from 0.095 to 235 mg dm⁻³. However, care must be taken when interpreting the results because of the significant effects of pH on the availability of aluminum. The wide range of L(E)C₅₀ values probably reflects variable bioavailability. Short- and long-term toxicity tests on fish have been carried out under a variety of conditions and, most importantly, at a range of pH values. The data show that significant effects have been observed at monomeric inorganic aluminum levels as low as 25 µg dm⁻³. However, the complex relationship between acidity and aluminum bioavailability makes interpretation of the toxicity data more difficult. In the pH range 4.5 to 6.0 aluminum in equilibrium exerts its maximum toxic effect.

Amphibian eggs and larvae are affected by acidity and aluminum, with interaction between the two factors. Reduced hatching, delayed hatching, delayed metamorphosis, metamorphosis at small size, and mortality has been reported in various species and at aluminum concentrations below 1 mg dm⁻³. In acidic or poorly buffered environments subjected to strong acidifying inputs, concentrations of aluminum can increase to levels resulting in adverse effects on both aquatic organisms and terrestrial plants.

Exposure of roots of terrestrial plants to aluminum can cause diminished root growth, reduced uptake of plant nutrients and stunted plant development. Tolerance to aluminum has been demonstrated both in the laboratory and the field.

The acute toxicity of aluminum is low, the reported oral LD₅₀ values being in the range of several hundred to 1000 mg aluminum kg⁻¹ body weight per day. Information from toxicokinetic studies in animals is consistent with and complementary to that obtained in humans. Available studies indicate that oral bioavailability is low (< 1%). The target tissues in animals are similar to those in humans and include the bone and nervous system. In developmental studies in rodents, reduced intrauterine weight gains were noted in the female offspring of dams gavaged with aluminum nitrate at doses as low as 13 mg Al kg⁻¹ body weight per day, whereas male offspring were not affected at this dose level.

There is considerable evidence that aluminum is neurotoxic in experimental animals, although there is considerable variation among species. Neurobehavioural and motor development were affected at 100 and 200 mg Al kg⁻¹ body weight per day respectively. There is no indication that aluminum is carcinogenic.

Aluminum can form complexes with DNA and cross-link chromosomal proteins and DNA, but it has not been shown to be mutagenic in bacteria or induce mutation or transformation in mammalian cells in vitro. Chromosomal aberrations have been observed in bone marrow cells of exposed mice and rats. Aluminum has not been demonstrated to pose a health risk to healthy, non-occupationally exposed humans. There is no evidence to support a primary causative role of aluminum in Alzheimer's disease (AD), and aluminum does not induce AD pathology in vivo in any species, including humans.

Under good operating conditions, concentrations of aluminum of 0.1 mg dm^{-3} or less are achievable in large water treatment facilities. For small facilities, 0.2 mg dm^{-3} or less is a practicable level for aluminum in finished water.

Boron

Amorphous boron powder oxidizes slowly in air and water. Adsorption-desorption reactions are expected to be the only significant mechanism influencing the fate of boron in water. The extent of boron adsorption depends on the pH of the water and the concentration of boron.

Boron is adsorbed onto soil particles, with the degree of adsorption depending on the type of soil, pH, salinity, organic matter content, iron and aluminum oxide content, iron and aluminum hydroxy content, and clay content.

The octanol/water partition coefficient of boric acid has been measured as 0.175, indicating a low bioaccumulation potential. Plants accumulate boron; however, uptake is affected by the pH of the soil solution, temperature, light intensity, and the concentration of other elements (e.g. calcium and potassium).

Acute tests with aquatic organisms yielded toxicity values ranging from about 10 to $1376 \text{ mg boron dm}^{-3}$.

Lowest-observed-effect concentrations (LOECs) ranged from 1.1 to $1.73 \text{ mg boron dm}^{-3}$. However, laboratory tests with reconstituted water exposures appear to overestimate the toxicity determined in natural waters, possibly as a result of nutrient deficiency in the former.

Boron is an essential micronutrient for plants, with interspecies differences in the levels required for optimum growth. There is a small range between deficiency and excess uptake (toxicity) in plants. Irrigation water is one of the main sources of high boron levels resulting in toxicity in the field.

Duckling growth was adversely affected at dietary levels of 30 and $300 \text{ mg boron kg}^{-1}$, and reduced at 1000 mg kg^{-1} .

The oral LD_{50} values for boric acid and borax in laboratory mammals are in the range of 200 to $700 \text{ mg boron per kg body weight}$.

The data regarding developmental and reproductive toxicity show that lower foetal body weight in rats is the critical effect. The no-observed-adverse-effect level (NOAEL) for lowered foetal body weight is $9.6 \text{ mg boron per kg body weight per day}$.

The Tolerable Daily Intake for humans is $0.16 \text{ mg/kg body weight}$, based on a NOAEL of $9.6 \text{ mg per kg body weight per day}$ for developmental toxicity (decreased foetal body weight in rats) and an uncertainty factor of 60 (10 for interspecies variation and 6 for intraspecies variation).

Animal studies on mice and rats showed no evidence of carcinogenicity of boric acid. Boron is not classifiable as to its human carcinogenicity based on the lack of human data and the limited animal data.

The Provisional World Health Organization drinking water guideline value for boron is 0.5 mg dm^{-3} . The guideline is designated as provisional because it will be difficult to achieve in areas with high natural boron levels with the treatment technology available.

Magnesium

Magnesium powder reacts slowly with freshwater and soil pore water to form magnesium hydroxide. It reacts more rapidly in sea water to produce chloride and sulfate salts. Below pH 7.5 most magnesium minerals are too soluble to persist in soils and sediments and are dissolved predominantly as the Mg^{2+} ion.

Magnesium compounds in soil are removed by weathering. Magnesium compounds become more soluble as soils weather. Subsequently, below pH 7.5, most magnesium minerals are too soluble to persist in soils and sediments. Volatilization of magnesium compounds from moist soil surfaces is not an important fate process because these compounds are ionic and will not volatilize.

Natural water systems acquire magnesium through weathering reactions, which involve the interaction of water and atmosphere with the earth's crust and subsequent leaching of magnesium compounds into water. The Mg^{2+} ion is the predominant form of dissolved magnesium. However, some magnesium complexes do form. The magnesium sulfate ion pair complex is the most significant complex present.

If released into water, magnesium compounds may be removed by incorporation into sediment. Volatilization of magnesium compounds from water surfaces is not an important fate process because these compounds are ionic and will not volatilize.

Magnesium is an essential nutrient for humans, animals and plants, is widespread in living cells and does not bioconcentrate in aquatic organisms. Magnesium has low acute toxicity to aquatic organisms with L(E)C_{50} values ranging from 15.6 to $>5000 \text{ mg dm}^{-3}$. Magnesium has low acute toxicity to laboratory mammals. Inhalation of dust may irritate mucous membranes or upper respiratory tract.

Exposure to magnesium oxide fumes subsequent to burning, welding or molten metal work can result in metal fume fever with the following temporary symptoms: fever, chills, nausea, vomiting and muscle pain.

Magnesium is not suspected of being carcinogenic, mutagenic or teratogenic; however, no tests are available. Humans take in between 250 and 350 mg of magnesium per day and require at least 200 mg. There is no evidence that magnesium produces systemic poisoning although persistent over-indulgence in taking magnesium supplements and medicines can lead to muscle weakness, lethargy and confusion.

There are no drinking water guidelines on magnesium. However, the optimum magnesium levels in drinking water should lie within the range 40 to 80 mg dm^{-3} .

Magnesium/aluminum alloy

The ratings for magnesium/aluminum alloy are based on the properties of the constituent metals.

Pyrotechnic oxidants

The results for the oxidants including perchlorates are given in Table 13. In general all of the oxidants showed high persistence with perchlorate having a medium rating for bioaccumulation, toxicity and ecotoxicity.

Potassium dinitramide, copper oxide and manganese oxide were found to have either a high bioaccumulation or toxicity rating. Copper oxide also showed high ecotoxicity. As a result of these ratings; these three materials were not used for the formulation studies.

	Persistence	Bioaccumulation	Toxicity	Ecotoxicity
Barium nitrate	High	Medium	Low	Low
Copper oxide	High	High	Medium	High
Iron oxide	High	Medium	Low	Low
Nitrates (Potassium, sodium & calcium nitrate)	High	Low	Medium	Low
Manganese oxide	High	High	Medium	Low
Molybdenum trioxide	High	Low	Medium	Low
Perchlorates	High	Medium	Medium	Medium
Polytetrafluoroethylene	High	Low	Low	Low
Potassium dinitramide)	Medium	High	High	High
Strontium nitrate & sulfate	High	Medium	Low	Low
Sulfates (Potassium & calcium sulfate)	High	Low	Low	Low
Tungsten oxide	High	Medium	Low	Low

Table 13; Environmental screening results for the pyrotechnic oxidants.

Barium nitrate

Elemental barium undergoes oxidation in air and is oxidized readily in moist air. The residence time of barium in the atmosphere may be several days, depending on the size of the particulate formed, the chemical nature of the particulates, and environmental factors such as rainfall.

Barium reacts with metal oxides and hydroxides in soils limiting its mobility and increasing adsorption. Barium nitrate is expected to be mobile in the environment. It is soluble, reacting with sulfates and carbonates in water to form insoluble barium sulfate and barium carbonate salts. Soluble barium compounds, such as barium nitrate, are expected to lead to moderate bioconcentration of barium in aquatic organisms.

Barium is not expected to volatilize from moist soils, dry soils or water surfaces.

Barium has low acute toxicity to aquatic organisms with L(E)C₅₀ levels ranging from 70 to >4000 mg dm⁻³. A barium (nitrate) concentration of 5.8 mg dm⁻³ has been observed to impair reproduction and growth in daphnids during 21 day tests. The acute oral toxicity of barium compounds in experimental mammals is slight to moderate.

There is no conclusive evidence that barium compounds, are carcinogenic in humans, nor is there any conclusive evidence that barium produces reproductive, embryotoxic or teratogenic effects in humans.

The critical end-points in humans for toxicity resulting from exposure to barium and barium compounds appear to be hypertension and renal function.

Using a NOAEL in humans of 0.21 mg barium kg⁻¹ body weight per day, a tolerable intake value of 0.02 mg kg⁻¹ body weight per day for barium and barium compounds has been developed by the WHO.

The WHO drinking water guideline for barium is 0.7 mg dm⁻³.

Copper oxide

Copper oxide is practically insoluble in water. Most copper deposited in soil is strongly adsorbed and remains in the upper few centimeters of soil.

Copper oxide can accumulate in soils and this has been reported following the long-term application of fertilizers or fungicides. Bioaccumulation of copper from the environment occurs if the copper is biologically available. Accumulation may lead to exceptionally high body burdens in certain animals and terrestrial plants. However, many organisms are capable of regulating their body copper concentration.

Bioavailability is a critical factor in assessing the hazard of copper; the physical and chemical environment can greatly alter the degree to which it will be accumulated and elicit effects.

Copper is an essential element and adverse health effects are related to deficiency as well as excess.

Although plants require copper as a trace element, copper can be extremely toxic at high soil levels. The acute toxicity of copper to freshwater and marine fish is highly variable.

Copper oxide has low bioavailability, although other copper salts including chloride, acetate, sulfate and carbonate are highly bioavailable in animal nutrition. The toxicity of a single oral dose of copper varies widely between species and copper salts. The more soluble sulfate and chloride salts are generally more toxic than the less soluble hydroxide and oxides salts.

Copper (II) sulfate was not mutagenic in bacterial assays, while reproductive toxicity and carcinogenicity data are inadequate for risk assessment.

Iron Oxide

Iron oxides have low solubility in water. Iron in soil exists in ferrous (Fe²⁺) and ferric (Fe³⁺) forms. Soil pH and aeration status of the soil determine which form dominates. Ferric iron compounds have low solubility in soil solution, and conditions that favor formation of these compounds decrease iron availability.

Aquatic organisms accumulate iron but also rapidly excrete iron under clean water conditions.

As the water-soluble iron chloride, iron has low toxicity to aquatic organisms while as iron nitrate it has moderate to low toxicity.

Total iron concentrations of 0.3 to 10 mg dm⁻³ have been observed to cause physiological impairments or decreased growth, survival, or reproductive success in various fish species. Wide variations in toxicity have been reported for different iron salts and animal species. The threshold level of iron for harmful physiological effects depends mainly on ambient water chemistry.

Iron compounds were not teratogenic in the chicken embryo test. In a study of iron (II) sulfate and iron (III) sodium diphosphate in mice and rats, neither maternal toxicity nor teratogenic effects were found.

Iron (II) gluconate was mutagenic for indicator strain TA1538 in activation tests with primate liver preparations and iron (II) sulfate was active in suspension tests with activation. Iron (II) lactate, iron (III) diphosphate, iron (III) orthophosphate, and iron (III) diphosphate were inactive in all systems used.

Iron is an essential element in human nutrition and adults have often taken iron supplements for extended periods without deleterious effects.

Nitrates

Nitrates are very soluble in water. They dissociate to metal and nitrate ions in the environment. Nitrate ions are highly mobile and this may lead to the presence of nitrate ions in pore water, ground water and surface waters. Nitrate is persistent in groundwater.

Nitrates are not accumulated by organisms.

The acute oral toxicity of nitrate in experimental mammals is low.

A low percentage of the nitrate ingested by mammals is converted to the more toxic nitrite.

Manganese oxide

Manganese oxide is insoluble in water and will adsorb to suspended particles in water and soil pore water, sediment and soil.

Manganese in soil can migrate as particulate matter to air or water and soluble manganese compounds can be leached from the soil. The solubility of manganese in soils is determined by pH and redox potential.

Manganese in water can be significantly bioconcentrated by aquatic biota at lower trophic levels. The high reported BCFs probably reflect that manganese is an essential element for a wide variety of organisms.

Most toxicity tests have been performed using ionic manganese salts. Consequently, little is known about the aquatic toxicity of colloidal, particulate, and complexed manganese; however, in general, the toxicities of metals bound into these forms are assumed to be less than those of the aqua-ionic forms.

Toxic manganese concentrations in crop plant tissues vary widely, with critical values ranging from 100 to 5000 mg kg⁻¹. Manganese toxicity is a major factor limiting crop growth on acidic, poorly drained, or steam-sterilized mineral soils.

Little is known about the relative toxicity of different manganese compounds, although most health effects are associated with chronic inhalation exposure.

Effects on the nervous system include neurological and neuropsychiatric symptoms that can culminate in a Parkinsonism-like disease known as manganism.

Studies in animals indicate that manganese can cause direct damage to the testes and late resorptions.

Information on the carcinogenic potential of manganese is limited and no conclusion can be made about its genotoxic potential to humans. Adverse neurological and respiratory effects exposure can occur in occupational settings.

Molybdenum trioxide

The aqueous solubility of molybdenum trioxide is 1 g dm^{-3} . The predominant form of molybdenum occurring in soil and natural waters is the molybdate anion, MoO_4^{2-} . Unlike most micronutrients, molybdenum becomes more available as the soil becomes more alkaline.

No bioaccumulation of molybdenum has been observed in lipid rich biota and it is not expected to biomagnify in the food web.

Molybdenum has low toxicity in humans as it does not combine sufficiently strongly with physiological important compounds to have a serious blocking effect on metabolic processes. It is a confirmed animal carcinogen but there is no evidence of human carcinogenicity.

Molybdenum trioxide is an essential nutrient for plant and animals and has low acute toxicity to aquatic organisms. It was not mutagenic in tests with *Bacillus subtilis* or *Escherichia coli*.

Perchlorates

Potassium perchlorate will dissociate almost completely to potassium and perchlorate ions in aqueous environments. Perchlorate has high solubility and is a powerful oxidizer. Despite its oxidative potential, perchlorate is very stable and persistent in soil and groundwater.

The bioaccumulation of perchlorate in aquatic organisms is low. Perchlorate was found to readily accumulate in plant tissues.

Perchlorate interferes with iodide uptake into the thyroid gland in fish and inhibits amphibian metamorphosis.

Effects on laboratory mammals are related to the effect on iodine uptake. Functional hyperplasia of the thyroid in rodents (goitres) leads to thyroid tumors; goitrogens are not normally carcinogenic in humans.

Ammonium perchlorate is not a mutagen, a carcinogen, a reproductive toxin or an immunotoxin.

Polytetrafluoroethylene

Polytetrafluoroethylene (PTFE) is insoluble in water and largely inert under environmental conditions.

No toxicity was observed in rats fed PTFE at up to 25% in the diet for 90 days. Exposure to dust may cause irritation of the eyes, skin or the digestive tract, while aspiration may lead to pulmonary oedema.

No data on the carcinogenicity of PTFE in humans were available and there is inadequate evidence to determine its carcinogenicity in animals.

Potassium dinitramide

No information was obtained regarding the fate and toxicity of potassium dinitramide. A review of ammonium dinitramide has been conducted.

Ammonium dinitramide is hydrolytically stable in acidic, neutral and slightly alkaline water at 25°C, with an estimated half-life of 370 years at pH 7. However, it is photolyzed within minutes in sunlight.

The acute oral toxicity of ammonium dinitramide in experimental mammals is low and no information was identified on its toxicity to aquatic organisms.

Ammonium dinitramide is a reproductive toxicant in laboratory mammals and a mutagenic toxicant in both in vitro and in vivo tests.

Strontium nitrate and strontium sulfate

Strontium nitrate has high aqueous solubility whereas strontium sulfate has low solubility. Strontium has moderate mobility in soils and sediments, and sorbs moderately to metal oxides and clays.

Strontium is required for the normal development of some unicellular microorganisms, gastropods, cephalopods, corals and calcareous algae.

Earthworms do not accumulate strontium in soils high in calcium; however, strontium accumulation may occur in acidic, calcium-poor soils.

Strontium has low acute toxicity to aquatic organisms and to laboratory mammals.

The adequacy of calcium nutrition is a critical factor regarding strontium toxicity; skeletal abnormalities have been observed in animals administered oral doses of strontium in conjunction with low levels of dietary calcium.

Young animals are more sensitive than adult animals to excessive strontium intakes as their bones are actively growing. No teratogenic effects of strontium have been reported.

Sulfates

Potassium sulfate is highly soluble in water whereas calcium sulfate is only slightly soluble. The fate of sulfate in soil is influenced by many chemical, biological and physical factors.

Sulfate is the most important form of inorganic sulfur in soils and is the most readily available form to plants.

The acute toxicity of sulfate to aquatic organisms and laboratory mammals is low.

Cathartic effects are commonly reported to be experienced by people consuming drinking water containing sulfate in concentrations exceeding 600 mg dm⁻³. Some subpopulations, such as children, transients and the elderly may be more sensitive to the cathartic effects of exposure to high concentrations of sulfate.

The existing data do not identify a level of sulfate in drinking water that is likely to cause adverse human health effects.

Tungsten oxide

When released to soil, tungsten compounds will have moderate to low mobility. Tungsten in natural waters is predominantly in the form of tungstate ions and other tungsten polyanions. Insoluble tungsten in water can settle to the bottom where it enters sediment.

Elemental tungsten is, by definition, persistent.

Tungsten is regarded as having low bioavailability and a low capacity for leaching into groundwater. Accumulation is moderate with plants and invertebrates taking up tungsten increasingly with increasing concentration in the medium.

Tungsten has low acute toxicity to *Daphnia*, *Chlorella* and bacteria. Adverse effects on plants occur only at high soil concentrations. Tungsten is inhibitory to soil micro-organisms at concentrations around 1% w/w and above. The effect appears to relate to lethality to more sensitive species.

Limited reports associate tungsten exposure with reproductive and developmental effects such as decreased sperm motility, increased embryotoxicity, and delayed foetal skeletal ossification in animals.

No adequate animal data are available to assess the carcinogenic potential of tungsten or tungsten compounds.

Pyrotechnic binders and other ingredients

A summary of the environmental screening results for the binders and other ingredients is given in Table 14. Except for calcium resinate which has low persistence, the binders and other ingredients showed high persistence. They all show low values for bioaccumulation, toxicity and ecotoxicity. All of these ingredients were therefore suitable for formulation studies.

	Persistence	Bioaccumulation	Toxicity	Ecotoxicity
Antimony (tri)sulfide				
Calcium resinate				
GAP				
Hexafluoropropylene vinylidene fluoride copolymer				
PolyGlyN				
PolyNIMMO				
PVC				

Table 14; Environmental screening results for the pyrotechnic binders.

Antimony (tri)sulfide

Antimony trisulfide is relatively insoluble in water and has little toxic action except through liberation of hydrogen sulfide (see hydrogen sulfide).

Antimony trisulfide has been shown to be approximately 3.5 times more acutely toxic to rats than antimony trioxide. Several studies reported interstitial fibrosis in rats exposed for 12 to 14.5 months to antimony trisulfide at concentrations ranging from 1.6 to 83.6 mg antimony m⁻³.

Inhalation of fumes from heated antimony trisulfide may cause irritation of nose and contact with eyes causes irritation. Contact of molten material with the skin may cause burns.

Chronic poisoning from handling antimony sulfide from mining in Morocco has been reported. Symptoms included headache, muscular pains, vertigo, anorexia, and altered blood makeup.

There is limited evidence for the carcinogenicity of antimony trisulfide in experimental animals and in humans. Antimony trisulfide's carcinogenicity to humans is therefore not classified.

L(E)C₅₀ and NOEC concentrations in algae, aquatic invertebrates and fish for the soluble antimony trichloride salt ranged from 0.01 to >80 mg dm⁻³; however, the insoluble antimony trioxide salt gave L(E)C₅₀ values ranging from 400 to >1000 mg dm⁻³.

Calcium resinate

Calcium resinate exists as yellow-white amorphous powder that is insoluble in water. It biodegrades readily under anaerobic conditions. It was not found to be irritating in acute dermal irritation/corrosion tests. However, inhalation of the fumes of the heated material may cause irritation of nose, while contact with eyes will also cause irritation.

Calcium resinate exhibits acute oral toxicity to laboratory mammals (>2000 mg kg⁻¹). In aquatic organisms, the L(E)C₅₀ levels range from 100 mg dm⁻³ (zebra fish) to >1000 mg dm⁻³ (algae).

GAP

GAP is insoluble in water.

No further hazard or risk information was found for this polymer.

The polymer is unlikely to be bioavailable to organisms; therefore, the likelihood of bioaccumulation or toxicity is low.

Hexafluoropropylene-vinylidene fluoride copolymer

No hazard, risk or environmental fate information was found for this polymer. The polymer is unlikely to be bioavailable to organisms; therefore, the likelihood of bioaccumulation or toxicity is low. The following information is based on the components of the polymer.

Hexafluoropropylene is unlikely to bioaccumulate. It has low toxicity after acute exposure and is not considered to be a genotoxin, although tests on the structurally related tetrafluoroethylene, indicate that it may be a carcinogen.

Vinylidene fluoride would not be expected to bioaccumulate or biomagnify in the food chain.

Model calculations predict that vinylidene fluoride will not be toxic to algae, aquatic invertebrates or fish. Vinylidene fluoride had a low acute toxicity in laboratory animals; it is not genotoxic either in vitro or in vivo. A teratology study did not indicate any embryotoxic, foetotoxic or teratogenic effects, even at high concentrations.

There is inadequate evidence to evaluate the carcinogenicity of vinylidene fluoride in animals or humans.

PolyGlyN

Uncured PolyGlyN prepolymer is chemically stable. PolyGlyN cured rubber has poor stability unless treated by an end modification process prior to curing.

No hazard or risk information was found for this polymer.

The polymer is unlikely to be bioavailable to organisms; therefore, the likelihood of bioaccumulation or toxicity is low.

PolyNIMMO

No hazard or risk information was found for this polymer.

Under environmental conditions PolyNIMMO is very stable. The polymer is unlikely to be bioavailable to organisms; therefore, the likelihood of bioaccumulation or toxicity is low

PVC

PVC is stable under environmental conditions and soluble in water. Biodegradation by fungal species has been observed under nutrient limiting conditions. There was no evidence of biodegradation of PVC buried in soil for 32 years.

The bioaccumulation potential of the vinyl chloride monomer is low.

The aquatic toxicity of the vinyl chloride monomer is low. There are insufficient data to evaluate the carcinogenicity or mutagenicity of PVC to animals or humans.

Combustion modeling

For each system, the species predicted by the CEA program were ranked according to mass fraction. The ten most abundant materials are shown as a function of second oxidant content in Figure 1 to Figure 24.

Analysis of the results shows that the chemistry of each system is complex and related to the amount of each reactant present, the combustion temperature and the thermal properties, of both the reactants and the combustion products.

For all three systems, the major products observed were the oxides of the fuel, in the case of the alloy this was a mixed fuel oxide. As the systems were generally fuel-rich, a proportion of the fuels did not react but they were vaporized. The cations of the oxidants were also present in the gas phase along with oxides and sulfides depending on the oxidant used in the formulation.

Most of the predicted species are in the gaseous state and during or after cooling would decompose, oxidize or hydrolyze possibly over an extended time period. A final list of compounds to environmentally screen which considers these reactions is shown in Table 15.

Ammonia, hydrogen sulfide, sulfur and sulfur dioxide were amongst the combustion products along with a range of metal oxides, hydroxides and sulfides.

Two additional combustion products were examined, these were magnesium fluoride and aluminum fluoride, which are produced when magnesium-PTFE-Viton compositions are burned.

CEA predicted	Comments	Final predicted species
AlN	AlN	Aluminum nitride
Al ₂ O	Reacts to form aluminum oxide	-
Al ₂ O ₂	Reacts to form aluminum oxide	-
Al ₂ O ₃	Aluminum oxide	Aluminum oxide
Al ₂ S	Reacts to form aluminum sulfide(Al ₂ S ₃)	Aluminum sulfide
Al ₂ S ₂	Reacts to form aluminum sulfide	-
AlS	Reacts to form aluminum sulfide	-
Ba	Reacts to form barium hydroxide (Ba(OH) ₂)	Barium hydroxide
BaN	Ba ₂ N ₃	Barium nitride
BaO	Reacts to form barium hydroxide	-
BaS	BaS will also react to produce hydrogen sulfide	Barium sulfide Hydrogen sulfide
Ca	Reacts to form calcium hydroxide or calcium nitride and ammonia	Ammonia
CaO	Reacts to form calcium hydroxide (Ca(OH) ₂)	Calcium hydroxide
CaS	Reacts to produce hydrogen sulfide	Calcium sulfide
K	Reacts to form potassium hydroxide	-
K ₂ N	Reacts to form potassium hydroxide	-
K ₂ O	KOH	Potassium hydroxide
KS	Reacts to form potassium hydroxide and hydrogen sulfide	-
Mg	Reacts to form magnesium hydroxide	Magnesium hydroxide
MgAl ₂ O ₄	MgAl ₂ O ₄	Magnesium aluminate
MgN	Reacts to form magnesium hydroxide and ammonia	-
MgO	Reacts to form magnesium hydroxide	-
MgS	Magnesium sulfide	Magnesium sulfide
Na	Reacts to form sodium hydroxide	Sodium hydroxide
Na ₂ N	Reacts to form sodium hydroxide	-
Na ₂ O	Sodium hydroxide	-
NaS	Reacts to produce hydrogen sulfide and sodium hydroxide	Sodium sulfide
S	Sulfur	Sulfur
SO ₂	Sulfur dioxide	Sulfur dioxide
Sr	Reacts to form strontium oxide and hydroxide	Strontium oxide Strontium hydroxide
SrN	Reacts to form strontium hydroxide, and ammonia	-
SrO	Strontium oxide	-
SrS	Reacts to produce hydrogen sulfide	Strontium sulfide

Table 15; Predicted species after combustion and further reaction.

Combustion products environmental screening study

A summary of the environmental screening results for the combustion products is given in Table 16. For toxicity both the chronic and acute toxicity were considered.

	Persistence	Bioaccumulation	Toxicity	Ecotoxicity
Aluminum fluoride		Low for Aluminum		
Aluminum nitride, oxide and sulfide				
Ammonia				
Barium hydroxide			Low for chronic exposure	
Barium nitride			Low for chronic exposure	Low for chronic exposure
Barium sulfide			Low for chronic exposure	Low for chronic exposure
Hydrogen sulfide				
Hydroxides (calcium, potassium & sodium)			Low for chronic exposure	
Magnesium aluminate				
Magnesium hydroxide and sulfide				
Magnesium fluoride		Low for Magnesium		Low for aquatic toxicity
Sodium nitride			Low for chronic exposure	Low for chronic exposure
Strontium hydroxide, strontium oxide & strontium sulfide			Low for chronic exposure	
Sulfides (inc. calcium, potassium and sodium sulfide)				
Sulfur			Low for chronic exposure	Low for chronic exposure
Sulfur dioxide			Low for chronic exposure	Low for chronic exposure

Table 16; Environmental screening results for the products of combustion.

Aluminum fluoride

Aluminum fluoride can be absorbed into the body by inhalation of the dust and by ingestion. Evaporation at 20°C is negligible; a harmful concentration of airborne particles can, however, be reached quickly. The aerosol is irritating to the eyes, the skin and the respiratory tract. Repeated or prolonged inhalation exposure may cause asthma. The substance may have effects on the bone, nervous system, resulting in bone alterations (fluorosis), and nervous system impairment. Aluminum fluoride is not classifiable as a human carcinogen.

See also the profile for aluminum.

Fluorides in the atmosphere may be in gaseous or particulate form. Atmospheric fluorides can be transported over large distances as a result of wind or atmospheric turbulence or can be removed from the atmosphere via wet and dry deposition or hydrolysis. The transport and transformation of fluoride in water are influenced by pH, water hardness and the presence of ion-exchange materials such as clays. Fluoride is usually transported through the water cycle complexed with aluminum.

The transport and transformation of fluoride in soil are influenced by pH and the formation of predominantly aluminum and calcium complexes. Adsorption to the soil solid phase is stronger at slightly acidic pH values (5.5–6.5). Fluoride is not readily leached from soils. Soluble fluorides are bioaccumulated by some aquatic and terrestrial biota. However, no information was identified concerning the biomagnification of fluoride in aquatic or terrestrial food-chains. Terrestrial plants may accumulate fluorides following airborne deposition and uptake from soil.

In humans and laboratory animals, approximately 99% of the total body burden of fluoride is retained in bones and teeth. Effects on the skeleton, such as inhibition of bone mineralization and formation, delayed fracture healing and reductions in bone volume and collagen synthesis, have been observed in a variety of studies in which rats received fluoride orally for periods of 3–5 weeks.

Reproductive, developmental, mutagenic or carcinogenic effects of fluorides have not been reported. Acute L(E)C₅₀s for fluorides in aquatic organisms range from 50 to 500 mg dm⁻³. Twenty-day L(E)C₅₀s for rainbow trout ranged from 2.7 to 4.7 mg fluoride dm⁻³ in static renewal tests.

Signs of inorganic fluoride phytotoxicity (fluorosis), such as chlorosis, necrosis and decreased growth rates, are most likely to occur in the young, expanding tissues of broadleaf plants and elongating needles of conifers. The induction of fluorosis has been clearly demonstrated in laboratory, greenhouse and controlled field plot experiments.

Fluorosis has been observed in cattle and sheep. The lowest dietary level observed to cause an effect on wild ungulates was in a controlled captive study with white-tailed deer (*Odocoileus virginianus*) in which a general mottling of the incisors characteristic of dental fluorosis was noted in the animals at the 35 mg kg⁻¹ diet dose.

The WHO recommended guideline value for fluoride in drinking-water is 1.5 mg dm⁻³.

Aluminum nitride, oxide and sulfide

Aluminum nitride reacts with water to form ammonia and nitrogen oxides while aluminum sulfide reacts with water to form hydrogen sulfide and oxides of sulfur. Aluminum nitride dust is an irritant to the eyes, respiratory system and skin. See profile for aluminum.

Ammonia

Ammonia is a colorless gas with a strong, penetrating odor and exists in the environment as a part of the nitrogen cycle. It volatilizes into the atmosphere where it may undergo a variety of reactions. Photolytic reactions destroy some of the ammonia and reactions with sulfur dioxide or ozone produce aerosols, most importantly of ammonium sulfate or nitrate, which return to the earth's surface as wet deposition (Acid rain) or dry deposition.

In surface waters, ammonia may be assimilated by aquatic plants as a nitrogen source or transferred to sediments or volatilized.

In soil, major sources of ammonia are the aerobic degradation of organic matter and atmospheric deposition of synthetic fertilizers. Most ammonium undergoes nitrification (the nitrate ion is mobile and is removed by leaching, plant root uptake, or denitrification).

Non-ionized ammonia (NH_3) is recognized as the principal toxic form of ammonia rather than the ammonium ion (NH_4^+). However, only very limited acute and chronic ammonia toxicity data for salt-water organisms are available. Mean L(E)C_{50} values for marine invertebrate species range from 0.9 to 18.3 $\text{mg NH}_3 \text{ dm}^{-3}$ and, for marine fish species, from 0.3 to 1.3 mg dm^{-3} .

There is no evidence that ammonia is mutagenic or carcinogenic in mammals.

Ammonia can be tasted in water at levels above about 35 mg dm^{-3} . Most people can identify the odor of ammonia in air at about 35 mg m^{-3} and can detect it at about one-tenth of this level.

Barium hydroxide, nitride and sulfide

The barium compounds barium hydroxide and barium oxide are quite soluble in water. Barium oxide reacts rapidly with carbon dioxide in water to form barium hydroxide and barium carbonate. Aqueous solutions of barium hydroxide are strongly alkaline and can cause severe burns to the eye and skin irritation

Barium sulfide decomposes slowly in water, forming barium hydroxide and barium hydrosulfide. Barium sulfide is also known to undergo slow oxidation in solution to form elemental sulfur and various oxidized sulfur species including the sulfite, thiosulfate, polythionates, and sulfate.

Also see profile for barium nitrate.

Hydrogen sulfide

Hydrogen sulfide exists as a colorless gas with a characteristic odor of rotten eggs. Partitioning to the air is likely to occur after environmental releases. It is also soluble in oil and water and may therefore partition to surface waters, ground waters, or moist soils and, subsequently, travel great distances.

The primary chemical transformation of hydrogen sulfide in the atmosphere is oxidation by oxygen containing radicals to sulfur dioxide and sulfates. These are eventually removed from the atmosphere through absorption by plants and soils or through precipitation.

Hydrogen sulfide oxidation by oxygen may readily occur in surface waters. Oxidation by hydrogen peroxide may also occur, primarily in rainwater and marine aerosols. In warm, damp environments hydrogen sulfide may be oxidized by autotrophic bacteria to sulfuric acid. Ionization in water may also occur, depending upon pH.

Soils may adsorb considerable amounts of hydrogen sulfide from the air, retaining most of it in the form of elemental sulfur. Anhydrous hydrogen sulfide has a boiling point of -60.3°C

and consequently much will evaporate. However, due to its solubility in water, the presence of water in soil may contribute to movement in the soil. It is unlikely to bioconcentrate and biomagnify in the food-chain.

Acute inhalation toxicity of hydrogen sulfide to laboratory mammals ranges from 470 mg m⁻³ after 6 hours to 820 mg m⁻³ after 2 hr.

In experimental animals, single inhalation exposures to hydrogen sulfide result in death and respiratory, immunological/lymphoreticular, cardiovascular, and neurological effects. Reported health effects in animals following short-term exposures include ocular, cardiovascular, neurological, metabolic, hepatic, and developmental effects. Medium-duration inhalation studies of hydrogen sulfide in animals have reported respiratory, neurological, and olfactory effects.

There are no studies on effects of long-term exposure to hydrogen sulfide in animals. There are no studies on cancer effects in animals exposed to hydrogen sulfide. Ingestion is of no relevance for humans. There are no human ingestion data. It is not possible to evaluate the carcinogenic potential of hydrogen sulfide.

Hydroxides (calcium, potassium & sodium)

Atmospheric emissions of hydroxides are rapidly neutralized by carbon dioxide or other acids to form salts which are washed out by rain. Hydroxides are very mobile in soil and very soluble in water but do not transport to air.

Hydroxides are strong alkaline substances that dissociate fully. The concentration of OH⁻ (pH) is in general regulated by the equilibria between CO₂, HCO₃⁻ and CO₃²⁻. The buffer capacity depends on the concentration of these substances. Sodium hydroxide can be absorbed into the body by inhalation of its aerosol and by ingestion.

The hydroxides are potent corrosives and the observed acute toxicity and reported dermatitis following prolonged exposure appear to be a consequence of this corrosive potential. There are no data to indicate the hydroxides to be skin sensitizers, genotoxic, carcinogenic, or reproductive toxicants.

The hazard of the hydroxides for the environment is caused by the pH effect of the hydroxide ion. Consequently, the effect of hydroxide on the organisms depends on the buffer capacity of the aquatic or terrestrial ecosystem.

Acute L(E)C₅₀s for hydroxides (calcium, potassium and sodium) range from 30 to 190 mg dm⁻³ for fish and 273 to 7340 mg dm⁻³ for rats.

Magnesium hydroxide and sulfide

Magnesium compounds become more soluble as soils weather. Consequently, most magnesium minerals are too soluble to persist in soils and sediments below pH 7.5.

Magnesium compounds in soil are removed by weathering. Natural water systems therefore acquire magnesium through these weathering reactions, which involve the interaction of water and the atmosphere with the earth's crust, and the subsequent leaching of magnesium compounds into water. Magnesium hydroxide is practically insoluble and magnesium sulfide decomposes in water. The magnesium sulfate ion pair complex (MgSO₄) is the most significant complex present.

See profile for magnesium.

Magnesium aluminate

Refer to the profiles on magnesium and aluminum.

Magnesium fluoride

Magnesium fluoride reacts with mineral acids to release highly toxic hydrogen fluoride gas. Magnesium fluoride is harmful by inhalation or ingestion, and is a skin and eye irritant. Long-term chronic exposure may cause fluorosis.

See also the profiles for magnesium and aluminum fluoride.

Strontium hydroxide, strontium oxide and strontium sulfide

Strontium oxide reacts with moisture and carbon dioxide in air to form strontium hydroxide and strontium carbonate respectively. Strontium hydroxide in contact with water will ionize to form Sr^{2+} and SrOH^+ ions. There is no evidence of interaction of strontium oxide with other compounds in the atmosphere.

See also the profile for strontium nitrate.

Sulfides (including calcium, potassium and sodium sulfide)

Calcium sulfide exists as a deep orange liquid while potassium sulfide exists as white cubic crystals or fused plates. Sodium sulfide exists as cubic crystals or granules. All three of these materials are soluble in water.

Alkaline sulfides are strong local irritants; 25% sodium sulfide caused skin corrosion in rabbits in a 4 hr patch test.

If free gastric acidity is high, the ingestion of sulfide salts may result in their decomposition to hydrogen sulfide in the stomach, with subsequent systemic poisoning (see hydrogen sulfide). Sulfide is so rapidly detoxified in the body and any decrease in exposure intensity may result in rapid and spontaneous revival.

Frequent exposure to low concentrations of sulfides leads to tolerance; however, exposure to high concentrations can lead to sensitization.

Calcium polysulfide (lime sulfur) solution is a common agricultural product used as a fungicide. Aqueous solutions of calcium polysulfide at a concentration of 120 ml dm^{-3} , applied at a rate of 336 L of calcium polysulfide per hectare to dormant grapevines in spring, killed cleistothecia of *Uncinula necator* (powdery mildew) on the bark of the vines and delayed the development of epidemics of powdery mildew.

Calcium polysulfide ingestions cause direct caustic injury to the upper gastrointestinal tract, coma and severe metabolic acidosis. Oral LD_{50} s of 205 and 208 mg kg^{-1} have been reported in laboratory mammals for sodium sulfide. Forty-eight hour L(E)C_{50} values for aquatic invertebrates range from 0.1 to 3.3 mg dm^{-3} for sodium sulfide.

Sulfur and sulfur dioxide

Sulfur irritates the eyes, the skin and the respiratory tract. Inhalation of sulfur powder may cause inflammation of the nose and the respiratory tract. Repeated or prolonged contact with skin may cause dermatitis. Sulfur may have effects on the respiratory tract, resulting in chronic bronchitis.

Sulfur dioxide is typically present in the gaseous phase. Anthropogenic and natural releases are considered to be its primary source to the atmosphere. Some of the sulfur dioxide emitted into the air moves unchanged to various surfaces including soil, water, grass, and vegetation. In the atmosphere, sulfur dioxide can be transformed into sulfuric acid or sulfates by a variety of processes.

Oceans are considered to be a sink for sulfur dioxide as it is extremely soluble in water. Potential release of sulfur dioxide from water would be by partition to the atmosphere.

Sulfur dioxide is oxidized less rapidly in freshwater lakes than in seawater because of the much lower salt content. Aqueous-phase oxidation of sulfur dioxide can also occur in cloud, fog, rain, deliquescent aerosol particles, and in surface liquid films on these particles. Once dissolved in these droplets, sulfur dioxide may be oxidized to sulfate via a variety of mechanisms, thus forming “acid rain”.

A 4 hour L(E)C₅₀ for inhalation of sulfur dioxide in mice was reported at 1000 ppm. Rats exposed to sulfur dioxide at 0.5 mg m⁻³ for 96 days showed interstitial pneumonia, bronchitis, tracheitis and peribronchitis. However, rats given 750 mg dm⁻³ in drinking water for 3 years (3 generations) showed no effect on growth, food and fluid intake, fertility, weight of newborns or the frequency of tumor development.

There is inadequate evidence for the carcinogenicity of sulfur dioxide in humans and limited evidence for that in experimental animals. Consequently, sulfur dioxide is not classifiable as to its carcinogenicity to humans (Group 3). However, sulfur and sulfur dioxide both irritate the eyes, skin and respiratory tract, resulting in chronic bronchitis.

Sulfur dioxide can be removed from air by the uptake of plant leaves. Green plants are extremely sensitive to atmospheric sulfur dioxide. Alfalfa, barley, cotton, and wheat can be injured at levels between 0.15 and 0.20 ppm, while potatoes, onions, and corn are far more resistant.

Formulation and performance studies

Magnesium/aluminum alloy based compositions

Combustion studies

Magnesium/aluminum alloy-barium nitrate-potassium perchlorate system

IM-28 incendiary flash composition which is used in the 0.50" caliber ammunition contains 50% magnesium/aluminum alloy, 40% barium nitrate and 10% potassium perchlorate. A range of control compositions containing these ingredients including IM-28 were prepared and tested.

The burning rate curve as a function of potassium perchlorate content for the range of binary and ternary compositions containing 50% magnesium/aluminum alloy is shown in Figure 25. The binary composition containing 50% alloy-50% barium nitrate had the highest burning rate. The addition of potassium perchlorate caused a reduction in the burning rate and the composition containing only potassium perchlorate as the oxidant had the lowest burning rate of around 2.5 mm s^{-1} .

Magnesium/aluminum alloy-potassium perchlorate-2% calcium resinate

RS-41 used in the explosive train of the 20mm PGU 28/B and the PGU-28A/B semi-armor-piercing high explosive incendiary ammunition contains 49% magnesium/aluminum alloy-49% potassium perchlorate and 2% calcium resinate as the binder. This composition and others with different fuel to oxidant ratios were examined. The burning rates as a function of perchlorate content are shown in Figure 26.

As the potassium perchlorate content of the compositions increased, the burning rate was found to decrease steadily from 4.7 mm s^{-1} to 1.3 mm s^{-1} ; the composition equivalent to RS-41 had a burning rate of 3.4 mm s^{-1} .

In addition, the effect on burning rate of changing the calcium resinate content from 2% to 12% was examined the burning rate results are shown in Figure 27. An almost linear decrease in burning rate from 3.4 mm s^{-1} to 1.4 mm s^{-1} was observed as the calcium resinate content of the compositions was increased.

Magnesium/aluminum alloy-barium nitrate

Binary magnesium/aluminum alloy-barium nitrate compositions were found to support combustion over the range 30% to 50% barium nitrate (Figure 28). The burning rate of the compositions showed only a small change over this range with the maximum burning rate occurring at around 45% barium nitrate.

Magnesium/aluminum alloy-barium nitrate-nitrate systems

Compositions containing magnesium/aluminum alloy, barium nitrate and potassium, sodium and strontium nitrate as the second oxidizer were studied. All three systems showed sustained combustion across the entire range of compositions (Figure 29). The burning rates of the compositions decreased with decreasing barium nitrate content with potassium and sodium nitrate showing higher initial reductions in burning rate. The burning rates of the compositions containing strontium nitrate were slightly greater than the equivalent compositions containing potassium perchlorate.

Magnesium/aluminum alloy-barium nitrate-sulfate systems

Compositions containing 50% magnesium/aluminum alloy-barium nitrate and either barium, calcium or strontium sulfate burned across the entire range examined. They showed a considerable increase in burning rate with increasing sulfate content (Figure 30). The highest burning rate, of 25 mm s^{-1} , was given by the binary magnesium/aluminum alloy strontium sulfate formulation. Compositions containing potassium and sodium sulfate burned up to the 30% and 40% sulfate levels respectively; the burning rates for these compositions initially decreased slightly before increasing at higher sulfate contents.

Magnesium/aluminum alloy-strontium nitrate-potassium nitrate

The addition of potassium nitrate to a binary magnesium/aluminum alloy-strontium nitrate composition decreased the burning rate (Figure 31). The binary compositions containing strontium nitrate had a burning rate of 4.2 mm s^{-1} compared to 2.5 mm s^{-1} for that containing potassium nitrate.

Magnesium/aluminum alloy-strontium nitrate-sodium nitrate

The burning rates for ternary compositions containing magnesium/aluminum alloy, strontium nitrate and sodium nitrate showed only small changes over the entire range; the maximum and minimum burning rates were around 4.3 mm s^{-1} and 3.3 mm s^{-1} respectively (Figure 32).

Magnesium/aluminum alloy compositions containing energetic binders

Two systems containing from 0% to 10% of three binders GAP, polyGlyN and polyNIMMO were studied. These were magnesium/aluminum alloy-barium nitrate-binder and magnesium/aluminum alloy-barium nitrate-strontium nitrate-binder. For each system the fuel to oxidant ratio was maintained at 1:1 and for the system containing two oxidants their ratio was kept at 1:1.

The binary compositions had significantly different burning rates; 8.5 mm s^{-1} for the magnesium/aluminum alloy-barium nitrate compositions compared to 6.4 mm s^{-1} for magnesium/aluminum alloy-barium nitrate-strontium nitrate one.

Magnesium/aluminum alloy compositions containing GAP as the binder

For both systems the burning rate decreased as the amount of GAP increased (Figure 33 and Figure 34). At binder levels above 3%, the burning rates of the compositions were similar; those containing only barium nitrate were slightly higher than the mixed oxidant combination.

Magnesium/aluminum alloy compositions containing PolyGlyN as the binder

For both systems, increasing the amount of PolyGlyN in the compositions resulted in a reduced burning rate (Figure 35 and Figure 36). Partial burns were recorded at relatively low binder levels so the data available on these systems are limited. The compositions based on barium nitrate had higher burning rates than the equivalent compositions containing the mixed oxidants.

Magnesium/aluminum alloy compositions containing PolyNIMMO as the binder

Increasing the amount of PolyNIMMO in the compositions also caused a reduction in burning rate (Figure 37 and Figure 38). Partial burns were also observed with PolyNIMMO but at slightly greater binder levels than for the compositions containing PolyGlyN. Once again, the compositions based on barium nitrate had higher burning rates than the equivalent compositions containing the mixed oxidants.

Exothermicity measurements

Exothermicity measurements have been performed on compositions to establish the available energy during combustion.

Magnesium/aluminum alloy-barium nitrate-potassium perchlorate system

A combustion reaction was achieved for all the magnesium/aluminum alloy-barium nitrate-potassium perchlorate compositions studied. The exothermicity showed a linear increase with potassium perchlorate content (Figure 39). The binary alloy-barium nitrate composition gave an exothermicity value of 5.65 kJ g^{-1} . An increase of over 50% in the exothermicity was given when the barium nitrate was completely replaced by potassium perchlorate.

Magnesium/aluminum alloy-potassium perchlorate-calcium resinate system

Exothermicity measurements were performed on a range of magnesium aluminum-barium nitrate-calcium resinate compositions where the calcium resinate content was maintained at 2% and the magnesium/aluminum alloy content was varied between 35% and 63%. The results are shown as a function of magnesium/aluminum alloy content in Figure 40. The maximum exothermicity was shown by the composition containing 45% alloy which gave a value of $8.65 \pm 0.04 \text{ kJ g}^{-1}$.

Exothermicity determinations were also carried out on a range of ternary magnesium/aluminum alloy-potassium perchlorate-calcium resinate compositions where the fuel to oxidant ratio was maintained at 1:1 and the calcium resinate content was increased from 2% to 12%. The results are shown as a function of calcium resinate content in Figure 41. A linear reduction in the exothermicity was observed when the calcium resinate content was increased. The addition of 12% resinate resulted in a decrease in the exothermicity of around 34%.

Magnesium/aluminum alloy-barium nitrate

Over the range 30% to 55% barium nitrate, the binary compositions containing magnesium/aluminum alloy as the fuel showed a linear increase in exothermicity as the barium nitrate content increased (Figure 42). Compositions containing more than 55% barium nitrate failed to ignite.

Magnesium/aluminum alloy-barium nitrate-nitrate systems

The exothermicities of compositions containing 50% magnesium/aluminum alloy-barium nitrate and either sodium, potassium or strontium nitrate were determined. A small increase in exothermicity was observed as the barium nitrate was replaced by the nitrates (Figure 43). The compositions containing either sodium or potassium nitrate ignited up to the level where 20% of the barium nitrate had been replaced. Combustion for the strontium nitrate compositions was observed across the entire range.

Magnesium/aluminum alloy-barium nitrate-sulfates

The addition of the sulfates to magnesium/aluminum alloy-barium nitrate compositions resulted in a linear decrease in exothermicity (Figure 44). Ignitions were only achieved up to the 30% sulfate level with potassium sulfate. Over the range 0% to 50% sulfate, the greatest reduction was observed with barium sulfate, strontium caused the next largest while sodium and calcium gave a similar reduction to around 5.5 kJ g^{-1} for the compositions containing 50% sulfate.

Thermal analysis studies

Thermal analysis was performed on the ingredients and the pyrotechnic compositions to investigate the role of potassium perchlorate and calcium resinate in the pyrotechnic reactions. The work was extended to examine the DSC behavior of compositions at higher heating rates which are generally termed ignition DSC experiments and at lower heating rates under non-ignition conditions.

Thermal studies on the ingredients

Magnesium/aluminum alloy

The DSC curve for the magnesium/aluminum alloy, shown in Figure 45 exhibits a sharp fusion peak with an extrapolated onset temperature of 456 °C. The melting point of the alloy is therefore considerably lower than that of either aluminum (660 °C) or magnesium (650 °C).

Simultaneous TG-Differential Thermal Analysis (DTA) measurements were carried out to study the oxidation of the magnesium/aluminum alloy in air. The experiments were performed using a Stanton Redcroft STA 1500 unit, heating 20 mg samples at 10 °C min⁻¹ in ceramic crucibles. The results of duplicate measurements are shown in Figure 46. The alloy showed a complex oxidation pattern giving a total mass gain of 75.6 ± 0.6%. The initial rapid mass gain above 500 °C was accompanied by a sharp exothermic DTA peak at 580 ± 1 °C. The sample then gained mass steadily until about 800 °C when the oxidation rate accelerated rapidly. This resulted in a sharp temperature rise giving a large DTA peak at 862 °C in one experiment and at 912 °C in the other.

Oxidants

The DSC curves for barium nitrate and potassium perchlorate and mixtures of barium nitrate and potassium perchlorate containing 10%, 30% and 50% of the perchlorate are shown in Figure 47. As it melted, barium nitrate gave a broad endotherm with an extrapolated onset temperature of 544 °C. This was followed by a larger endotherm, due to the decomposition of the nitrate, with a peak temperature of 730 °C. Potassium perchlorate showed a small endotherm at 300 °C corresponding to a rhombic-cubic transition, with fusion occurring at 599 °C. The fusion was followed immediately by the exothermic decomposition of the perchlorate.

The addition of potassium perchlorate to barium nitrate produced an endothermic peak with an extrapolated onset temperature in the region of 465 °C. This peak increased in magnitude with increasing perchlorate content and has been attributed to the formation of a eutectic between the nitrate and the perchlorate. Above 650 °C, the curve for the mixture containing 10% perchlorate showed an endothermic peak that was similar in shape to that observed for barium nitrate. As the amount of potassium perchlorate increased this peak decreased in size and the small exothermic peak following the eutectic, which corresponds to the decomposition of the potassium perchlorate, increased in size.

The TG curves for barium nitrate and potassium perchlorate are shown in Figure 48. Barium nitrate showed a single stage weight loss starting at around 510 °C corresponding to the formation of barium oxide. Potassium perchlorate which starts to decompose at around 590 °C gave an initial weight loss at around 49% at a temperature of 640 °C corresponding to

the formation of potassium chloride. This was followed by a further loss of around 30% by 830 °C attributed to the sublimation/volatilization of potassium chloride.

The TG curves for the barium nitrate-potassium perchlorate mixtures are given in Figure 49, they show that the onset of the decomposition starts the region of 510 °C. The magnitude of the initial mass loss stage was found to increase in a linear manner with potassium perchlorate content (Figure 50). Simultaneous TG-mass spectrometry studies showed that this mass loss was due solely to the evolution of oxygen (Figure 51). The loss is therefore attributed to the accelerated decomposition of potassium perchlorate in the presence of barium nitrate and gives rise to the small exothermic peak observed on the DSC curves.

DSC experiments

Magnesium/aluminum alloy-barium nitrate-potassium perchlorate compositions

DSC measurements on 20 mg samples at 50 °C min⁻¹ (Figure 52) failed to show an ignition reaction for any of the magnesium/aluminum alloy-barium nitrate-potassium perchlorate compositions.

The replacement of barium nitrate with potassium perchlorate resulted in a significant decrease in the temperature of the main exothermic reaction and for the compositions containing from 35 to 45% perchlorate, this reaction overlapped with the endotherm at around 500 °C).

The lowest DSC peak temperature of 547 °C was given by the composition containing 35% perchlorate. This represents a decrease of over 290 °C compared to the binary barium nitrate composition. The binary composition containing 50% alloy-50% potassium perchlorate gave a strongly exothermic reaction in the region of 600 °C.

Magnesium/aluminum alloy-potassium perchlorate-calcium resinate compositions

DSC studies have been carried out at 50 °C min⁻¹ on a range of compositions containing equal amounts of magnesium/aluminum alloy and potassium perchlorate and from 2% to 12% calcium resinate, the DSC curves are shown in Figure 53. The introduction of 2% calcium resinate into the system produces additional exothermic peak in the region of 565 °C.

Increasing the calcium resinate content of the ternary compositions above the 2% level gave an ignition reaction in the region of 550 °C. Thereafter, the ignition temperatures showed a small increase with increasing calcium resinate content. Ternary compositions containing 2% calcium resinate and from 35% to 63 % magnesium/aluminum alloy were also studied (Figure 54); in all cases a non-ignition reaction was given.

Non-ignition DSC studies at 10 °C min⁻¹ on a mixture of calcium resinate and potassium perchlorate showed that the additional peak observed at 550 °C during the ignition DSC experiments was due to the interaction of these two components (Figure 55). The magnesium/aluminum alloy and calcium resinate gave only a shallow exothermic reaction above 500°C, while calcium resinate itself did not show any significant thermal effects.

Further investigations were carried out on the reaction between potassium perchlorate and calcium resinate using a binary mixture containing 78.6% perchlorate which was chosen to correspond to the perchlorate:resinate ratio in the ternary composition containing 12% calcium resinate. DSC experiments were performed at both 50 C min⁻¹ and 10 °C min⁻¹ and the results are shown in Figure 56 and Figure 57 respectively. They confirmed that a strongly exothermic reaction was given between potassium perchlorate and calcium resinate and showed that, at the slower heating rate, this commenced in the region of 440 °C.

A simultaneous TG-mass spectrometry experiment was also performed on the 78.6% perchlorate mixture by heating a 20 mg sample in a ceramic crucible at $10\text{ }^{\circ}\text{C min}^{-1}$ in an argon atmosphere. The results given in Figure 58 show that the main product of the reaction between potassium perchlorate and calcium resinate is carbon dioxide (44). Rapid evolution of oxygen (32), associated with decomposition of the perchlorate, was given in the region of $550\text{ }^{\circ}\text{C}$ and this was accompanied by the evolution of both carbon monoxide (28) and carbon dioxide. A small amount of water (18) was also observed.

On completion of the experiment the inside and outside of the crucible were covered with a black coating which was also present on the balance beam and the furnace work tube. This probably accounts for the slow evolution of carbon monoxide at higher temperatures due to oxidation of the deposited carbon by oxygen impurities in the argon gas stream.

Duplicate infrared heating-mass spectrometry experiments were performed on the 78.6% potassium perchlorate-21.4% calcium resinate mixture. The results, which are given in Figure 59, indicate that carbon dioxide was the main product given under these fast heating conditions and that the amount of oxygen evolved was reduced.

Magnesium/aluminum alloy-barium nitrate compositions

DSC experiments were performed on a range of magnesium/aluminum alloy-barium nitrate compositions under ignition conditions (Figure 60). The small exotherm which followed the melt of the magnesium/aluminum alloy generally increased in size as the amount of alloy increased but some variability in the results was observed. Increasing the amount of alloy present caused a reduction in the temperature of the exotherm observed in the $770\text{ }^{\circ}\text{C}$ (70% alloy) to $849\text{ }^{\circ}\text{C}$ (30% alloy) range but in no case did an ignition reaction take place.

Magnesium/aluminum alloy-barium nitrate-potassium nitrate composition

The addition of potassium nitrate to the magnesium/aluminum alloy-barium nitrate composition initially caused the exotherm following the fusion of the alloy to increase in size (Figure 61); the greatest increase was observed at the 30% potassium nitrate level. Very little exothermic activity below $800\text{ }^{\circ}\text{C}$ was observed for the binary magnesium/aluminum alloy-potassium nitrate composition.

The high temperature exothermic activity observed for all of the compositions was complex and the peak positions varied widely.

Magnesium/aluminum alloy-barium nitrate-sodium nitrate compositions

A similar result was obtained with sodium nitrate as that observed for potassium nitrate, except that the exothermic activity following the fusion of the alloy was also observed for the binary alloy-sodium nitrate composition (Figure 62).

Magnesium/aluminum alloy-barium nitrate-strontium nitrate compositions

Figure 63 shows the ignition DSC curves for the compositions containing strontium nitrate. The exotherm following the fusion of the alloy increased in size in when strontium nitrate was present. The high temperature exotherms were once again complex in nature.

Binary magnesium/aluminum alloy-nitrate compositions

The ignition DSC curves for the binary magnesium/aluminum alloy-nitrate compositions are compared in Figure 64. Only the compositions containing sodium and potassium nitrate showed high temperature exothermic reactivity. With sodium nitrate the exothermic activity was sufficiently high that the sample began to self heat; as a result, a 'looped' exotherm was observed.

Binary magnesium/aluminum alloy-sulfate compositions

The DSC curves for the binary compositions containing the magnesium/aluminum alloy with the sulfates are shown in Figure 65. All the compositions gave an ignition reaction apart from that containing potassium sulfate.

The highest reactivity towards the alloy was shown by sodium sulfate and that for the alkaline earth sulfates the reactivity decreased with increasing cation size. In the case of the alkaline earth sulfates around 60% of the sample mass was lost on ignition. This probably accounts for the smaller peaks shown by these compositions compared with those given by the composition containing sodium sulfate which only lost about 20% mass on ignition.

Magnesium/aluminum alloy-35% barium nitrate-15% sulfate systems

The DSC curves for the ternary compositions containing 50% magnesium/aluminum alloy-35% barium nitrate and either barium, calcium, potassium, sodium or strontium sulfate are shown in Figure 66.

Although the addition of a sulfate to the binary magnesium/aluminum alloy-barium nitrate composition did not result in ignition, the magnitude of the DSC exotherms was markedly increased in the presence of sodium, strontium and barium sulfates. That this increase was not so marked in the case of calcium sulfate is surprising in view of its reactivity with the alloy.

DSC on 50% magnesium/aluminum alloy-50% potassium perchlorate at different heating rates

DSC experiments were initially performed on 50% magnesium/aluminum alloy-50% potassium perchlorate composition in quartz crucibles at a heating rate of $10\text{ }^{\circ}\text{C min}^{-1}$ in an argon atmosphere. The results showed that the onset temperature of the main exothermic peak had reduced by over $90\text{ }^{\circ}\text{C}$, compared with the experiments carried out previously at $50\text{ }^{\circ}\text{C min}^{-1}$.

In view of this unexpectedly large decrease in the reaction temperature at the slower heating rate, a series of experiments were carried out to determine the influence of heating rate on the exothermic reaction between the alloy and potassium perchlorate. Single measurements were performed at heating rates from $2\text{ }^{\circ}\text{C min}^{-1}$ to $50\text{ }^{\circ}\text{C min}^{-1}$ and the results were adjusted for the effect of heating rate by applying corrections obtained from a series of DSC experiments on the fusion of aluminum at the same range of heating rates.

The DSC curves for the complete range of heating rates are shown in Figure 67, the corrected extrapolated onset (T_e) and peak temperatures (T_p) for the fusion of the alloy and for the main exothermic reaction are listed in Table 17.

Heating rate (°C min ⁻¹)	Magnesium/aluminum alloy fusion		Exothermic reaction	
	T _e (°C)	T _p (°C)	T _e (°C)	T _p (°C)
2	457.8	460.8	464.3	471.9
5	457.7	461.8	476.1	494.5
10	460.0	464.9	496.7	523.1
20	456.4	464.4	517.8	554.6
30	456.4	469.3	528.6	564.0
40	455.2	472.2	542.7	582.0
50	458.2	477.4	554.8	595.2

*Table 17; DSC temperatures for a 50% magnesium/aluminum alloy-50% potassium perchlorate composition at different heating rates.
(Sample mass, 20 mg; atmosphere, argon)*

The extrapolated onset temperatures for the exothermic reaction and the fusion of the alloy are plotted as a function of heating rate in Figure 68. The results demonstrate clearly that the onset temperature of the reaction between the alloy and potassium perchlorate is markedly affected by the heating rate and reduces from 555 °C to 462 °C on decreasing the heating rate from 50 °C min⁻¹ to 2 °C min⁻¹. At the slowest heating rate the exothermic reaction overlapped with the fusion peak of the alloy.

DSC on 49% magnesium/aluminum alloy-49% potassium perchlorate-2% calcium resinate at different heating rates

DSC studies were also carried out on the 49% magnesium/aluminum alloy-49% potassium perchlorate-2% calcium resinate composition at the same range of heating rates. The DSC curves for the complete range of heating rates are shown in Figure 69. The corrected extrapolated onset temperature for the fusion of the alloy and extrapolated onset and peak temperatures for the two exothermic peaks are listed in Table 18.

The extrapolated onset temperatures for the fusion of the alloy and the two exothermic reactions are plotted as a function of heating rate in Figure 70 and show that the temperatures for the first peak decreased in an approximately linear manner. The values obtained for the second peak decreased more rapidly at the lower heating rates and at 2 °C min⁻¹ the two peaks had merged.

A comparison of the DSC curves obtained at 2 °C min⁻¹ for the binary and ternary compositions show that the exothermic reaction for the ternary composition starts below the fusion of alloy. This appeared to delay the onset of the main exothermic reaction and this took place at a higher temperature than the exothermic reaction in the binary composition which was triggered by the fusion of the alloy.

Heating rate (°C min ⁻¹)	Magnesium/ aluminum alloy fusion T _e (°C)	First exothermic peak		Second exothermic peak	
		T _e (°C)	T _p (°C)	T _e (°C)	T _p (°C)
2	457.7	487.6	500.2	-	505.0
5	457.7	494.8	505.8	513.3	537.3
10	457.6	490.9	505.4	522.0	554.8
20	456.4	508.5	523.7	541.9	584.1
30	456.4	519.3	535.8	559.4	608.5
40	455.2	530.2	546.8	559.8	603.3
50	458.2	538.6	559.1	565.5	627.9

Table 18; DSC Temperatures for a 49% magnesium/aluminum alloy-49% potassium perchlorate-2% calcium resinate composition at different heating rates. (Sample mass, 20 mg; atmosphere, argon).

Non-ignition DSC

Binary magnesium/aluminum alloy-sulfate compositions

Experiments were also carried out at a reduced heating rate of 10 °C min⁻¹ on the binary compositions containing sodium, strontium and barium sulfates and the DSC plots are given in Figure 71. The binary sodium sulfate composition still ignited under these conditions giving a mean ignition temperature of 540 ± 4 °C. For the strontium and barium sulfate compositions a non-ignition reaction was given which in both cases started in the region of 550 °C.

Magnesium/aluminum alloy-35% barium nitrate-15% sulfate systems

DSC measurements were also made at a heating rate of 10 °C min⁻¹ on the ternary compositions containing 15% sodium, strontium or barium sulfate, the DSC curves are given in Figure 72. Surprisingly both experiments on the composition containing sodium sulfate resulted in ignition giving a mean ignition temperature of 517 ± 14 °C. The strontium and barium sulfate compositions both showed strongly exothermic reactions immediately following the fusion of the alloy.

Time to ignition studies

Magnesium/aluminum alloy-barium nitrate-potassium perchlorate compositions

Time to ignition studies, were carried out in triplicate on magnesium aluminum-barium nitrate compositions containing from 0-15% potassium perchlorate. The composition containing 15% perchlorate gave a vigorous ignition reaction with a mean time to ignition of 39.8 ± 0.4 s. This time corresponded to an ignition temperature of approximately 665°C. In addition, a photocell deflection was also observed in the region of 35 s. However, this deflection was not accompanied by a peak on the heating rate curve which is normally given by an ignition reaction.

The compositions containing 5% and 10% perchlorate did not appear to ignite although they also showed a photocell deflection in the region of 35 s. However, this again was not accompanied by a peak on the heating rate curve and the mass losses were much lower than those observed for the 15% perchlorate composition.

In view of the vigorous nature of the ignition reaction for the 15% perchlorate composition, the compositions containing more than 15% perchlorate were studied at a reduced sample mass of 20 mg. Under these conditions only the binary magnesium aluminum-potassium perchlorate composition ignited. This gave a mean time to ignition of 38.0 ± 0.1 s. Experiments were also carried out on the composition containing 40% perchlorate where the sample mass was increased in 10 mg stages to 50 mg. However, in no case was an ignition reaction given.

Magnesium/aluminum alloy-potassium perchlorate-calcium resinate compositions

The results of the time to ignition experiments on the magnesium/aluminum alloy-potassium perchlorate compositions containing from 2-12% calcium resinate are shown in Table 19 together with the values obtained for the 50% magnesium/aluminum alloy-50% potassium perchlorate composition.

Composition			Time to ignition (s)
Magnesium/ aluminum alloy (%)	Potassium perchlorate (%)	Calcium resinate (%)	
50	50	-	35.7 ± 0.2
49	49	2	$31.2 \pm 1.1^*$
48	48	4	32.0 ± 0.3
47	47	6	30.1 ± 0.2
46	46	8	30.7 ± 0.7
45	45	10	28.7 ± 0.0
44	44	12	28.9 ± 0.4

*plus 1 non-ignition

Table 19; Time to ignition experiments on the range of magnesium/aluminum alloy-potassium perchlorate-calcium resinate compositions.

(Sample mass, 20 mg; temperature, 900 °C; atmosphere, argon)

The faster heating rates obtained in the time to ignition experiments have resulted in ignition taking place for both the binary composition and the composition containing 2% calcium resinate, whereas a non-ignition reaction was given by these compositions in the DSC experiments. The addition of 2% calcium resinate to the binary composition resulted in a decrease of over 4 s in the time to ignition. The times to ignition are plotted in Figure 73 and it can be seen that there was a small linear decrease in the time to ignition as the resinate content was increased.

The time to ignition results obtained for the ternary compositions containing 2% calcium resinate are summarized in Table 20. For the compositions containing from 35-45% magnesium/aluminum alloy, ignition was only achieved in one experiment on the 40% magnesium/aluminum alloy composition. The compositions containing higher amounts of the

alloy ignited in the region of 31 s, with the exception of the 53% magnesium/aluminum alloy composition which gave a slightly shorter time to ignition.

Composition			Time to ignition (s)
Magnesium/ aluminum alloy (%)	Potassium perchlorate (%)	Calcium resinate (%)	
35	63	2	DNI
40	58	2	30.8 a
45	53	2	DNI
49	49	2	31.2 ± 1.1 b
53	45	2	29.6 ± 0.3
58	40	2	31.7 ± 0.5 c
63	35	2	31.2 ± 0.1

(a) 1 ignition in 3 experiments (30.8 s); (b) 1 non-ignition; (c) mean of 3 results

Table 20; Time to ignition experiments on the range of magnesium/aluminum alloy-potassium perchlorate-calcium resinate system.

(Sample mass, 20 mg; temperature, 900 °C; atmosphere, argon.

Magnesium/aluminum alloy-metal sulfates

Single time to ignition measurements on the compositions containing 50% magnesium/aluminum alloy and either sodium, potassium, strontium and barium sulfates showed that the most reactive composition was that containing sodium sulfate which gave a time of 33.9 s compared with values of 38.9 s and 41.8 s for the strontium and barium sulfate compositions, respectively. The composition containing potassium sulfate did not ignite.

Magnesium/aluminum alloy-barium nitrate-metal sulfates

Time to ignition experiments showed that although a strongly exothermic reaction was given, the faster heating rates achieved using this technique did not result in ignition (the calcium sulfate composition was not studied).

Magnesium/aluminum alloy-barium nitrate compositions containing metal nitrates

Single time to ignition experiments gave an ignition reaction for all the compositions containing sodium nitrate and the times are shown in Table 21. The shortest ignition time of 71 s was given by the binary sodium nitrate composition which corresponded to an ignition temperature of 876 °C.

Sodium nitrate (%)	Time to ignition (s)
0	Did not ignite
5	74.9
10	77.4
15	79.3
20	83.5
30	78.8
40	76.2
50	71.1

Table 21; Times to Ignition for magnesium aluminum-barium nitrate-sodium nitrate composition.

(Sample mass, 20 mg; temperature, 900 °C; atmosphere, argon)

Ignitions were observed for all of the ternary compositions containing potassium nitrate during single time to ignition experiments. The times to ignition, which are listed in Table 22, increased as the potassium nitrate content was raised from 5% to 30%. For the compositions containing 20 to 40% potassium nitrate ignition took place after the sample had self heated above the 900 °C set temperature. This is a reflection of the high ignition temperatures observed in the DSC experiments.

Single time to ignition experiments were also performed on the complete range of compositions containing strontium nitrate, even at this relatively faster heating rate ignitions did not occur.

Potassium nitrate (%)	Time to ignition (s)
0	Did not ignite
5	70.2
10	76.4
15	83.6
20	99.8
30	124.7
40	96.2
50	Did not ignite

Table 22; Times to Ignition for magnesium/aluminum alloy-barium nitrate-potassium nitrate compositions.

(Sample mass, 20 mg; temperature, 900 °C; atmosphere, argon)

Magnesium based compositions

Combustion studies

Pyrotechnic studies were performed initially on compositions containing magnesium, barium nitrate and potassium perchlorate to establish the performance of this pyrotechnic system. The work was then extended to study the effect of replacing the potassium perchlorate with a second nitrate or a sulfate.

Magnesium-barium nitrate-potassium perchlorate system

The compositions containing magnesium-barium nitrate-potassium perchlorate showed a reduction in burning rate as the perchlorate content increased Figure 74. The compositions had higher burning rates than the equivalent compositions containing the magnesium/aluminum alloy.

Magnesium-barium nitrate

Over the range 30% to 70% nitrate, the burning rate of binary magnesium-barium nitrate compositions showed an almost linear decrease from 15 mm s^{-1} to 4 mm s^{-1} (Figure 75).

Magnesium-barium nitrate-nitrates systems

The burning rate curves for the magnesium-barium nitrate-nitrate compositions are shown in Figure 76. The composition containing strontium nitrate showed an almost linear decrease with increasing strontium nitrate content. The ternary compositions containing potassium and sodium nitrate gave a complex burning rate curve which initially showed a decrease and then an increase in burning rate. All of the compositions had burning rates above those of the 50% magnesium/aluminum alloy-40% barium nitrate-10% potassium perchlorate composition.

Magnesium-barium nitrate-sulfate systems

Figure 77 shows the burning rate curves for the magnesium-barium nitrate-sulfate compositions; in general only a small range of burning rates was observed and they were above those of the 50% magnesium/aluminum alloy-40% barium nitrate-10% potassium perchlorate composition. The compositions containing potassium sulfate showed a decrease in burning rate with increasing sulfate content. Those containing barium, sodium and strontium initially showed an increase in burning rate followed by a decrease. For calcium sulfate the burning rate increased as the sulfate content increased.

Exothermicity measurements

Magnesium-barium nitrate-potassium perchlorate

As the potassium perchlorate content was increased from 0% to 50%, the exothermicity of magnesium-potassium perchlorate-barium nitrate compositions (Figure 78) showed a linear increase from 6 kJ g^{-1} to around 9 kJ g^{-1} .

Magnesium-barium nitrate-nitrate

The exothermicity curves for ternary compositions containing magnesium, barium nitrate and either potassium, sodium or strontium nitrate are shown in Figure 79. For all three systems, increasing the amount of second nitrate present resulted in an increase in the exothermicity. The largest increases were observed for the addition of sodium nitrate.

Magnesium-barium nitrate-sulfate

The exothermicity curves for ternary compositions containing magnesium, barium nitrate and either barium, calcium, sodium or strontium sulfate are shown in Figure 80. For all four systems, increasing the amount of sulfate present resulted in a decrease in the exothermicity. The decreases observed for calcium and sodium were very similar; the largest decreases were observed for the addition of barium sulfate.

Ignition DSC

Magnesium-barium nitrate-potassium perchlorate

DSC studies under ignition conditions were carried out in duplicate on a range of magnesium-barium nitrate-potassium perchlorate compositions containing 50% magnesium and from 0 to 50% perchlorate.

An ignition reaction was observed for all of the compositions containing potassium perchlorate with the exception of the 40% perchlorate composition, the DSC curves are plotted in Figure 81. The majority of the compositions ignited within a narrow temperature range and did not show any trend with increasing perchlorate content.

The ignition DSC curve for magnesium-barium nitrate showed an exotherm, peaking at around 630 °C, with a shoulder on the lower temperature side.

Magnesium-barium nitrate-potassium nitrate

The results of single DSC measurements on the ternary compositions containing potassium nitrate are plotted in Figure 82. An ignition reaction was observed for the compositions containing more than 5% potassium nitrate.

Magnesium-barium nitrate-sodium nitrate

DSC studies under ignition conditions were carried out in duplicate on a range of magnesium-barium nitrate-sodium nitrate compositions containing 50% magnesium and from 0 to 50% sodium nitrate.

An ignition reaction was observed for all of the compositions containing sodium nitrate, the DSC curves are plotted in Figure 83. The ignition temperatures increased with increasing sodium nitrate content up to the 15% level and then decreased as more sodium nitrate was added.

Although the 50% magnesium-50% sodium nitrate composition showed a lower ignition temperature than the binary potassium nitrate composition, the presence of sodium nitrate in the ternary composition resulted in higher ignition temperatures compared with the ternary compositions containing potassium nitrate.

Magnesium-sulfate compositions

Figure 84 shows the DSC curves for each of the binary 50% magnesium-50% sulfate compositions and for comparison purposes the curve for 50% magnesium-50% barium nitrate. All the compositions gave an ignition reaction apart from that containing potassium sulfate.

The most reactive composition was that containing calcium sulfate which gave a mean ignition temperature of 566°C. The ignition temperatures increased with increasing cation size and barium sulfate composition gave a value over 110°C higher than that containing the calcium salt.

Magnesium-barium nitrate-15% sulfate compositions

Ternary compositions containing 15% of the sulfates were also examined and the ignition DSC, curves are shown in Figure 85. All the compositions, apart from that containing potassium sulfate ignited.

The addition of sodium sulfate to the binary magnesium-barium nitrate composition had the greatest effect and lowered the ignition temperature by some 50°C. The addition of calcium and strontium sulfates resulted in only a small reduction in the ignition temperature while the addition of barium sulfate did not have a significant effect.

Non-ignition DSC

Magnesium-sulfate compositions

The high reactivity of magnesium with sodium, calcium and barium sulfates was confirmed by DSC studies at a reduced heating rate of 10 °C min⁻¹. All three compositions ignited and in the case of calcium sulfate it was so violent that it destroyed the DSC head. The composition containing strontium sulfate gave a broad exothermic reaction extending from 550 °C to 760 °C. The endothermic fusion peak for the unreacted magnesium was superimposed upon this exotherm.

Magnesium-barium nitrate-15% sulfate compositions

Duplicate DSC studies performed at 10 °C min⁻¹ on the ternary compositions containing sodium, strontium and barium sulfates gave a non-ignition reaction for the sodium, and strontium sulfate compositions. In one of the experiments on the barium sulfate composition an ignition reaction was given at 609 °C. The curves which are shown in Figure 86 confirm that the composition containing sodium sulfate reacts at the lowest temperature.

Time to ignition

Magnesium-barium nitrate-potassium perchlorate

Single time to ignition measurements gave a mean time to ignition of 31.7 ± 0.9 s for the ternary compositions containing from 5% to 45% potassium perchlorate.

Magnesium-barium nitrate-potassium nitrate

The results of time to ignition measurements on the ternary mixtures containing potassium nitrate are given in Table 23. Over the range 0-50% potassium nitrate only a small change in the time to ignition was observed.

Potassium nitrate (%)	Time to ignition (s)
0	31.2
5	31.5 ± 0.5
10	30.1 ± 0.2
15	30.3 ± 0.3
20	30.1 ± 0.2
30	31.2 ± 0.2
40	32.5 ± 0.5
50	32.6 ± 0.3

Table 23; Times to ignition for magnesium-barium nitrate-potassium nitrate compositions. (Sample mass, 20 mg, temperature, 900 °C, atmosphere, argon)

Magnesium-barium nitrate-sodium nitrate

Time to ignition measurements on the ternary magnesium-barium nitrate-sodium nitrate compositions (Table 24) gave a mean value of 30.7 ± 0.7 s for compositions containing from 5% to 40% sodium nitrate. The times were similar to those observed for similar compositions containing potassium nitrate, and the mean values were also similar to the mean value for the ternary magnesium-barium nitrate-perchlorate compositions.

Sodium nitrate (%)	Time to ignition (s)
0	31.2
5	30.6
10	29.9
15	30.1
20	30.8
30	30.7
40	31.9
50	31.7

Table 24; Times to ignition for magnesium-barium nitrate-sodium nitrate compositions. (Sample mass, 20 mg; temperature, 900 °C; atmosphere, argon)

Magnesium-barium nitrate-strontium nitrate

Duplicate time to ignition measurements were also performed on the ternary compositions containing strontium nitrate. All the ternary compositions ignited and the times are shown in Table 25.

Significantly longer times to ignition were given by the ternary compositions containing strontium nitrate compared with those containing sodium and potassium nitrates. In one experiment on each of the compositions containing from 5-15% strontium nitrate a second ignition reaction appeared to be given in the region of 42-43 s.

Strontium nitrate (%)	Time to ignition (s)
0	31.2
5	34.7 ± 1.1
10	33.3 ± 0.0
15	34.1 ± 0.3
20	33.3 ± 0.0
30	32.3 ± 0.5
40	32.9 ± 0.3
50	32.8 ± 0.3

Table 25; Times to ignition for magnesium-barium nitrate-strontium nitrate compositions. (Sample mass, 20 mg; temperature, 900 °C; atmosphere, argon)

Aluminum based compositions

Combustion studies

Aluminum-barium nitrate-potassium perchlorate system

The burning rate curve as a function of potassium perchlorate content for the range of binary and ternary compositions containing 50% aluminum, barium nitrate and potassium perchlorate is shown in Figure 87. The binary composition containing barium nitrate had the highest burning rate. The addition of potassium perchlorate caused a reduction in the burning rate up to the 35% level to around 5 mm s⁻¹, thereafter the burning rate increased. The binary composition containing 50% aluminum-50% potassium perchlorate had a burning rate of around 7.5 mm s⁻¹.

Aluminum-barium nitrate

Burning rates of the binary aluminum-barium nitrate compositions are shown in Figure 88. Compositions containing 30 to 40% barium nitrate failed to ignite; the maximum burning rate, of 10 mm s⁻¹, was observed at the 55% barium nitrate level.

Aluminum-barium nitrate-nitrate systems

Only two of these systems (potassium and strontium nitrates) sustained combustion across the entire range of compositions (Figure 89). The compositions containing potassium and sodium nitrates showed an initial decrease in burning rate as the amount of barium nitrate present reduced. The minimum burning rate was observed at around the 15-20% barium nitrate content where burning rates of around 1 mm s⁻¹ and 3 mm s⁻¹ were observed for potassium and sodium nitrate respectively. The binary aluminum-potassium nitrate compositions had a

burning rate of 2 mm s^{-1} . The compositions containing strontium nitrate had similar burning rates to the binary aluminum-barium nitrate composition.

Magnesium/aluminum alloy-barium nitrate-sulfate systems

Except for potassium and sodium sulfate, the ternary compositions containing aluminum, barium nitrate and a sulfate burned across the entire range (Figure 90). Ternary composition containing up to 20% potassium or 30% sodium sulfate sustained combustion. The burning rates at these points were 5 mm s^{-1} and 7.5 mm s^{-1} for potassium and sodium sulfate compositions respectively.

The addition of barium sulfate to aluminum-barium nitrate caused an almost linear decrease in burning rate; for the binary aluminum-sulfate composition it was around 6 mm s^{-1} . Strontium sulfate initially caused a reduction in the burning rate and further additions gave an increase, which for the binary aluminum-sulfate composition, was just greater than that of aluminum-barium nitrate.

An increase in burning rate was observed as the calcium sulfate content of the ternary compositions increased; the maximum burning rate observed for the binary aluminum-calcium sulfate mix was around 15 mm s^{-1} .

Exothermicity measurements

Aluminum-barium nitrate

Over the range 30-55% barium nitrate binary compositions exhibited a linear increase in exothermicity as the barium nitrate content increased (Figure 91). In comparison with the burning rate determinations, the compositions containing lower quantities of barium nitrate ignited in the bomb calorimeter but those containing 60% and 70% barium nitrate failed to ignite. This difference may reflect the difference in igniting a loose powder compared to a pressed column of material and/or the two different ignition techniques used in each test.

Aluminum-barium nitrate-nitrate systems

Ternary 50% aluminum-35% barium nitrate-15% nitrate compositions where the second oxidant was either potassium, sodium or strontium nitrate were prepared and examined. A combustion reaction was only achieved for the composition containing sodium nitrate which gave an exothermicity of $6.41 \pm 0.2 \text{ kJ g}^{-1}$. This equates to an approximately 15% increase over that expected for the composition containing 50% aluminum-50% barium nitrate.

DSC studies under ignition conditions

Aluminum-barium nitrate

The DSC curves for a range of binary aluminum-barium nitrate compositions are shown in Figure 92. At the high heating rates used during these experiments the temperature recorded for the fusion of the nitrates and aluminum is some 20°C higher than the literature values.

The binary compositions show the barium nitrate fusion endotherm which peaks at 610°C . This was followed by strong exothermic activity which is quenched by the melting of the aluminum. The aluminum fusion endotherm which has a peak temperature of around 680°C is followed by further exothermic activity which increases in magnitude as the barium nitrate content of the compositions increases. Except for the composition containing 70% barium nitrate a shoulder was apparent on the low temperature side of the exotherm. The peak temperature of the exotherm was significantly greater for the composition containing 70%

barium nitrate. The compositions containing 30% to 55% aluminum produced a third exotherm with a peak temperature of around 800 °C.

Aluminum-barium nitrate-potassium nitrate

The DSC curves for the aluminum-barium nitrate-potassium nitrate compositions are shown in Figure 93. The 50% aluminum-50% potassium nitrate composition has an endotherm at around 350 °C corresponding to the fusion of the oxidant. Exothermic activity is apparent just before the aluminum fusion endotherm. The addition of potassium nitrate reduces the size of the endotherm associated with fusion of barium nitrate. The ternary compositions containing 5% and 15% potassium nitrate gave stronger exothermic reactions at 730°C, compared to similar binary aluminum-barium nitrate compositions.

Aluminum-barium nitrate-sodium nitrate

Figure 94 shows the DSC curves for the compositions containing aluminum, barium nitrate and sodium nitrate. In addition to the fusion of the nitrate (335 °C) and the aluminum (680 °C) the DSC curve of the binary 50% aluminum-50% sodium nitrate composition showed a broad endotherm before a strongly exothermic reaction which peaked at around 885 °C. The ternary composition containing 15% sodium nitrate also increased the size of the exotherm associated with the presence of barium nitrate.

Aluminum-barium nitrate-strontium nitrate

The DSC curves for the aluminum-barium nitrate-strontium nitrate compositions are shown in Figure 95. For the 50% aluminum-50% strontium nitrate mix a complex pattern showing both endo and exothermic activity was observed. The fusion of the nitrate (640 °C) appears to be followed by a reaction which is exothermic in nature; the fusion of the aluminum is superimposed on this peak.

A complex pattern of endotherms and exotherms was similarly observed for ternary compositions containing 5% or 15% strontium nitrate. The addition of strontium nitrate reduced the exothermic activity, at 730 °C, associated with the barium nitrate.

The results suggest that the reactivity of aluminum-nitrate compositions is influenced by the strong endothermic nature of the aluminum fusion. The addition of potassium, sodium or strontium did not reduce the temperature of the exotherm associated with a reaction between aluminum and barium nitrate mixtures but the addition of potassium and sodium nitrate at relatively low levels increased the size of the exotherm.

Gun firing trials

The aims of first gun firing trial were to establish that the ammunition maintained stability over the short range selected, that the interaction between the bullet and the target material was small and that initiation of the control composition containing magnesium/aluminum alloy, barium nitrate and potassium perchlorate was attained; the results are presented in Table 26.

The tests using bullets filled with an inert wax against a steel target showed a significant reaction (Figure 96), this was reduced by changing to a target made from an aluminum alloy (Figure 97). Figure 98 shows that on impact with the target the control composition containing 50% magnesium/aluminum alloy, 40% barium nitrate and 10% potassium perchlorate produced a bright flash with a duration of around 10 ms. A comparison of the video stills (Figure 98 and Figure 99) shows that the use of pellets increased the size of the fireball. Analysis of the results also showed a slightly increased in the flash duration.

The results obtained for ternary compositions containing 50% magnesium/aluminum alloy, 35% barium nitrate and 15% potassium nitrate or sodium (Figure 100 and Figure 101) are similar to those of the control composition. For the compositions containing 50% magnesium/aluminum alloy, 35% barium nitrate and 15% strontium nitrate the duration was similar but the fireball produced was smaller (Figure 102). To allow a comparison of composition performance, a single frame for each firing showing the largest output is reproduced in Figure 103. The results show that even for identical fillings there was some variability in the results, and of the composition tested those containing 15% strontium nitrate or 10% sodium nitrate gave a slightly lower output.

Bullet no.	Form	Mass (g)	Composition	Flash duration (ms)
1	Powder	0.71	50% Mg/Al alloy 40% Barium nitrate 10% Potassium perchlorate	9.5
2		0.74		10.5
3		0.72		10.3
4	Pellets	1.15		11.0
5		1.17		10.3
6		1.17		11.6
7	-	-	Wax	5.5 steel target
8				1.3
9				3.9
10	Powder	0.62	50% Mg/Al alloy 35% Barium nitrate 15% Strontium nitrate	10.0
11	Powder	0.74	50% Mg/Al alloy 40% barium nitrate 10% Sodium nitrate	11.0
12	Powder	0.56	50% Mg/Al alloy 17.5% Barium nitrate 17.5% Potassium nitrate	9.7
13	-	-	Plasticine	-
14				-
15				-

Table 26; Trial 1, Aluminum alloy target placed 10 m from muzzle.

The second trial allowed the control composition containing 49% magnesium/aluminum alloy-49% potassium perchlorate-2% calcium resinate to be studied along with a large number of the new formulations; the results are presented in Table 27. For each round, the camera frame which captured the largest output is shown in Figure 104 for the controls composition and Figure 105 for the new formulations. Once again some variability is apparent in the output from the control compositions and the increase in mass for pelleted formulations generally gave a larger output. The results also show the relatively poor output from the binary metal-sulfate mixes and the majority of the formulations containing barium nitrate and the metal sulfates. For this firing, the result for magnesium/aluminum alloy-barium nitrate-strontium nitrate was amongst the highest.

Two formulations which gave particularly high outputs but did not contain barium nitrate were the binary formulations containing sodium and potassium nitrate.

Bullet no.	Form	Mass (g)	Composition	Flash duration (ms)
16	Powder	0.85	50% Mg/Al alloy 35% Barium nitrate 15% Potassium sulfate	8.7
17	Powder	0.68	49% Mg/Al alloy 49% Potassium perchlorate 2% Calcium resinate	14.2
18		0.70		17.1
19	Pellets	1.17		16.3
20		1.05		18.9
21	Powder	1.19	50% Mg/Al alloy 35% Barium nitrate 15% Strontium nitrate	16.6
22	Powder	0.79	50% Mg/Al alloy 50% Sodium nitrate	15.5
23	Pellets	1.05		20.0
24	Powder	0.55	50% Mg/Al alloy 50% Potassium nitrate	11.1
25	Pellets	1.10		11.8
26	Powder	0.72	50% Mg/Al alloy 50% Barium nitrate 15% Strontium sulfate	10.5
27	Powder	0.78	50% Mg/Al alloy 50% Potassium sulfate	9.7
28	Powder	0.68	50% Mg/Al alloy 50% Sodium sulfate	21.8
29	Powder	0.64	50% Mg/Al alloy 50% Strontium sulfate	4.7
30	Powder	0.59	50% Mg/Al alloy 35% Barium nitrate 15% Potassium nitrate	15.0
31	Pellets	1.05		21.6
32		1.20		15.5
33	Powder	0.49	50% Magnesium 50% Sodium nitrate	13.4
34	Powder	0.62	49% Mg/Al alloy 49% Barium nitrate	11.8
35	Pellets	1.30	2% PolyNIMMO	15.3
36	Powder	0.47	46% Mg/Al alloy 46% Barium nitrate	11.6
37	Pellets	1.38	8% PolyNIMMO	14.5
38	Powder	0.41	45% Mg/Al alloy 45% Barium nitrate	9.2
39	Pellets	1.40	10% PolyGlyN	16.6

Table 27; Trial 2, Aluminum alloy target placed 6 m from muzzle.

The results from the third gun firing trial are detailed in Table 28 and illustrated in Figure 106, where the phantom camera was set with a narrow field of view, and Figure 107. This trial highlighted the low output from the sulfate based formulations and those containing thermite type materials including the one containing nano aluminum-boron. A number of the new formulations including several magnesium/aluminum alloy-sodium nitrate-binder combinations, magnesium-sodium nitrate and aluminum sodium nitrate produced results which were similar to the control compositions (bullets 67-69)

Bullet no.	Form	Mass (g)	Composition	Flash duration (ms)
40	-	-	Wax	-
41	-	-		1.3
42	Powder	0.79	50% Mg/Al alloy 50% Barium nitrate	13.4
43		0.71		13.2
44	Powder	0.64	50% Mg/Al alloy 50% Strontium nitrate	9.7
45		0.56		11.3
46	Powder	0.61	50% Mg/Al alloy 50% Calcium sulfate	5.5
47	Powder	0.74	50% Mg/Al alloy 35% Barium nitrate 15% Calcium sulfate	10.8
48	Powder	0.71	50% Mg/Al alloy 35% Barium nitrate 15% Sodium sulfate	12.6
49	Powder	0.69	50% Mg/Al alloy 35% Barium nitrate 15% Potassium sulfate	12.1
50	Powder	0.48	50% Magnesium 50% Sodium nitrate	15.5
51	Powder	0.49		15.0
52	Powder	0.45	50% Magnesium 50% Strontium nitrate	9.7
53	Powder	0.40	50% Magnesium 50% Strontium sulfate	4.7
54	Powder	0.53	50% Magnesium 50% Potassium sulfate	6.8
55	Powder	0.41	50% Magnesium 50% Calcium sulfate	5.8
56	Powder	0.62	50% Aluminum 50% Sodium nitrate	12.4
57	Powder	0.78	50% Aluminum 50% Strontium nitrate	7.6

58	Powder	0.51	50% Aluminum 50% Sodium sulfate	5.0
59	Powder	0.59	50% Aluminum 50% Barium sulfate	5.0
60	Powder	0.48	50% Aluminum 50% Strontium sulfate	8.2
61	Powder	0.74	50% Mg/Al alloy 35% Strontium nitrate 15% Sodium nitrate	13.9
62	Powder	0.59	50% Mg/Al alloy 35% Strontium nitrate 15% Potassium nitrate	10.8
63	Powder	0.57	49% Mg/Al alloy 49% Sodium nitrate 2% PolyGlyN	15.3
64	Powder	0.54		15.0
65	Powder	0.54	49% Mg/Al alloy 49% Strontium nitrate 2% PolyNIMMO	13.9
66	Powder	0.53		13.9
67	Powder	0.78	50% Mg/Al alloy 40% Barium nitrate 10% Potassium perchlorate	11.6
68	Powder	0.78		11.8
69	Powder	0.69	49% Mg/Al alloy 49% Potassium perchlorate 2% Calcium resinate	13.7
70	Powder	1.66	19% Aluminum 81% Tungsten oxide	11.0
71	Powder	0.48	27% Mg/Al alloy 73% Ferric oxide (Fe ₂ O ₃)	10.0
72	Powder	0.47	27% Aluminum 73% Ferric oxide (Fe ₂ O ₃)	8.4
73	Powder	0.28	27% Al-B nano 43% Ferric oxide (Fe ₂ O ₃)	1.8

Table 28; Trial 3, Aluminum alloy target placed 6 m from muzzle.

A fourth gun firing trial examined a range of formulations based on magnesium/aluminum alloy-potassium or sodium nitrate and a binder. These oxidants are amongst the most benign available and when similar formulations were gun fired they demonstrated a high light output. The binders examined were calcium resinate, boiled linseed oil, lithographic varnish, PVC and GAP. The duration of the flash recorded for each formulation were very similar (Table 29) and there was little difference between the outputs from the different oxidants. For each round, the frame with the largest fireball is reproduced in Figure 108 and Figure 109 for the formulations based on sodium and potassium nitrates respectively.

Bullet no.	Form	Mass (g)	Composition	Flash duration (ms)
74	Powder	0.63	49% Mg/Al alloy 49% Sodium nitrate 2% Calcium resinate	-
75	Powder	0.66	48% Mg/Al alloy 48% Sodium nitrate 4% Calcium resinate	21.0
76	Powder	0.61	49% Mg/Al alloy 49% Sodium nitrate 2% Boiled linseed oil	15.0
77	Powder	0.60	48% Mg/Al alloy 48% Sodium nitrate 4% Boiled linseed oil	20.8
78	Powder	0.57	49% Mg/Al alloy 49% Sodium nitrate 2% Lithographic varnish	19.7
79	Powder	0.53	48% Mg/Al alloy 48% Sodium nitrate 4% Lithographic varnish	26.3
80	Powder	0.67	49% Mg/Al alloy 49% Sodium nitrate 2% PVC powder	16.6
81	Powder	0.67	48% Mg/Al alloy 48% Sodium nitrate 4% PVC powder	23.1
82	Powder	0.71	49% Mg/Al alloy 49% Sodium nitrate 2% GAP	28.7
83	Powder	0.65	48% Mg/Al alloy 48% Sodium nitrate 4% GAP	17.4
84	Powder	0.62	49% Mg/Al alloy 49% Potassium nitrate 2% Calcium resinate	16.0
85	Powder	0.64	48% Mg/Al alloy 48% Potassium nitrate 4% Calcium resinate	17.1
86	Powder	0.55	49% Mg/Al alloy 49% Potassium nitrate 2% Boiled linseed oil	15.0
87	Powder	0.52	48% Mg/Al alloy 48% Potassium nitrate 4% Boiled linseed oil	13.4
88	Powder	0.54	49% Mg/Al alloy 49% Potassium nitrate 2% Lithographic varnish	14.2
89	Powder	0.45	48% Mg/Al alloy 48% Potassium nitrate 4% Lithographic varnish	13.9

90	Powder	0.71	49% Mg/Al alloy 49% Potassium nitrate 2% PVC powder	17.1
91	Powder	0.72	48% Mg/Al alloy 48% Potassium nitrate 4% PVC powder	16.6
92	Powder	0.57	49% Mg/Al alloy 49% Potassium nitrate 2% GAP	15.5
93	Powder	0.56	48% Mg/Al alloy 48% Potassium nitrate 4% GAP	18.7

Table 29; Trial 4, Aluminum alloy target placed 5.8 m from muzzle.

A final gun firing trial examined two formulations based on magnesium/aluminum alloy-sodium nitrate and calcium resinate which had provided high light output levels and showed good ageing properties. Control compositions based on potassium perchlorate were also examined. The flash durations recorded showed some variation (Table 30). This is in part due to the subjective nature of determining the end of the combustion. There was little difference between the sizes of the fireballs observed; the frames showing the maximum size are given in Figure 110.

Bullet no.	Form	Mass (g)	Composition	Flash duration (ms)
94	Powder	0.65	49% Mg/Al alloy 49% Sodium nitrate 2% Calcium resinate	19.2
95	Powder	0.63	49% Mg/Al alloy 49% Sodium nitrate 2% Calcium resinate	28.1
96	Powder	0.63	49% Mg/Al alloy 49% Sodium nitrate 2% Calcium resinate	21.0
97	Powder	0.77	49% Mg/Al alloy 49% Sodium nitrate 2% Calcium resinate	23.1
98	Powder	0.71	48% Mg/Al alloy 48% Sodium nitrate 4% Calcium resinate	27.3
99	Powder	0.66	48% Mg/Al alloy 48% Sodium nitrate 4% Calcium resinate	29.2
100	Powder	0.71	48% Mg/Al alloy 48% Sodium nitrate 4% Calcium resinate	28.4
101	Powder	0.65	48% Mg/Al alloy 48% Sodium nitrate 4% Calcium resinate	18.9
102	Powder	0.74	49% Mg/Al alloy 49% Potassium perchlorate 2% Calcium resinate	22.6
103	Powder	0.76	49% Mg/Al alloy 49% Potassium perchlorate 2% Calcium resinate	15.3
104	Powder	0.88	50% Mg/Al alloy 40% Barium Nitrate 10% Potassium perchlorate	15.8
105	Powder	0.89	50% Mg/Al alloy 40% Barium Nitrate 10% Potassium perchlorate	20.5

Table 30; Trial 5, Aluminum alloy target placed 6 m from muzzle.

Ageing studies

To investigate their ageing characteristics, isothermal heat flow calorimetry studies were carried out on a number of ingredients and compositions. The measurements were performed using a Thermometric TAM 2277 on 100 mg samples in closed ampoules. The relative humidity in the ampoule was maintained but inserting a small tube containing a saturated solution of either sodium nitrate (65%) or strontium nitrate (75%).

After six days at 50 °C and 65% RH the alloy (Figure 111) gave a very low heat flow signal of $13 \mu\text{W g}^{-1}$; this is around one tenth of the level observed previously for magnesium aged under identical conditions [2]. The heat flow for the alloy at 50 °C and 75% RH (Figure 112)

gave a larger initial peak heat flow value of $74.9 \mu\text{W g}^{-1}$ which reduced steadily and after six days a level of $40.3 \mu\text{W g}^{-1}$ was observed.

Potassium perchlorate showed essentially no reaction with water (Figure 113) but calcium resinate showed a large initial exothermic peak (Figure 114) and after six days a signal of $68.9 \mu\text{W g}^{-1}$ was given.

At 50°C and 65% RH the 50% the magnesium/aluminum alloy-50% potassium perchlorate composition and the 49% magnesium/aluminum alloy-2% calcium resinate compositions did not give marked heat flow effects; the heat flow curves are shown in Figure 115 and Figure 116 respectively. Experiments carried out on the ternary composition containing 12% calcium resinate exhibited a significantly higher heat flow (Figure 117) and after six days a heat flow of $25.2 \mu\text{W g}^{-1}$ was observed compared to less than $1 \mu\text{W g}^{-1}$ for the composition containing 2% calcium resinate.

DSC studies were carried out on the three compositions examined in the microcalorimeter in order to evaluate the effects of ageing. The plots for the samples aged in the microcalorimeter are compared with those measured for unaged samples in Figure 118 to Figure 120. No significant differences were observed between DSC curves for the aged and unaged compositions.

Isothermal microcalorimetry studies were also carried out on the composition containing 50% magnesium/aluminum alloy-40% barium nitrate and 10% potassium perchlorate (Figure 121) and the binary composition containing equal amounts of the alloy and barium nitrate (Figure 122). The compositions did not show significant heat flow signals and the DSC curves for the aged and unaged material showed no significant differences (Figure 123 and Figure 124).

A binary composition containing magnesium/aluminum alloy and sodium nitrate (Figure 125) gave an initial maximum heat flow of over $400 \mu\text{W g}^{-1}$ and after twelve days it was still around $100 \mu\text{W g}^{-1}$. Both of these values are considerably less than those previously observed for a 50% magnesium-50% sodium nitrate composition aged under the same conditions [3]. DSC showed significant reductions in the ignition temperature on ageing from around 780°C to between 670°C and 700°C (Figure 126).

Similar experiments with potassium nitrate as the oxidant gave a lower initial peak heat flow of $244 \mu\text{W g}^{-1}$ but unlike sodium nitrate the heat flow after 6 days was significantly higher at around $322 \mu\text{W g}^{-1}$ and continuing to increase (Figure 127). The DSC curves show a marked reduction in the magnitude of the exothermic reactions given above 600°C (Figure 128) and there also appears to be a reduction in the size of the alloy's fusion peak.

A further three magnesium/aluminum alloy and sodium nitrate compositions which had given a good performance in the gun firing trials were studied. The heat flow curves for the compositions containing 4% calcium resinate, lithographic varnish or GAP are given in Figure 129 to Figure 131. The heat flows observed were considerably lower than those seen for the binary magnesium/aluminum alloy-sodium nitrate composition and after seven days values of $1 \mu\text{W g}^{-1}$, $12 \mu\text{W g}^{-1}$ and $27 \mu\text{W g}^{-1}$ were observed for the compositions containing calcium resinate, lithographic varnish and GAP respectively.

Following the final gun firing trial, two compositions containing magnesium/aluminum alloy, sodium nitrate and either 2% or 4% calcium resinate were selected for additional ageing studies. Two samples of each composition along with two samples of a composition containing 50% magnesium/aluminum alloy-50% sodium nitrate were aged at 50°C and 65% RH for a period of 28 days. The heat flow and cumulative heat flow curves are shown in Figure 132 to Figure 137 and the values after 28 days are summarized in Table 31.

The addition of just 2% calcium resinate resulted in a significant reduction in the rate of ageing and the heat flows observed for both samples containing calcium resinate were extremely low and at the limits of the TAM heat flow calorimeter. Based on the mean heat flow levels observed the sample containing 4% calcium resinate was selected for hazard assessment.

Sample	Run	Heat flow ($\mu\text{W g}^{-1}$)	Cumulative heat (J g^{-1})
50% Magnesium/aluminum alloy- sodium nitrate	1	16.2	120.2
	2	26.9	95.7
	Mean	21.5 ± 5.3	107.9 ± 12.3
9% Magnesium/aluminum alloy- 49% sodium nitrate-2% calcium resinate	1	3.9	2.9
	2	2.1	0.8
	Mean	3.0 ± 0.9	1.9 ± 1.1
48% Magnesium/aluminum alloy- 48% sodium nitrate-4% calcium resinate	1	2.3	1.5
	2	0.1	-3.6
	Mean	1.2 ± 1.1	-1.1 ± 2.5

Table 31; Heat flow and cumulative heat values after 28 day at 50 °C and 65% RH

Hazard assessment

The small scale hazard assessment data for the compositions containing magnesium/aluminum alloy, sodium nitrate and 4% calcium resinate are given in Table 32. The results show that this composition has acceptable hazard characteristics.

Test	Results
Rotter test (Figure of Insensitiveness)	89
Rotary friction test (Figure of Friction)	3.8
Mallet friction test	
Steel on steel:	50
Nylon on steel:	0
Wood on hardwood:	0
Wood on softwood:	0
Wood on yorkstone:	0
Temperature of ignition	Decomposes slowly
Ease of ignition	Fails to ignite
Train test	Ignites and supports train vigorously throughout
Electric spark test	No ignitions at 4.5J

Table 32; Hazard data for magnesium/aluminum alloy, sodium nitrate and 4% calcium resinate.

Additional pyrotechnic and thermal studies

The burning rate of the compositions containing magnesium/aluminum alloy-sodium nitrate and from 2% to 12% calcium resinate were determined along with a binary mixture. The burning rate curves given in Figure 138 shows that the addition of calcium resinate results in a small continuous reduction in burning rate. The largest reduction occurs over the range 2% to 4% calcium resinate. The burning rate of the binary compositions is slightly lower than that observed previously but is consistent with typical batch to batch variations observed for pyrotechnic compositions.

The ignition DSC curves for the range of compositions are shown in Figure 139 and the ignition temperatures plotted as a function of calcium resinate in Figure 140. The addition of 2% calcium resinate caused a small reduction in ignition temperature, this increased further when 4% was present but thereafter the ignition temperature was essentially unchanged.

Conclusions and implications for future research/implementation

The project allowed a wide range of pyrotechnic formulations with potential as incendiary pyrotechnics for ammunition to be assessed. The objectives were met by:

- Environmental screening of the proposed pyrotechnic ingredients
- Pyrotechnic formulation and performance studies
- Thermal analysis
- Modeling of pyrotechnic combustion
- Environmental screening of the combustion products
- Gun firing trials
- Ageing studies
- Hazard assessment

An in-depth environmental and toxicity screen of the ingredients was performed prior to the formulation studies. As a result, potassium dinitramide, copper oxide and manganese oxide were not used for the formulation studies.

Burning rate and thermal studies showed that a large number of compositions had potential as replacement for the perchlorate based compositions currently used in incendiary ammunition.

Analysis of the combustion modeling results showed that the chemistry of each system was complex and related to the amount of each reactant present, the combustion temperature and the thermal properties, of both the reactants and the combustion products. For the main three systems examined, the major products observed were the oxides of the fuel and in the case of the alloy this was a mixed fuel oxide. Most of the predicted species are in the gaseous state and during or after cooling would decompose, oxidize or hydrolyze possibly over an extended time period. Ammonia, hydrogen sulfide, sulfur and sulfur dioxide were amongst the predicted combustion products along with a range of metal oxides, hydroxides and sulfides.

The results from the environmental screening study for the combustion products showed that a number were undesirable particularly the fluorides, hydrogen sulfide, sulfur dioxide and ammonia.

The gun firing trial showed that the most promising compositions were those based on magnesium/aluminum alloy with either sodium or potassium nitrate and a binder. These compositions produced a flash duration and signature which was similar to that of the control compositions containing potassium perchlorate. Preliminary ageing studies performed at 50 °C and 65% RH in closed ampoules using a heat flow calorimeter showed that the rate of ageing was considerably lower for the formulations based on sodium nitrate.

A further gun firing trial confirmed that the formulations containing magnesium/aluminum alloy-sodium nitrate and either 2% or 4% calcium resinate gave a performance that matched that of the control compositions containing potassium perchlorate in terms of flash size and duration. When subjected to longer term ageing at 50 °C and 65% RH, the composition containing 4% calcium resinate was found to have the lower heat flow. Ignition DSC showed that the ignition temperature for this formulation was also lower and hazard assessment confirmed that this formulation had acceptable safety characteristics.

It is therefore recommended that the formulation magnesium/aluminum alloy-sodium nitrate-4% calcium resinate is examined further as a replacement incendiary composition. The ingredients used in this formulation can be readily obtained and their cost is comparable with those presently used for the incendiary compositions.

Further work is needed to investigate the incendiary properties of this formulation and assess the flash brightness and duration at longer ranges. This work would involve filling ammunition and conducting the Incendiary Flash and Incendiary Ignition Tests [4]. Once the performance of the composition has been confirmed, it will be necessary to obtain additional data including Hazard Classification, Health Hazard and a Lifecycle Environmental Analysis before transition of the formulation into ammunition filling.

Literature cited

1. Environmental Microbiology, Perchlorate-reducing microorganisms isolated from contaminated sites, A S Waller, E E Cox and E A Edwards, Volume 6, Issue 5, 517-527 May 2004.
2. Studies on the Ageing of a Magnesium-Potassium Nitrate Pyrotechnic Composition using Isothermal Heat Flow Calorimetry and Thermal Analysis Techniques, S D Brown, E L Charsley, S J Goodall, P G Laye, J J Rooney and T T Griffiths, Thermchimica Acta 401 53-61, May 2003.
3. Studies of Ageing in Pyrotechnic Mixtures of Magnesium and Sodium Nitrate, Proceedings of the 12th Symposium on Chemical Problems Connected With The Stability of Explosives, Sweden, E L Charsley, P G Laye, S J Goodall and T T Griffiths, May 2001, Published 2004.
4. TECP 700-700 ORD M608, Volume 3, Test Methods for Small Arms Ammunition.

Figures

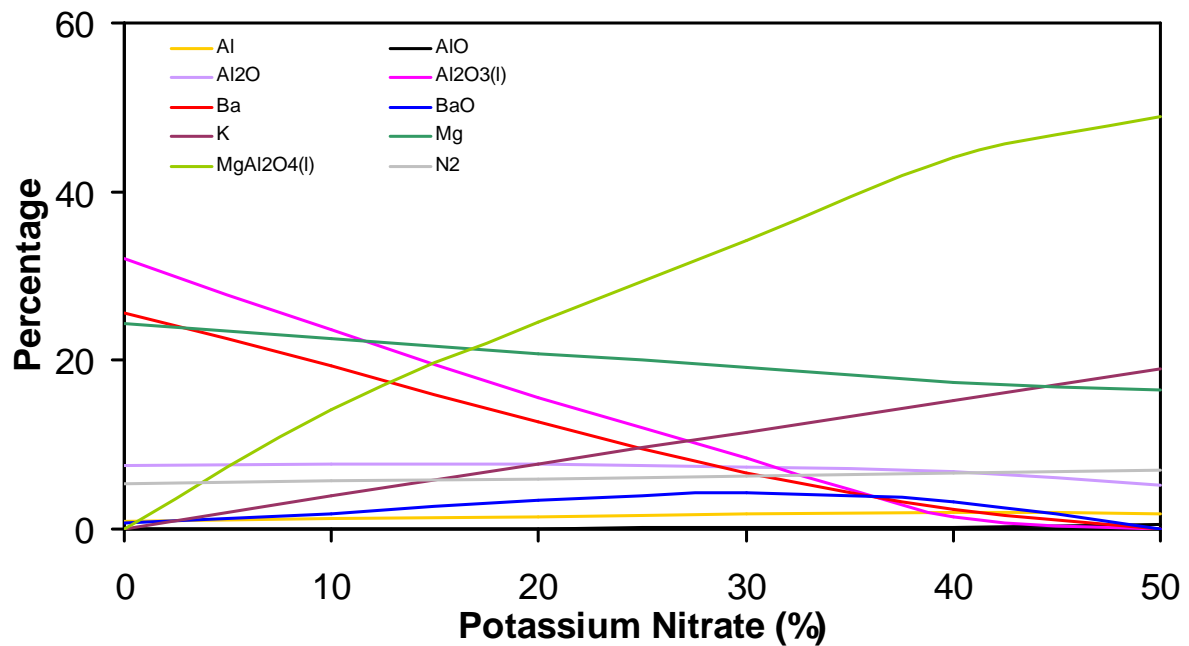


Figure 1; Main reaction products for 50% magnesium/aluminum alloy-barium nitrate-potassium nitrate.

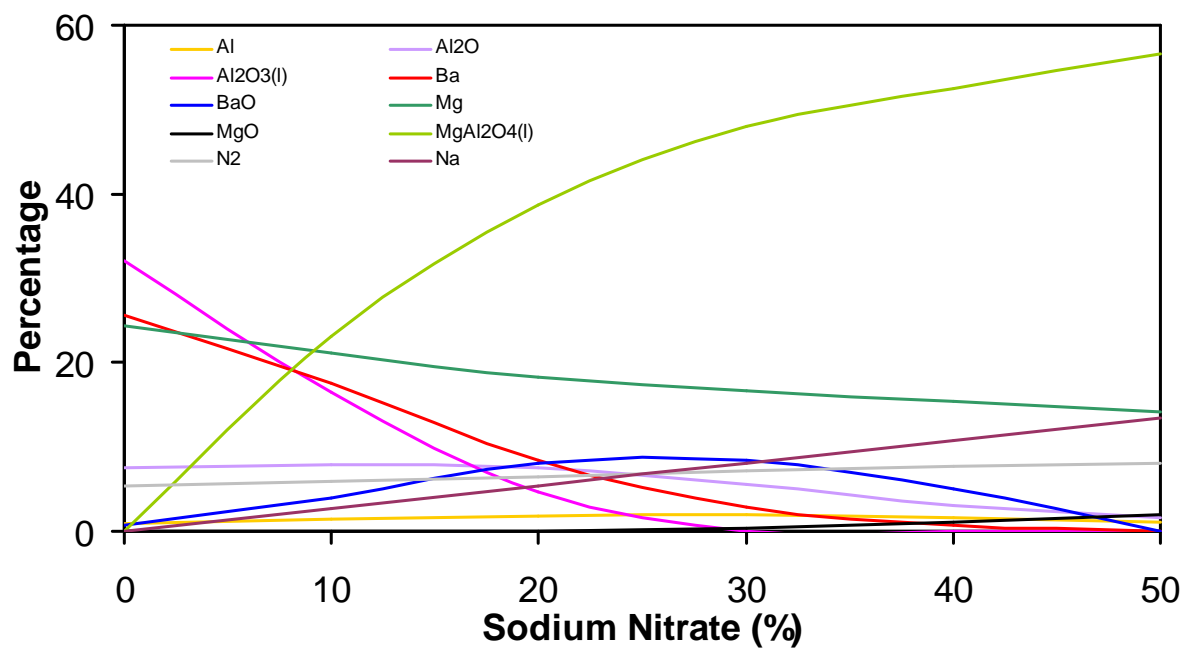


Figure 2; Main reaction products for 50% magnesium/aluminum alloy-barium nitrate-sodium nitrate.

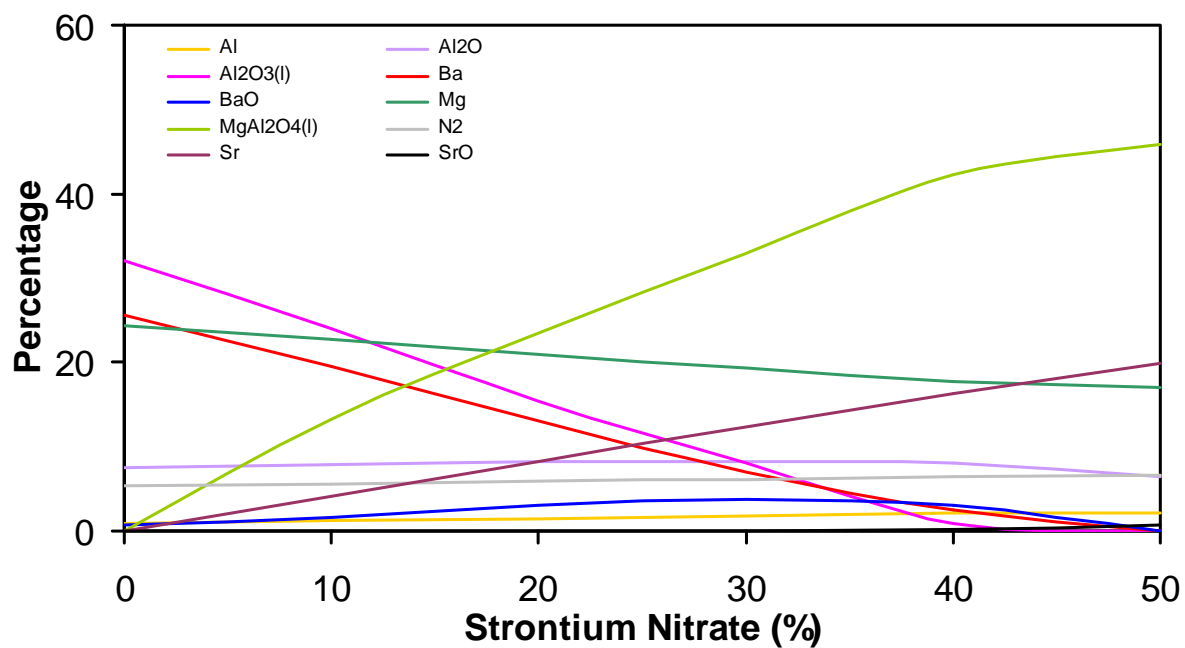


Figure 3; Main reaction products for 50% magnesium/aluminum alloy-barium nitrate-strontium nitrate.

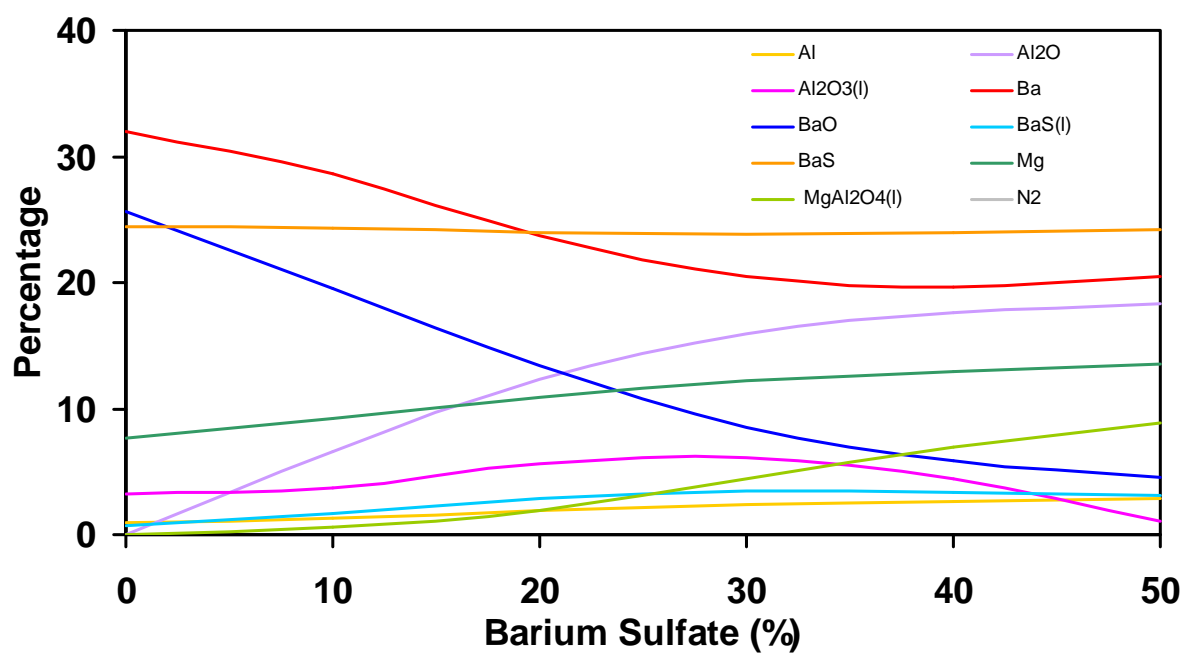


Figure 4; Main reaction products for 50% magnesium/aluminum alloy-barium nitrate-barium sulfate.

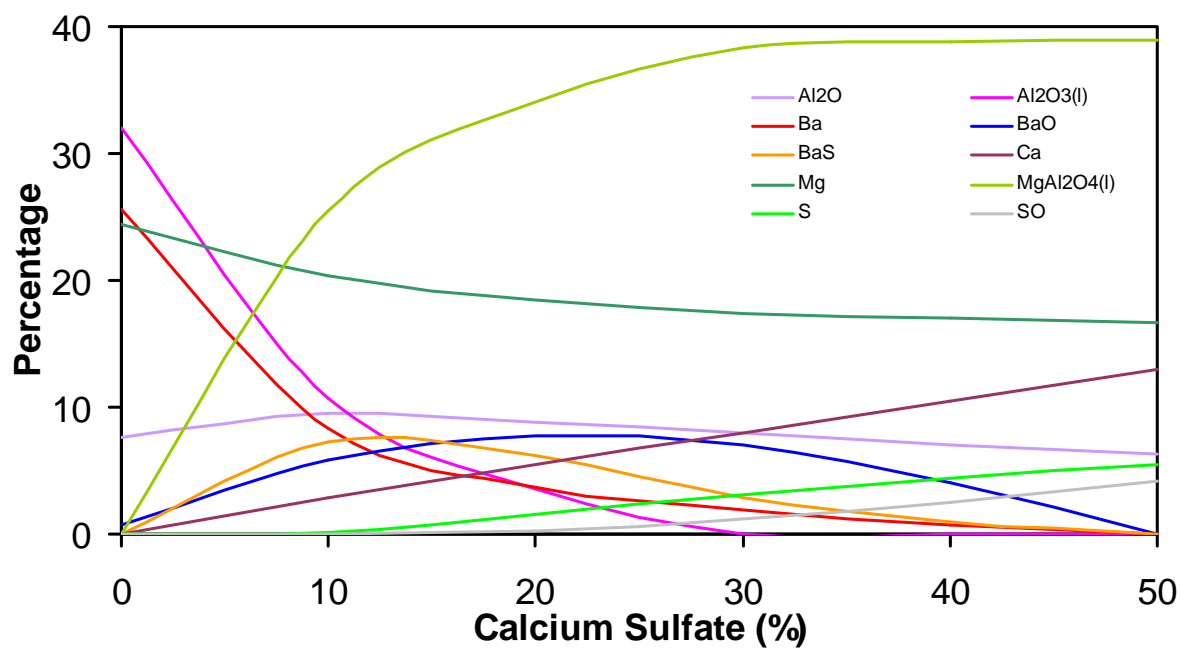


Figure 5; Main reaction products for 50% magnesium/aluminum alloy-barium nitrate-calcium sulfate.

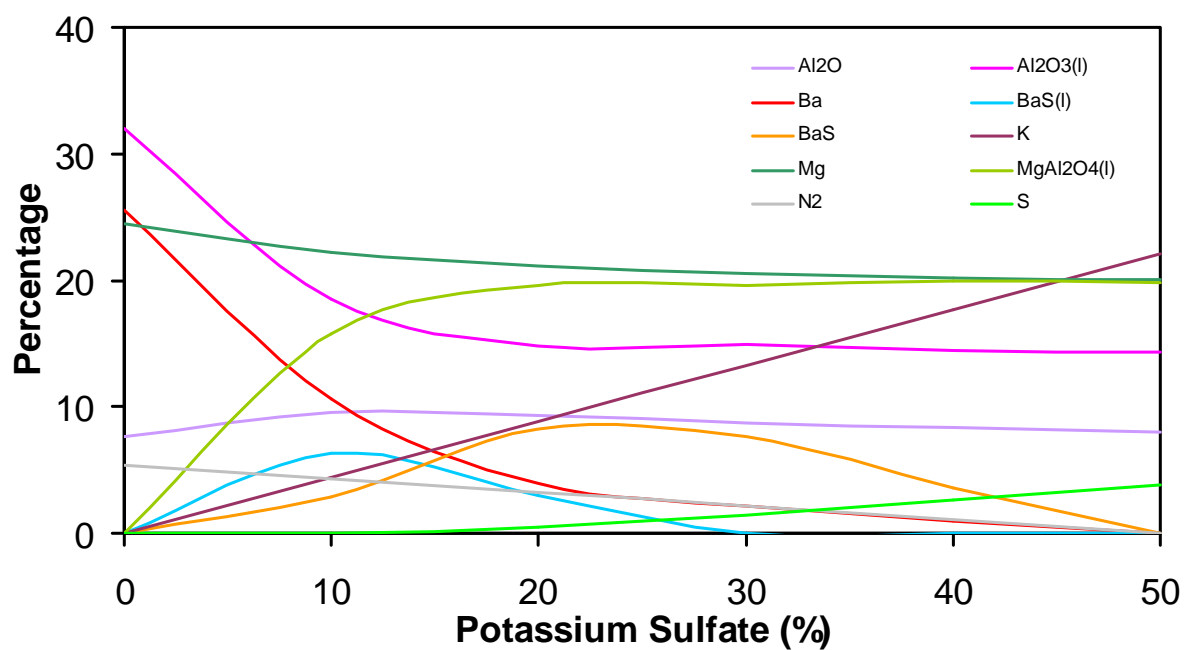


Figure 6; Main reaction products for 50% magnesium/aluminum alloy-barium nitrate-potassium sulfate.

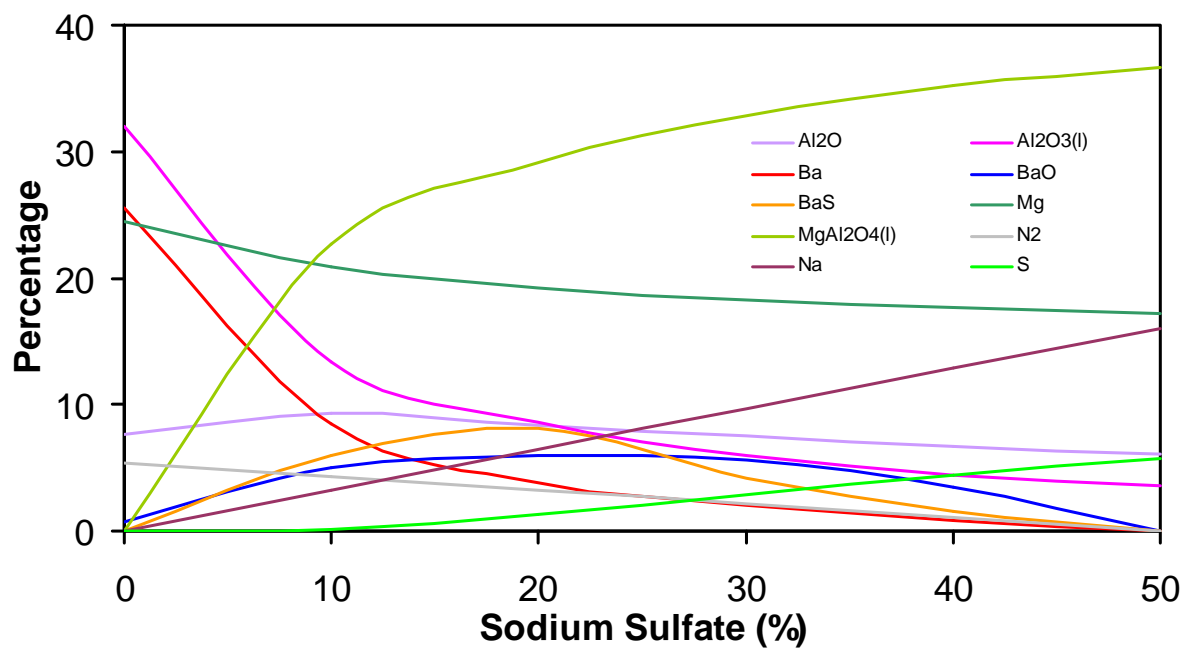


Figure 7; Main reaction products for 50% magnesium/aluminum alloy-barium nitrate-sodium sulfate.

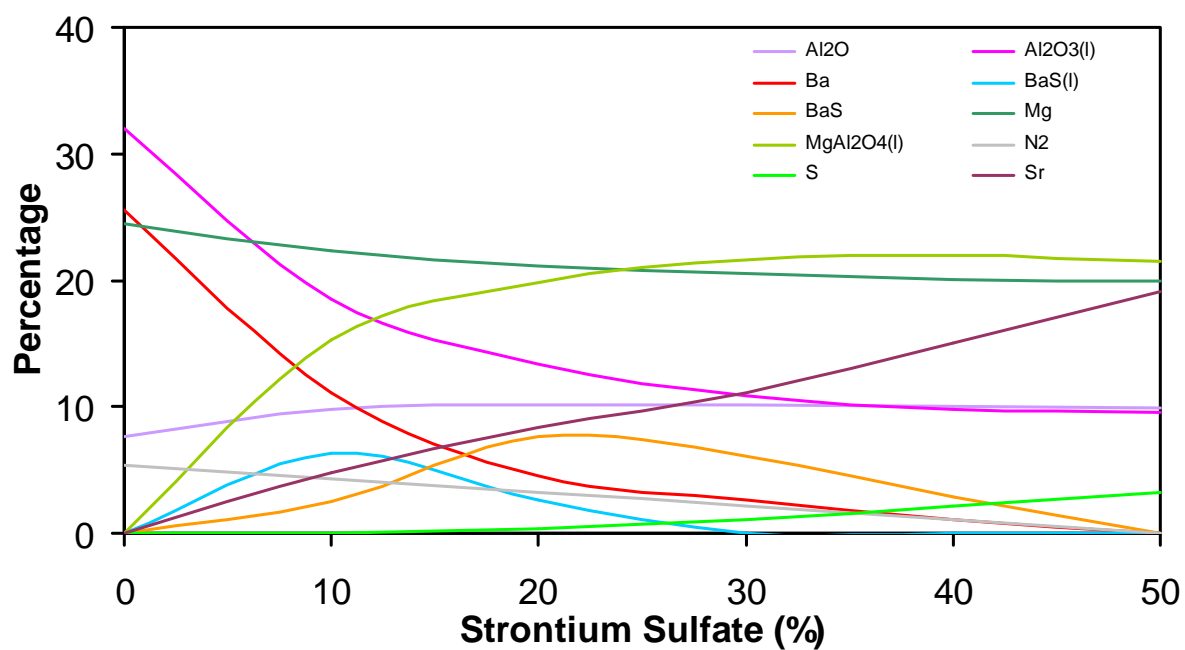


Figure 8; Main reaction products for 50% magnesium/aluminum alloy-barium nitrate-strontium sulfate.

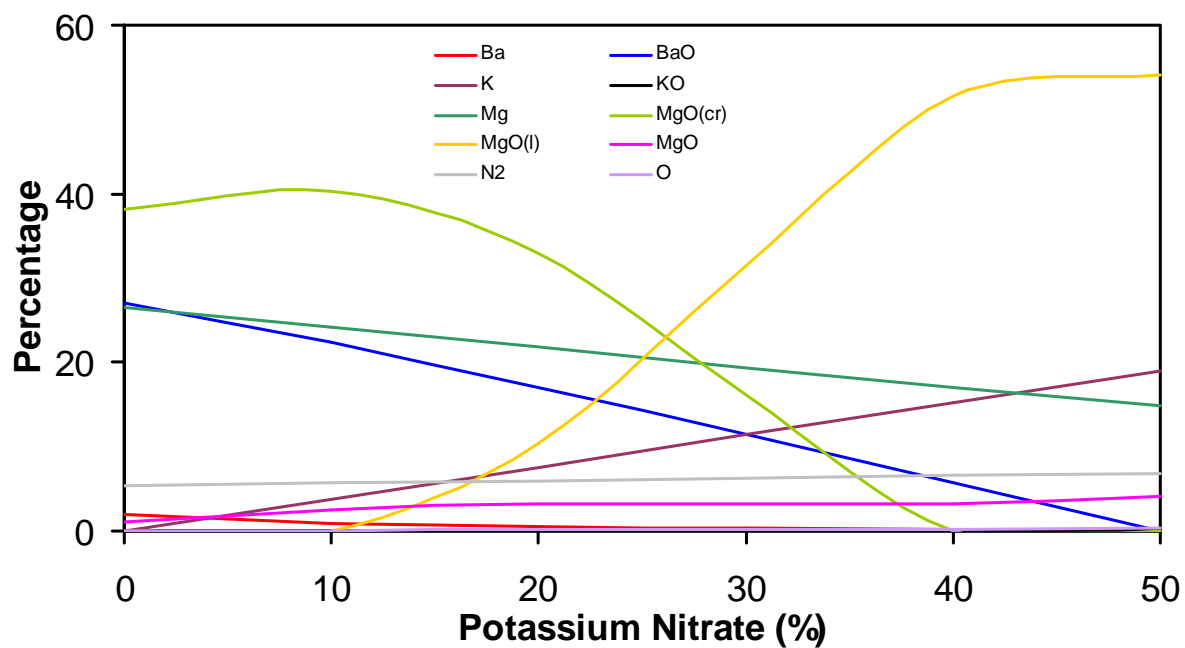


Figure 9; Main reaction products for 50% magnesium-barium nitrate-potassium nitrate.

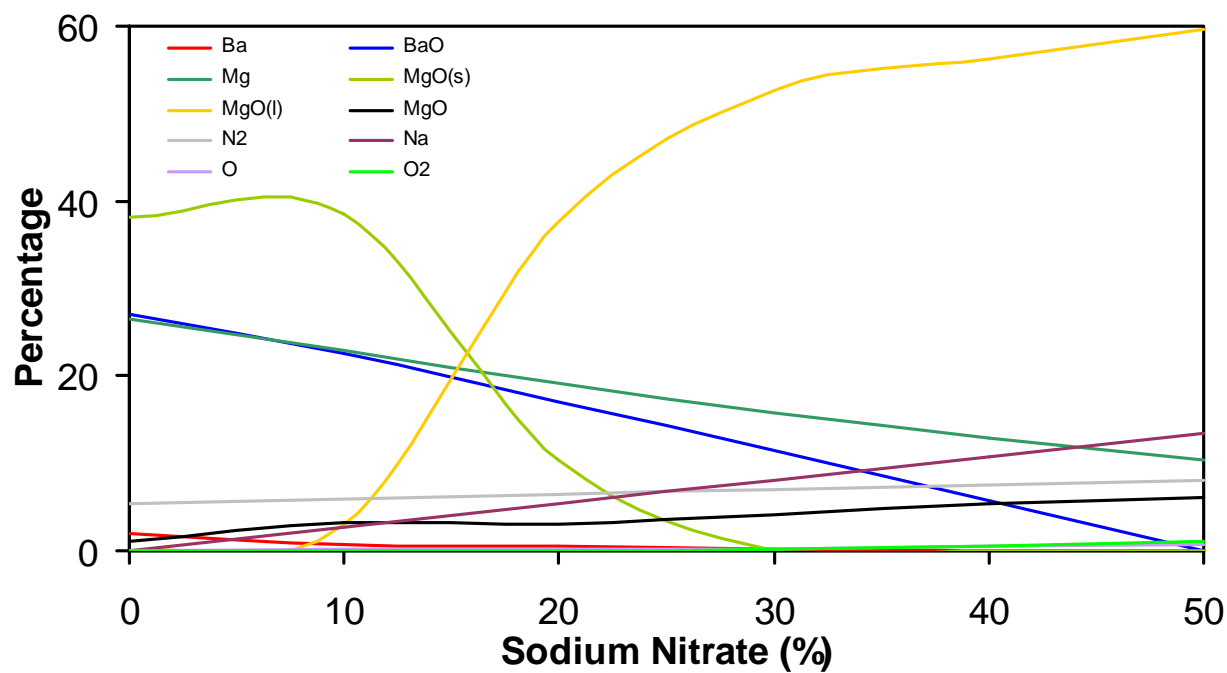


Figure 10; Main reaction products for 50% magnesium-barium nitrate-sodium nitrate.

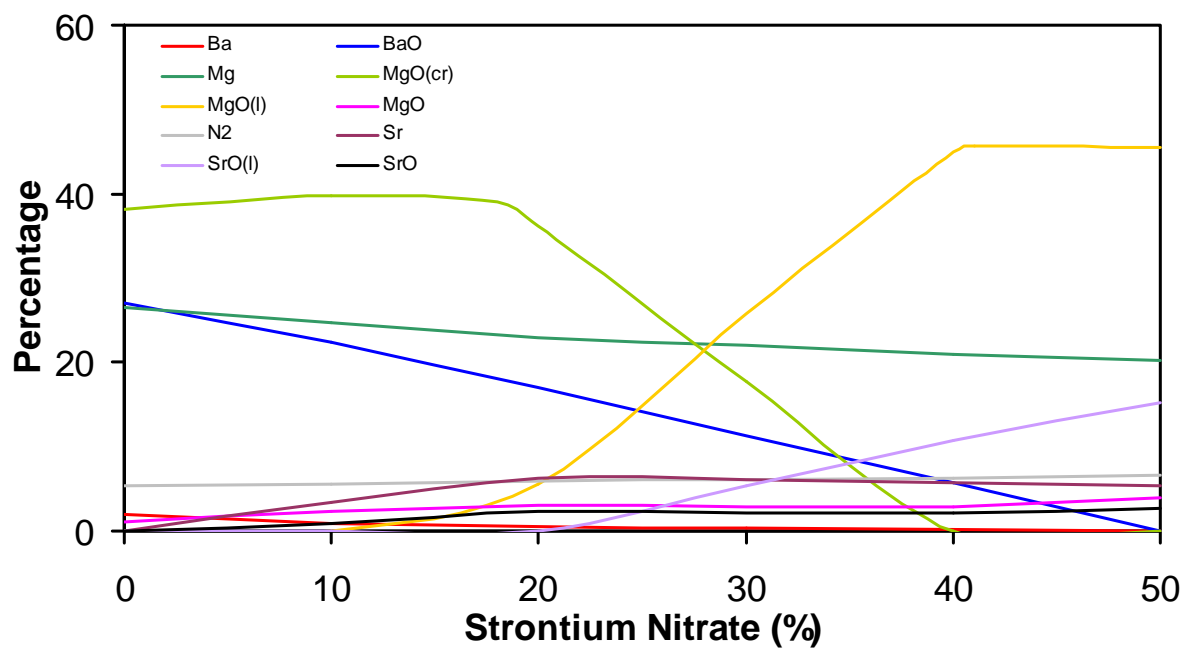


Figure 11; Main reaction products for 50% magnesium-barium nitrate-strontium nitrate.

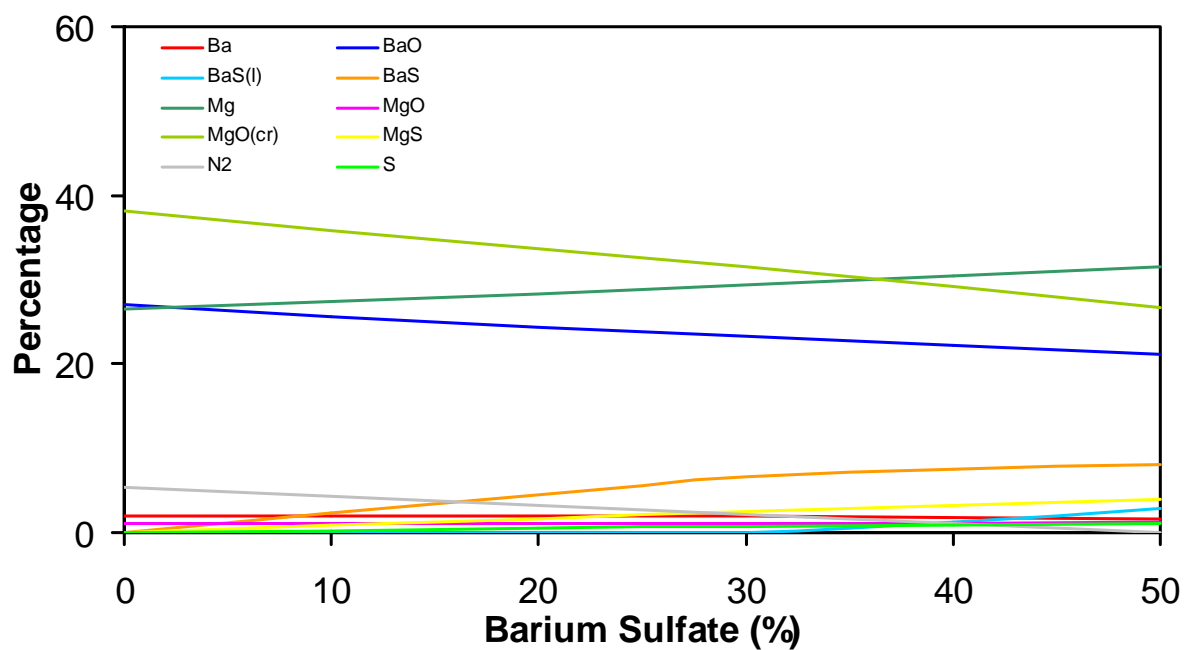


Figure 12; Main reaction products for 50% magnesium-barium nitrate-barium sulfate.

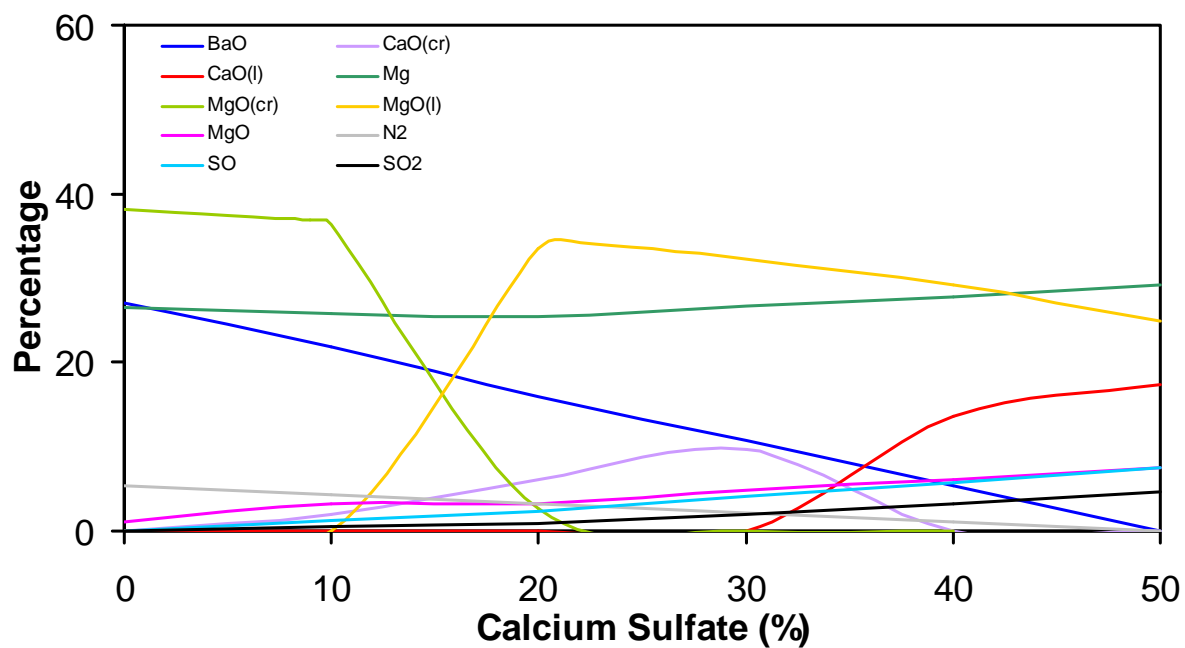


Figure 13; Main reaction products for 50% magnesium-barium nitrate-calcium sulfate.

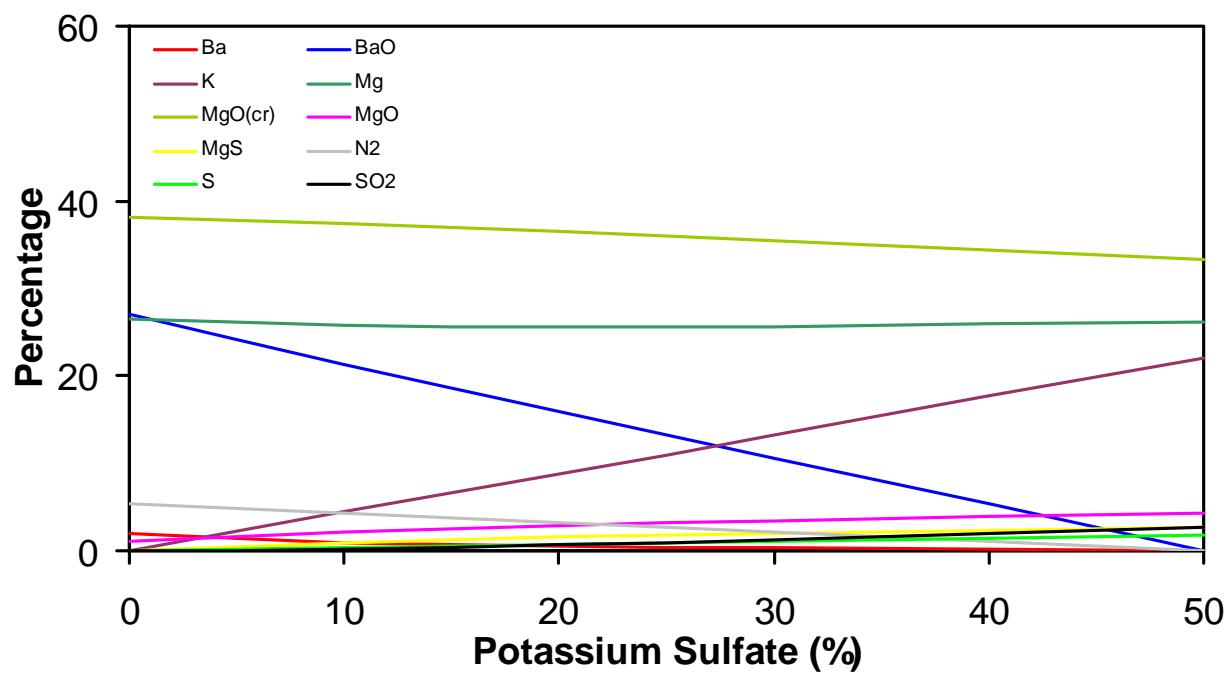


Figure 14; Main reaction products for 50% magnesium-barium nitrate-potassium sulfate.

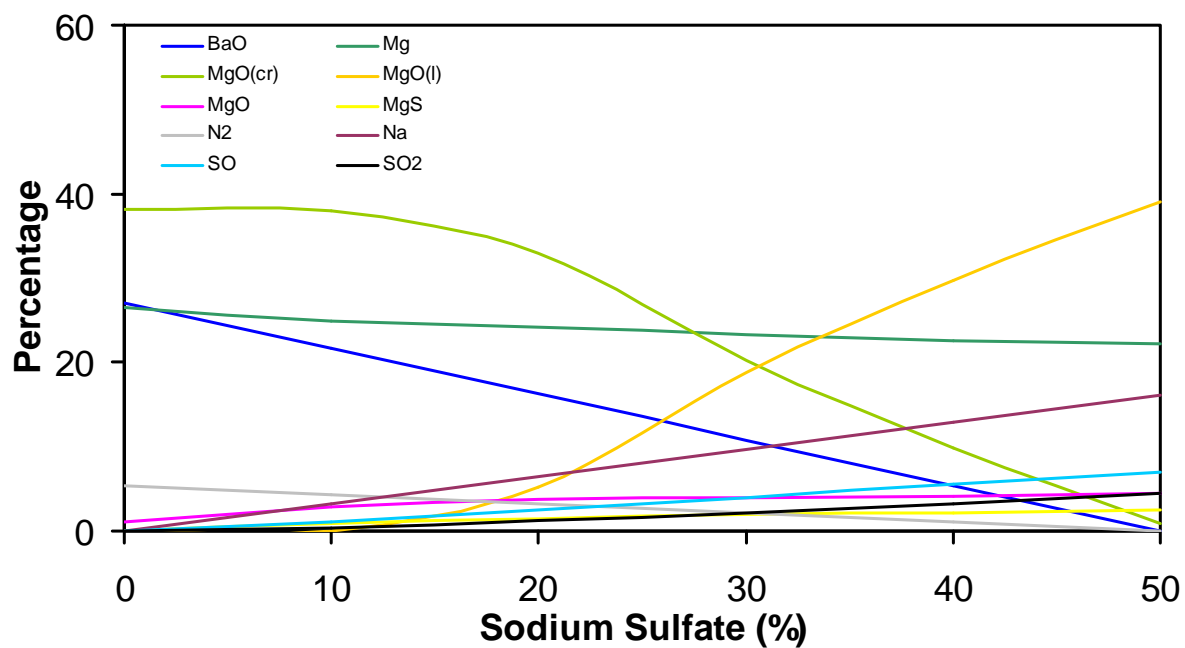


Figure 15; Main reaction products for 50% magnesium-barium nitrate-sodium sulfate.

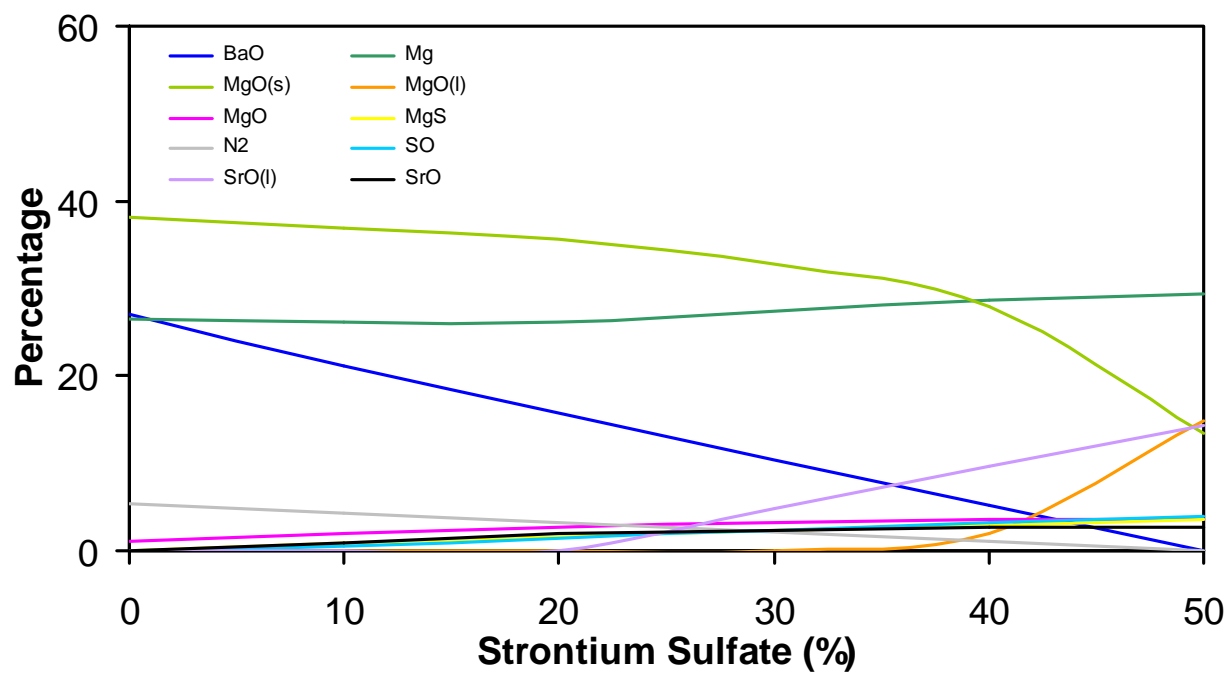


Figure 16; Main reaction products for magnesium-barium nitrate-strontium sulfate.

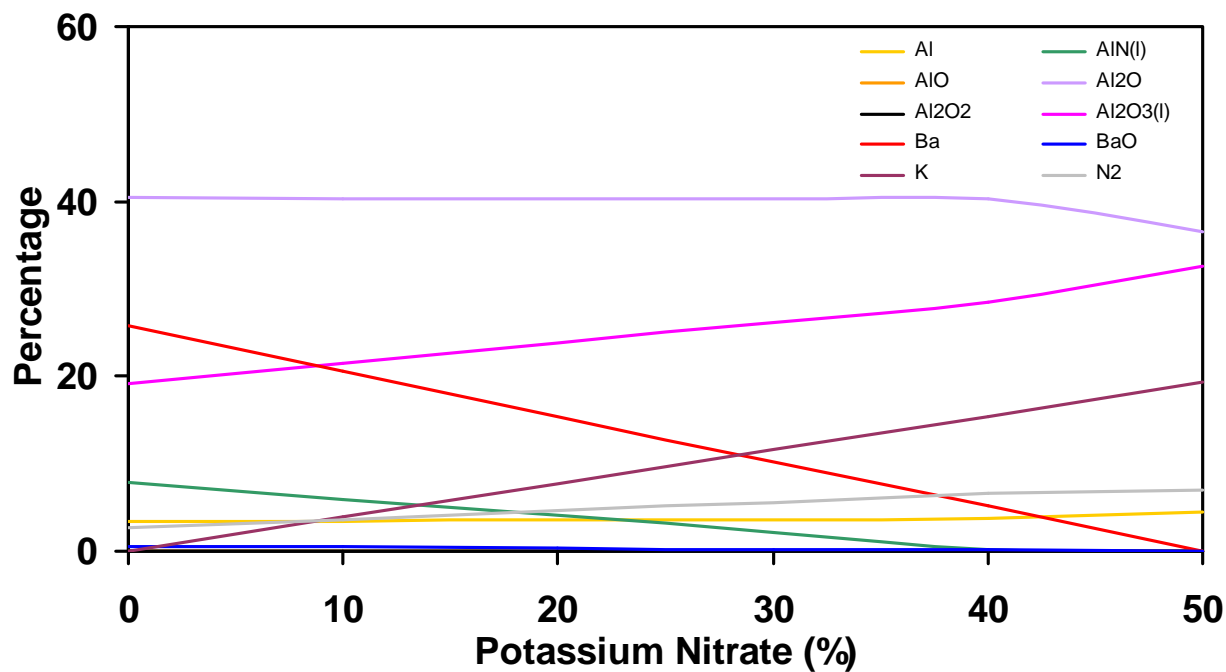


Figure 17; Main reaction products for aluminum-barium nitrate-potassium nitrate.

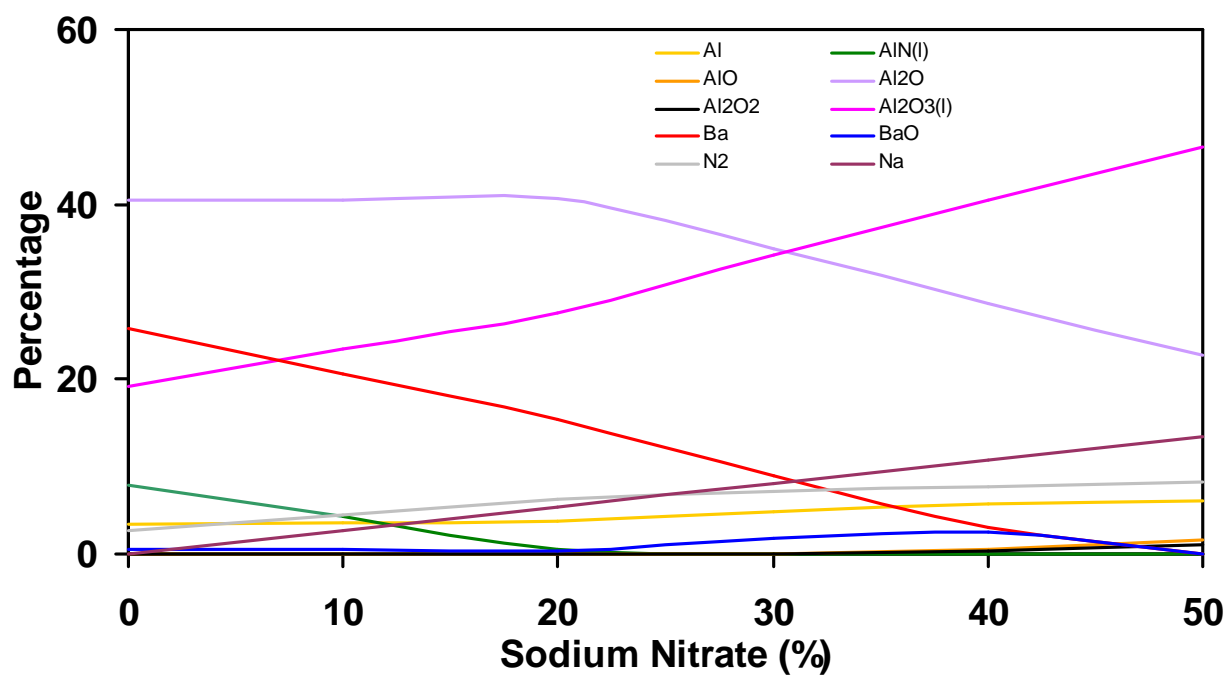


Figure 18; Main reaction products for 50% aluminum-barium nitrate-sodium nitrate.

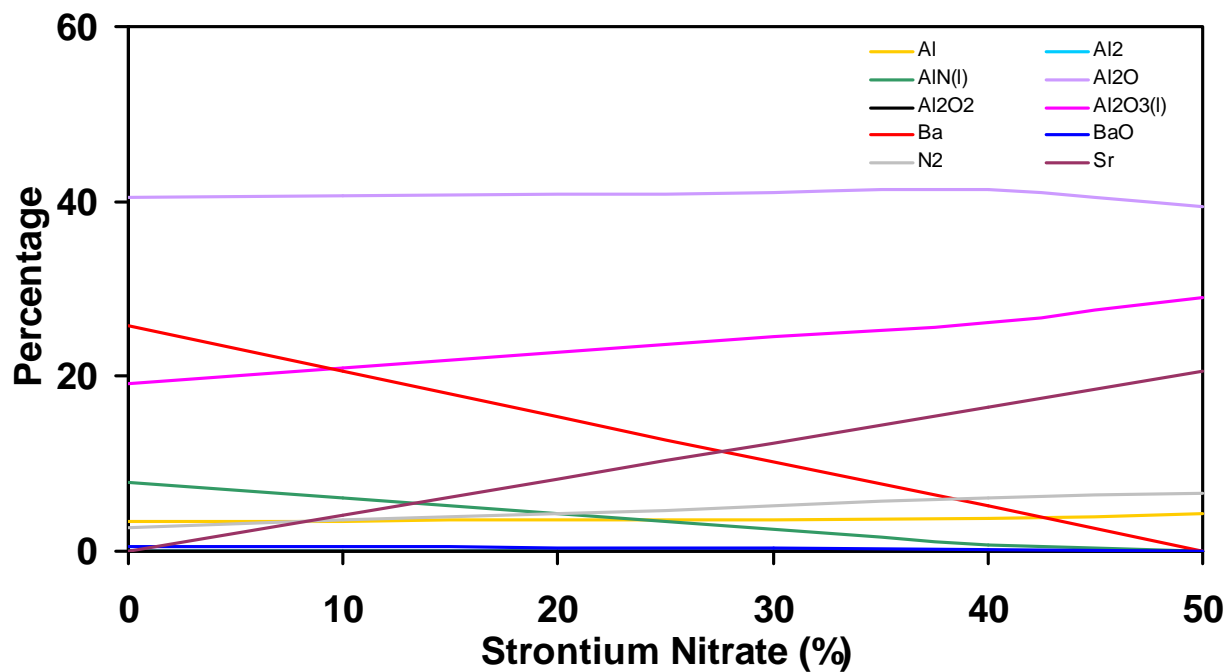


Figure 19; Main reaction products for 50% aluminum-barium nitrate-strontium nitrate.

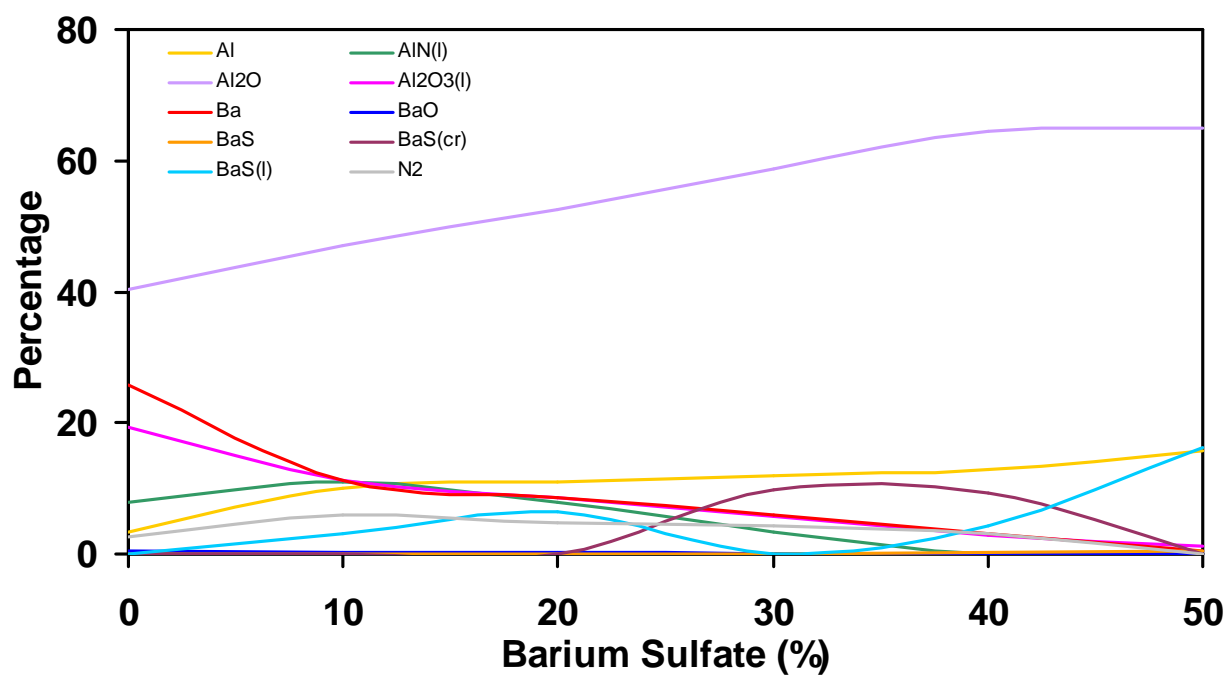


Figure 20; Main reaction products for 50% aluminum-barium nitrate-barium sulfate.

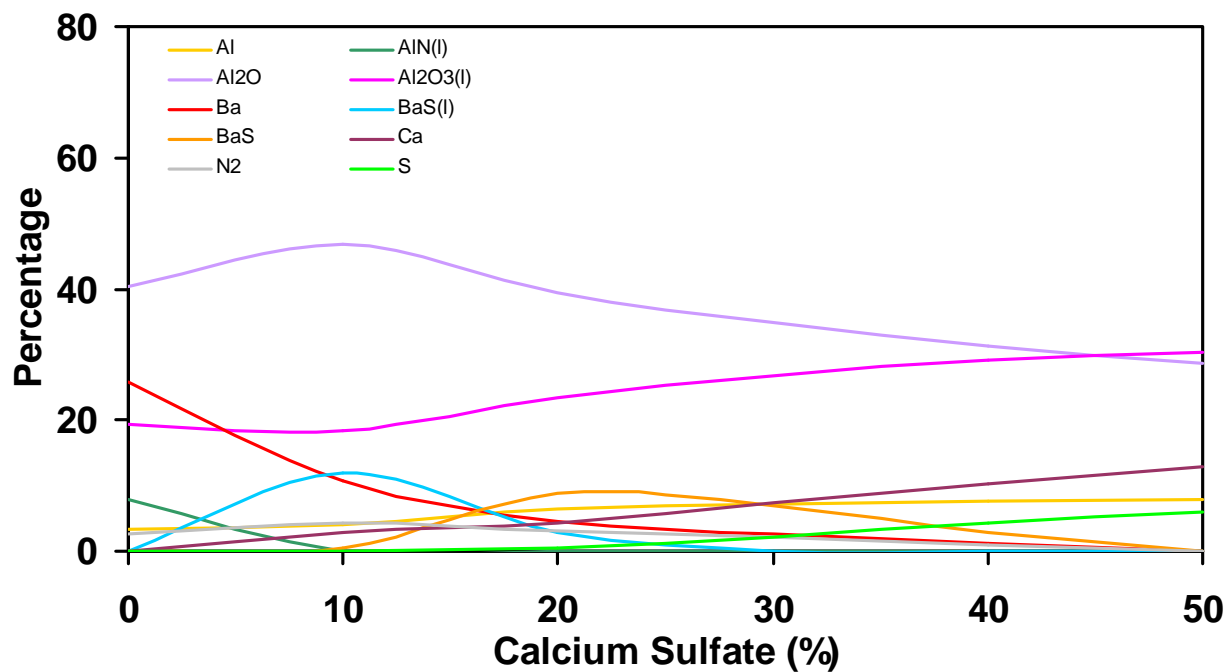


Figure 21; Main reaction products for 50% aluminum-barium nitrate-calcium sulfate.

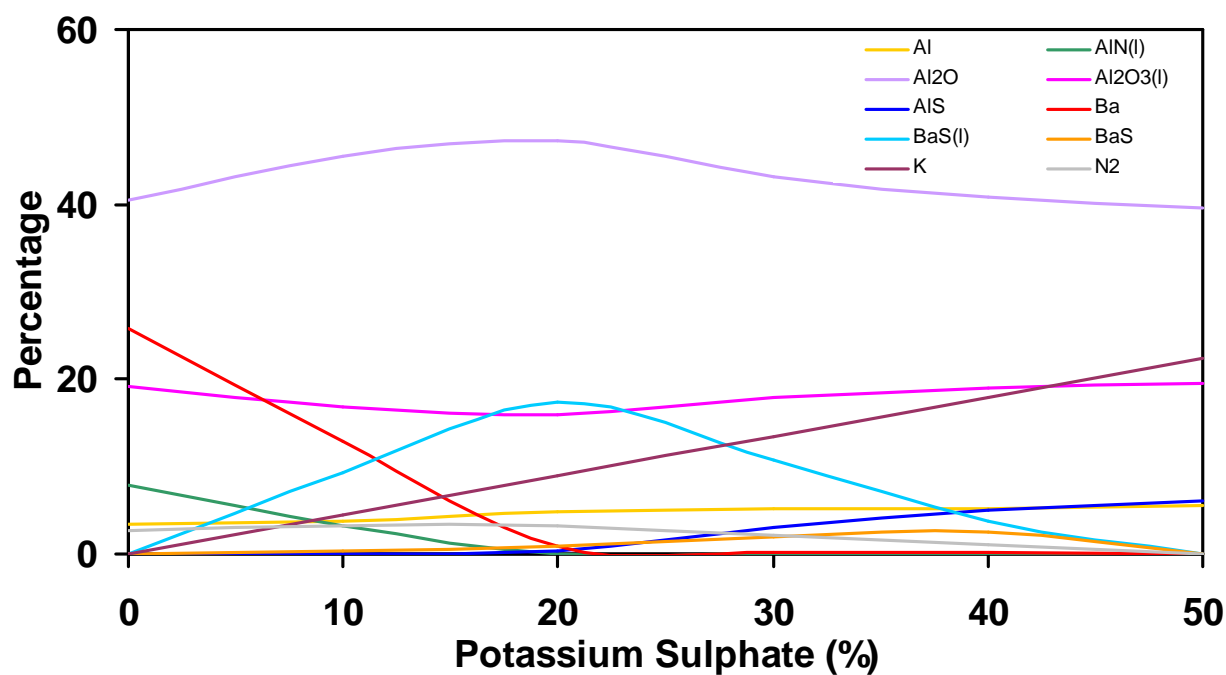


Figure 22; Main reaction products for 50% aluminum-barium nitrate-potassium sulfate.

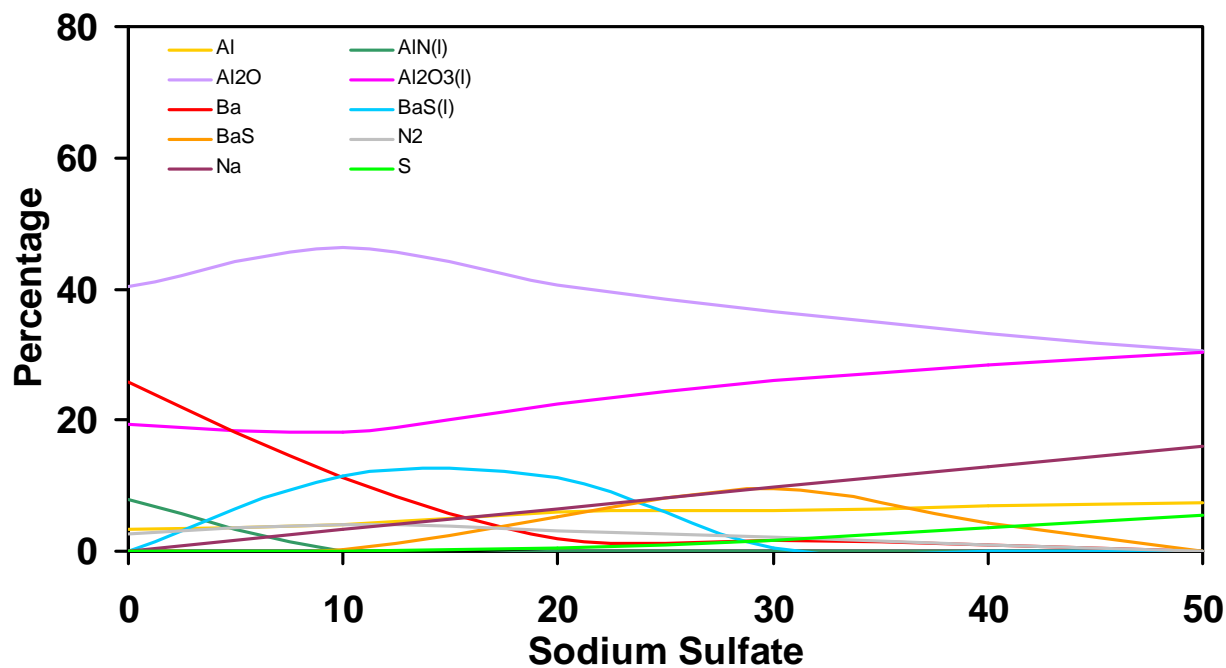


Figure 23; Main reaction products for 50% aluminum-barium nitrate-sodium sulfate.

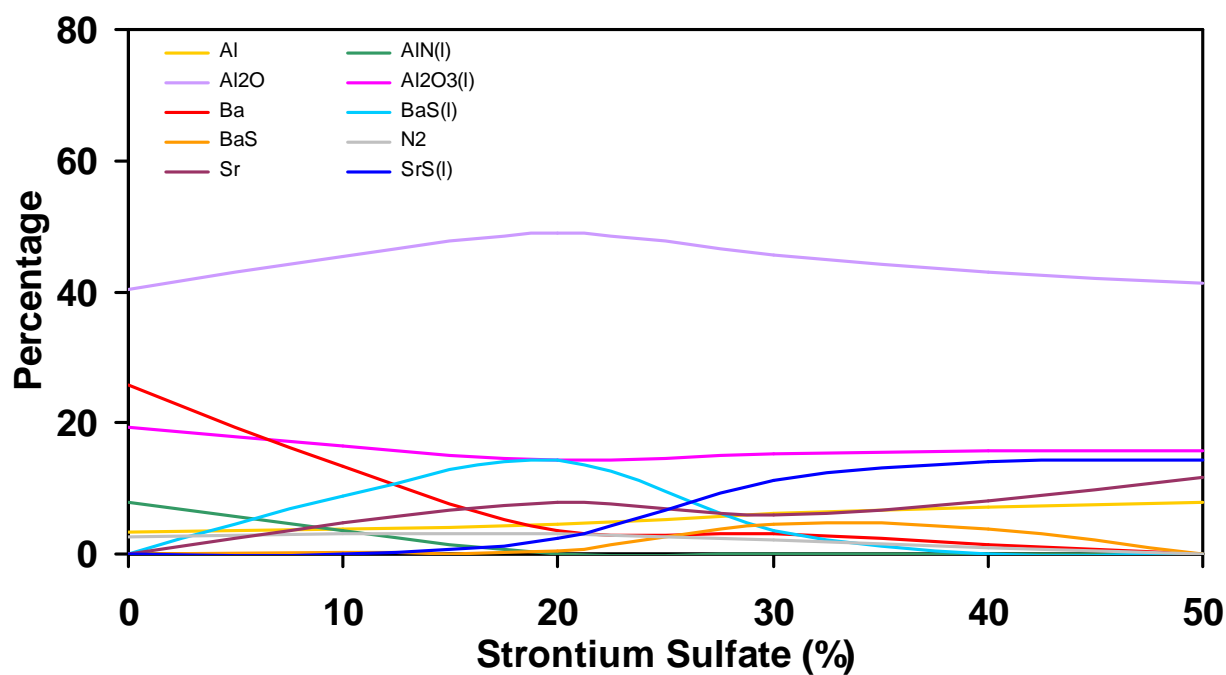


Figure 24; Main reaction products for 50% aluminum-barium nitrate-strontium sulfate.

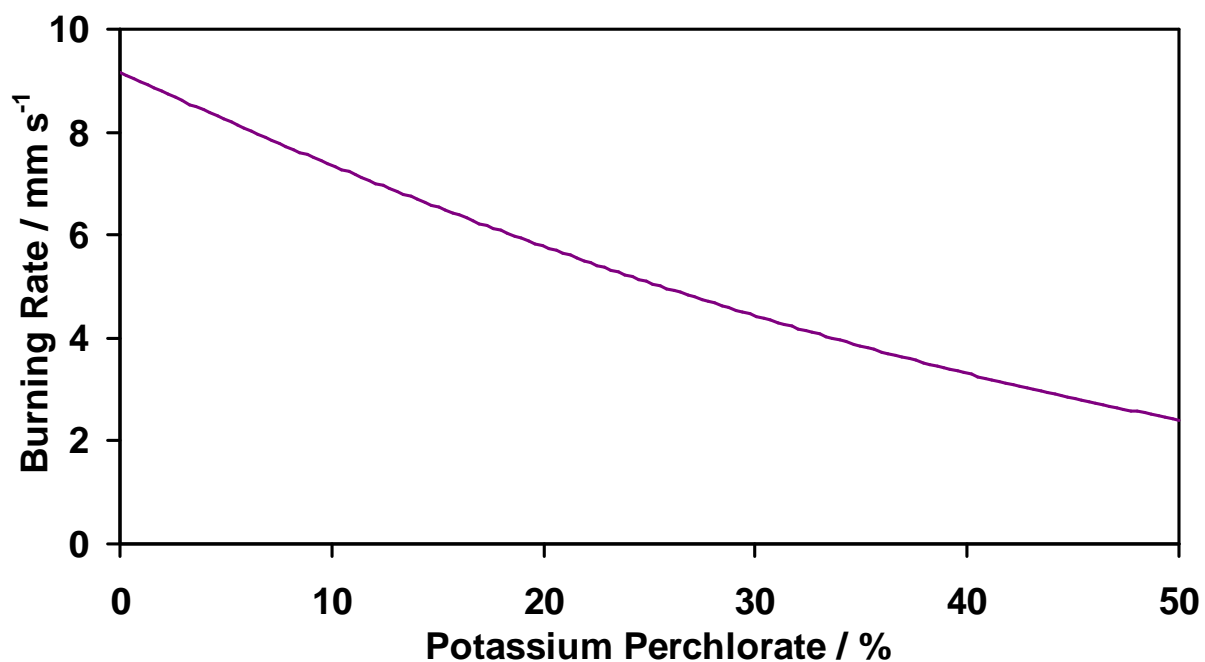


Figure 25; Burning rate curve for magnesium/aluminum alloy-barium nitrate-potassium perchlorate.

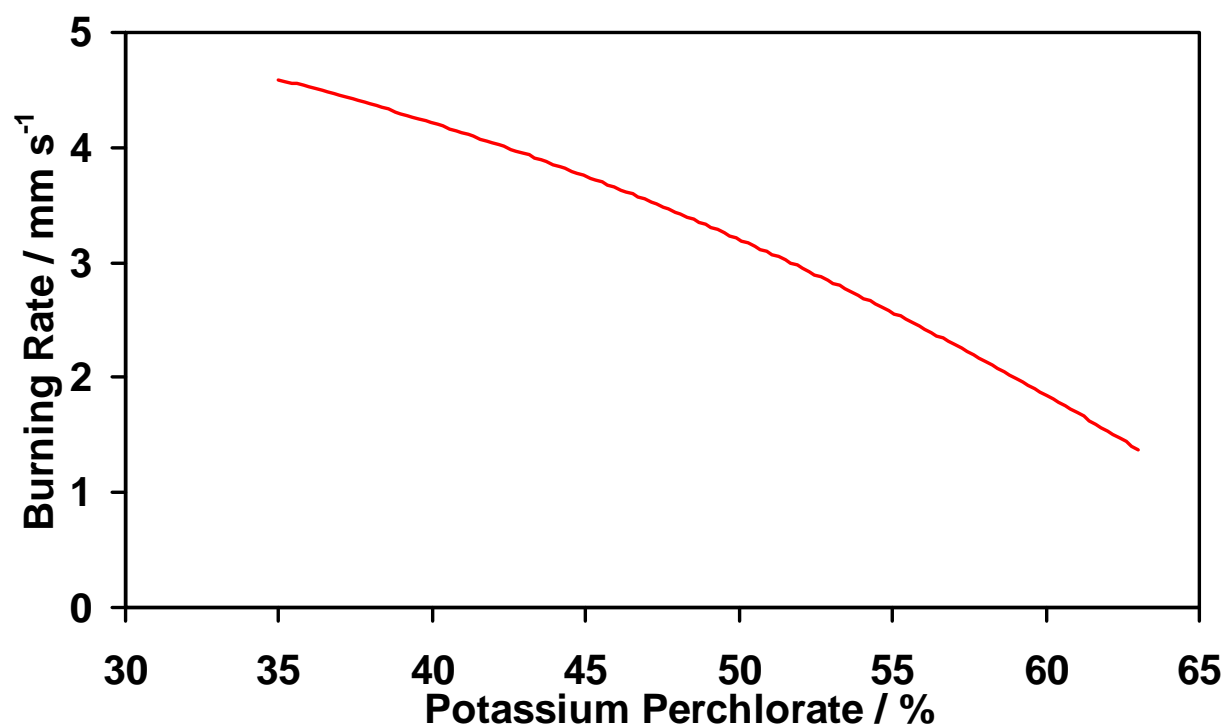


Figure 26; Burning rate curve for magnesium/aluminum alloy-potassium perchlorate-2% calcium resinate compositions.

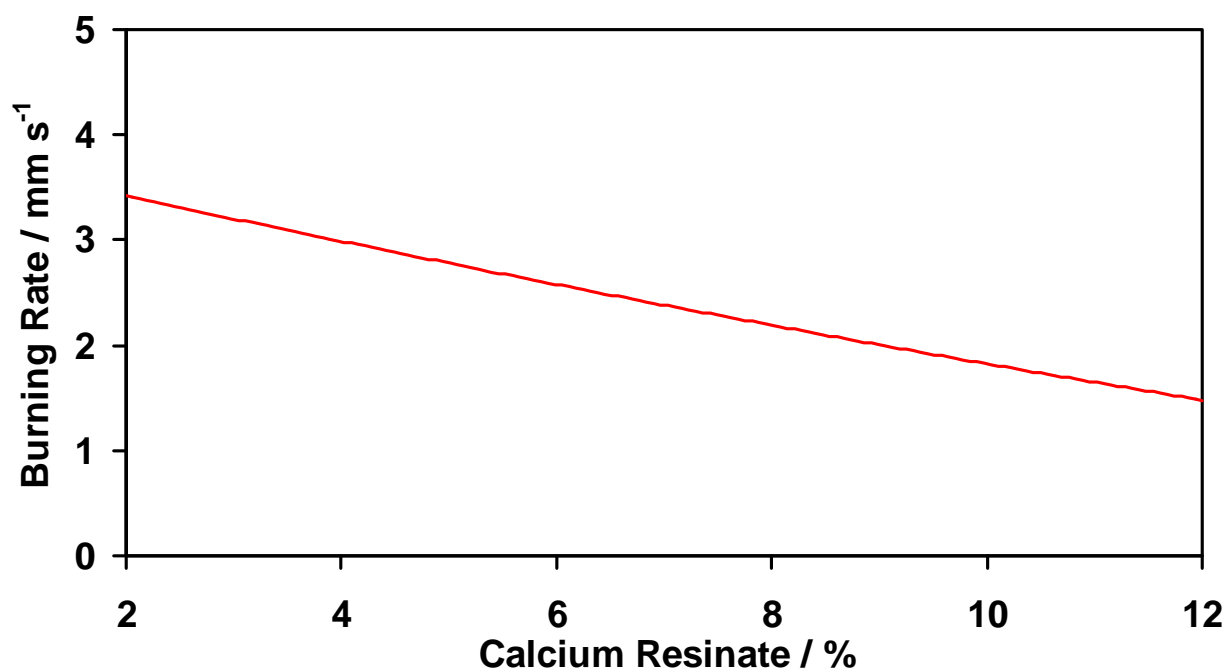


Figure 27; Burning rate curve for magnesium/aluminum alloy-potassium perchlorate-calcium resinate compositions with constant fuel:oxidant ratio and increasing calcium resinate content.

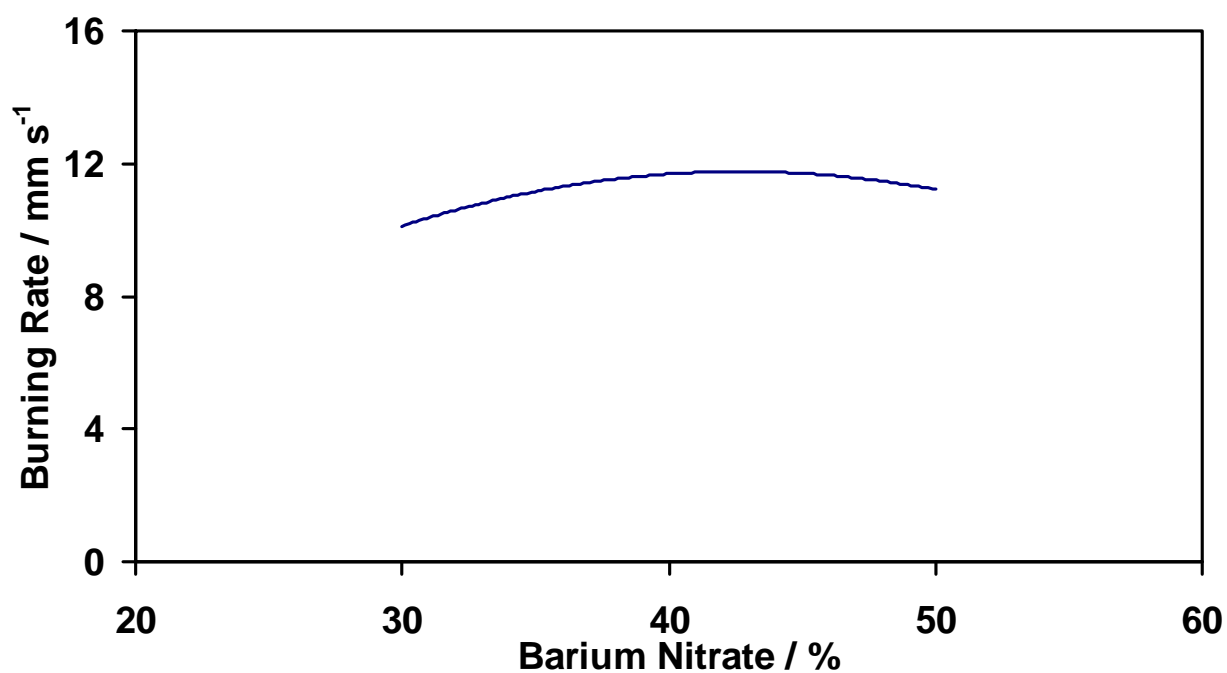


Figure 28; Burning rate curve for magnesium/aluminum alloy-barium nitrate compositions.

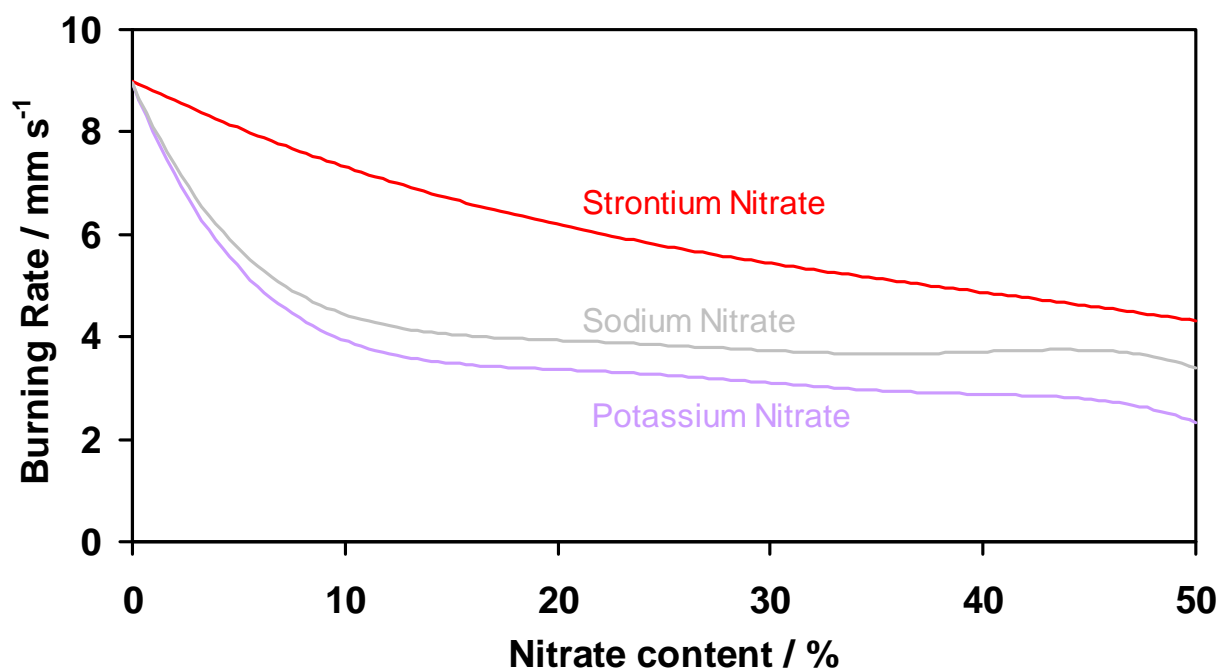


Figure 29; Burning rate curves for magnesium/aluminum alloy-barium nitrate-nitrate compositions.

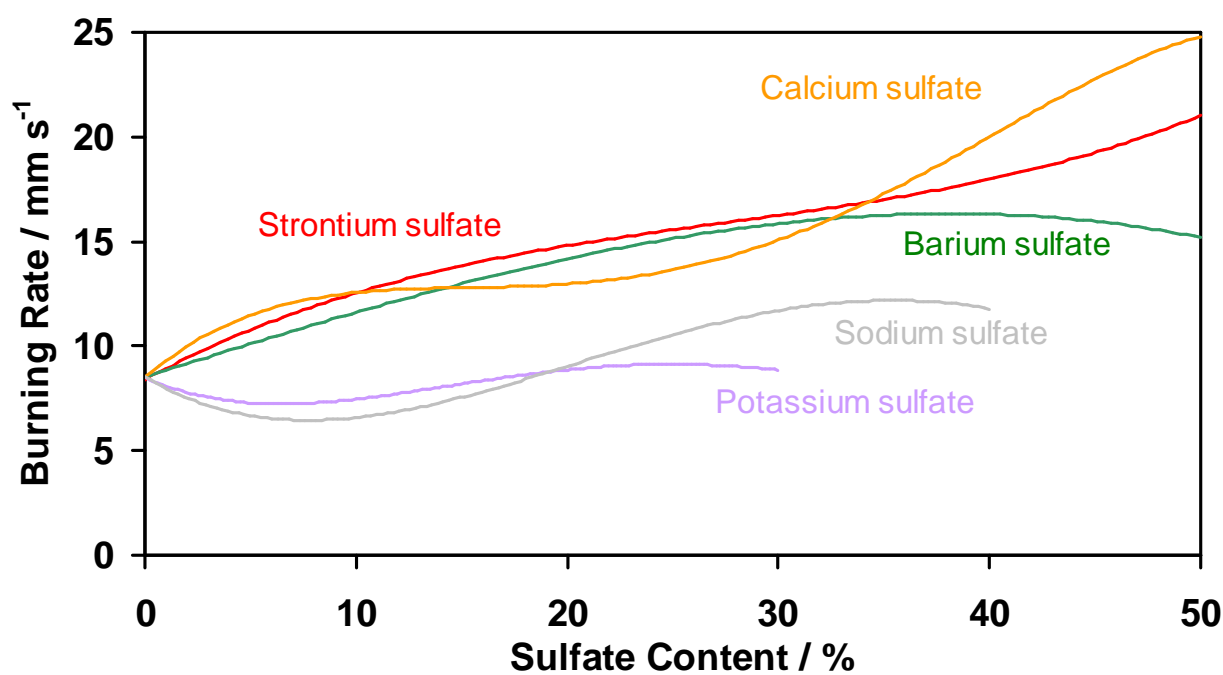


Figure 30; Burning rate curve for magnesium/aluminum alloy-barium nitrate-sulfate compositions.

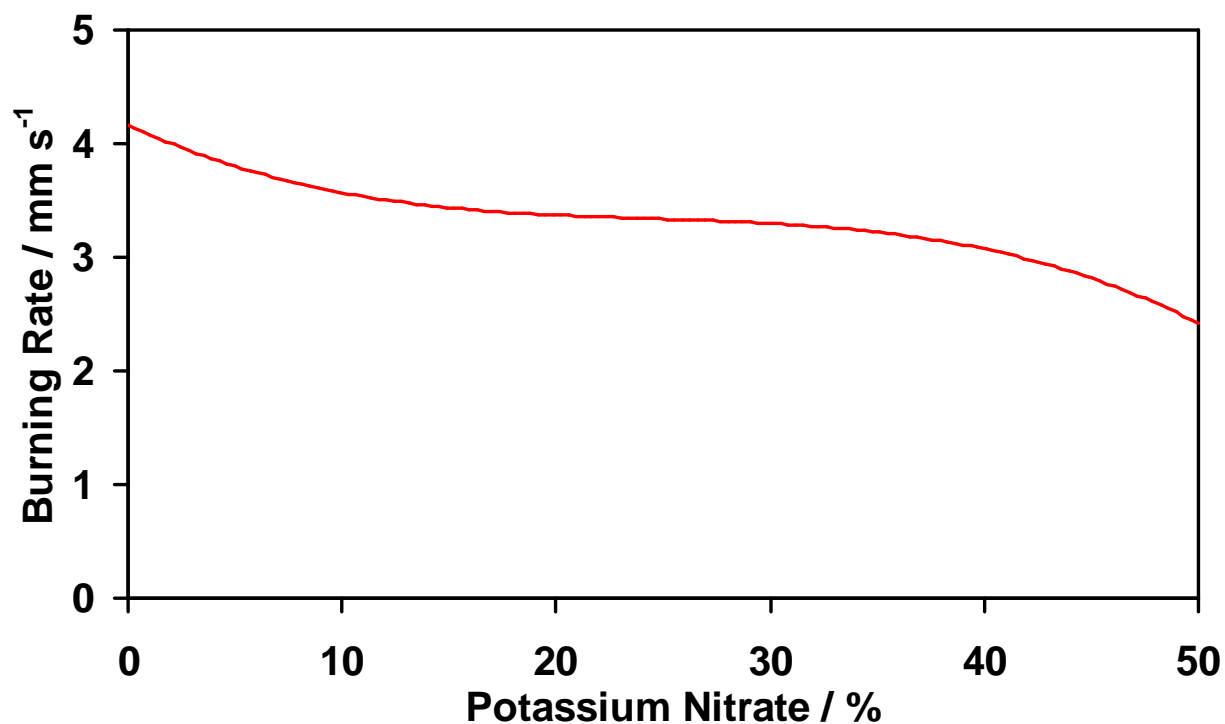


Figure 31; Burning rate curve for magnesium/aluminum alloy-strontium nitrate-potassium nitrate compositions.

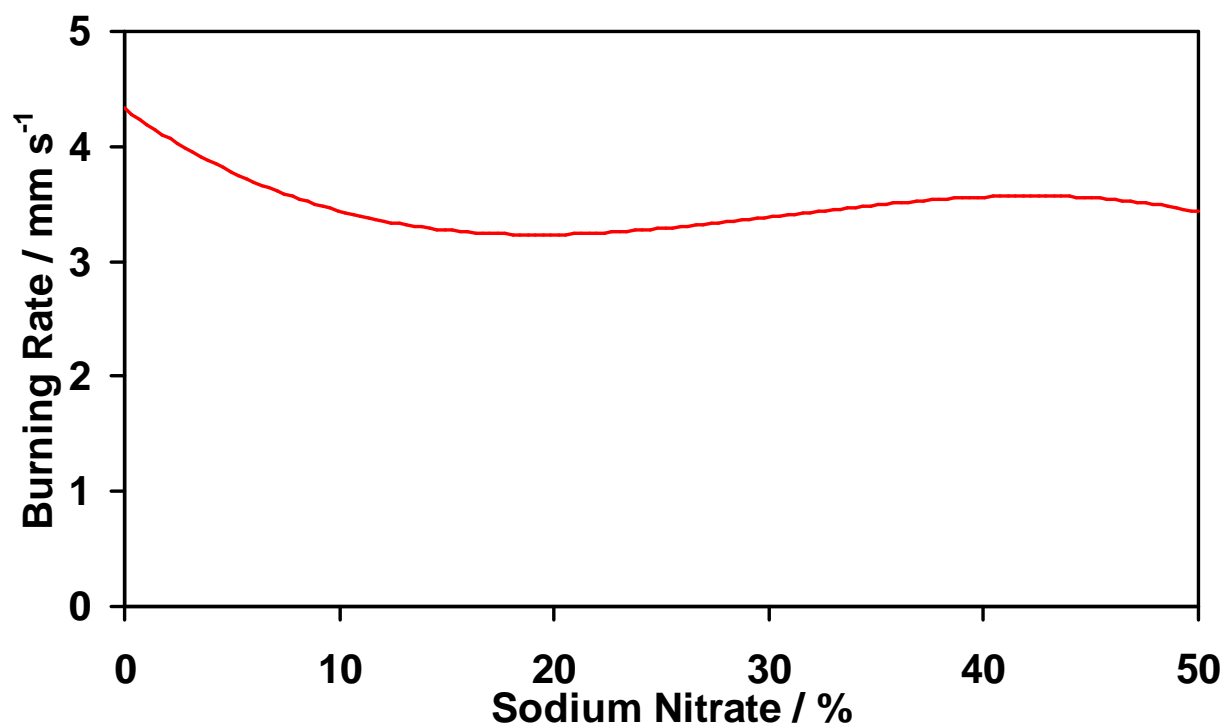


Figure 32; Burning rate curve for magnesium/aluminum alloy-strontium nitrate-sodium nitrate compositions.

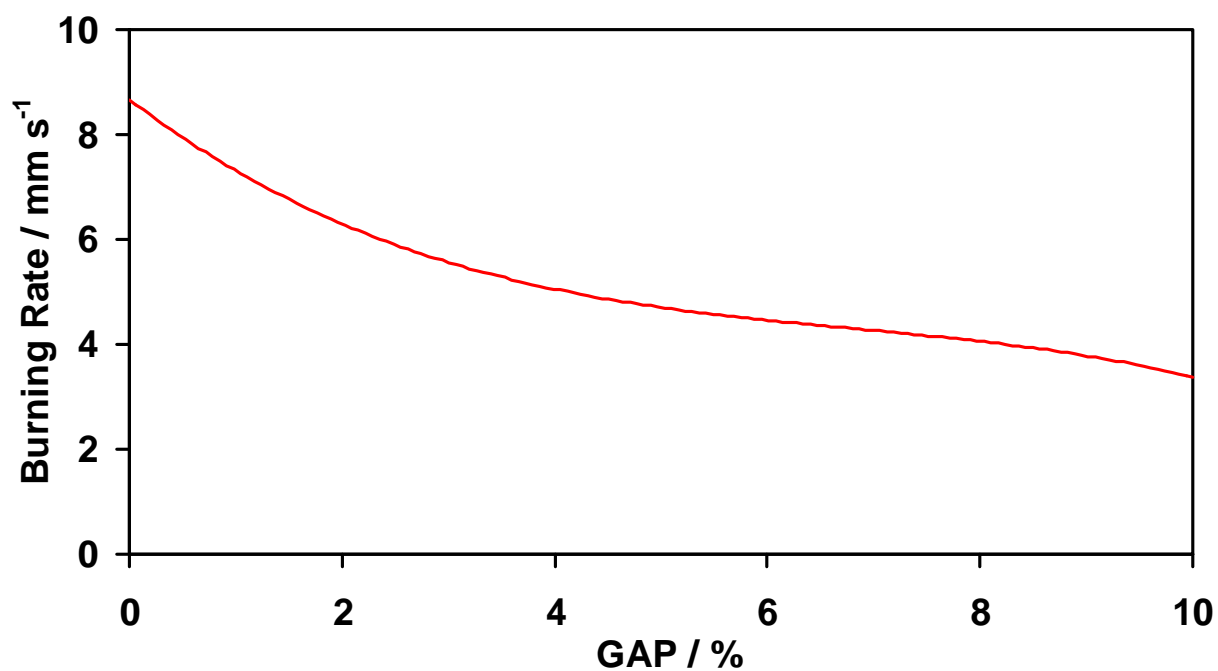


Figure 33; Burning rate curve for magnesium/aluminum alloy-barium nitrate-GAP compositions.

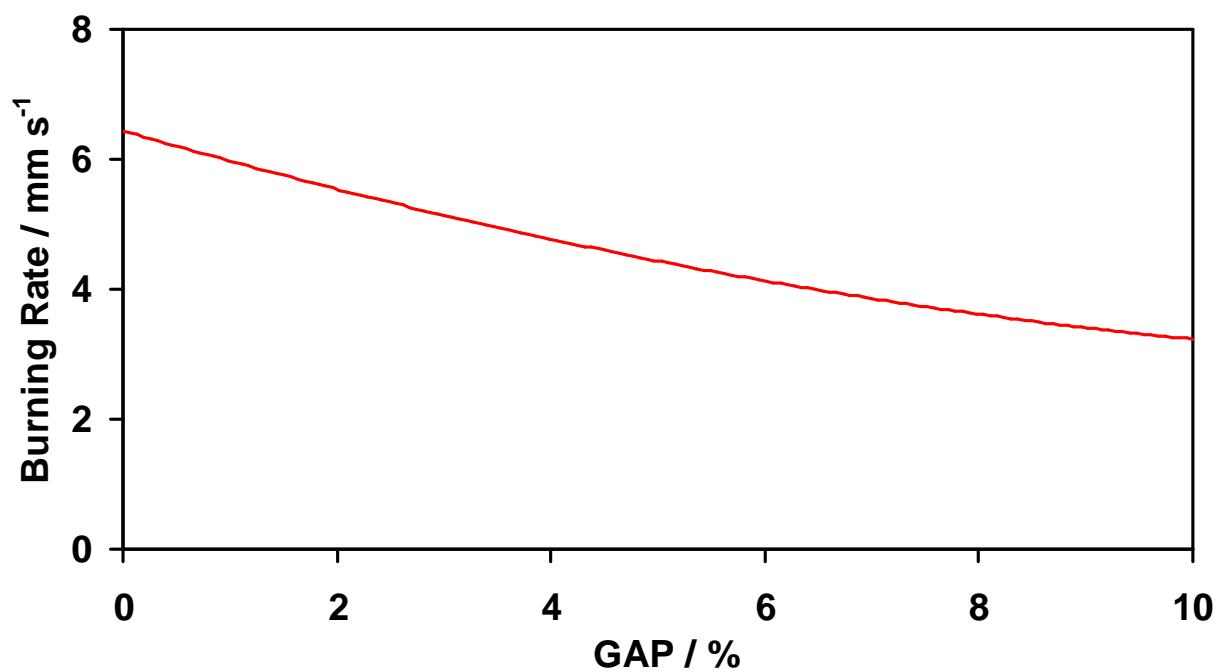


Figure 34; Burning rate curve for magnesium/aluminum alloy-barium nitrate-strontium nitrate-GAP compositions.

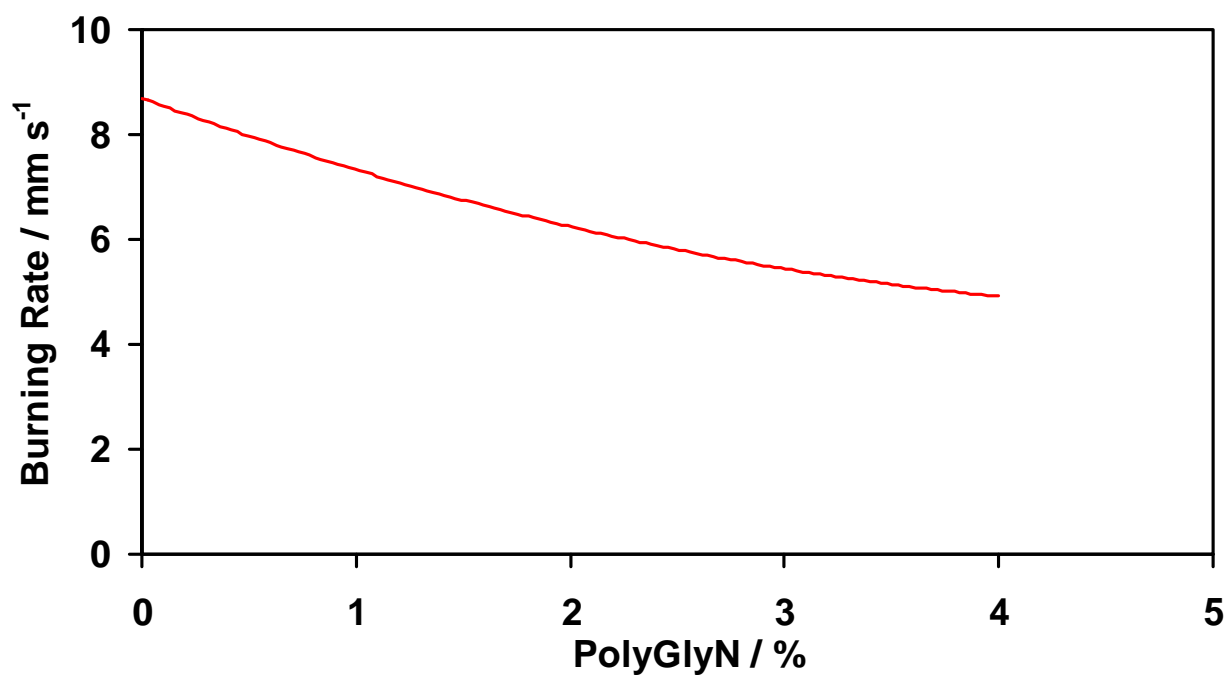


Figure 35; Burning rate curve for magnesium/aluminum alloy-barium nitrate-polyGlyN compositions.

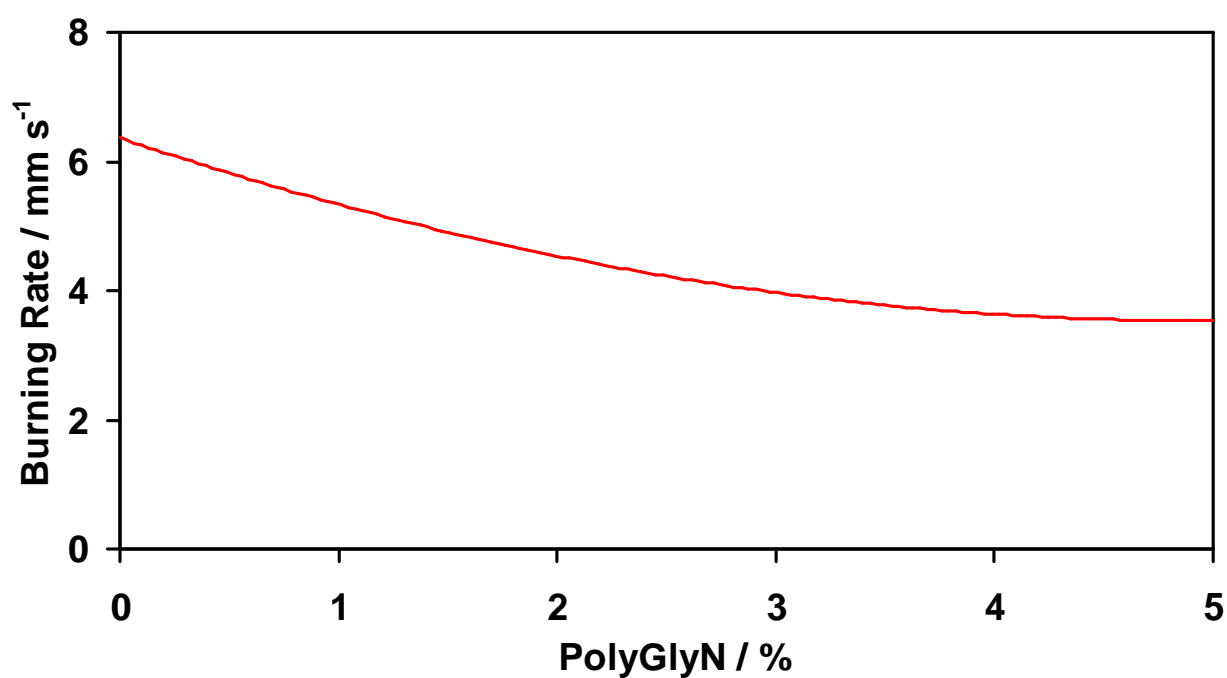


Figure 36; Burning rate curve for magnesium/aluminum alloy-barium nitrate-strontium nitrate-polyGlyN compositions.

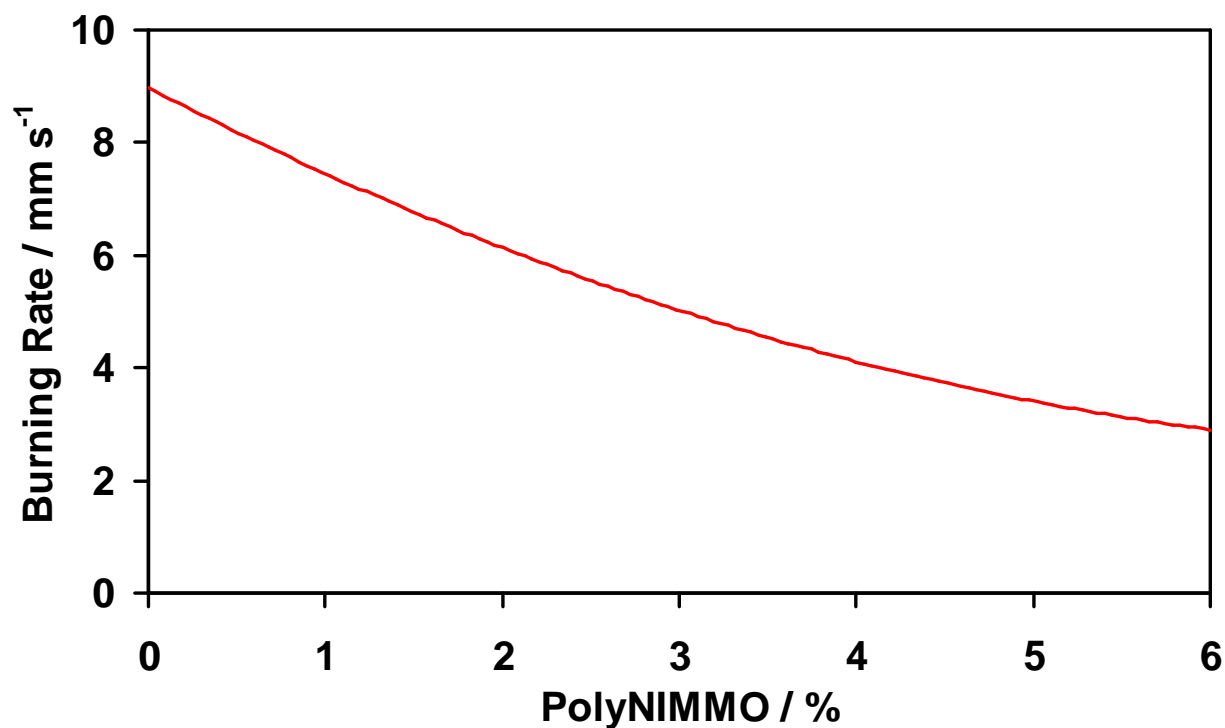


Figure 37; Burning rate curve for magnesium/aluminum alloy-barium nitrate-polyNIMMO compositions.

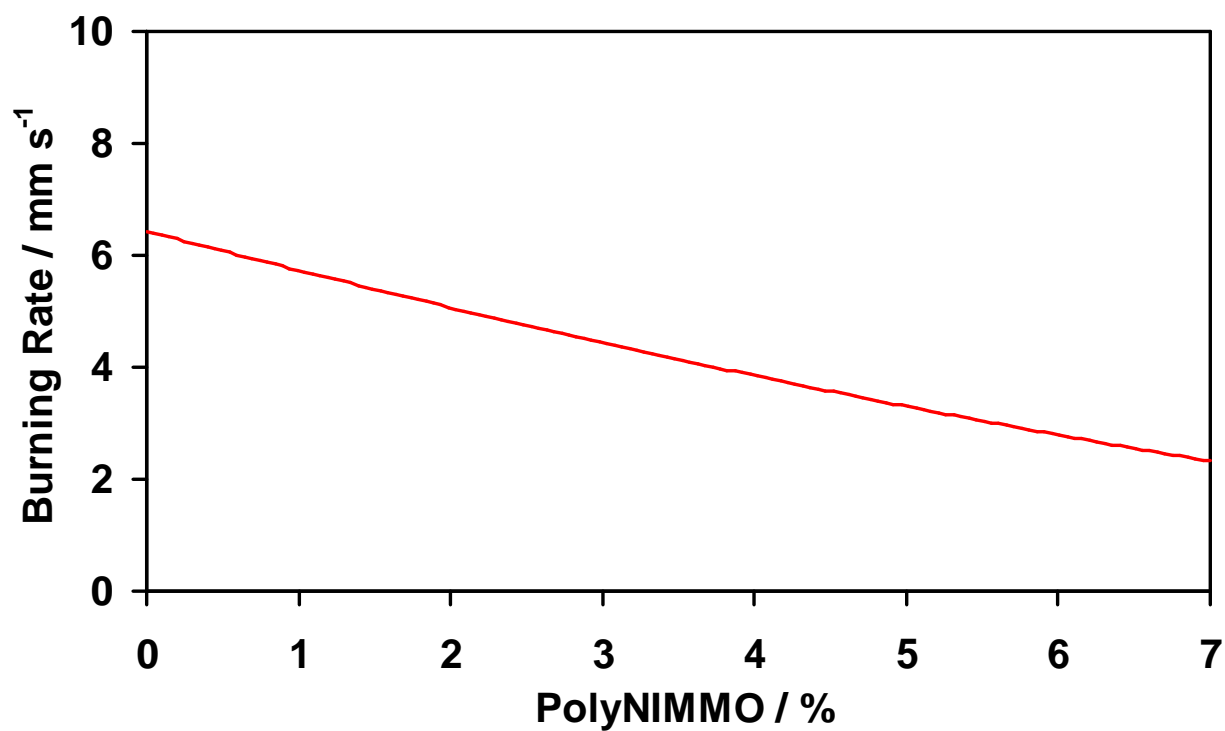


Figure 38; Burning rate curve for magnesium/aluminum alloy-barium nitrate-strontium nitrate-polyNIMMO compositions.

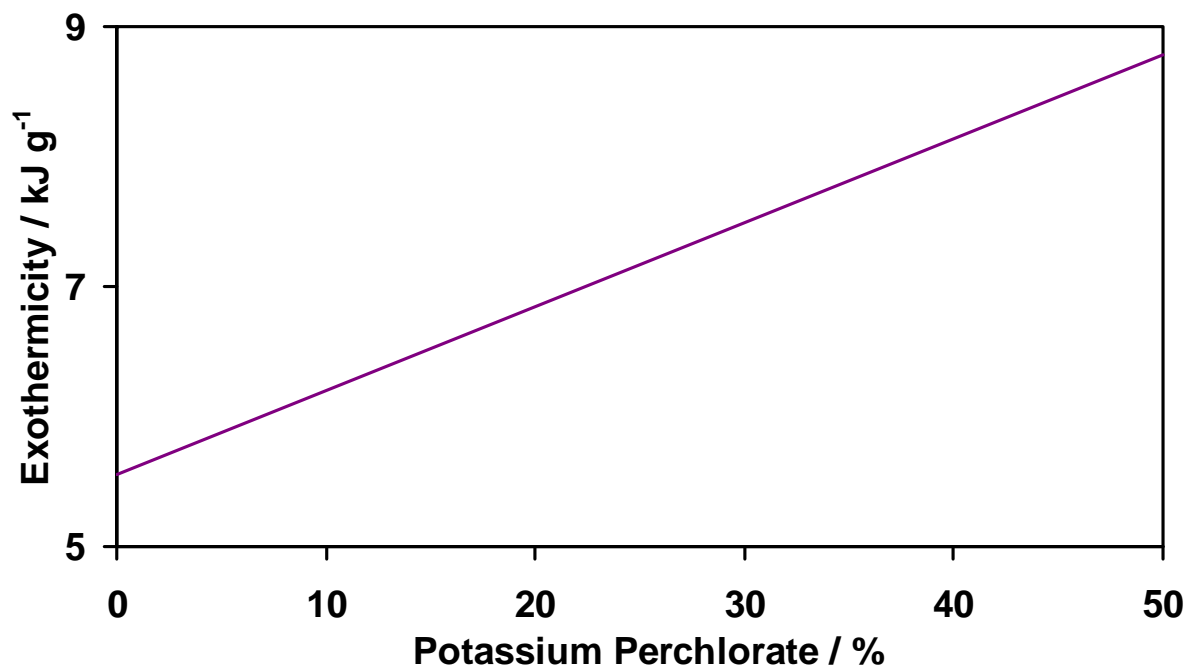


Figure 39; Exothermicity curve for magnesium/aluminum alloy-barium nitrate-potassium perchlorate.

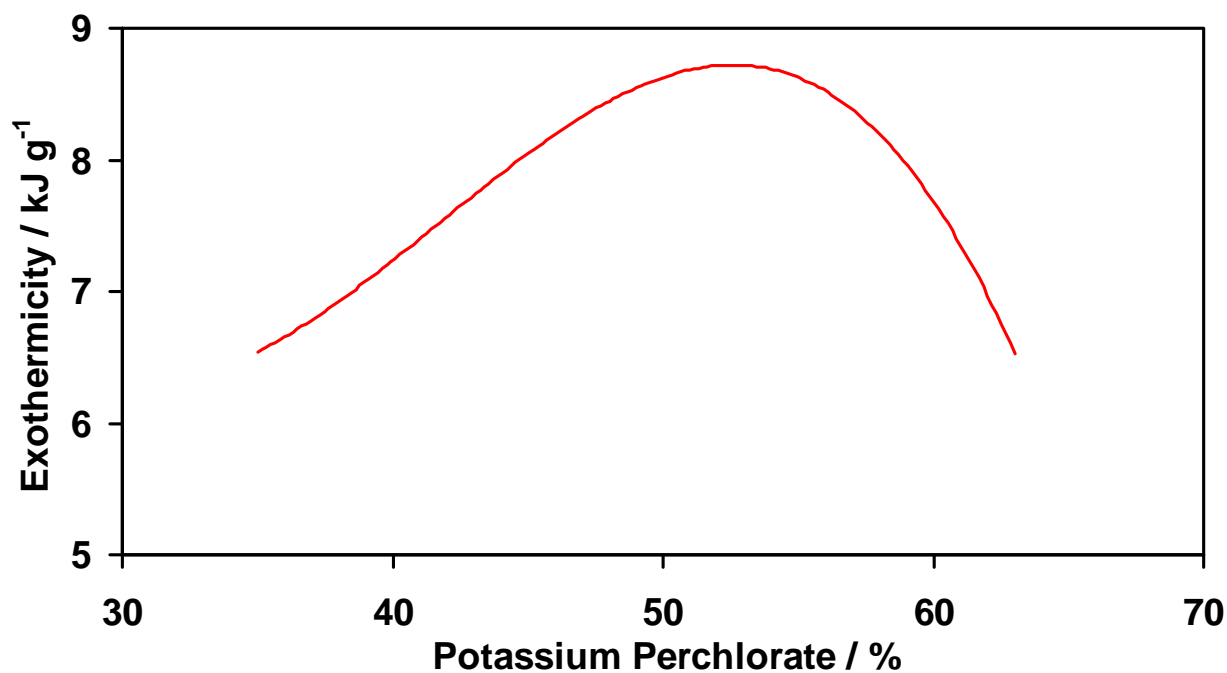


Figure 40; Exothermicity curve for magnesium/aluminum alloy-potassium perchlorate-2% calcium resinate.

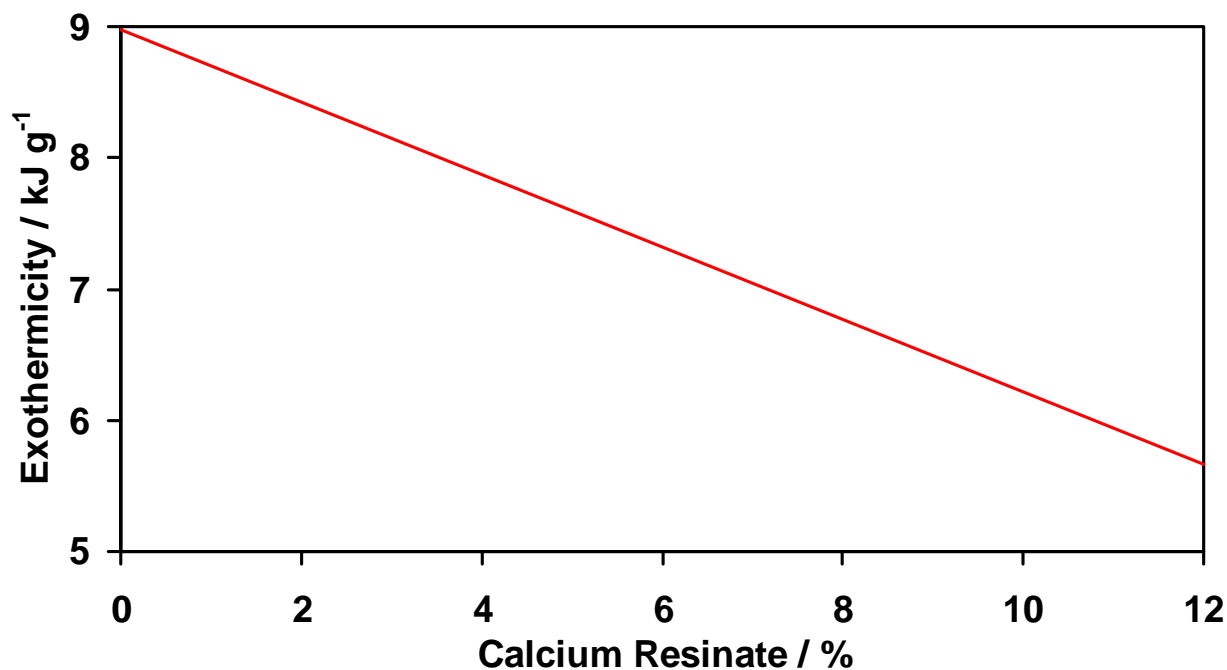


Figure 41; Exothermicity curve for magnesium/aluminum alloy-potassium perchlorate-calcium resinate compositions with constant fuel:oxidant ratio and increasing calcium resinate content.

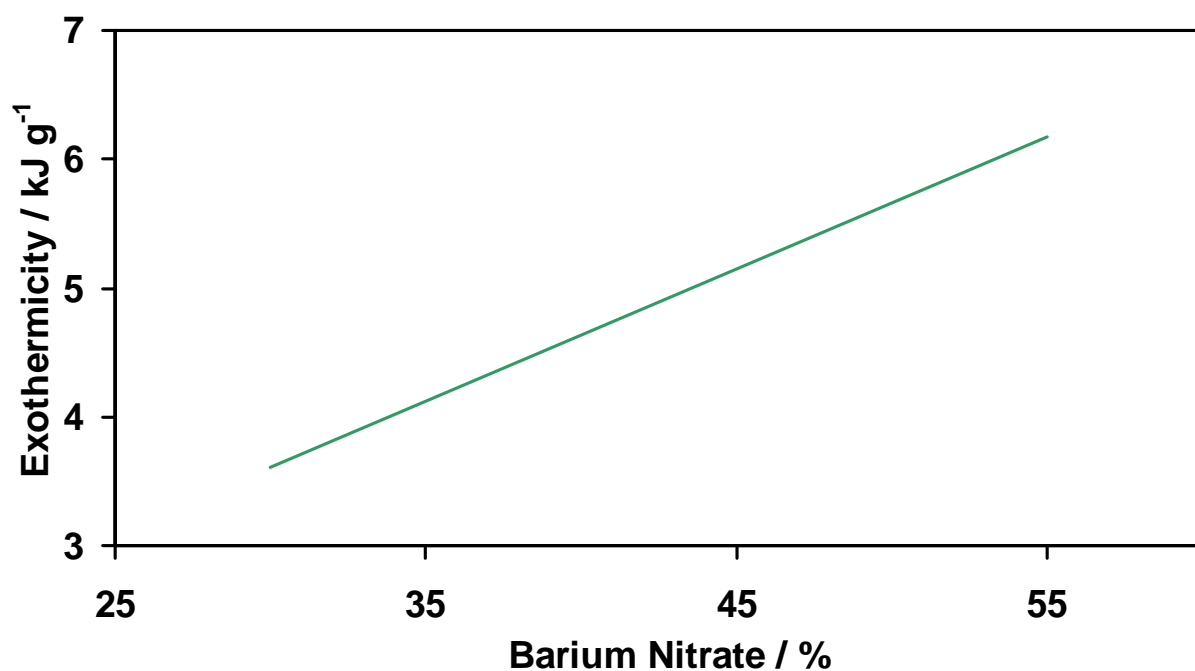


Figure 42; Exothermicity curve for magnesium/aluminum alloy-barium nitrate compositions. (Sample mass, 100 mg; 1 atmosphere, argon)

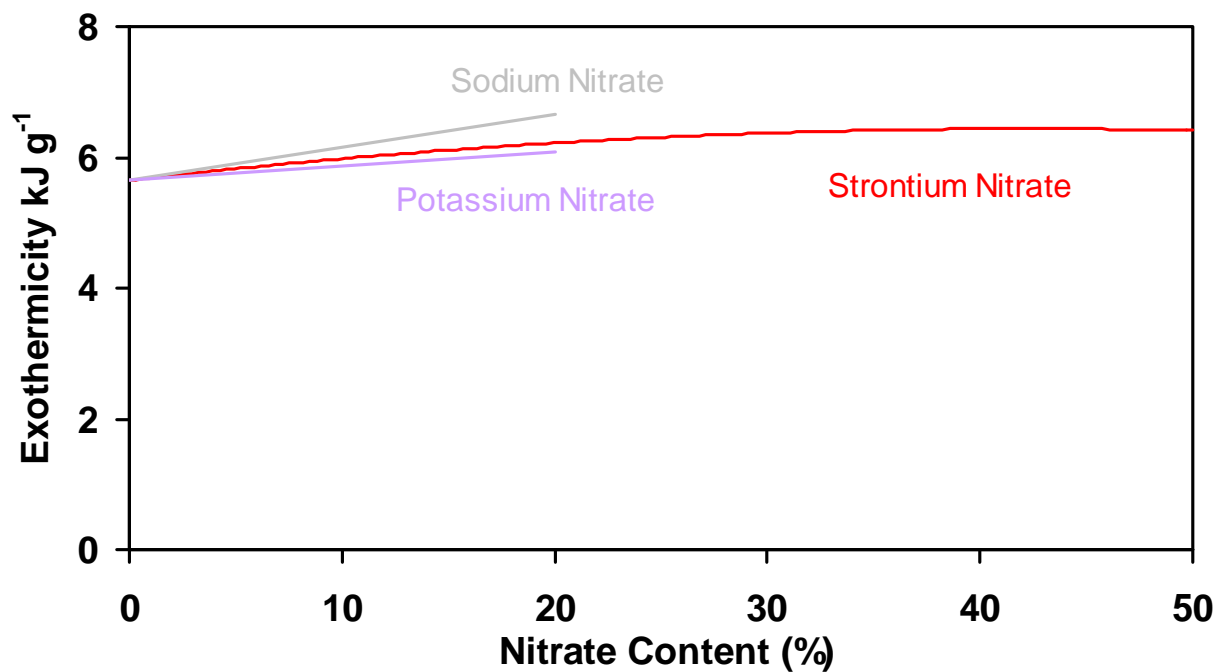


Figure 43; Exothermicity curve for magnesium/aluminum alloy-barium nitrate-nitrates.

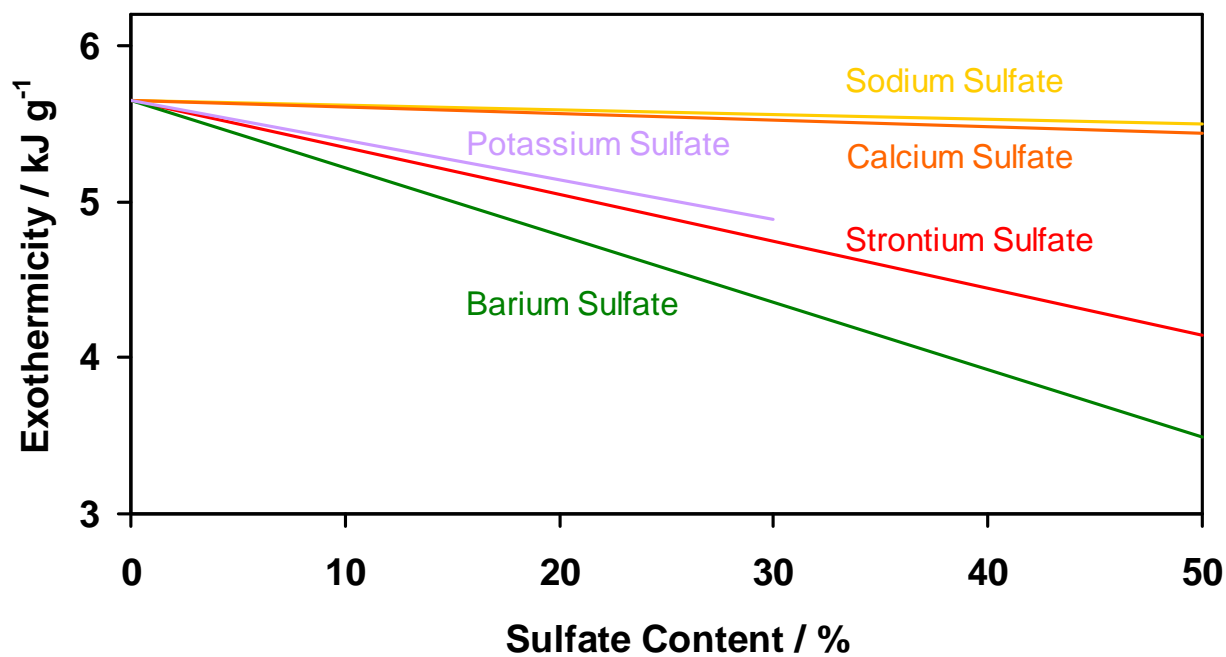


Figure 44; Exothermicity curve for magnesium/aluminum alloy-barium nitrate-sulfates.
(Sample mass, 100 mg; 1 atmosphere, argon)

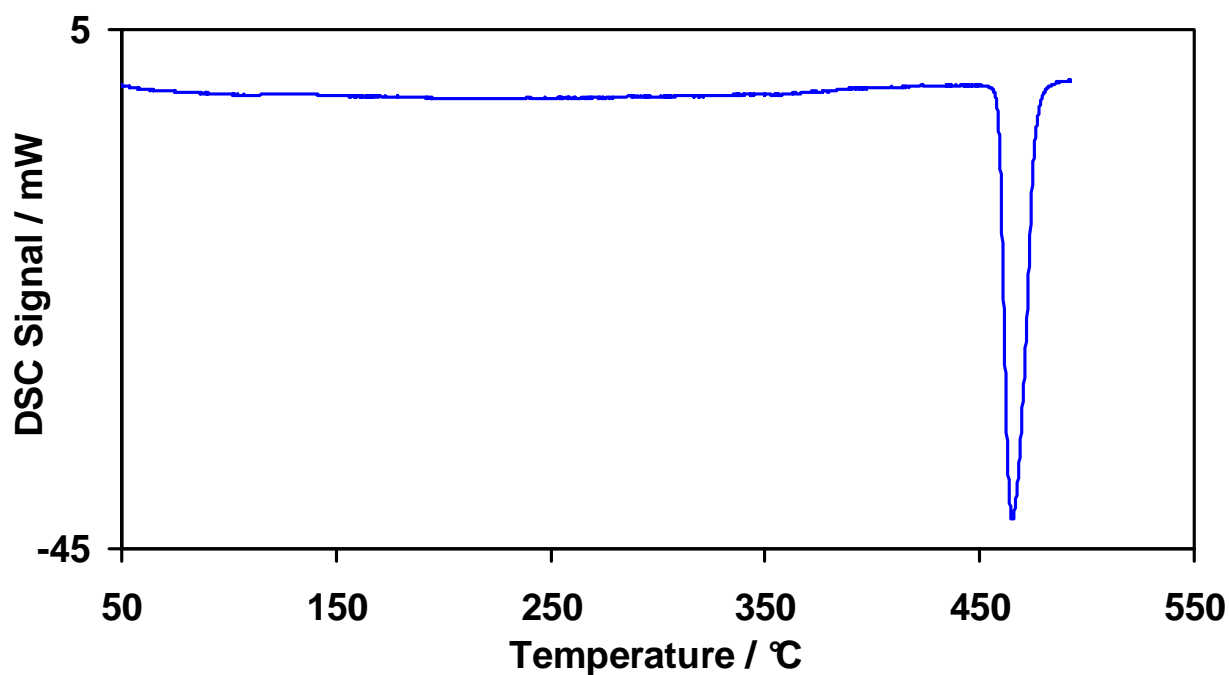


Figure 45; DSC Curve for a magnesium/aluminum alloy.
(Sample mass, 10 mg; heating rate, 10 °C min⁻¹; atmosphere, argon)

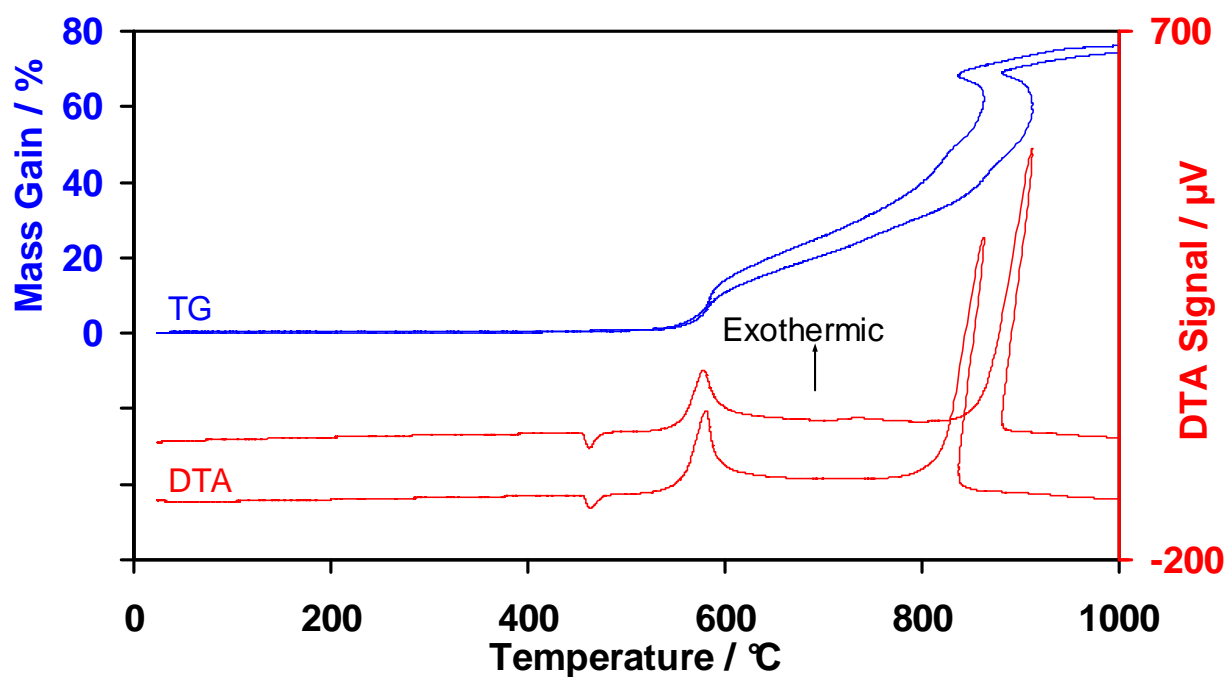


Figure 46; Simultaneous thermogravimetry-DSC curves for the oxidation of magnesium/aluminum alloy.
(Sample mass, mg; heating rate, 10 °C min⁻¹; atmosphere, air)

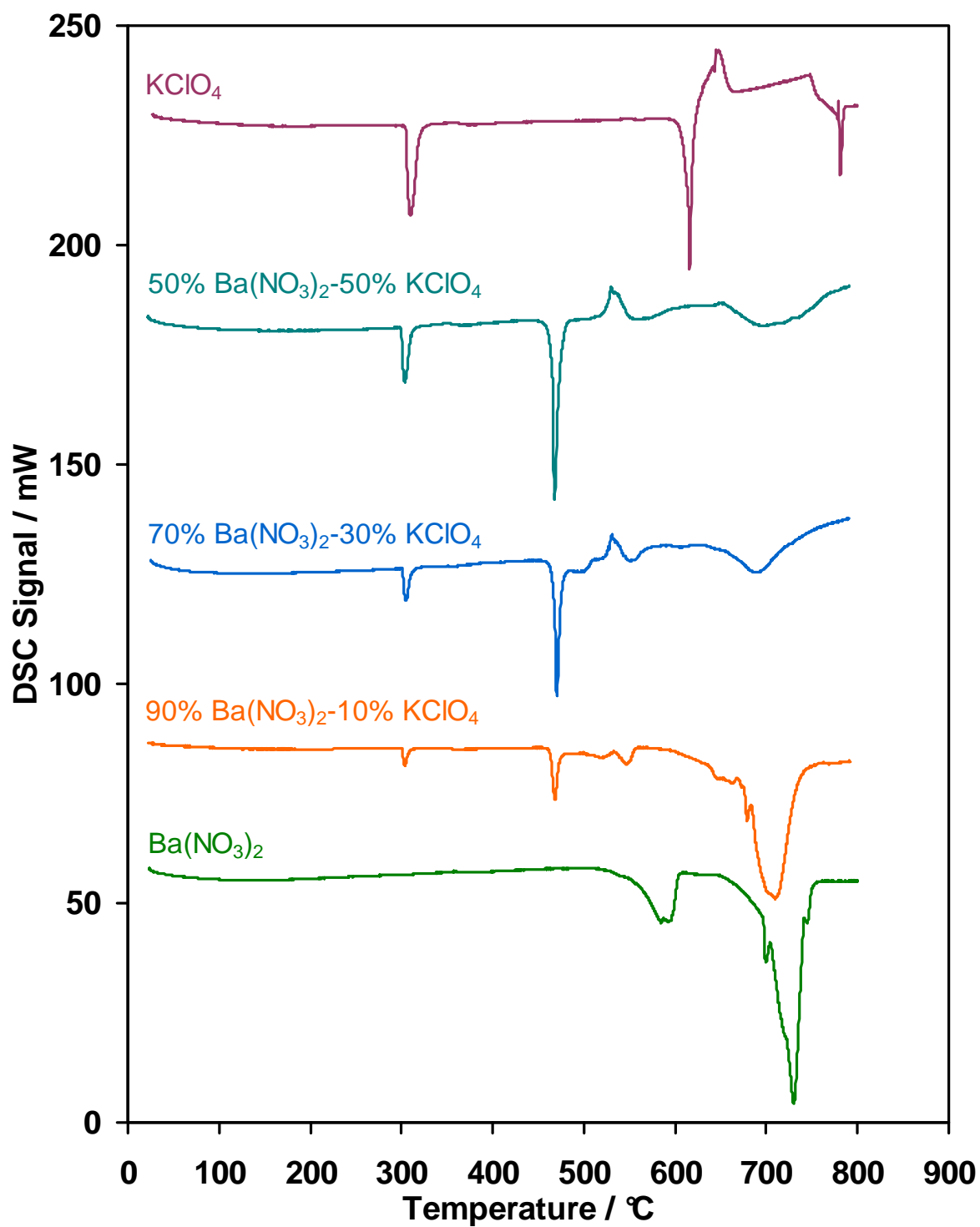


Figure 47; DSC curves for potassium perchlorate, barium nitrate and mixtures of these oxidants.

(Sample mass, 10 mg; heating rate, 10 °C min⁻¹; atmosphere, argon)

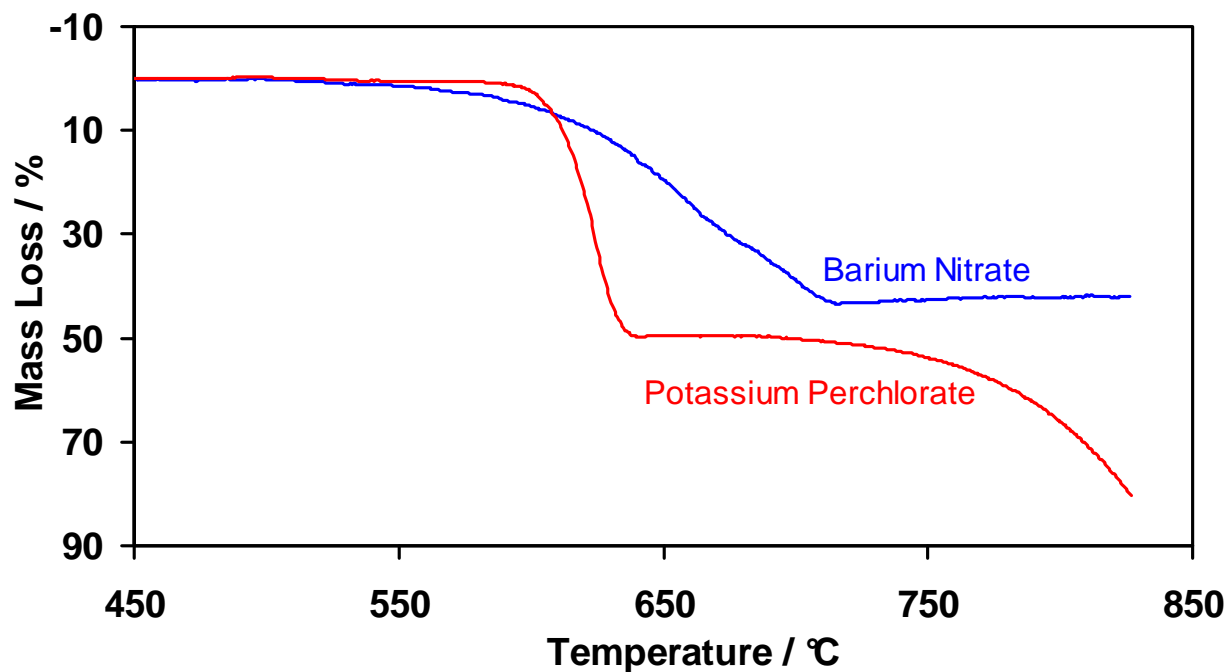


Figure 48; TG curves for barium nitrate and potassium perchlorate.
(Sample mass, 5 mg; heating rate, 10 °C min⁻¹; atmosphere, argon)

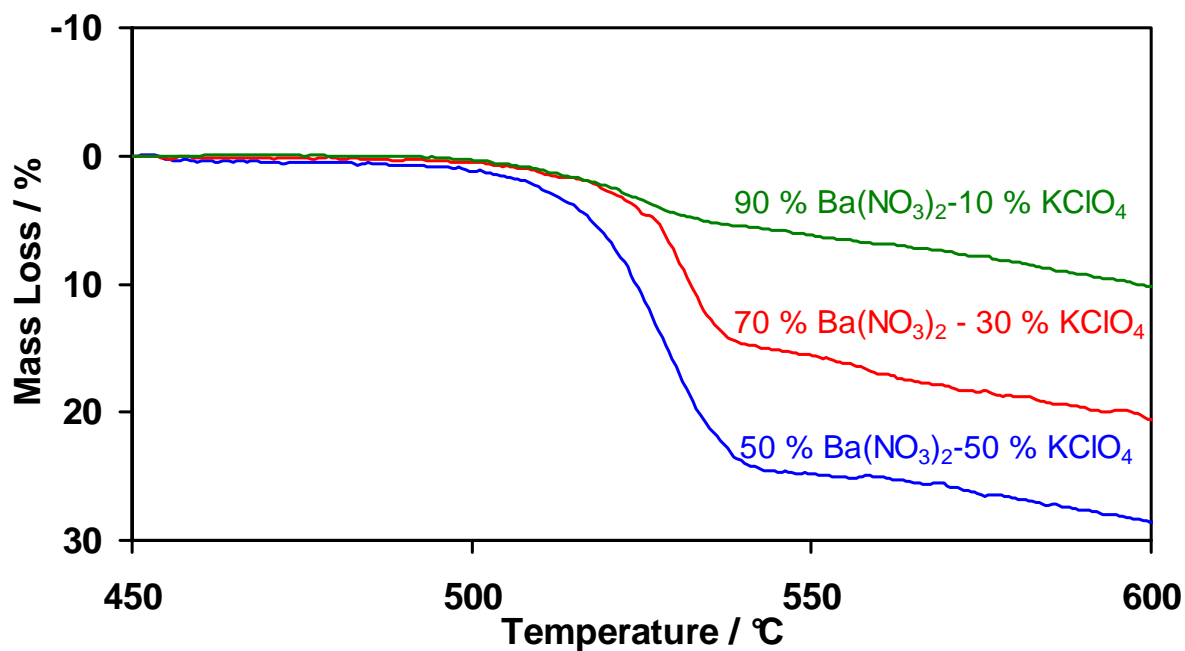


Figure 49; TG curves for barium nitrate potassium perchlorate mixtures.
(Sample mass, 5 mg; heating rate, 10 °C min⁻¹; atmosphere, argon)

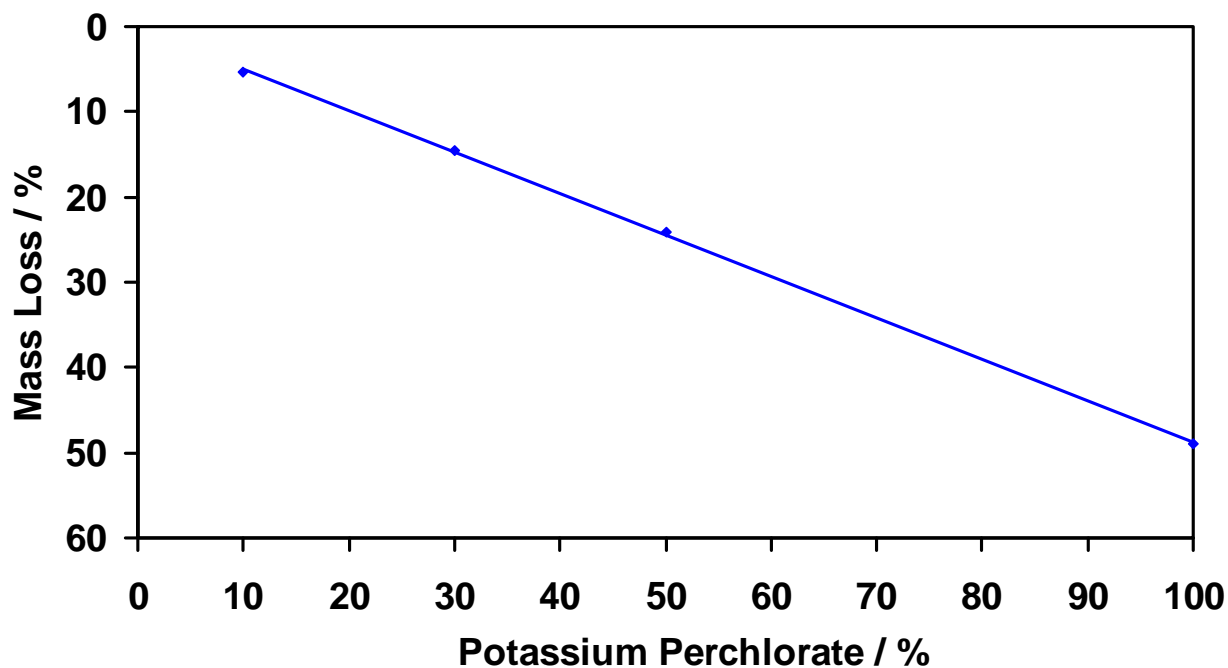


Figure 50; Initial mass loss stage against potassium perchlorate content for a range of barium nitrate-potassium perchlorate mixtures.
(Sample mass, 5 mg; heating rate, $10\text{ }^{\circ}\text{C min}^{-1}$; atmosphere, argon)

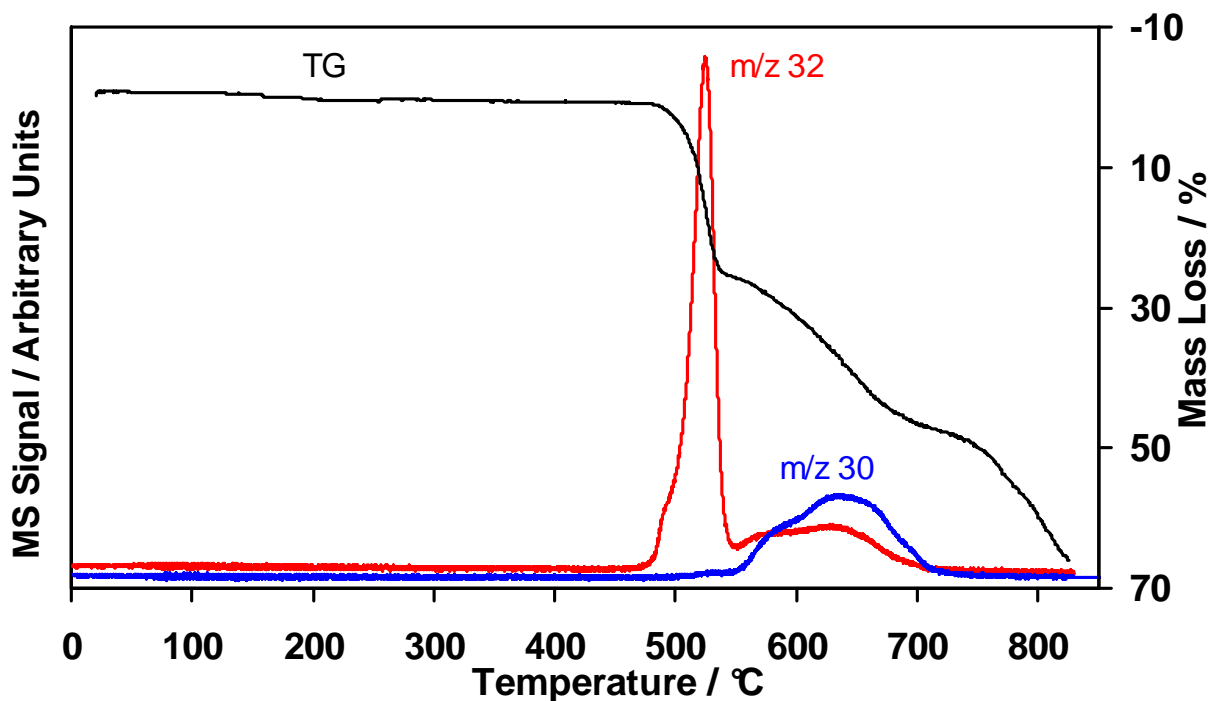


Figure 51; TG-mass spectrometry curves for the decomposition of a 50% barium nitrate-50% potassium perchlorate mixture.
(Sample mass, 5 mg; heating rate, $10\text{ }^{\circ}\text{C min}^{-1}$; atmosphere, argon).

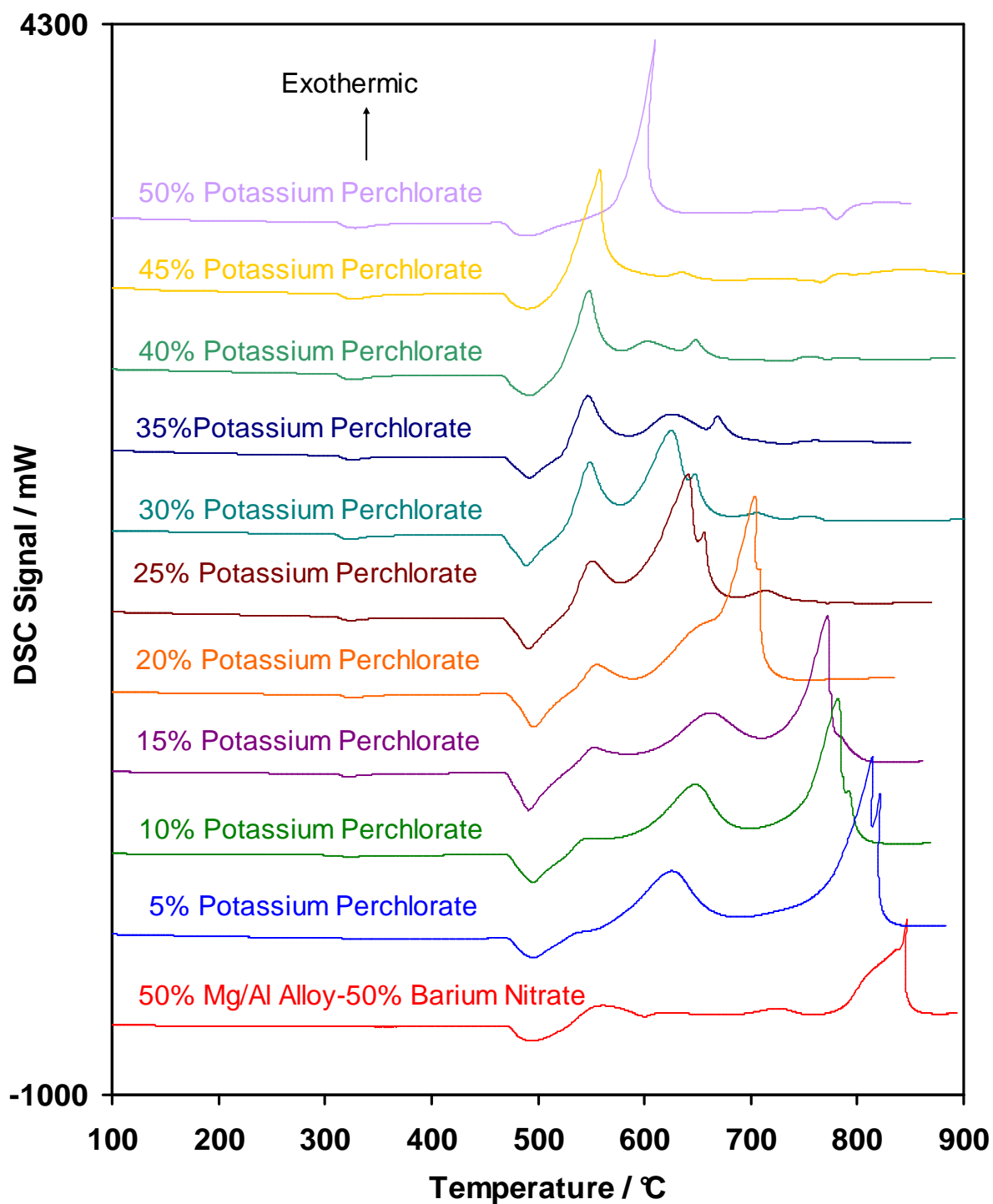


Figure 52; Ignition DSC curves for a range of magnesium/aluminum alloy-barium nitrate-potassium perchlorate compositions.
(Sample mass, 20 mg; heating rate, 50 °C min⁻¹; atmosphere, argon)

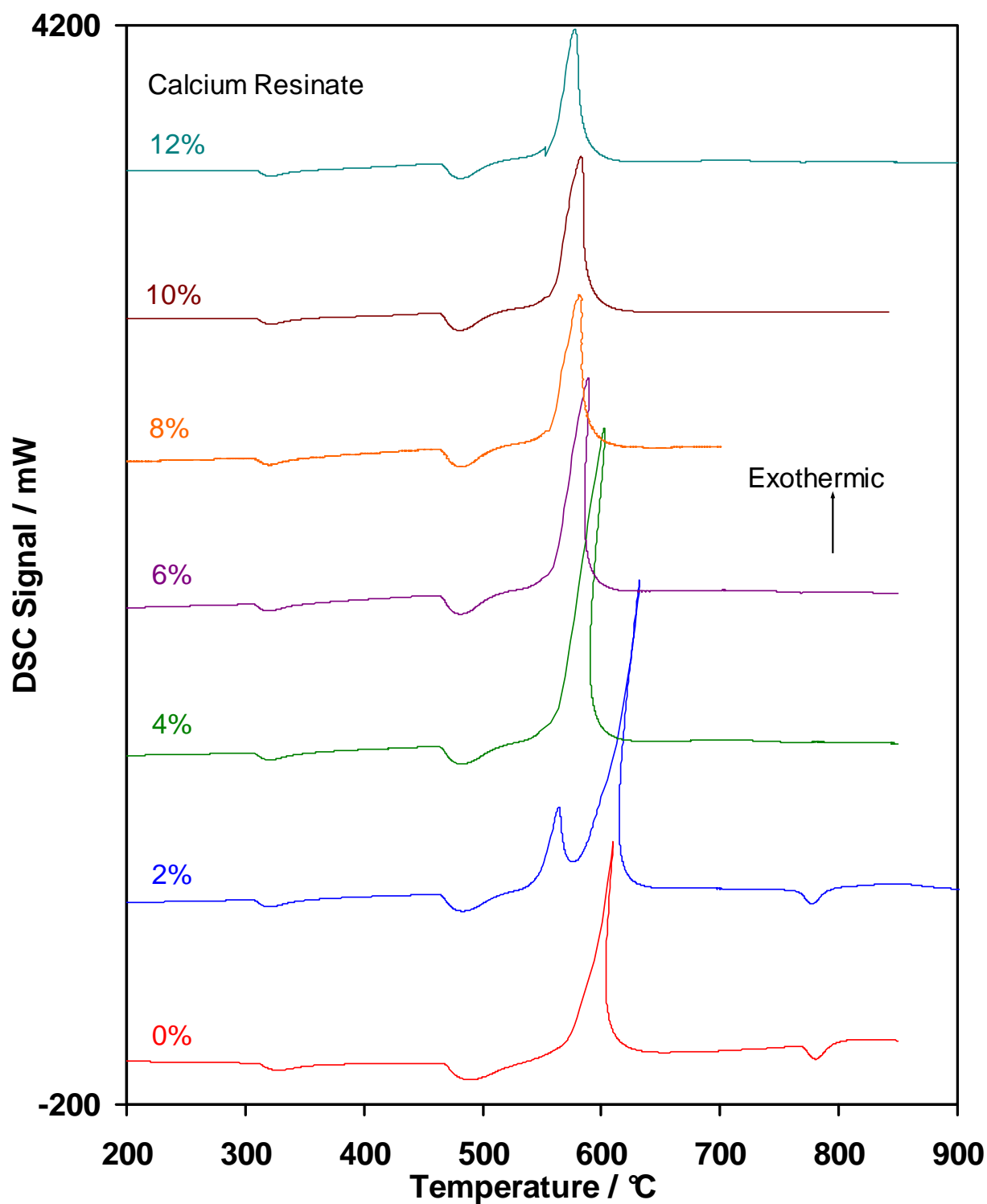


Figure 53; Ignition DSC curves for a range of magnesium/aluminum alloy-potassium perchlorate-calcium resinate compositions containing equal masses of magnesium/aluminum alloy and potassium perchlorate.
(Sample mass, 20 mg; heating rate, 50 °C min⁻¹; atmosphere, argon)

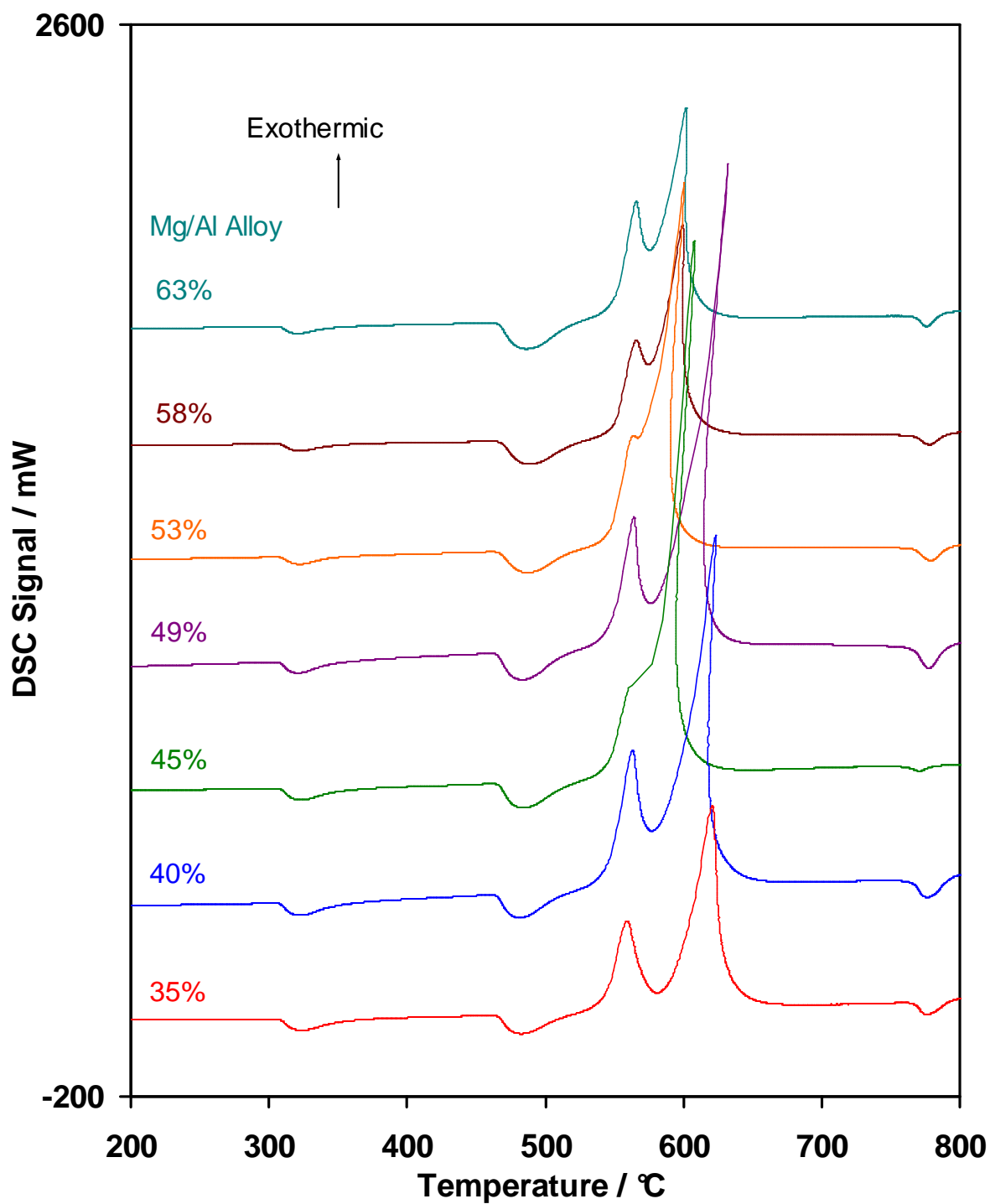


Figure 54; Ignition DSC curves for a range of magnesium/aluminum alloy-potassium perchlorate-2% calcium resinate compositions.
(Sample mass, 20 mg; heating rate, 50 °C min⁻¹; atmosphere, argon)

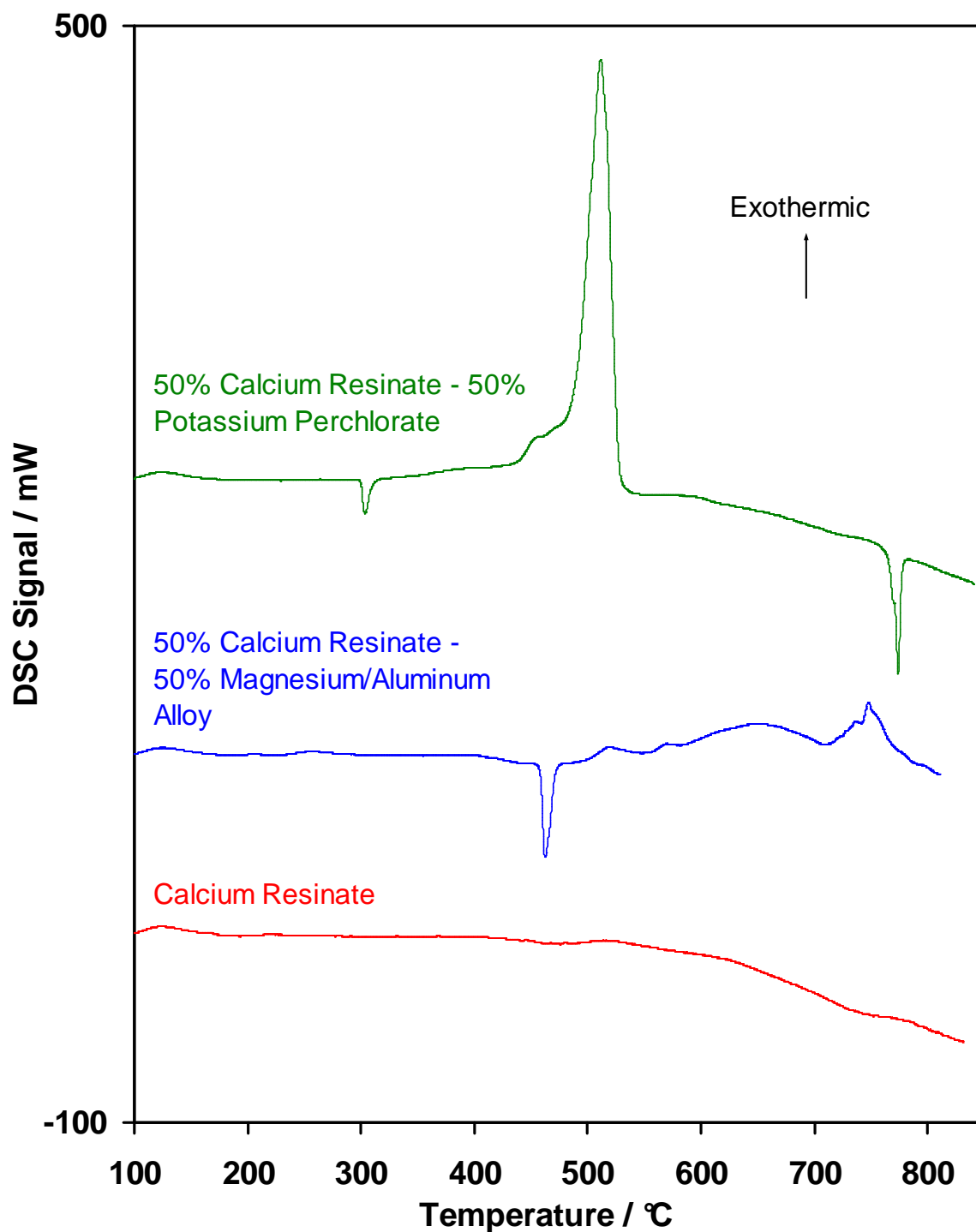


Figure 55; DSC curves for a range of mixtures of calcium resinate with magnesium/aluminum alloy and potassium perchlorate.
(Sample mass, 20 mg; heating rate, $10\text{ }^{\circ}\text{C min}^{-1}$; atmosphere, argon)

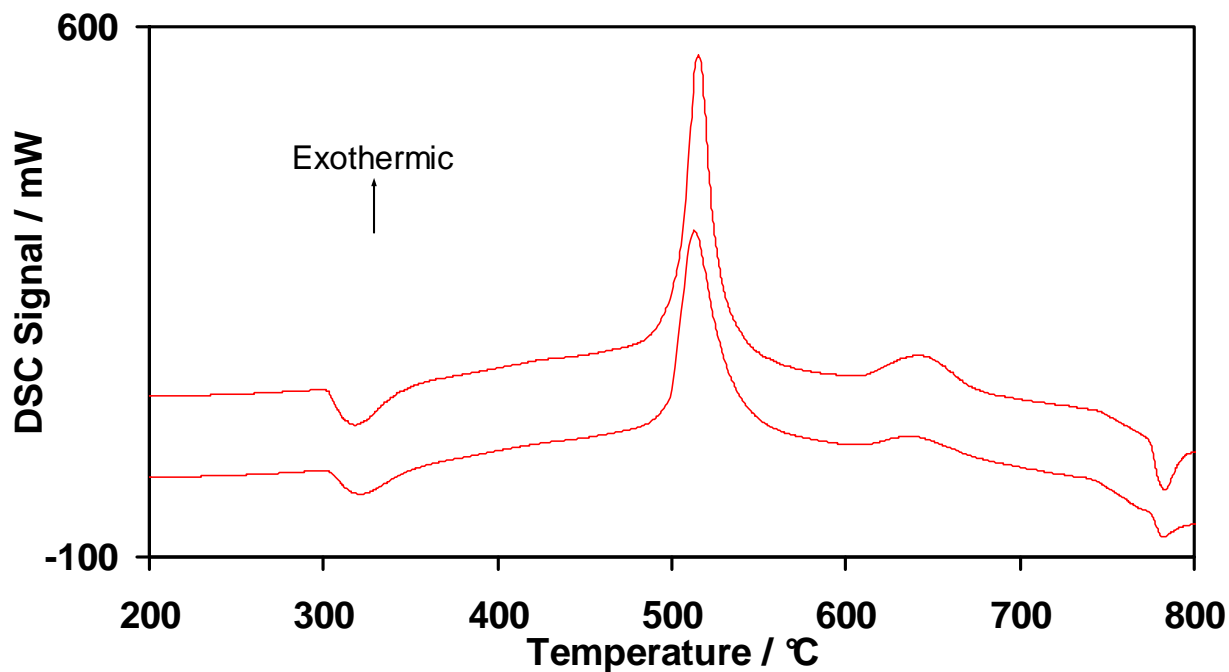


Figure 56; DSC curves for a 78.6% potassium perchlorate-21.4% calcium resinate mixture. (Sample mass, 20 mg; heating rate, 50 °C min⁻¹; atmosphere, argon)

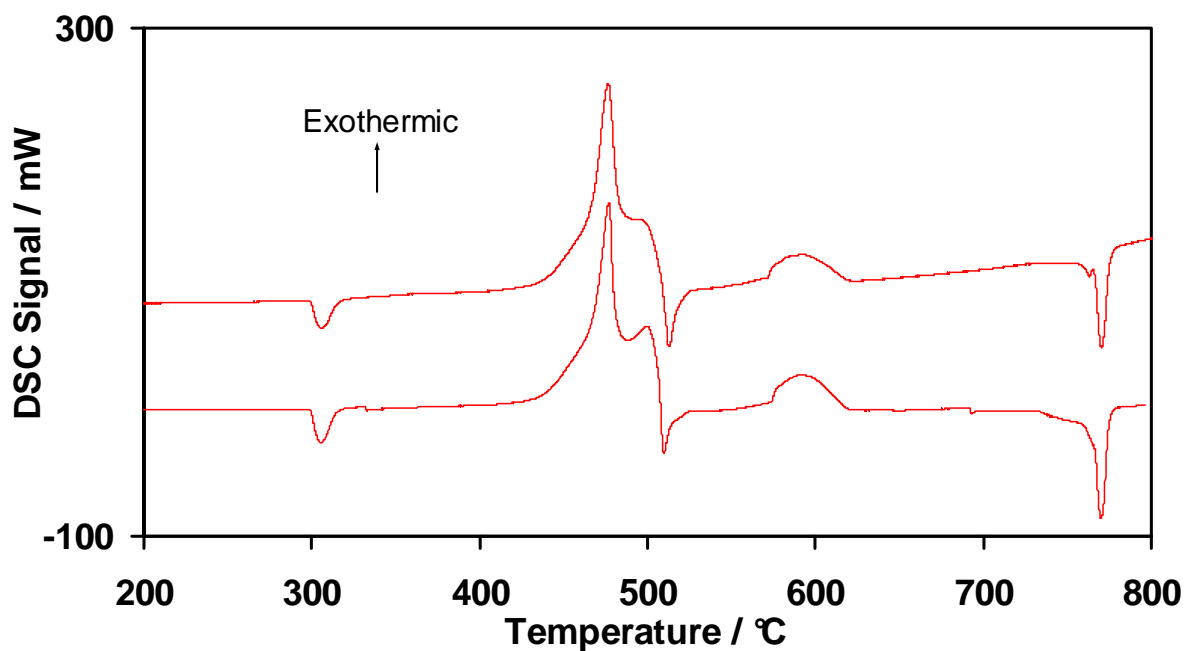


Figure 57; DSC curves for a 78.6% potassium perchlorate-21.4% calcium resinate mixture. (Sample mass, 20 mg; heating rate, 10 °C min⁻¹; atmosphere, argon)

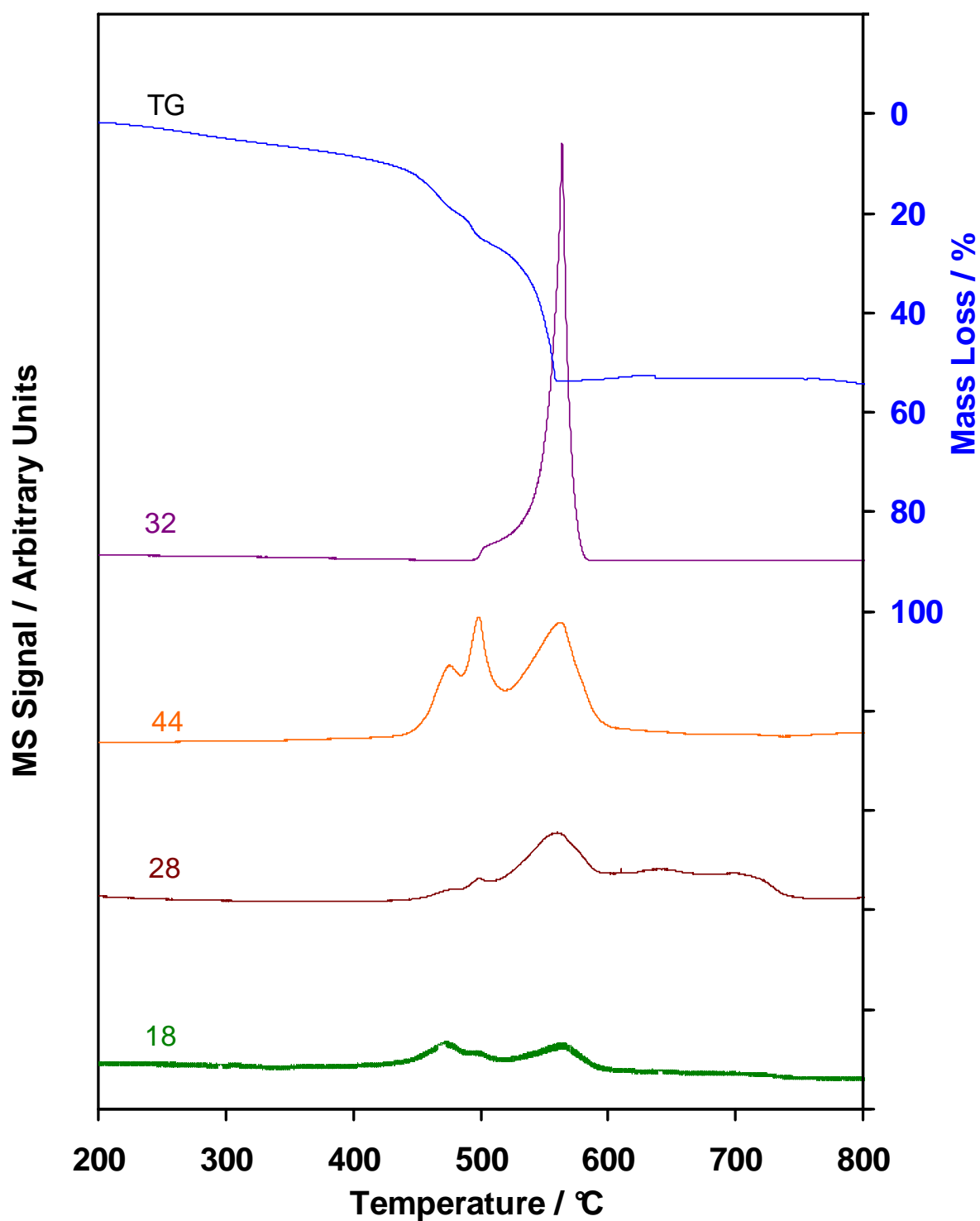
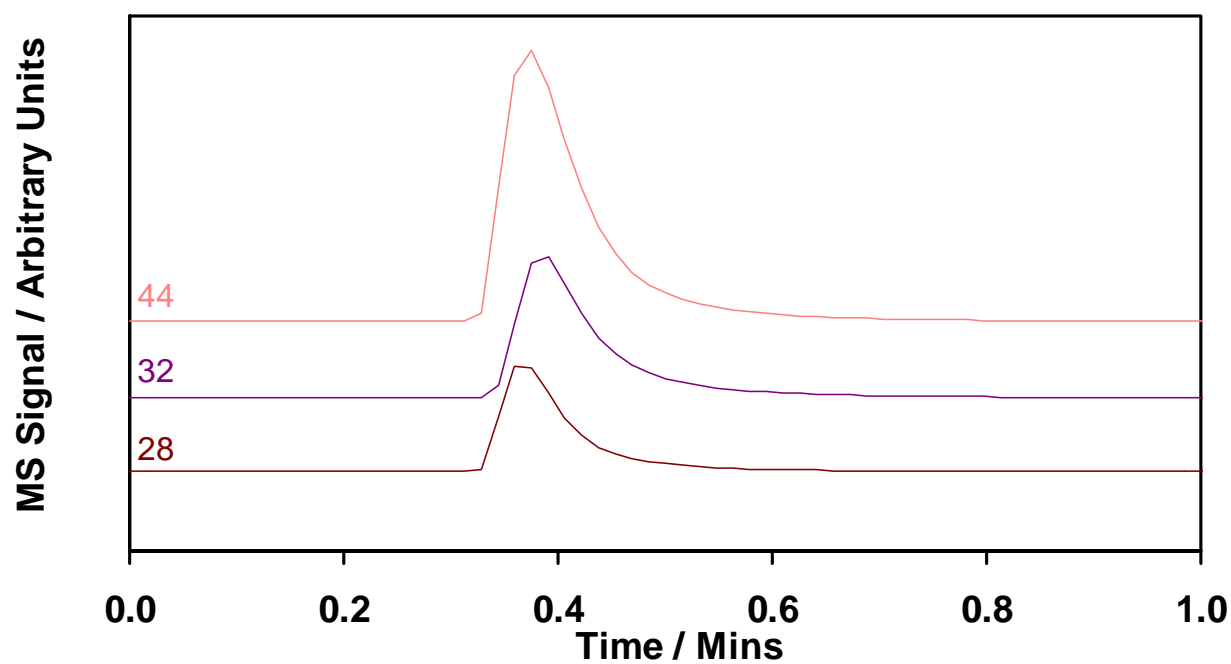


Figure 58; Simultaneous thermogravimetry-mass spectrometry curves for a 78.6% potassium perchlorate-21.4% calcium resinate mixture.
(Sample mass, 20 mg; heating rate, 10 °C min⁻¹; atmosphere, argon)



*Figure 59; Infra red heating-mass spectrometry heating curves for a 78.6% potassium perchlorate-21.4% calcium resinate mixture.
(Sample mass, 5 mg; atmosphere, argon)*

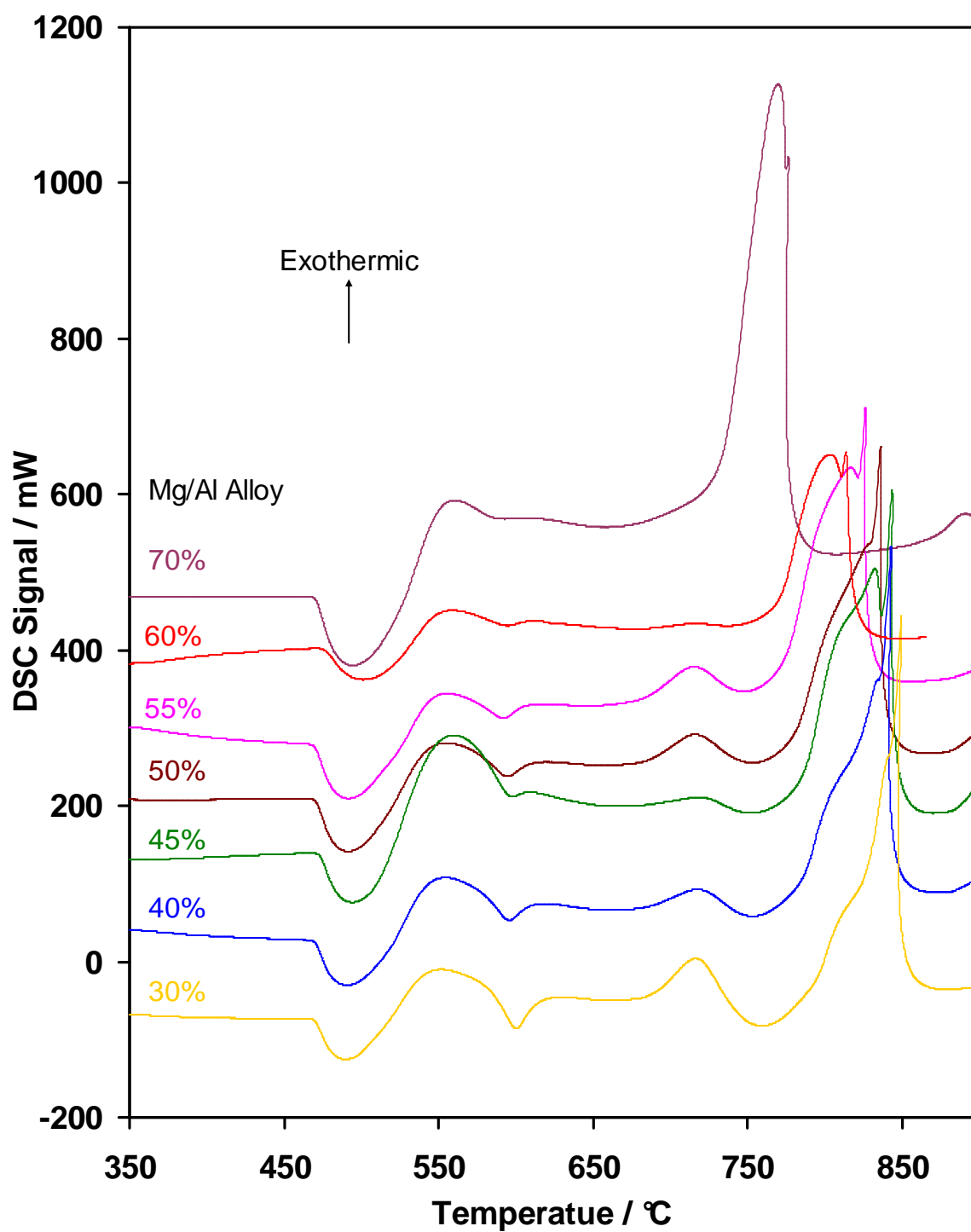


Figure 60; Ignition DSC curves for a range of magnesium/aluminum alloy-barium nitrate compositions.

(Sample mass, 20 mg; heating rate, 50 °C min⁻¹; atmosphere, argon)

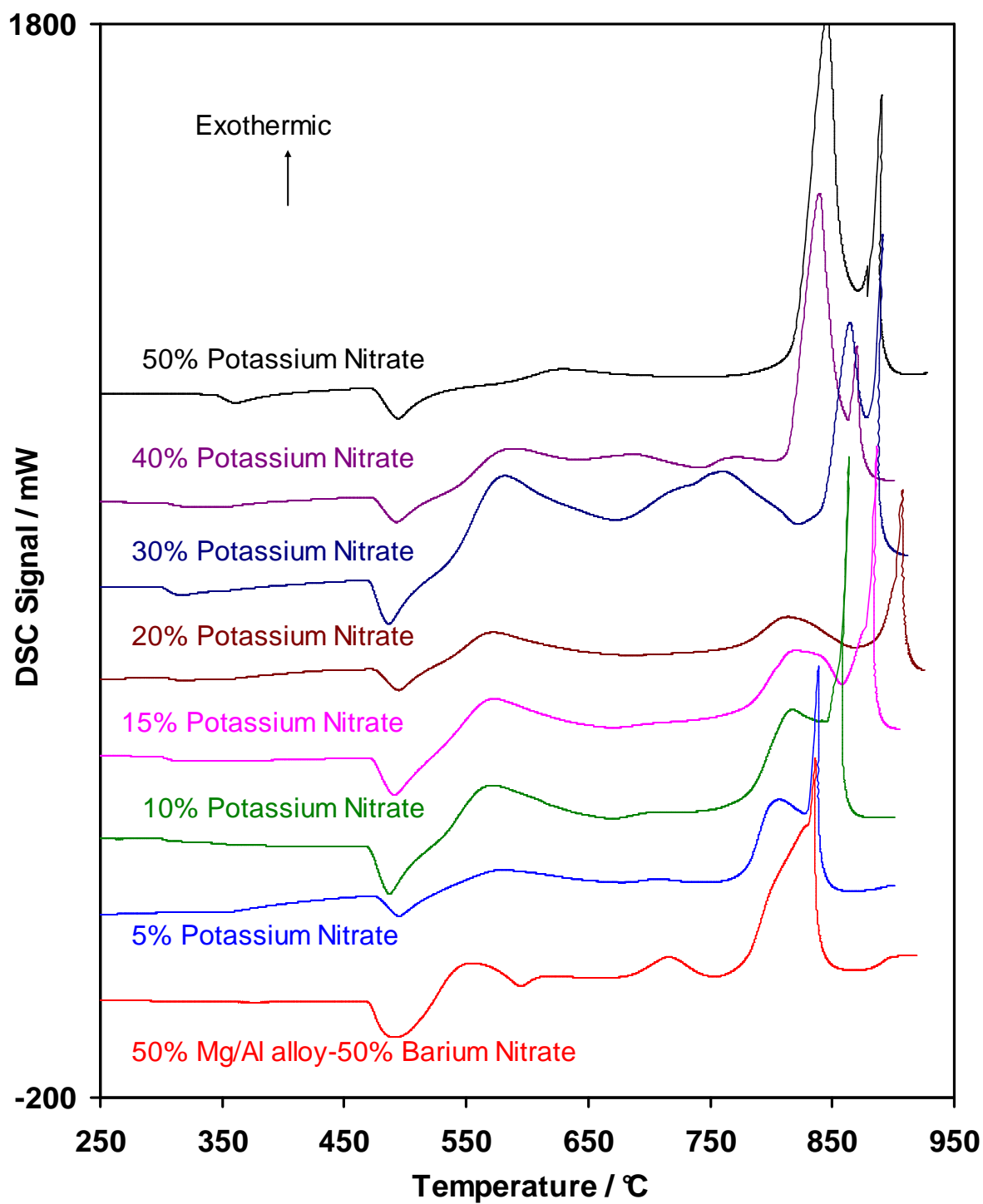


Figure 61 Ignition DSC; curves for a range of magnesium/aluminum alloy-barium nitrate-potassium nitrate compositions.

(Sample mass, 20 mg; heating rate, 50 °C min⁻¹; atmosphere, argon)

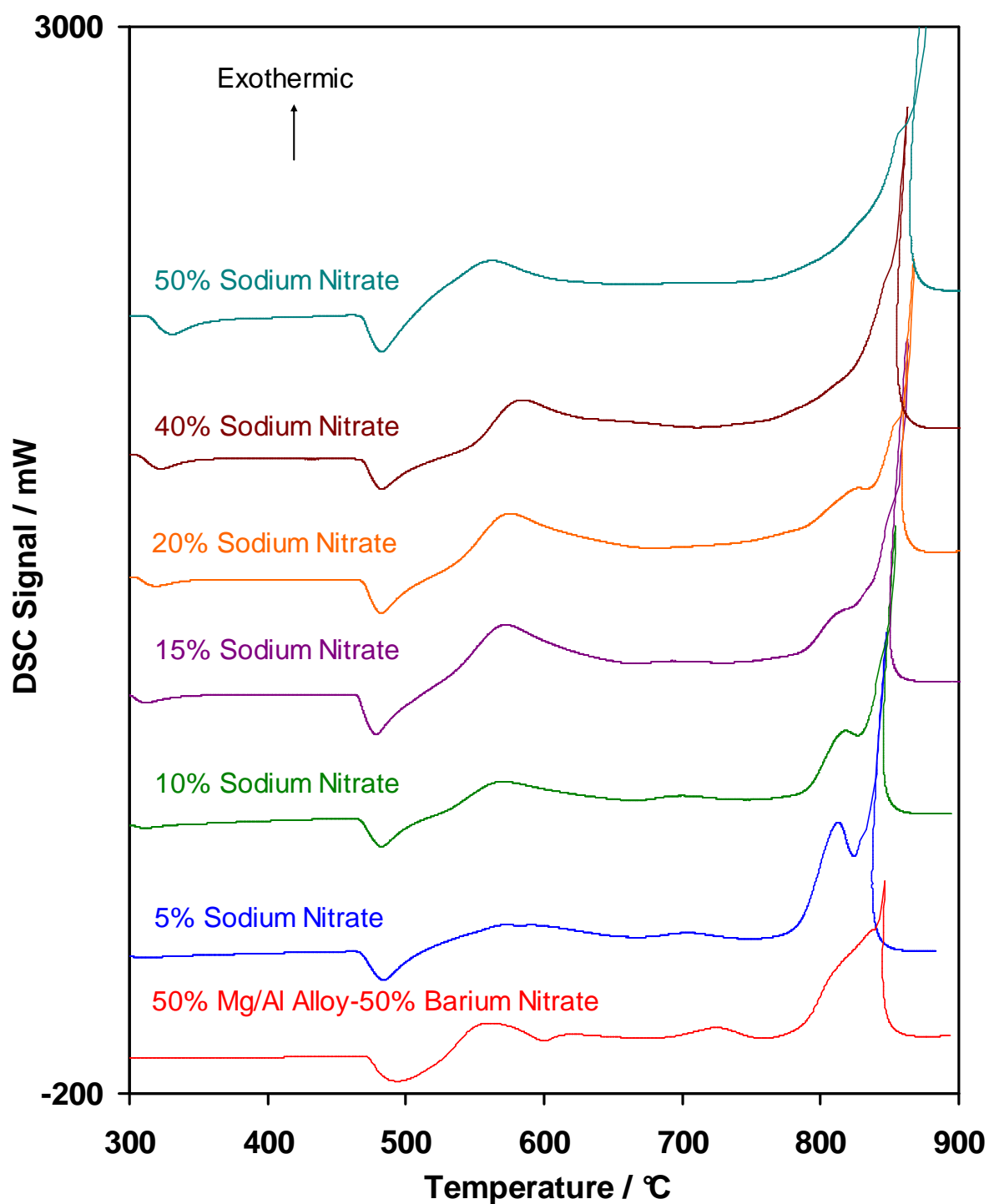


Figure 62; Ignition DSC curves for a range of magnesium/aluminum alloy-barium nitrate-sodium nitrate compositions.
(Sample mass, 20 mg; heating rate, 50 °C min⁻¹; atmosphere, argon)

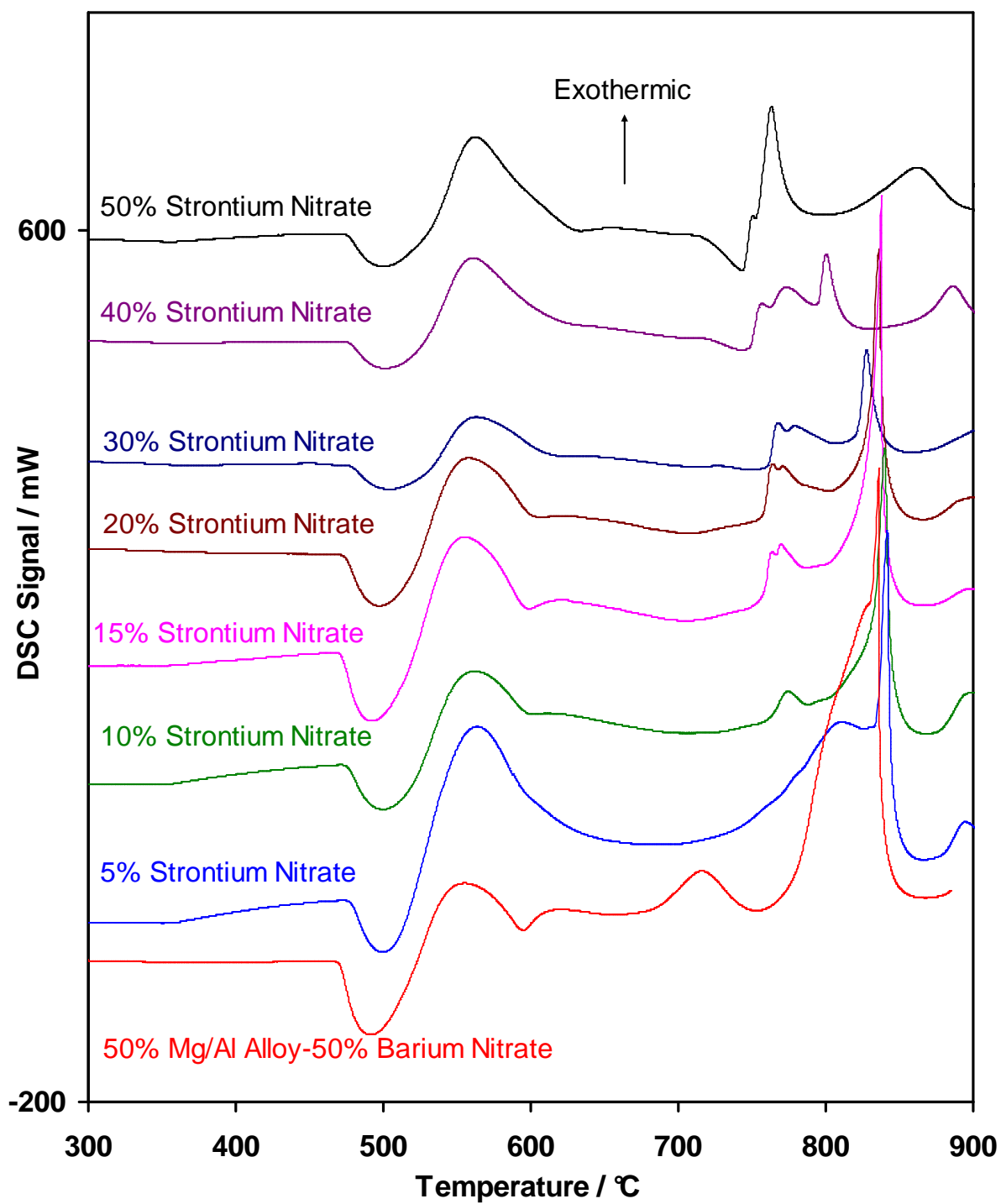


Figure 63; Ignition DSC curves for a range of magnesium/aluminum alloy-barium nitrate-strontium nitrate compositions.

(Sample mass, 20 mg; heating rate, 50 °C min⁻¹; atmosphere, argon)

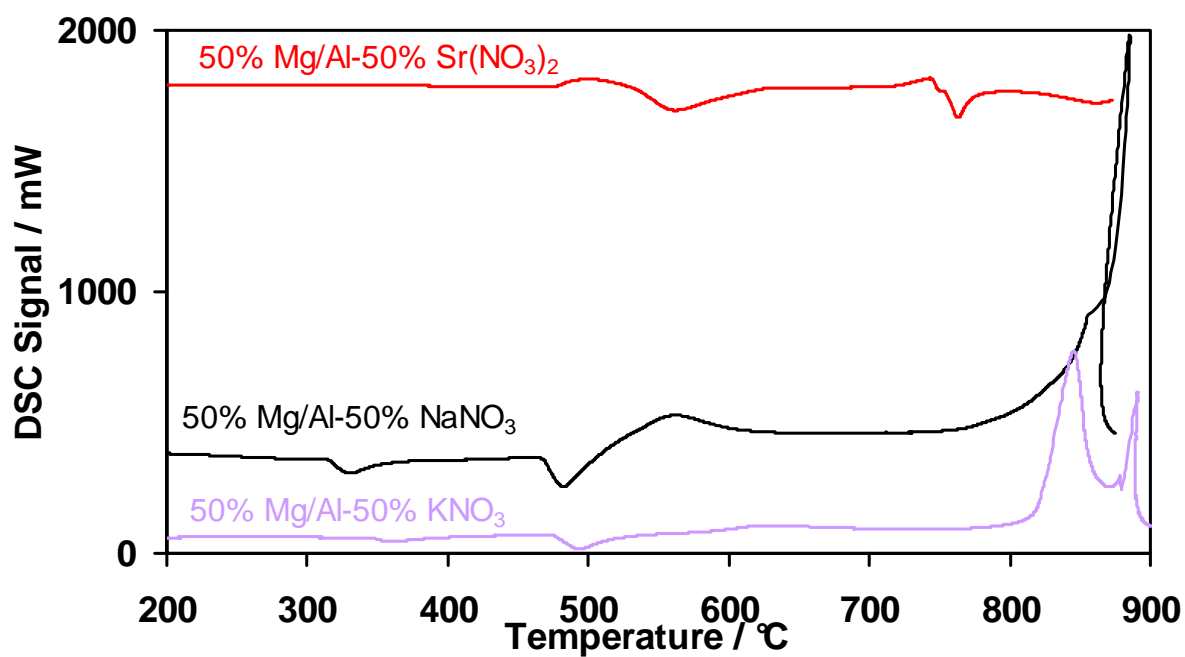


Figure 64; Ignition DSC curves for compositions containing 50% magnesium/aluminum alloy and 50% of the nitrates.
(Sample mass, 20 mg; heating rate, 50 °C min⁻¹; atmosphere, argon)

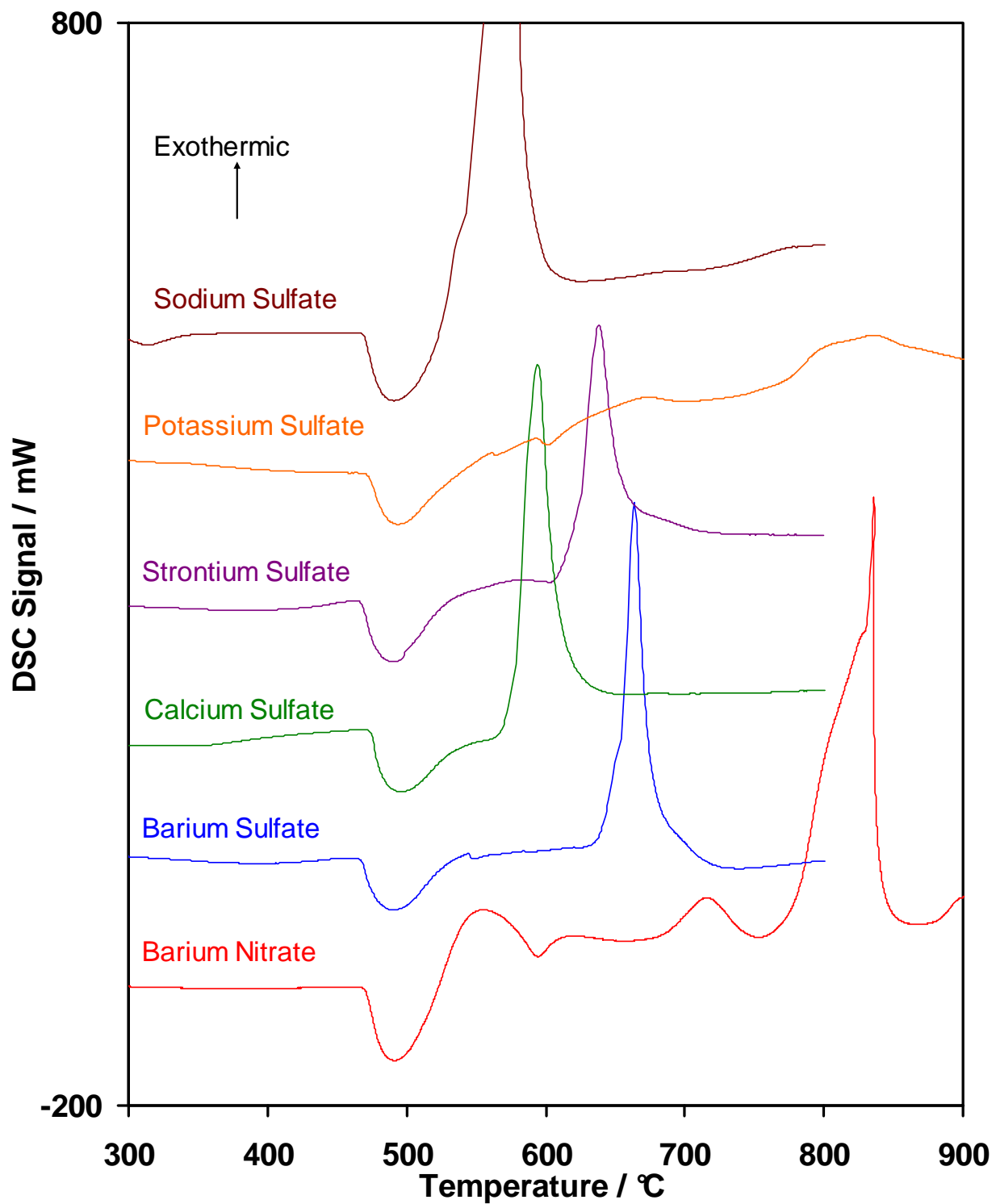


Figure 65; Ignition DSC curves for binary and ternary compositions containing 50% magnesium/aluminum alloy-50% sulfate.
(Sample mass, 20 mg; heating rate, 50 °C min⁻¹; atmosphere, argon)

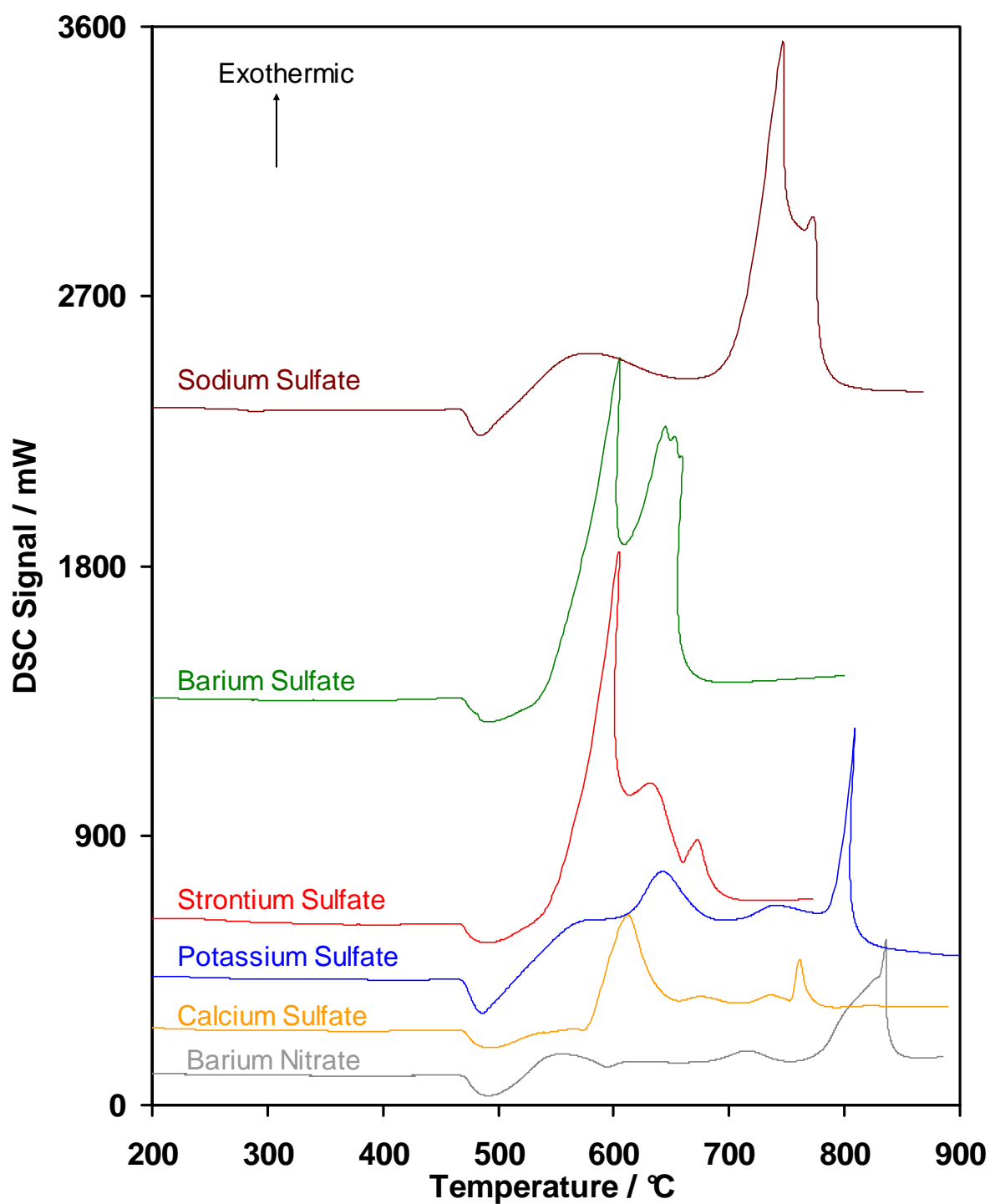


Figure 66; Ignition DSC curves for ternary compositions containing 50% magnesium/aluminum alloy-35% barium nitrate and 15% sulfate.
(Sample mass, 10 mg; heating rate, 50 °C min⁻¹; atmosphere, argon)

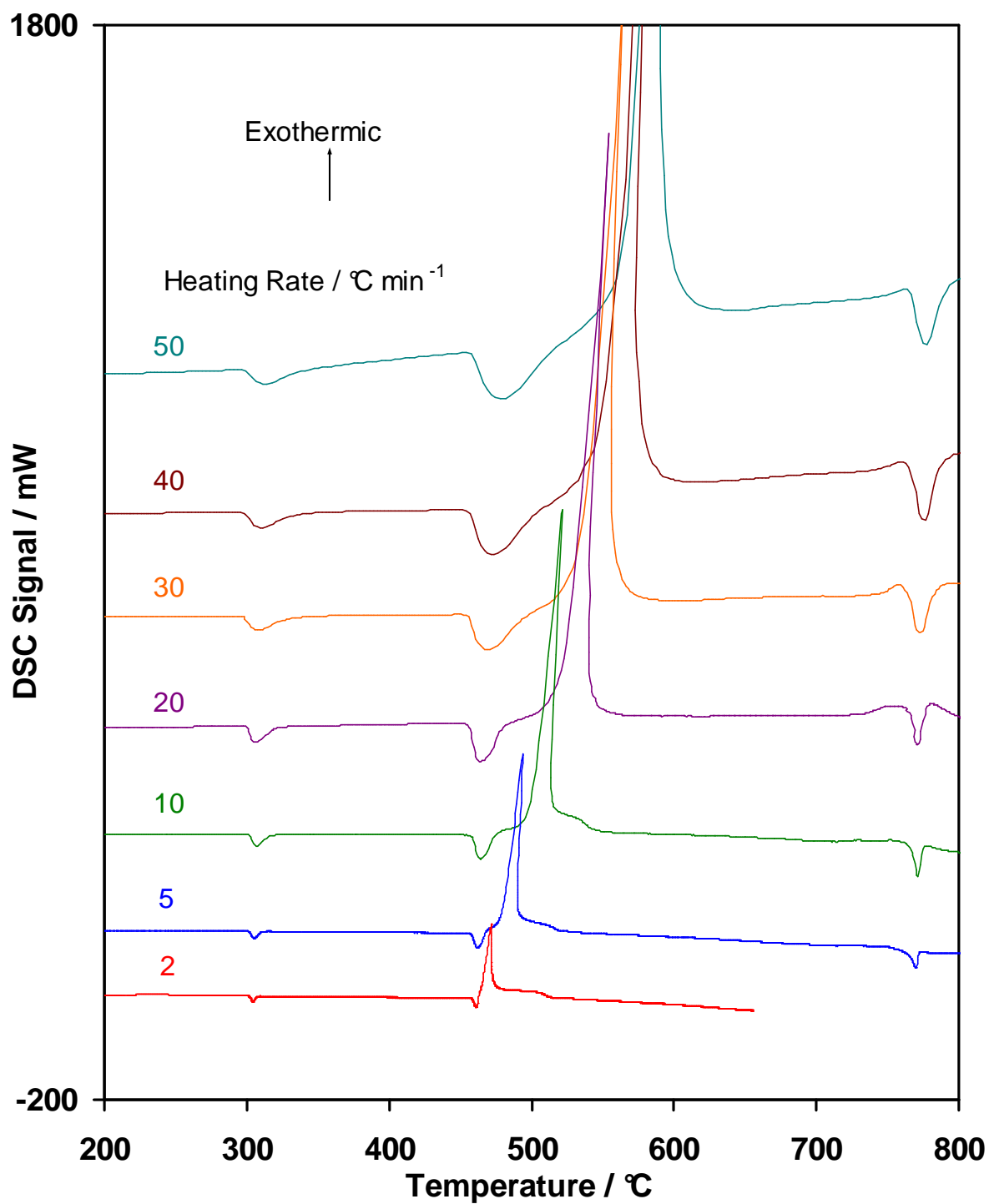


Figure 67; DSC curves at different heating rates for a binary composition containing 50% magnesium/aluminum alloy-50% potassium perchlorate.
(Sample mass, 20 mg; atmosphere, argon)

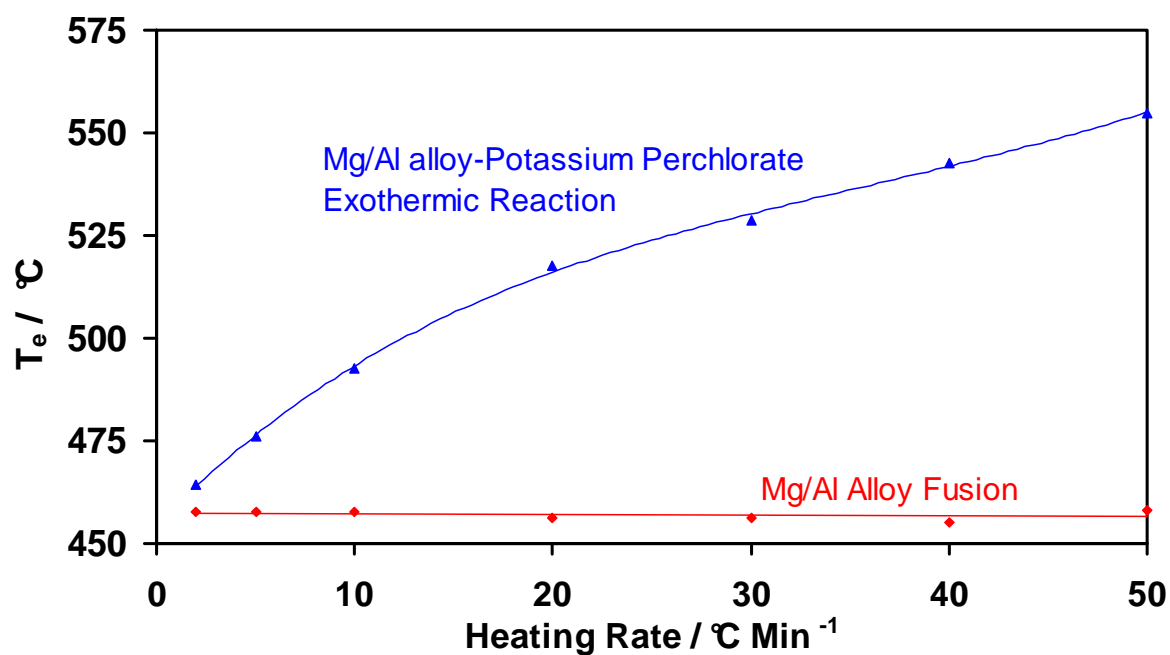


Figure 68; Plot of extrapolated onset temperature against heating rate for magnesium/aluminum alloy fusion and the exothermic reaction in 50% magnesium/aluminum alloy-50% potassium perchlorate.

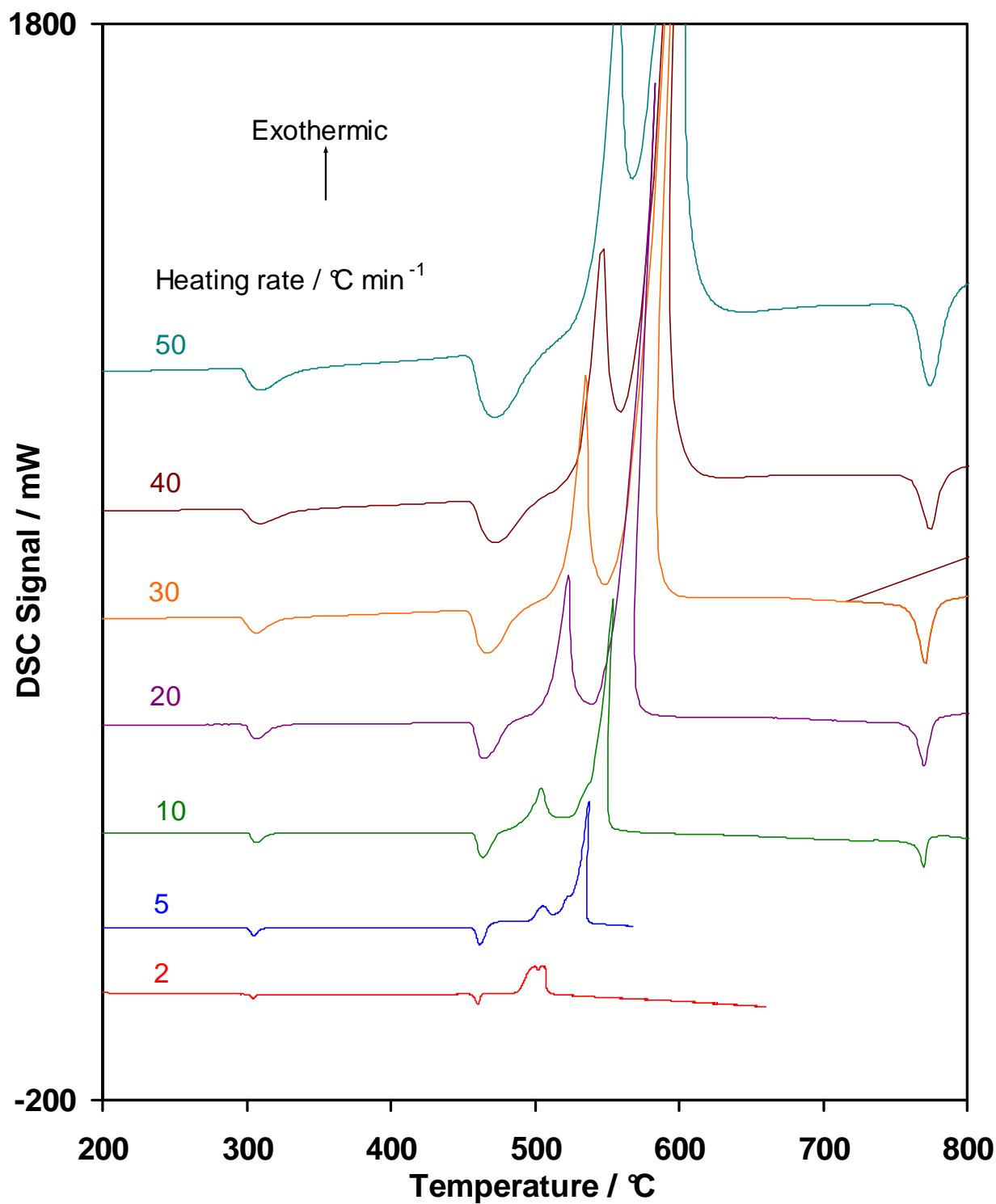


Figure 69; DSC curves at different heating rates for a binary composition containing 48% magnesium/aluminum alloy-48% potassium perchlorate-2% calcium resinate. (Sample mass, 20 mg; atmosphere, argon)

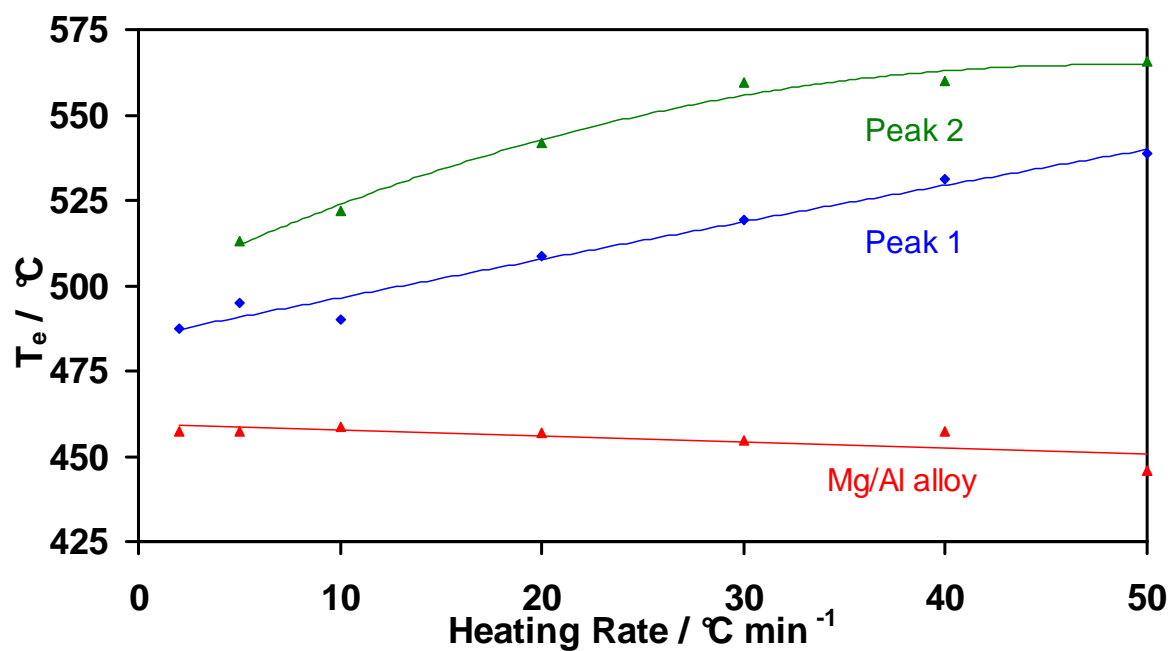


Figure 70; Plot of extrapolated onset temperature against heating rate for magnesium/aluminum alloy fusion and the exothermic reactions in 48% magnesium/aluminum alloy-48% potassium perchlorate-2% calcium resinate.

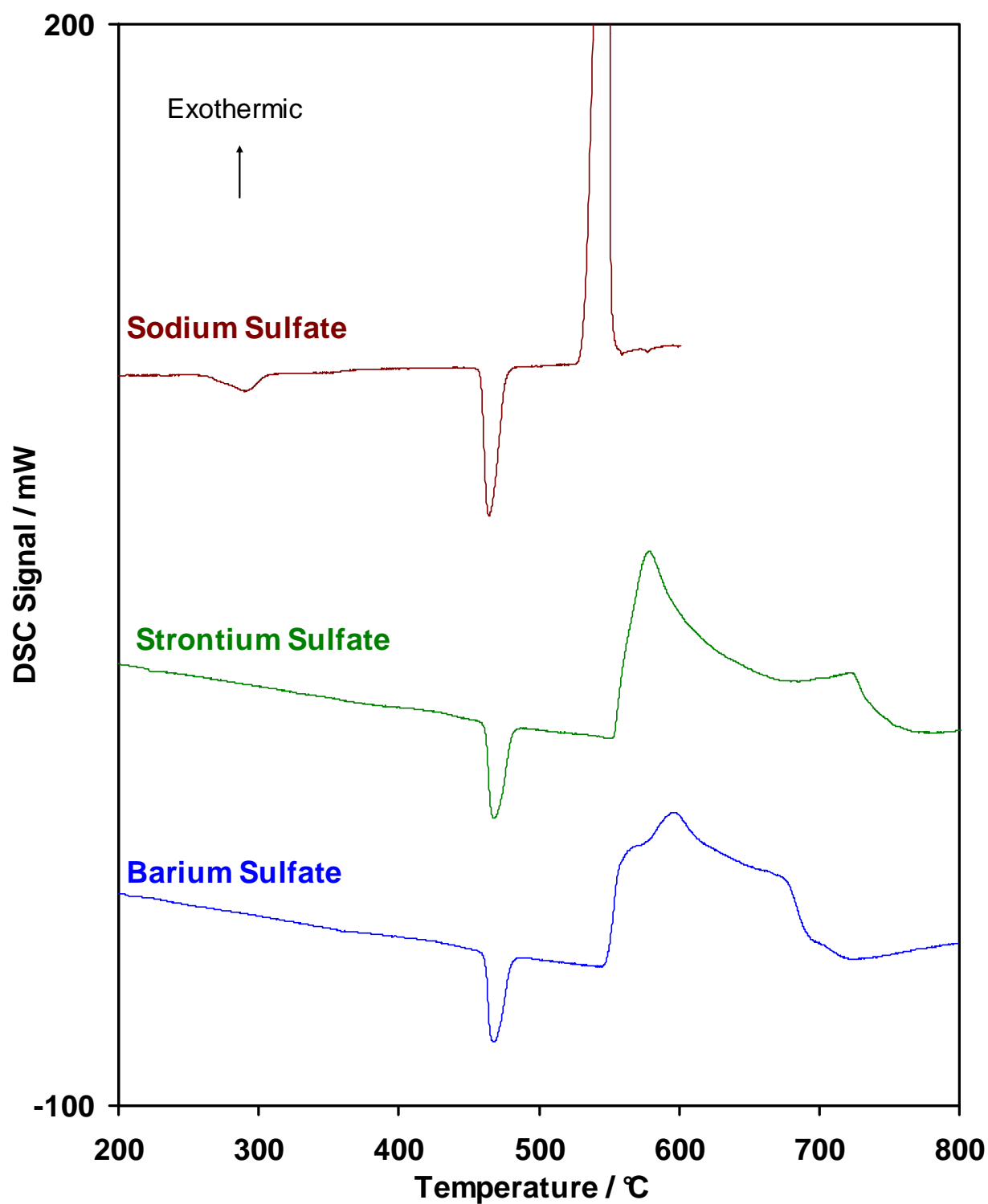


Figure 71; DSC curves for ternary compositions containing 50% magnesium aluminum-50% metal sulfate.
(Sample mass, 20 mg; heating rate, $10\text{ }^{\circ}\text{C min}^{-1}$; atmosphere, argon)

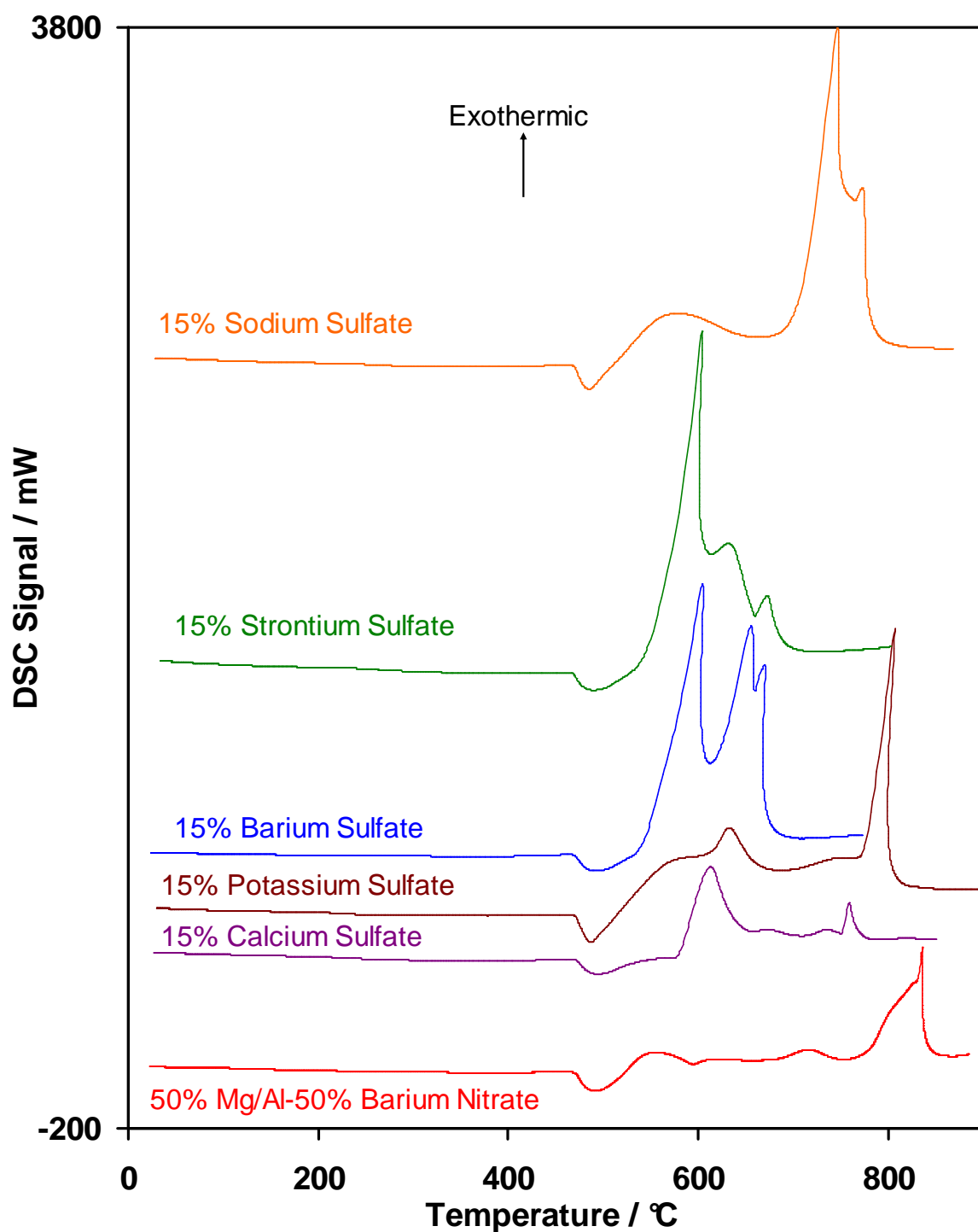


Figure 72; DSC curves for ternary compositions containing 50% magnesium aluminum-35% barium nitrate and 15% metal sulfate.
(Sample mass, 20 mg; heating rate, 10 °C min⁻¹; atmosphere, argon)

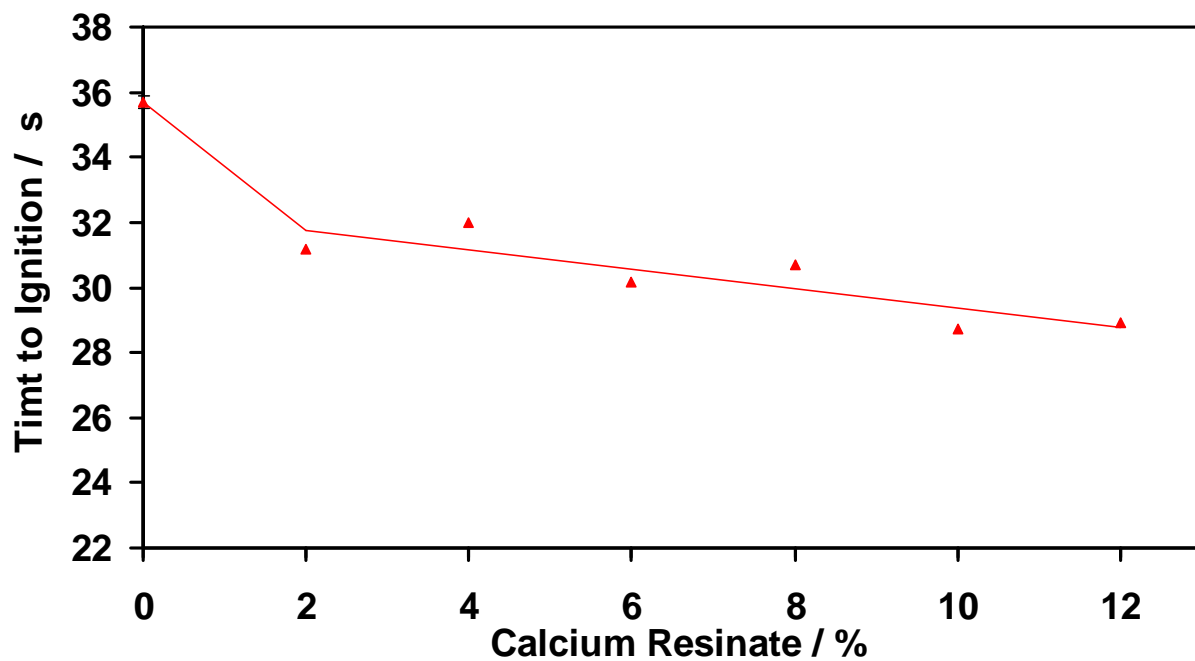


Figure 73; Time to Ignition for a range of magnesium/aluminum alloy-potassium perchlorate-calcium resinate compositions containing equal masses of magnesium/aluminum alloy and potassium perchlorate.
(Sample mass, 20 mg; temperature, 900 °C; atmosphere, argon)

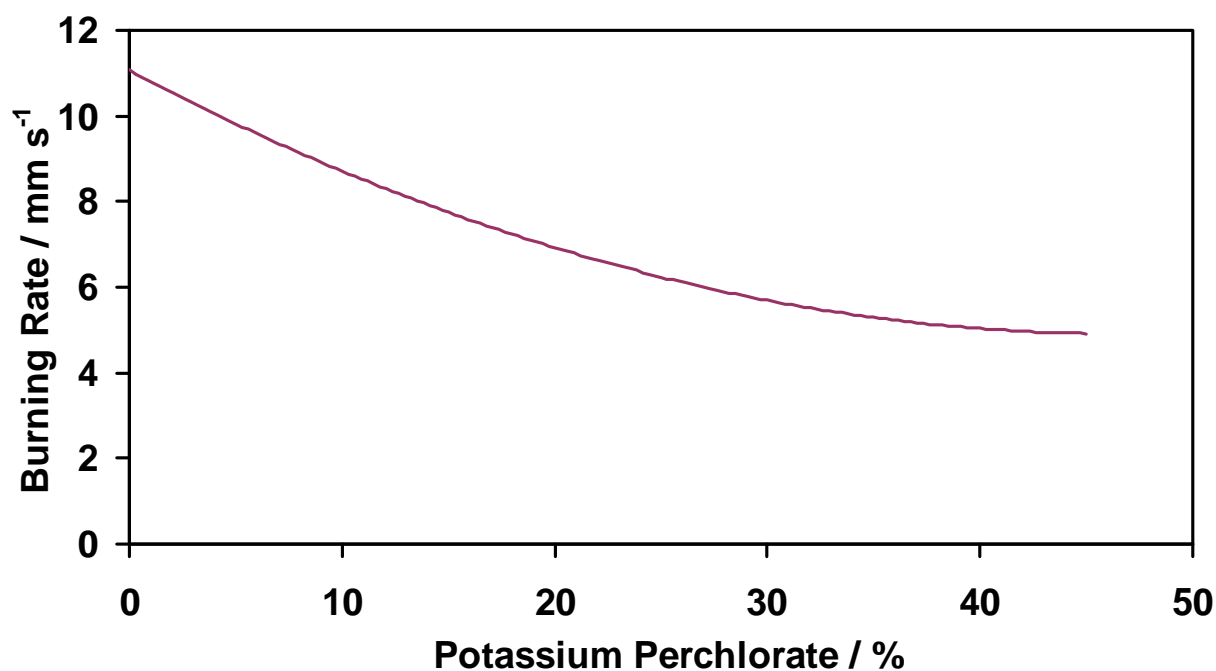


Figure 74; Burning rate curve for magnesium-barium nitrate-potassium perchlorate.

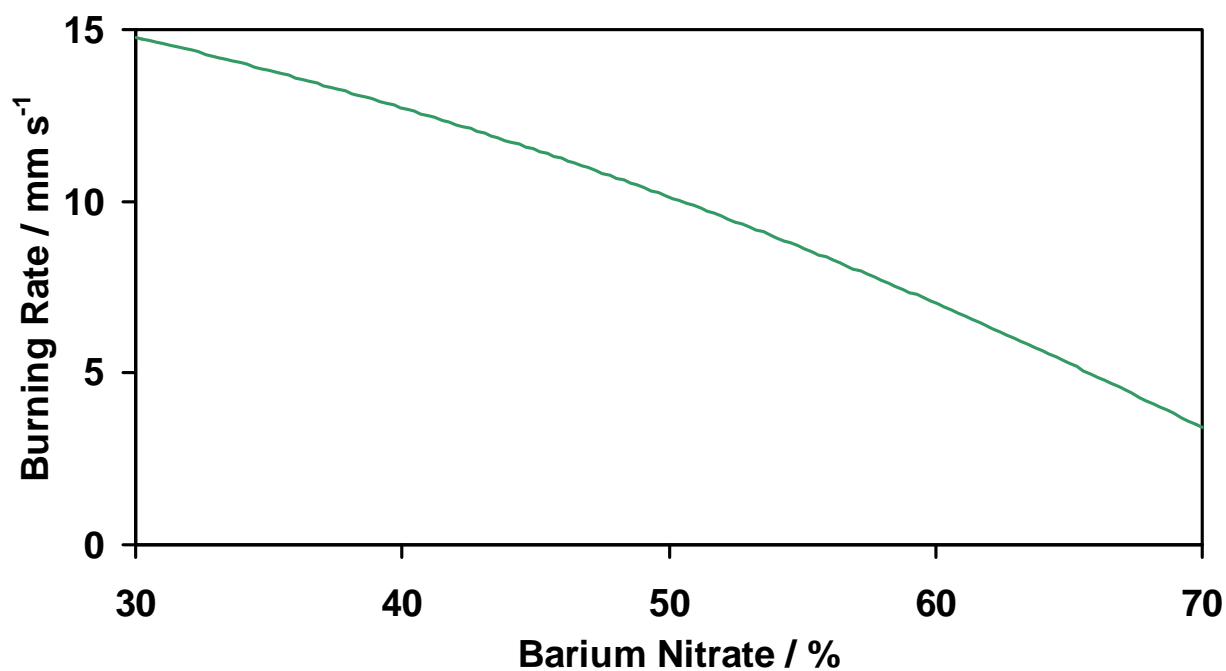


Figure 75; Burning rate curve for magnesium-barium nitrate compositions.

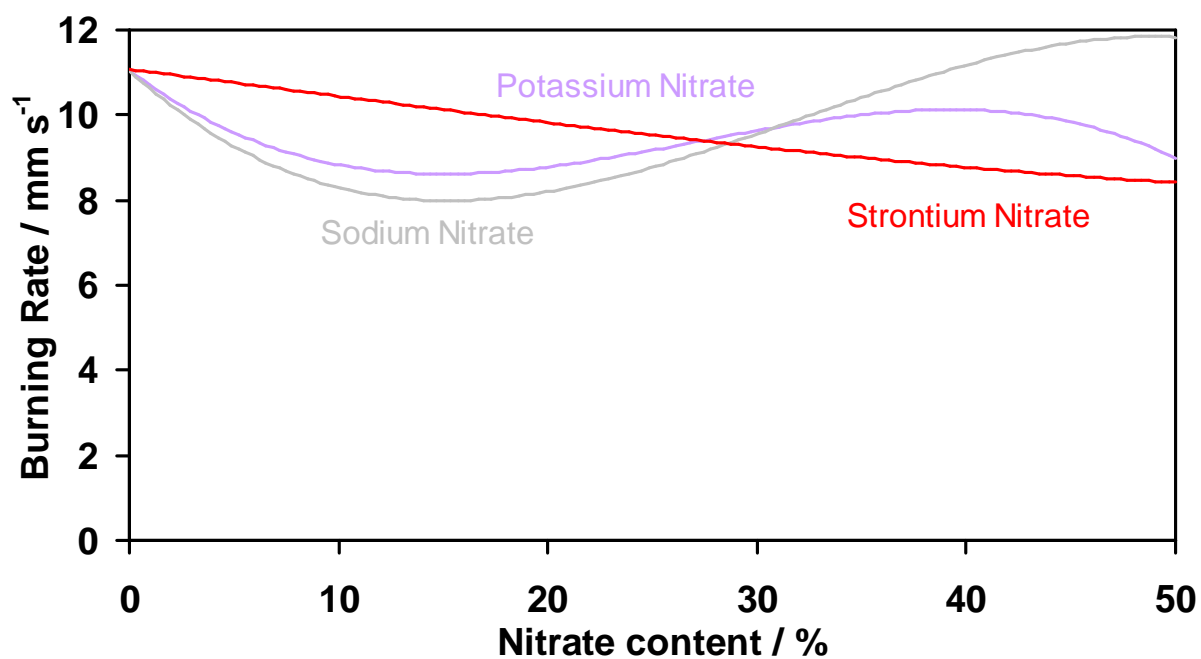


Figure 76; Burning rate curve for magnesium-barium nitrate-nitrates compositions.

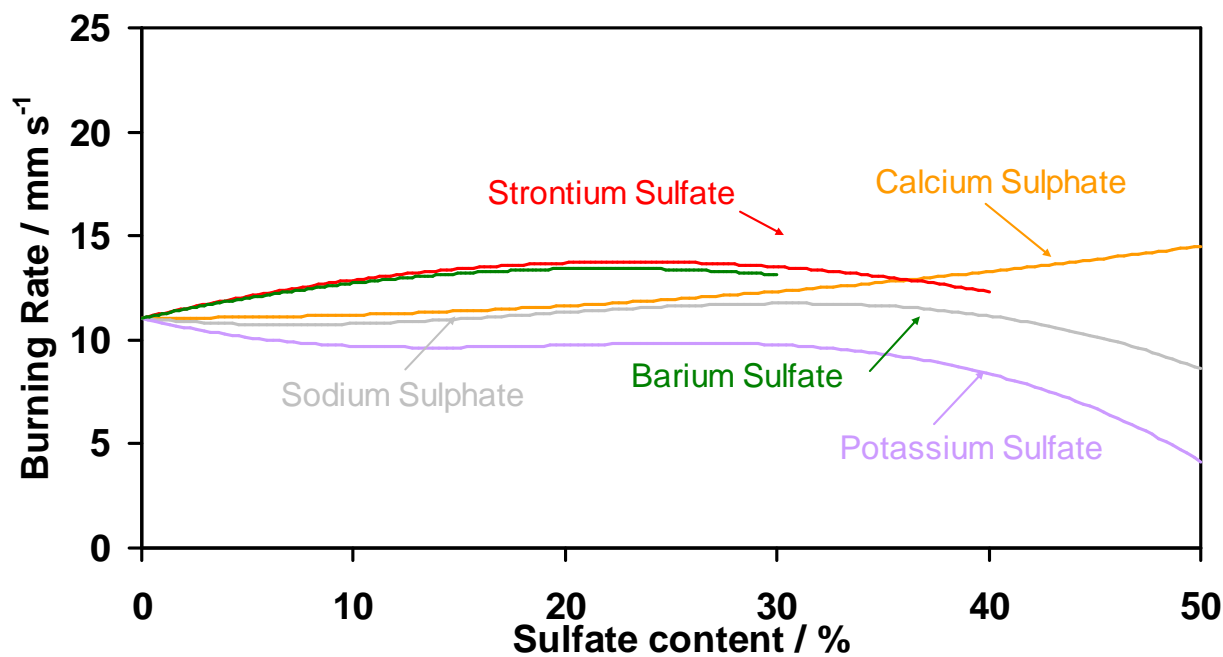


Figure 77; Burning rate curve for magnesium-barium nitrate-sulfate compositions.

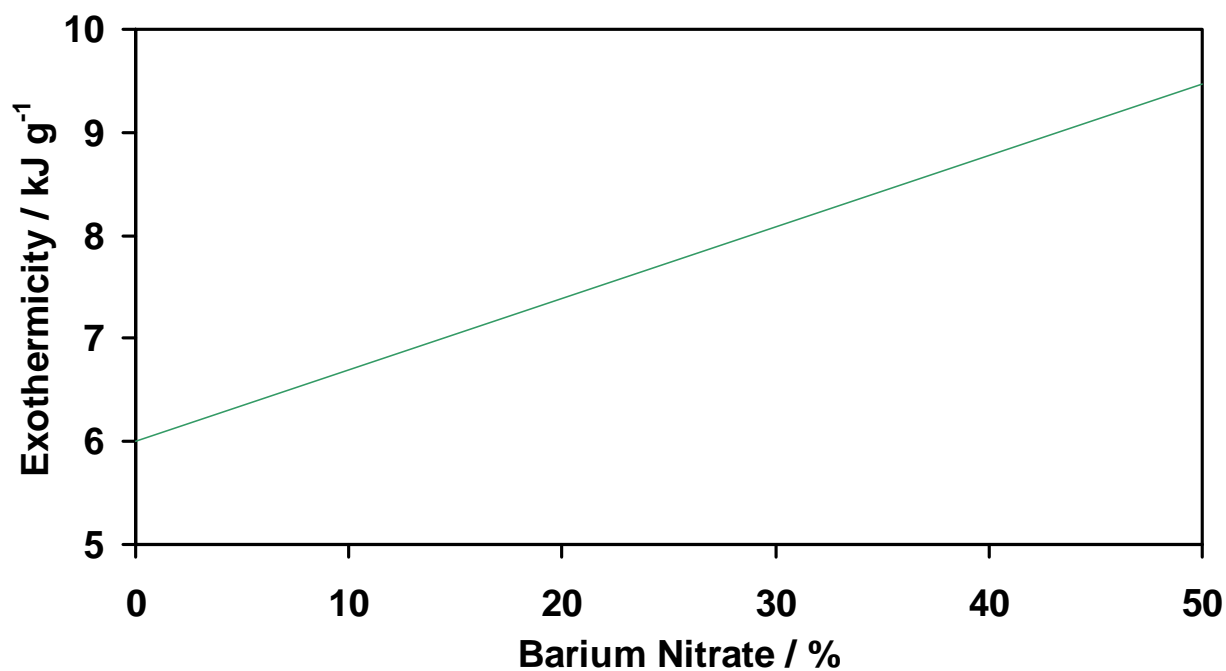


Figure 78; Exothermicity curve for magnesium-barium nitrate-potassium perchlorate compositions.
(Sample mass, 100 mg; 1 atmosphere, argon)

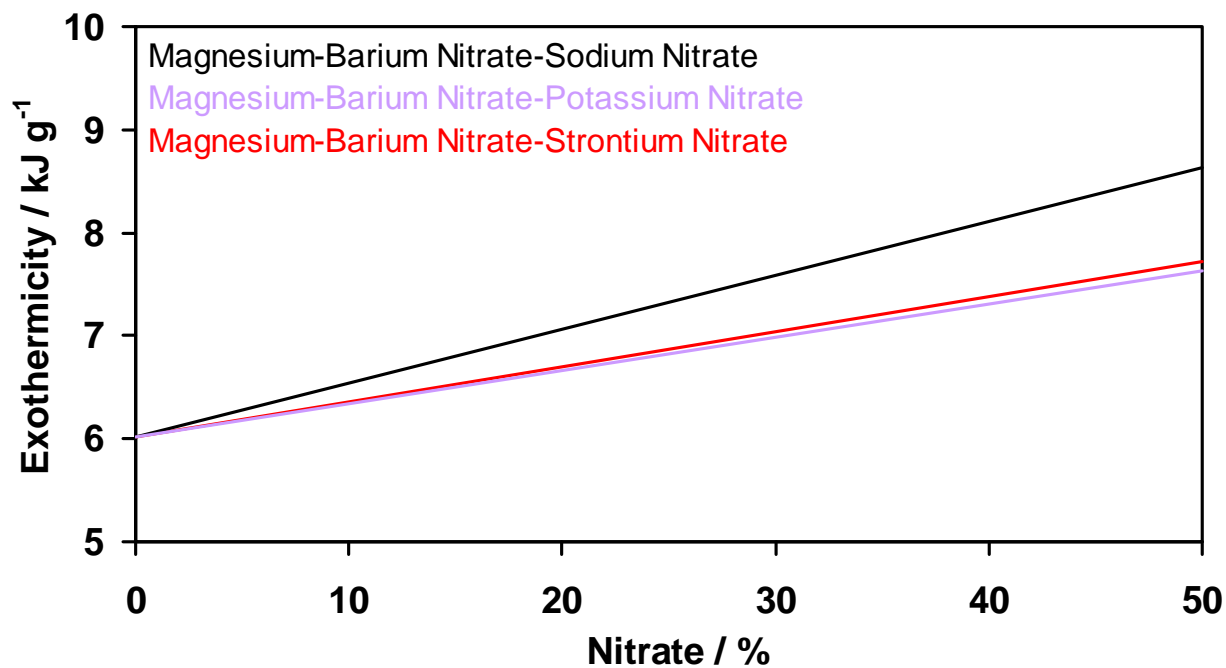


Figure 79; Exothermicity curves for magnesium-barium nitrate-nitrate compositions.
(Sample mass, 100 mg; 1 atmosphere, argon)

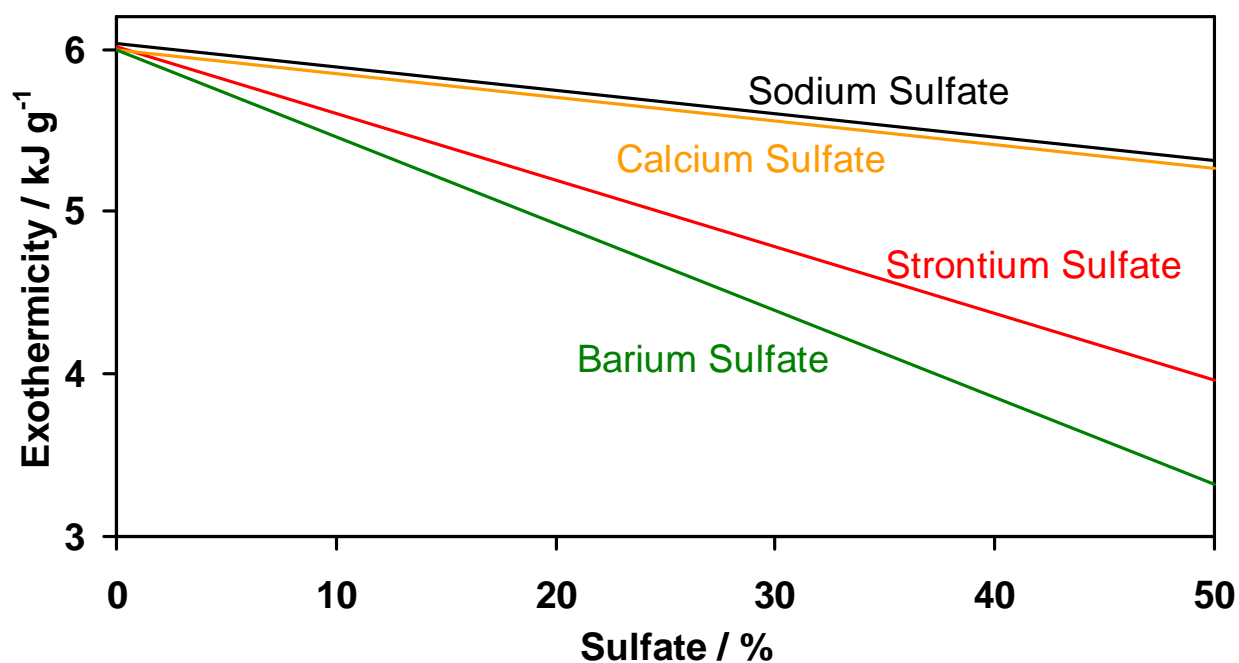


Figure 80; Exothermicity curves for magnesium-barium nitrate-sulfate compositions.
(Sample mass, 100 mg; 1 atmosphere, argon)

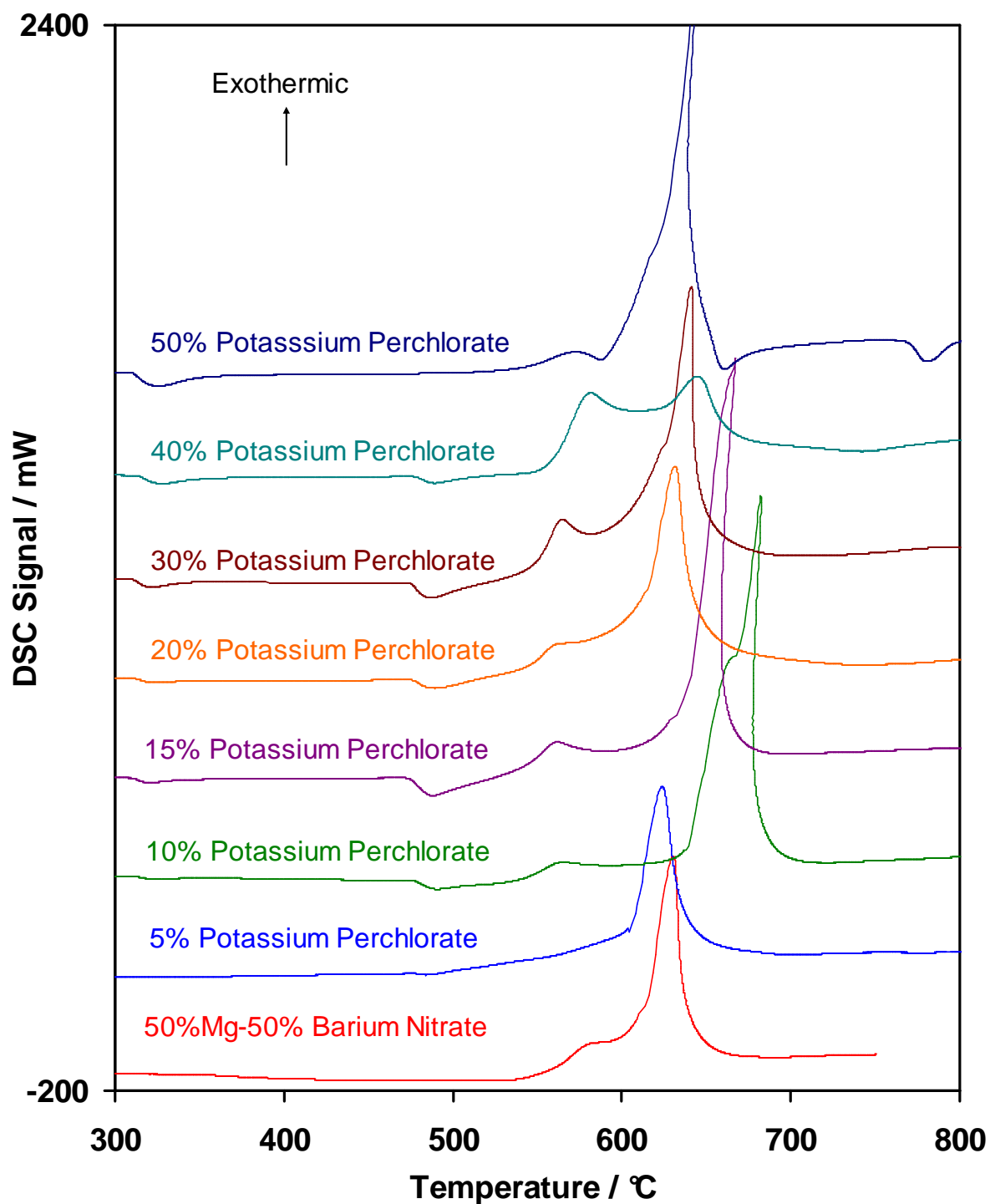


Figure 81; DSC Curves for a range of 50% magnesium-barium nitrate-potassium perchlorate compositions.
 (Sample mass, 20 mg; heating rate, 50 °C min⁻¹; atmosphere, argon)

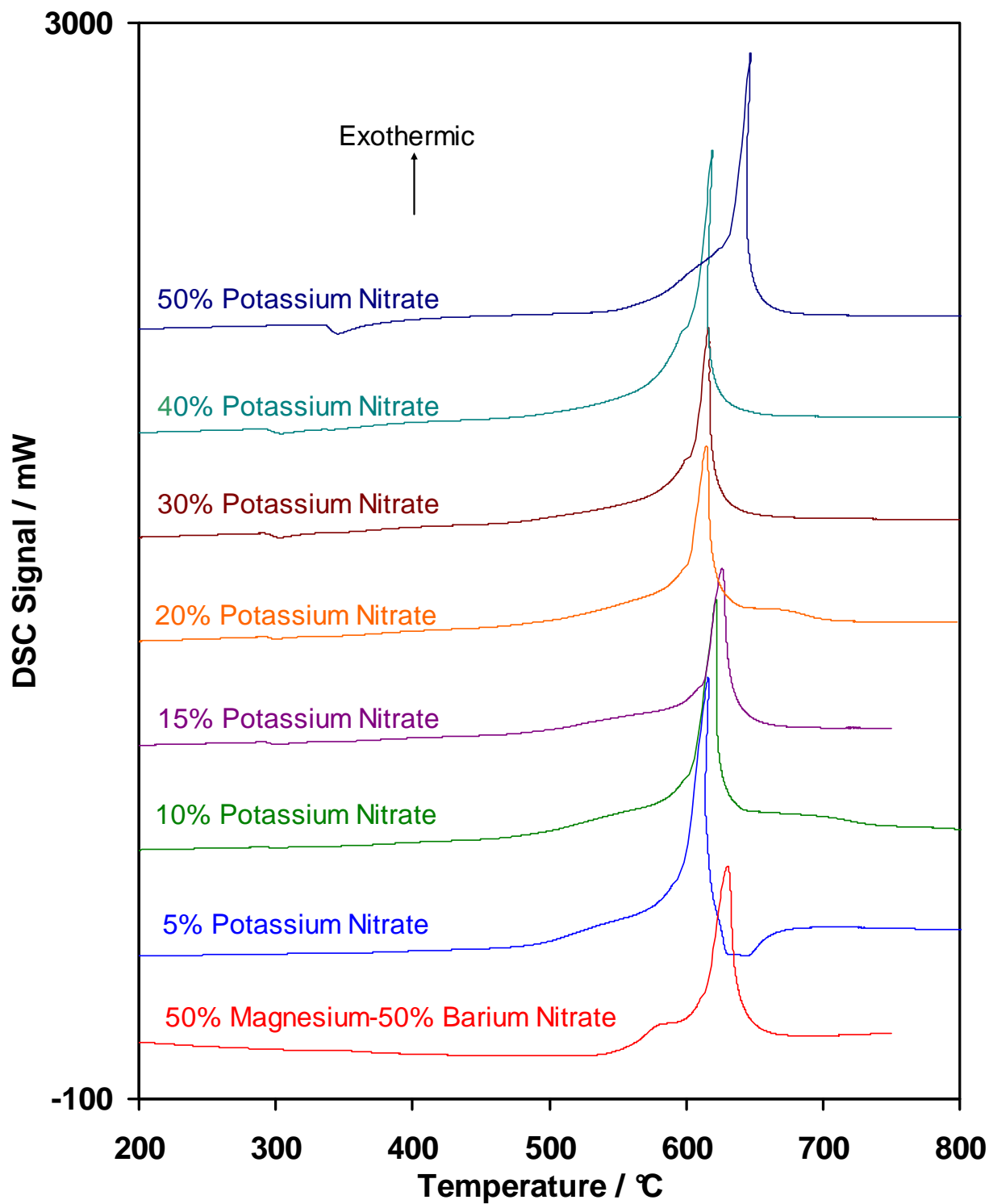


Figure 82; Ignition DSC curves for a range of magnesium-barium nitrate-potassium nitrate compositions.
(Sample mass, 20 mg; heating rate, 50 °C min⁻¹; atmosphere, argon)

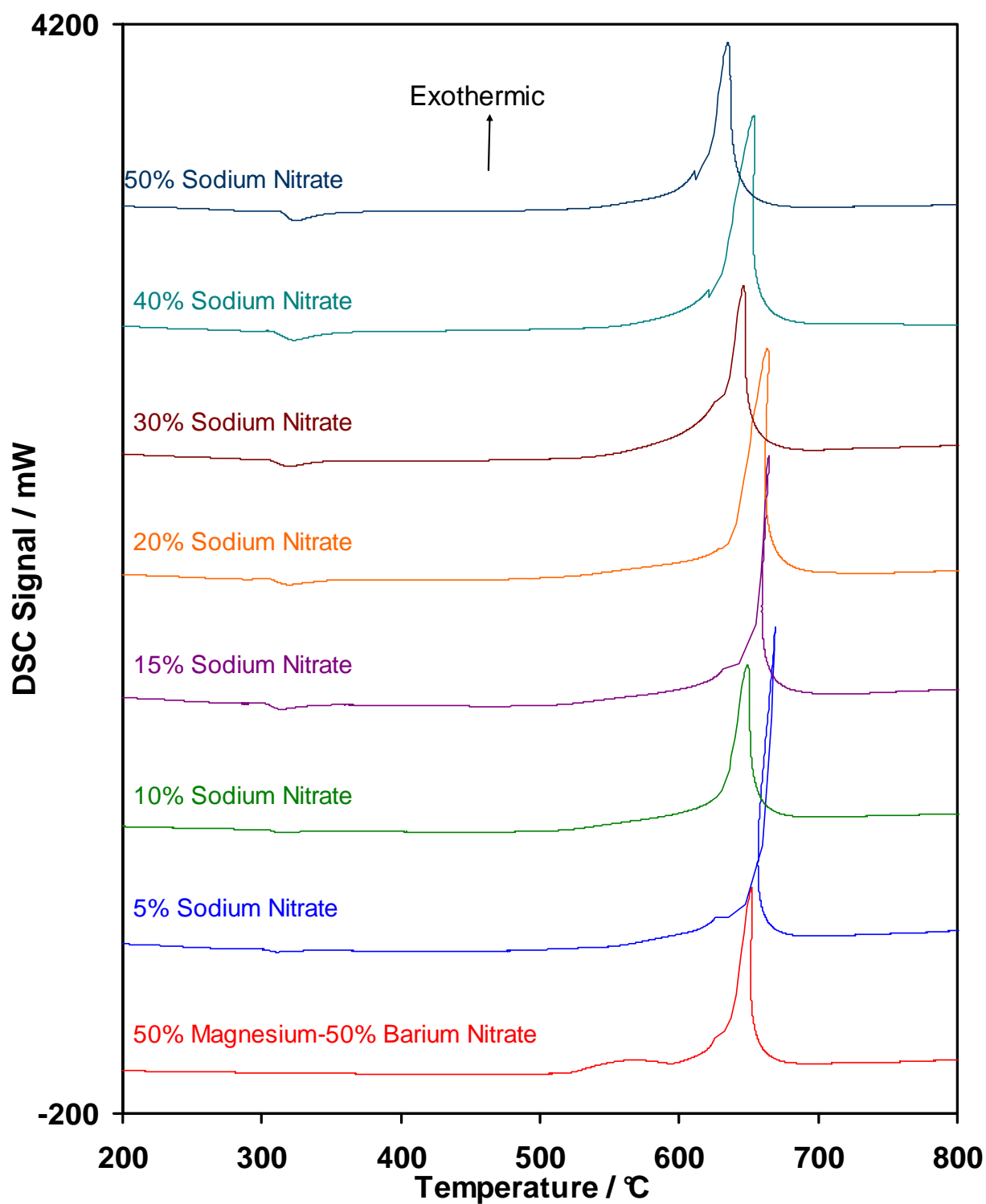


Figure 83; Ignition DSC curves for a range of magnesium-barium nitrate-sodium nitrate compositions.
(Sample mass, 20 mg; heating rate, 50 °C min⁻¹; atmosphere, argon)

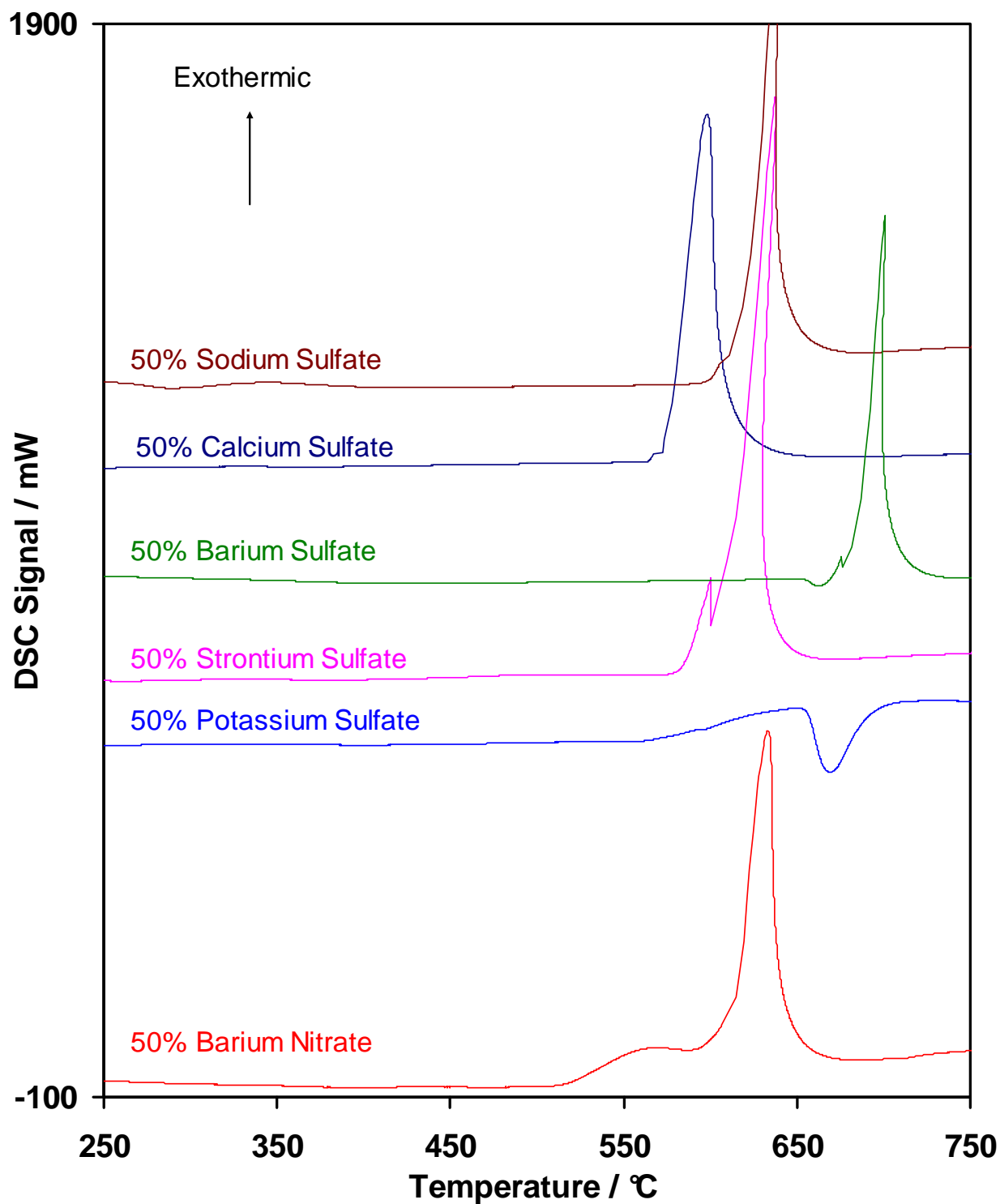


Figure 84; DSC curves for a range of magnesium-sulfate compositions.
(Sample mass, 20 mg; heating rate, 50 °C min⁻¹; atmosphere, argon)

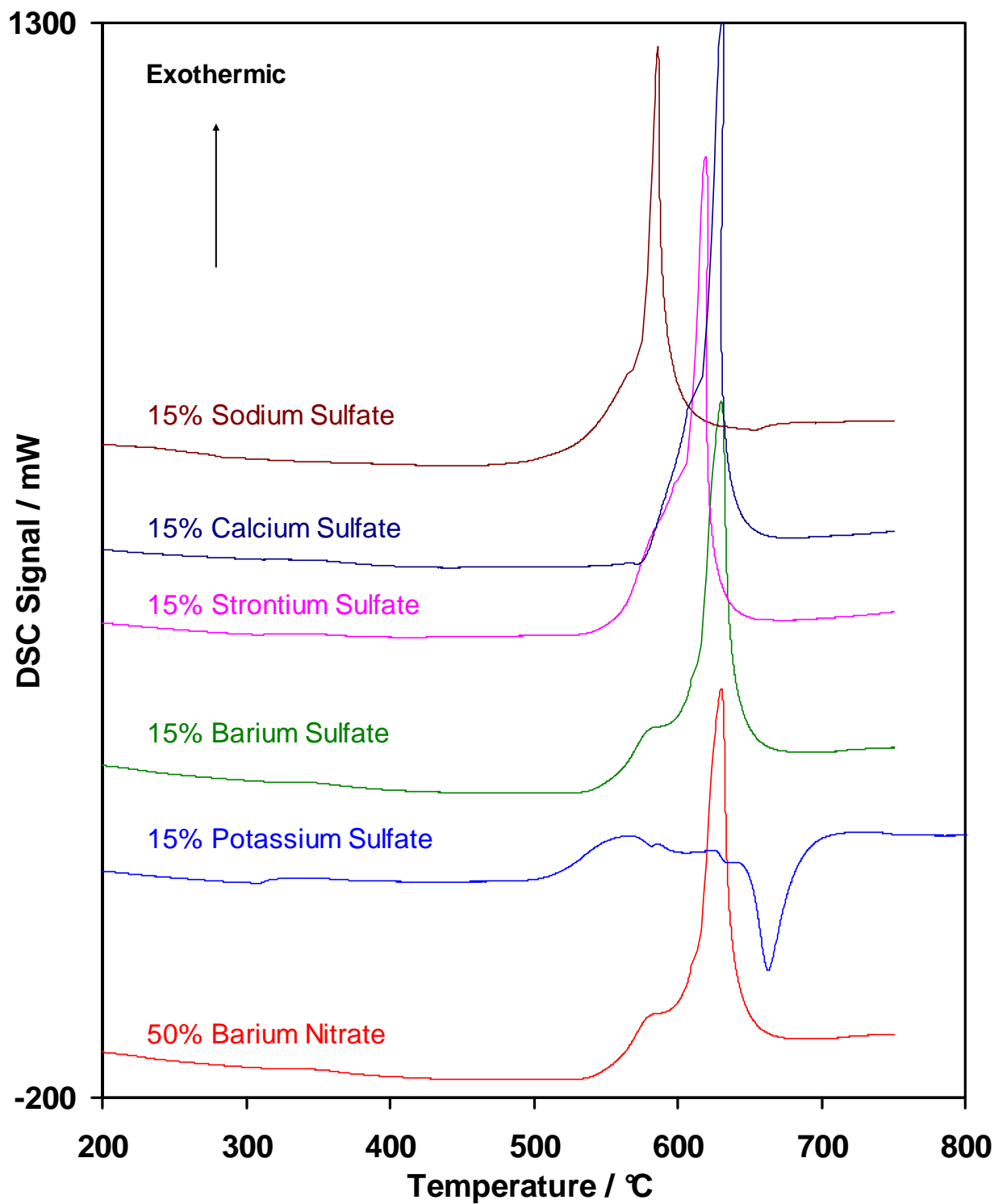


Figure 85; DSC curves for a range of ternary magnesium-barium nitrate-sulfate compositions.
(Sample mass, 20 mg; heating rate, 50 °C min⁻¹; atmosphere, argon)

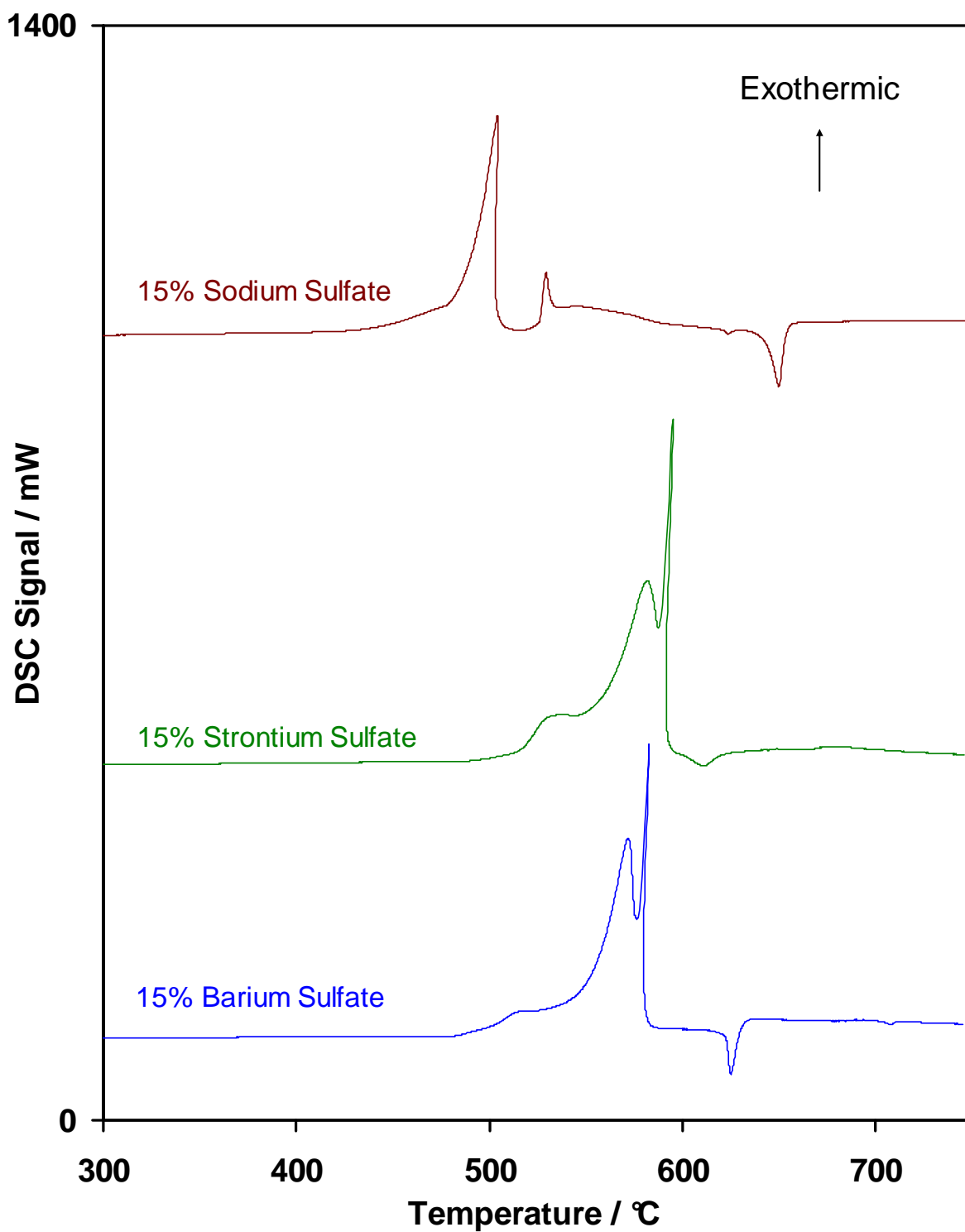


Figure 86; DSC curves for a range of ternary 50% magnesium-35% barium nitrate-15% metal sulfate compositions.
(Sample mass, 20 mg; heating rate, 10 °C min⁻¹; atmosphere, argon)

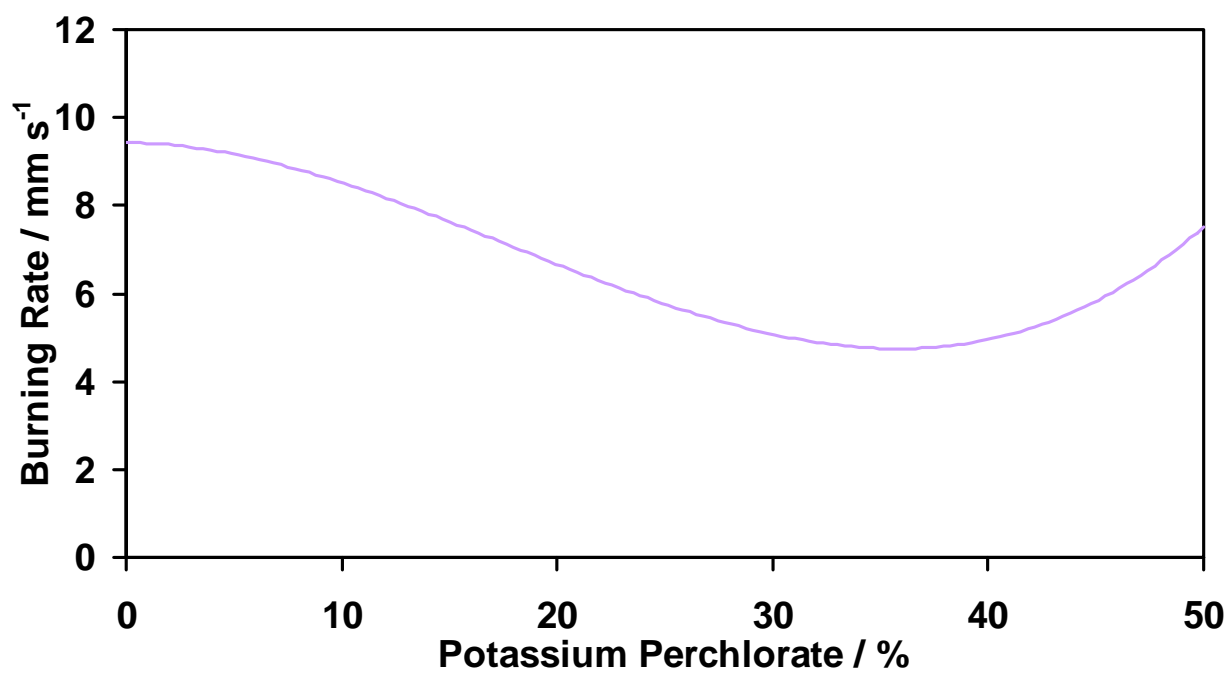


Figure 87; Burning rate curve for aluminum-barium nitrate-potassium perchlorate compositions.

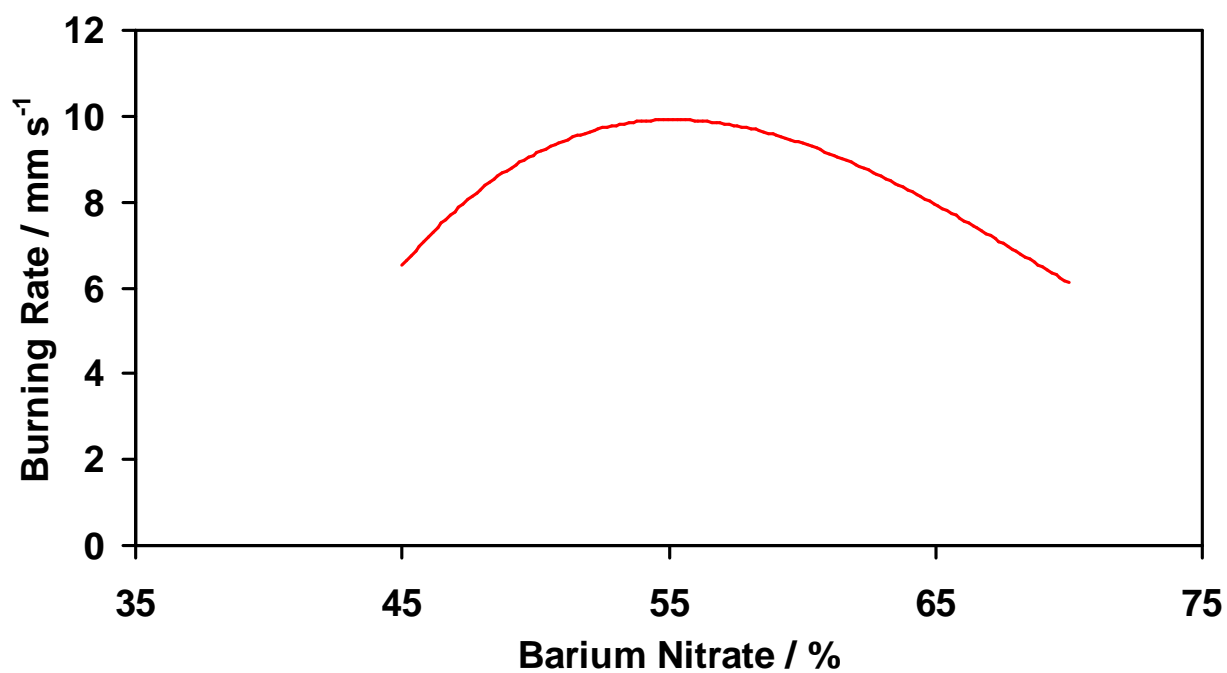


Figure 88; Burning rate curve for aluminum-barium nitrate compositions.

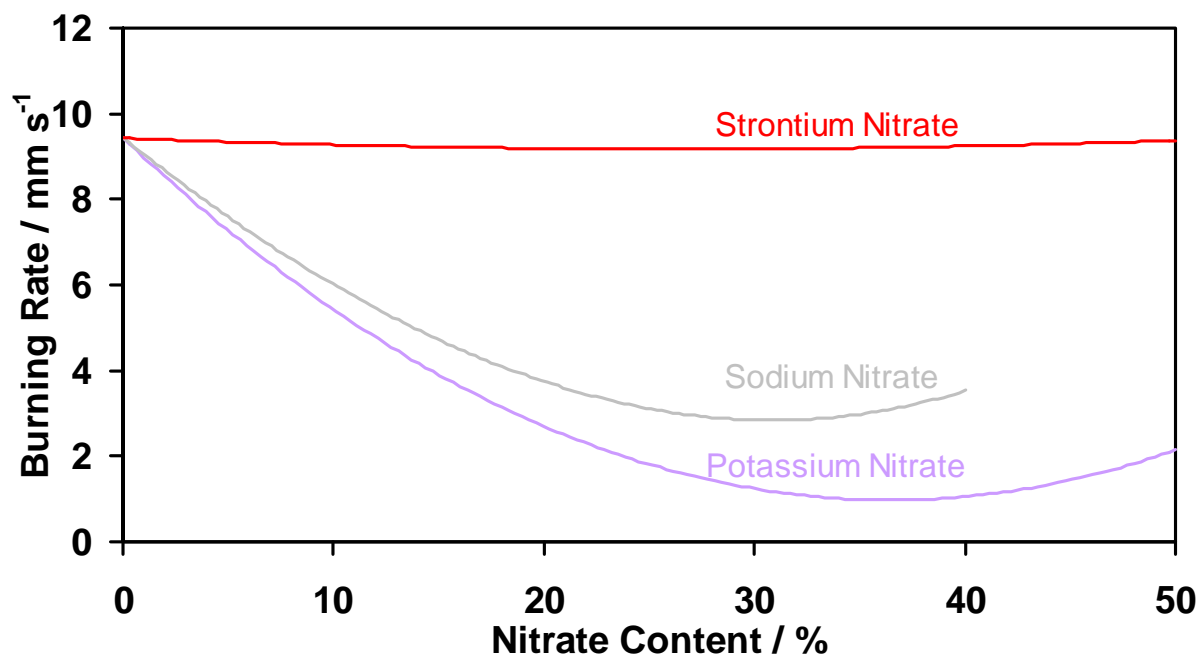


Figure 89; Burning rate curves for aluminum-barium nitrate-nitrate compositions.

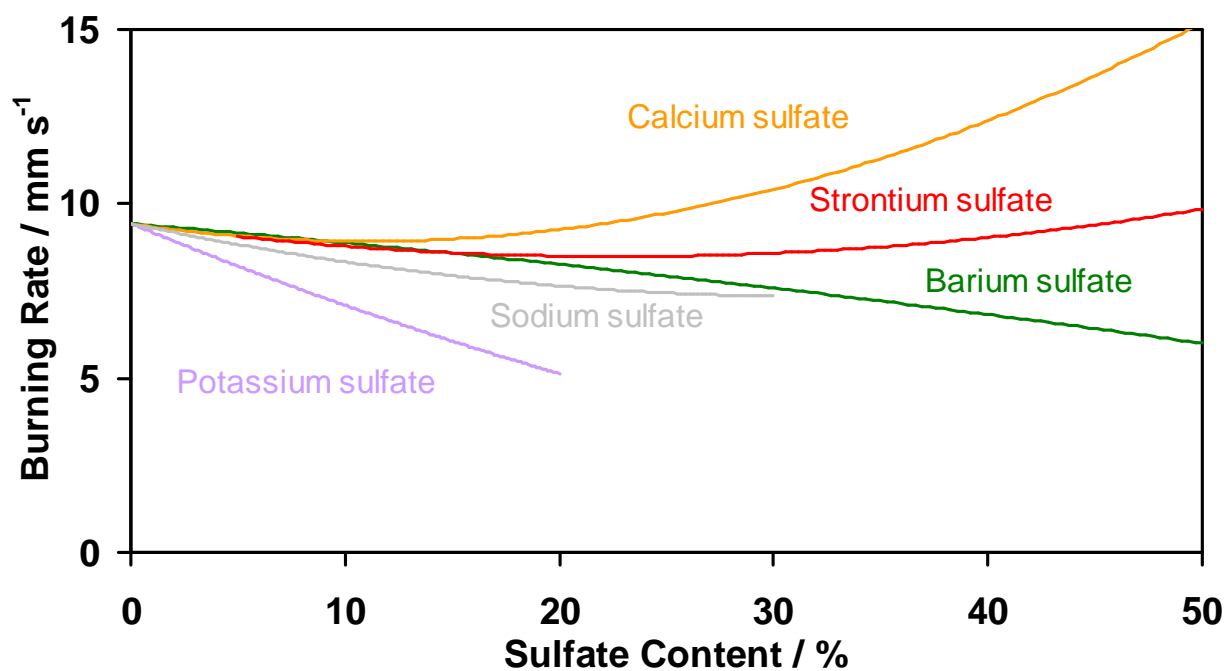


Figure 90; Burning rate curve for aluminum-barium nitrate-sulfate compositions.

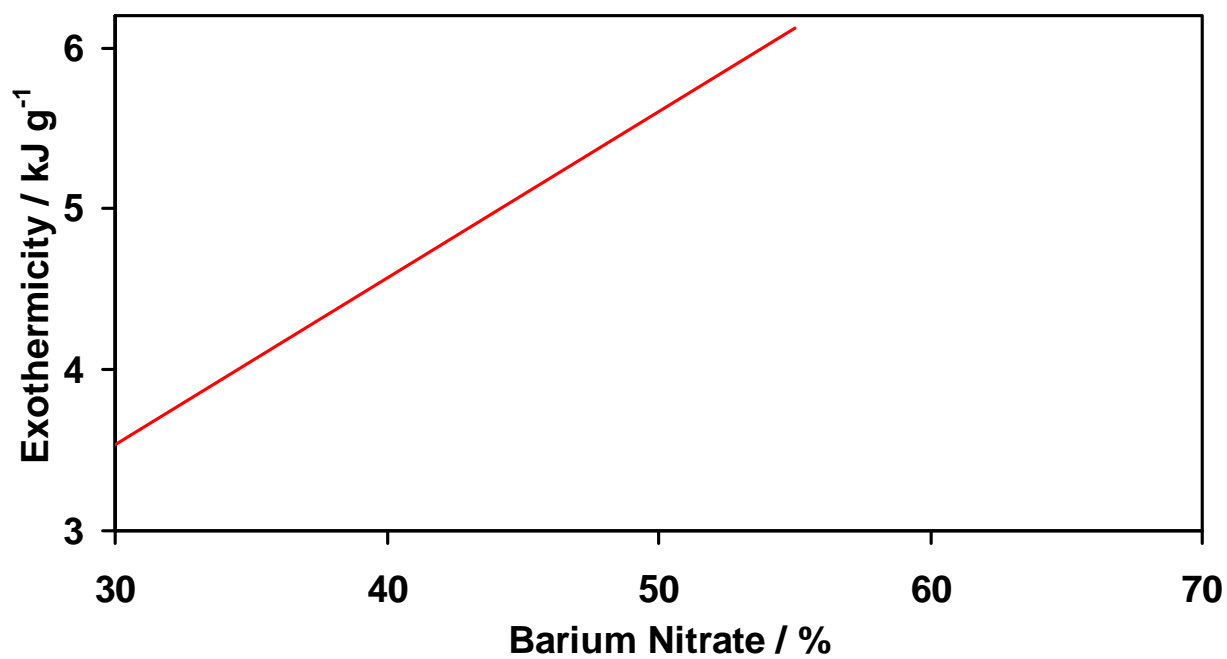


Figure 91; Exothermicity curve for aluminum-barium nitrate compositions.

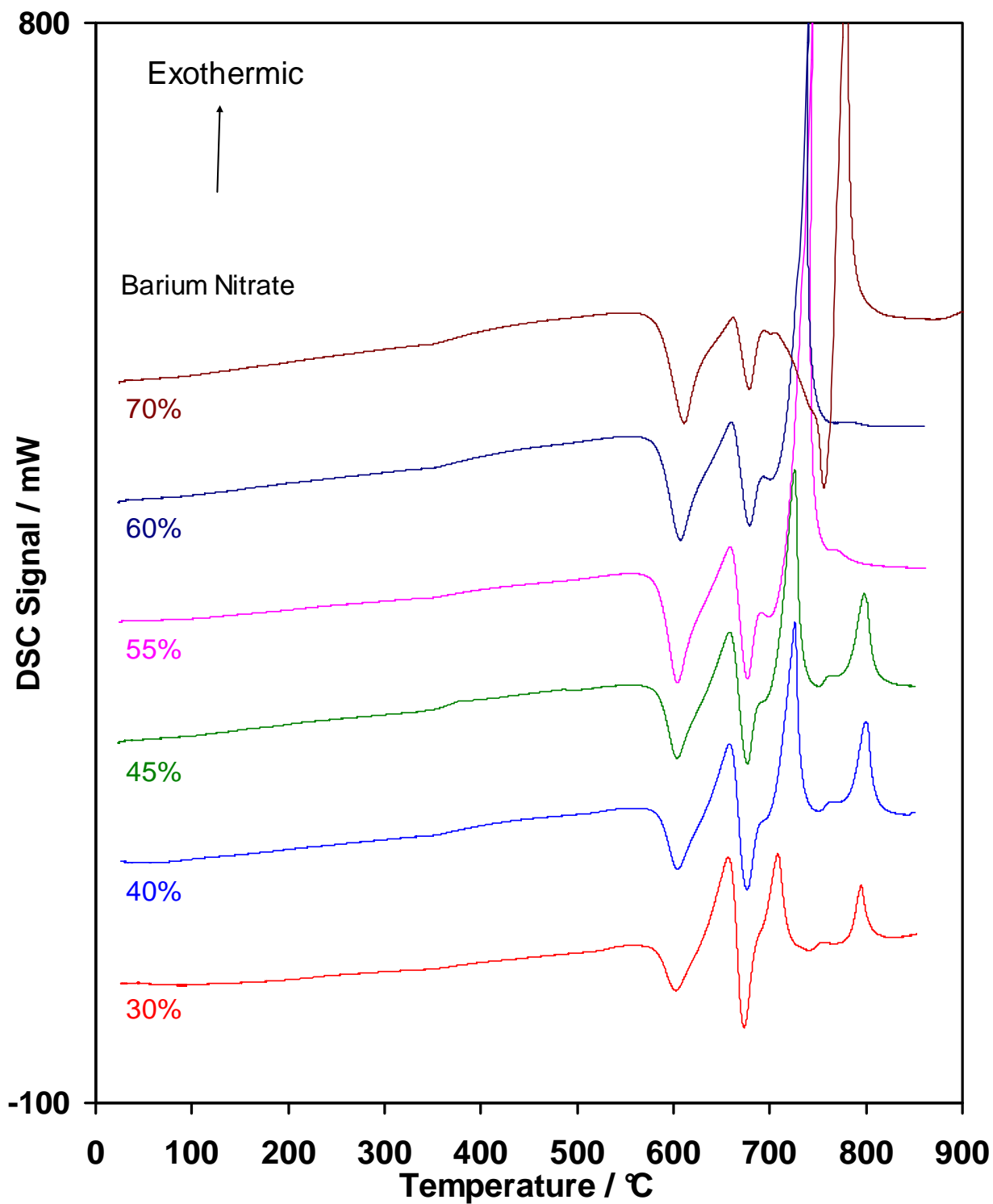


Figure 92; DSC curves for a range of aluminum-barium nitrate compositions.
(Sample mass, 20 mg; heating rate, 50 °C min⁻¹; atmosphere, argon)

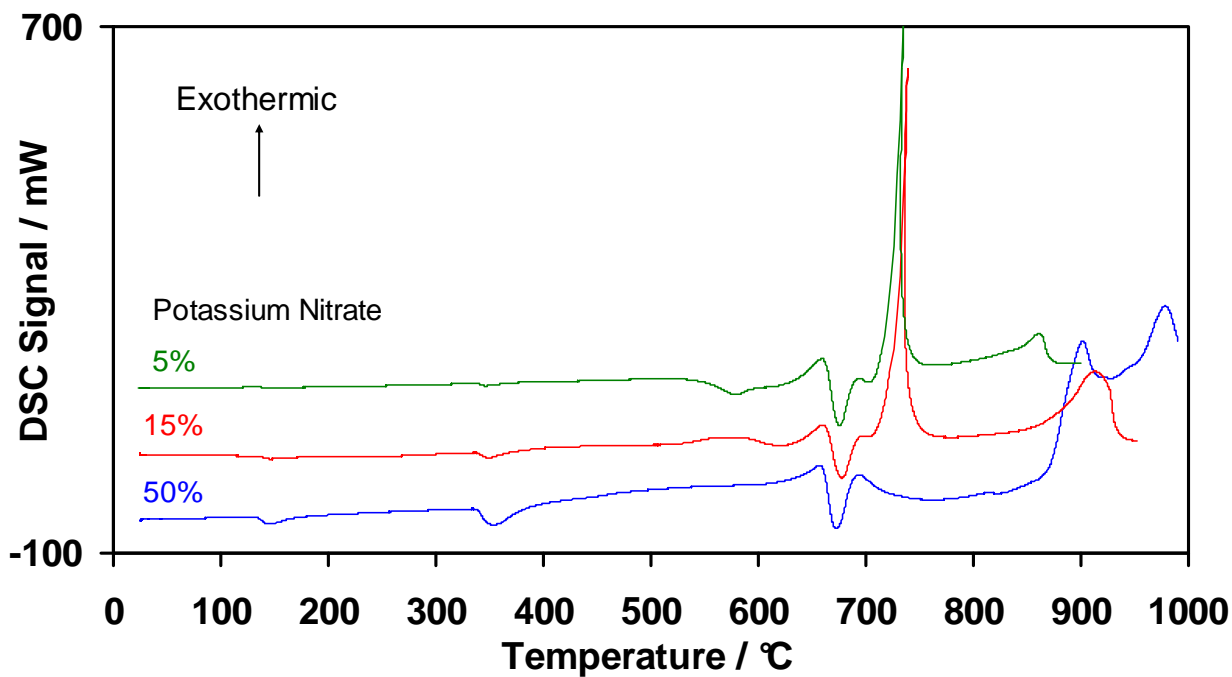


Figure 93; DSC curves for a range of aluminum-barium nitrate-potassium nitrate compositions.

(Sample mass, 20 mg; heating rate, 50 °C min⁻¹; atmosphere, argon)

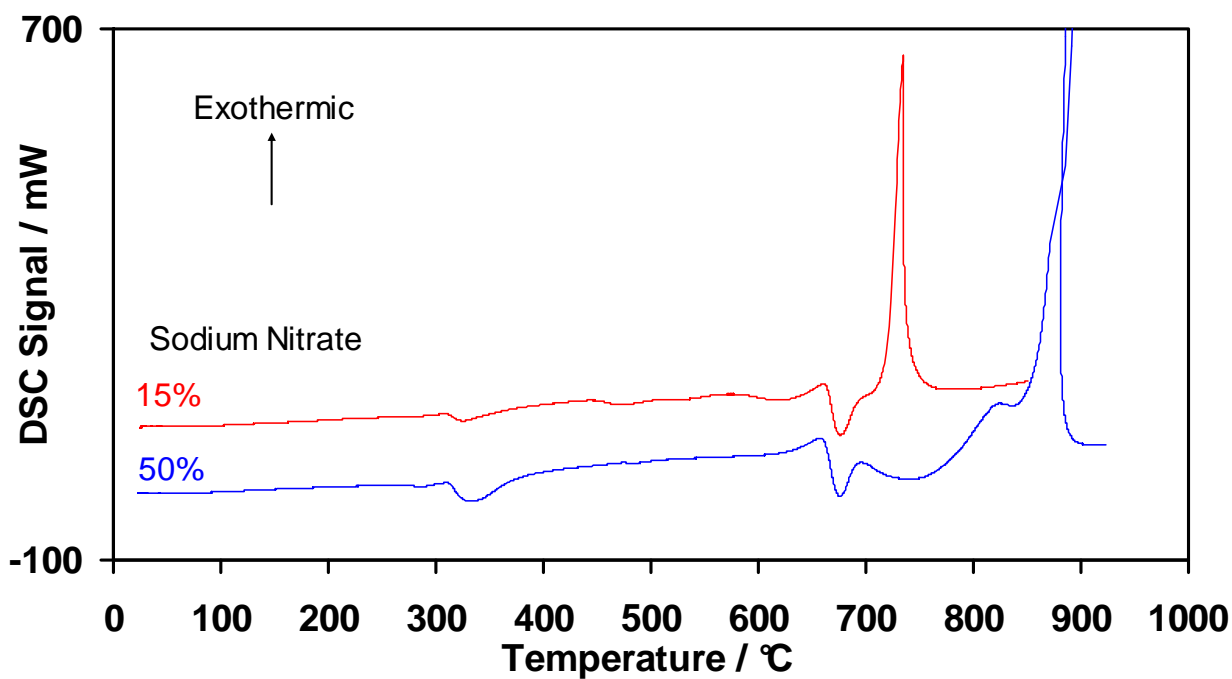


Figure 94; DSC curves for a range of aluminum-barium nitrate-sodium nitrate compositions.

(Sample mass, 20 mg; heating rate, 50 °C min⁻¹; atmosphere, argon)

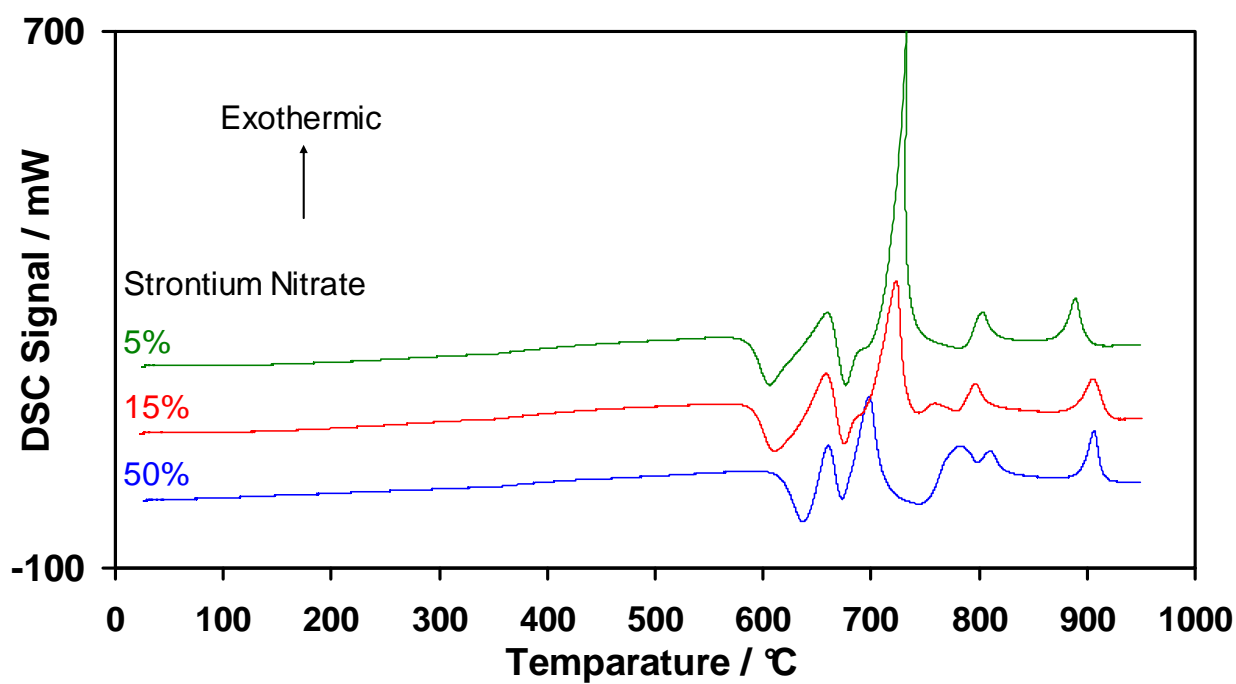


Figure 95; DSC curves for a range of aluminum-barium nitrate-strontium nitrate compositions.

(Sample mass, 20 mg; heating rate, 50 °C min⁻¹; atmosphere, argon)

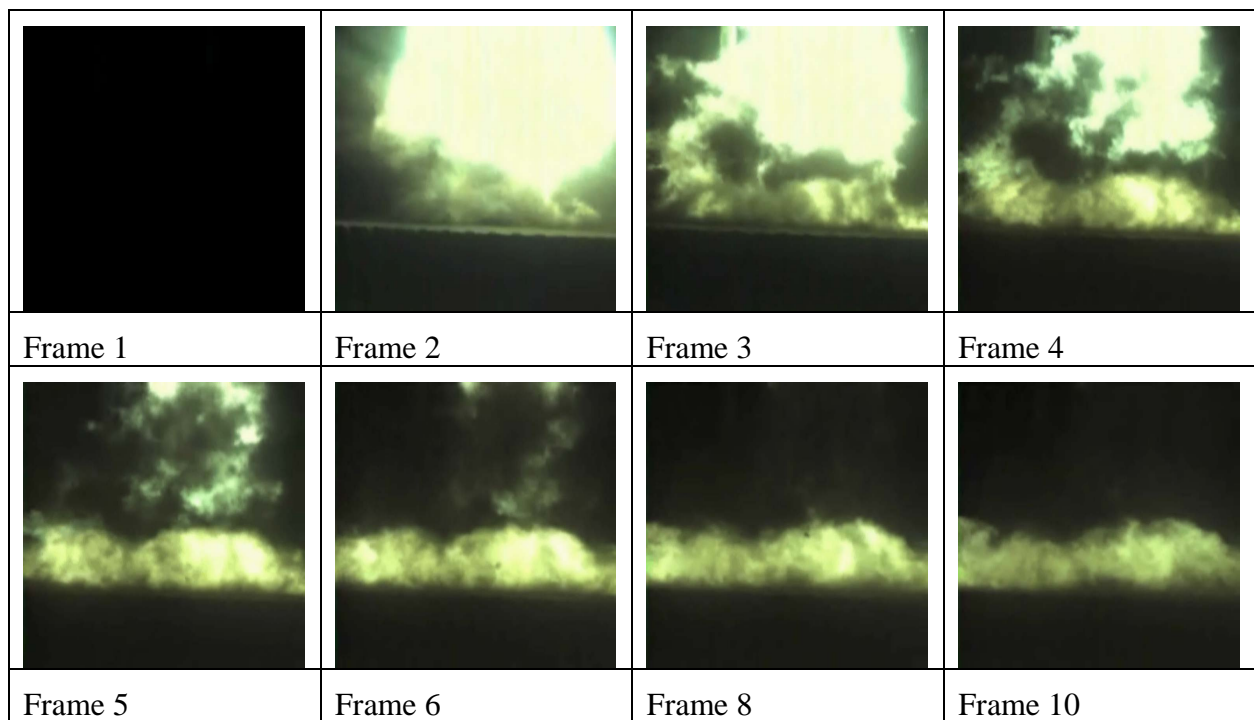


Figure 96; Trial 1, stills for gun firing of bullet containing wax against steel target.



Figure 97; Trial 1, stills for gun firing of bullet containing wax against aluminum alloy target.

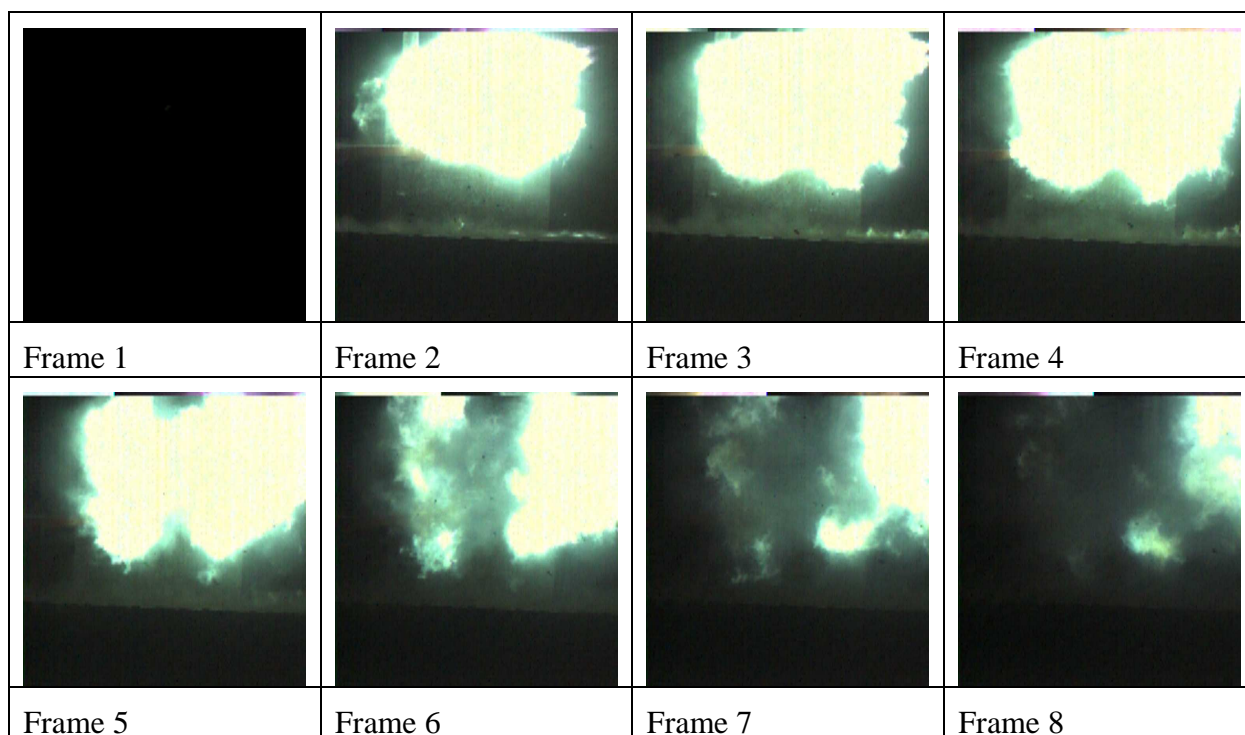


Figure 98; Trial 1, stills for gun firing of bullet containing 50% magnesium/aluminum alloy-40% barium nitrate-10% potassium perchlorate.

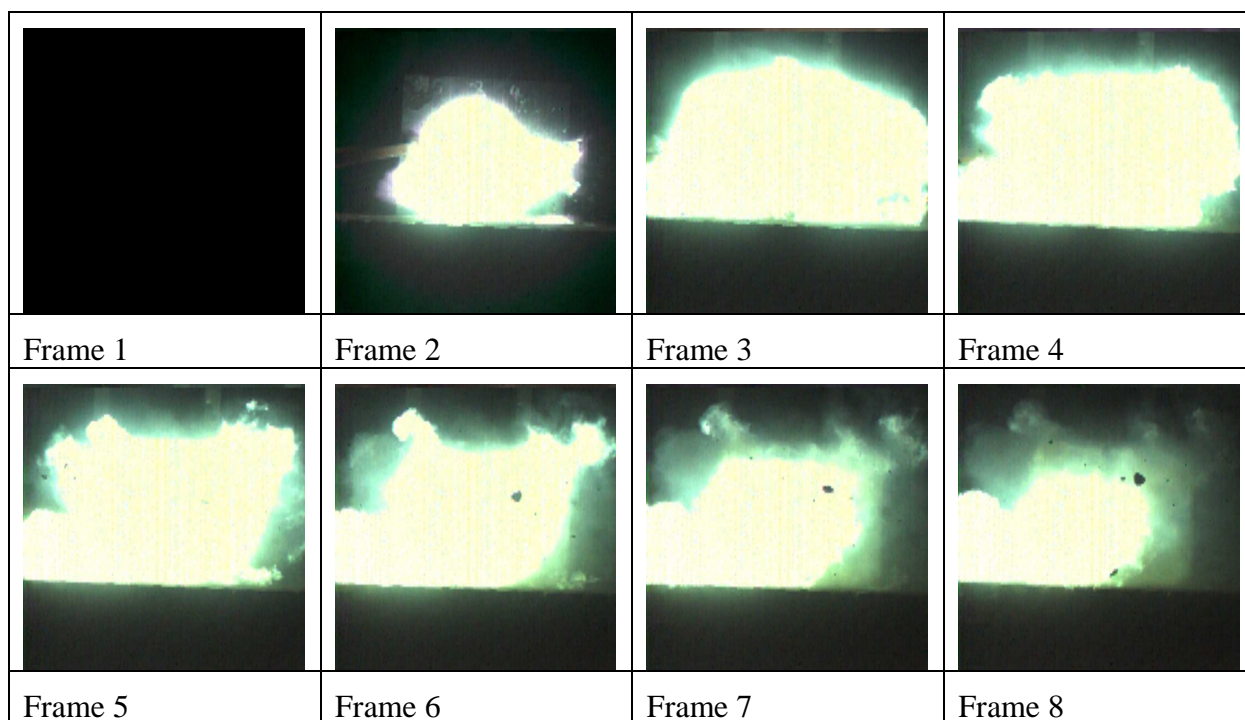


Figure 99; Trial 1, stills for gun firing of bullet containing pellets of 50% magnesium/aluminum alloy-40% barium nitrate-10% potassium perchlorate.

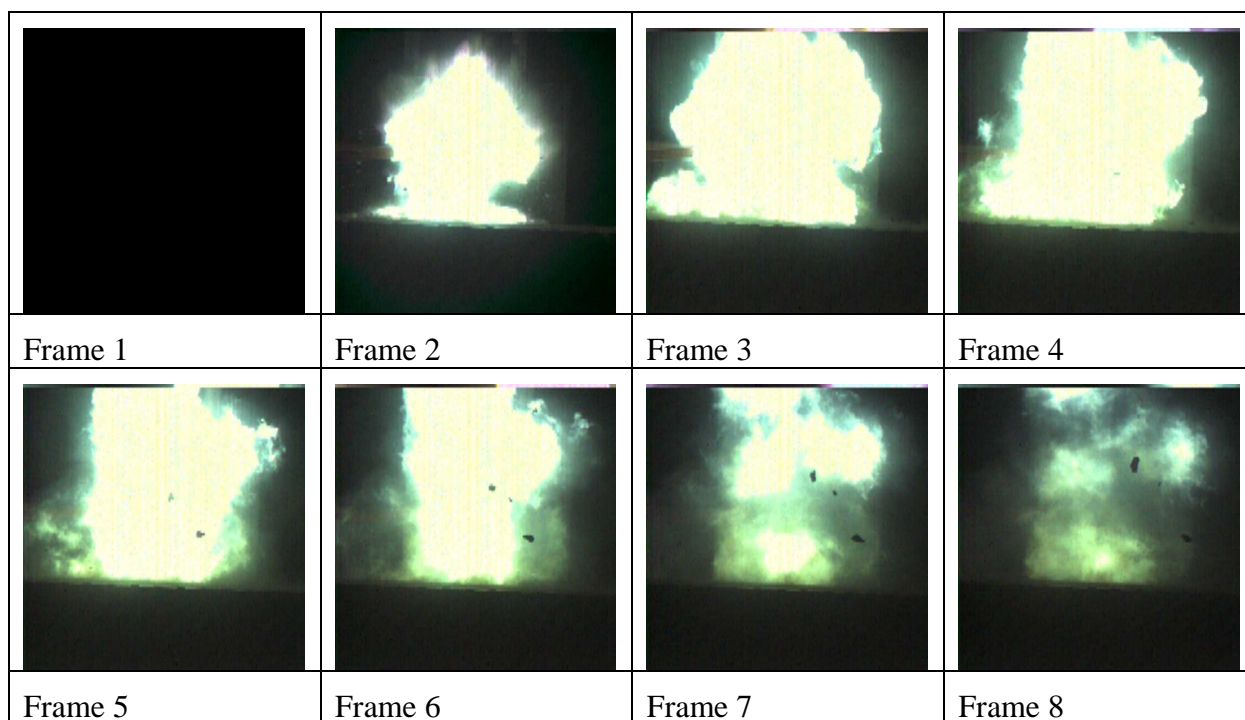


Figure 100; Trial 1, stills for gun firing of bullet containing 50% magnesium/aluminum alloy-35% barium nitrate-15% potassium nitrate.

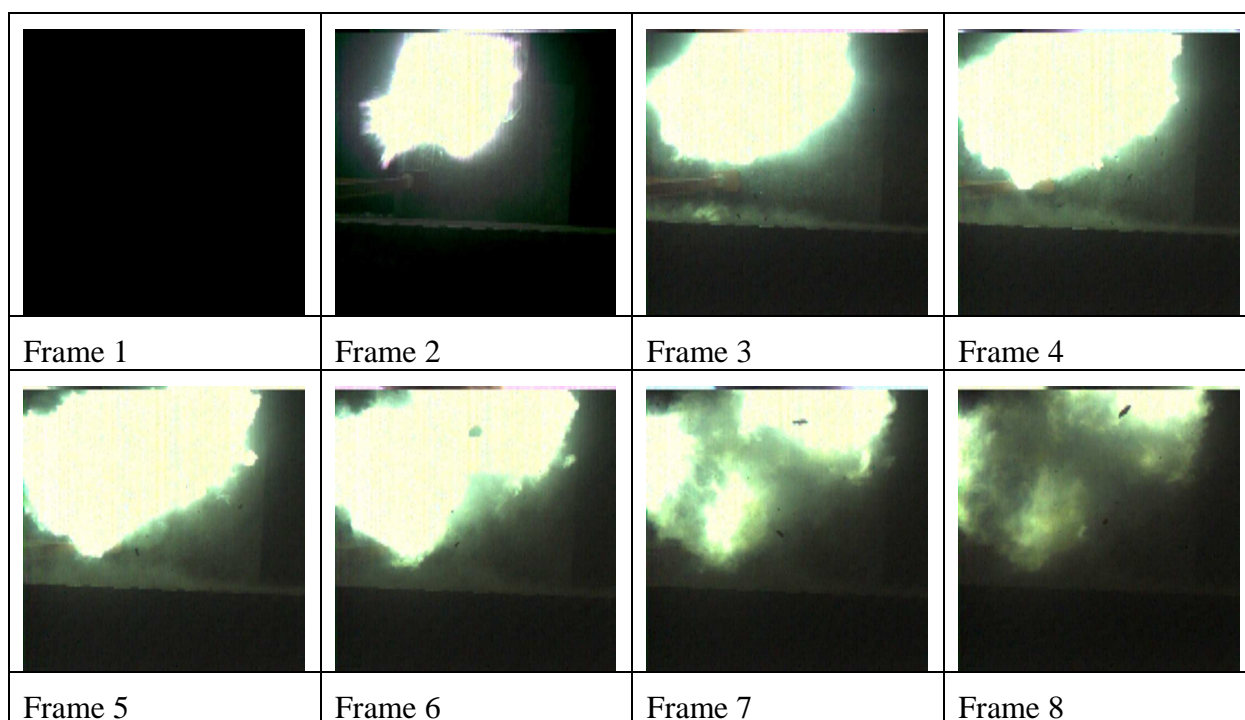


Figure 101; Trial 1, stills for gun firing of bullet containing 50% magnesium/aluminum alloy-35% barium nitrate-15% sodium nitrate.

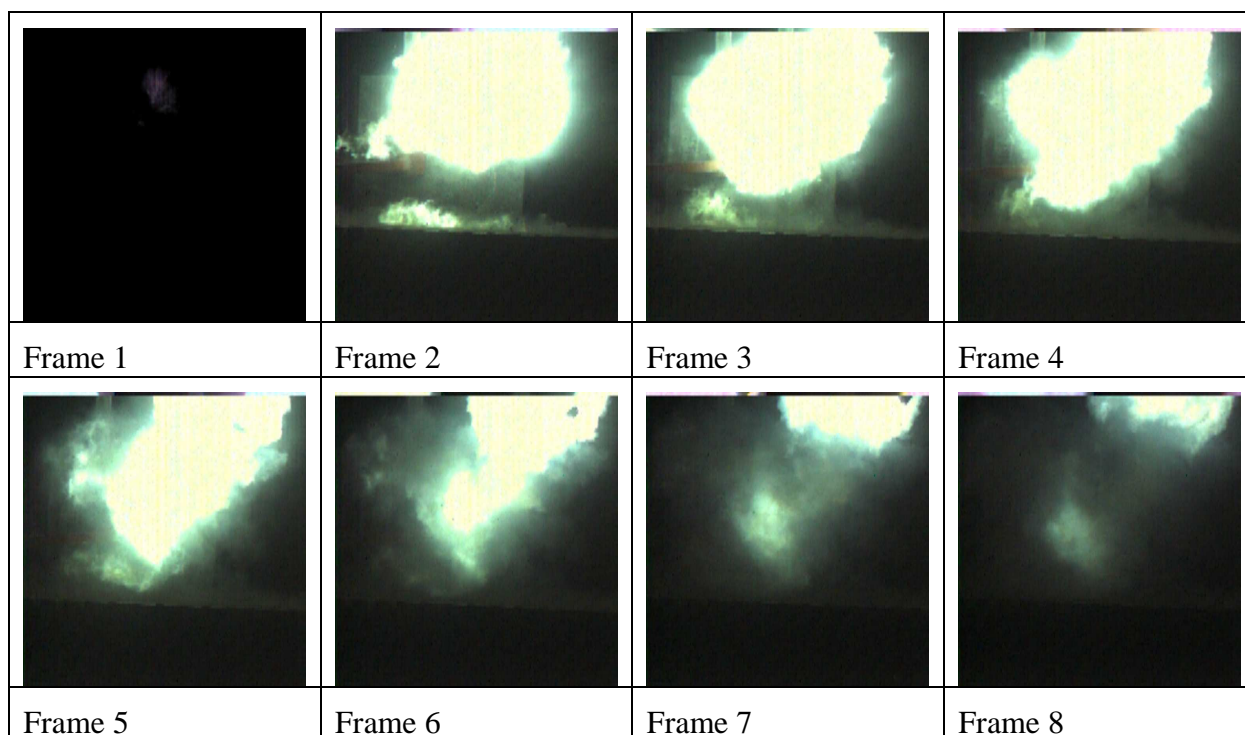


Figure 102; Trial 1, stills for gun firing of bullet containing 50% magnesium/aluminum alloy-35% barium nitrate-15% strontium nitrate.


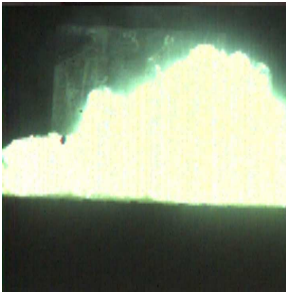
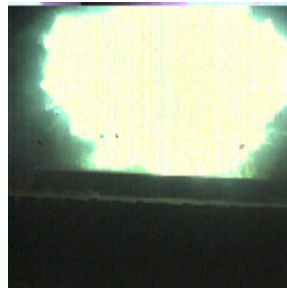
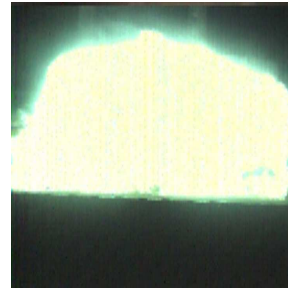
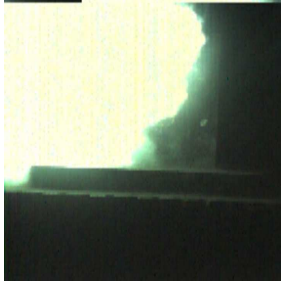
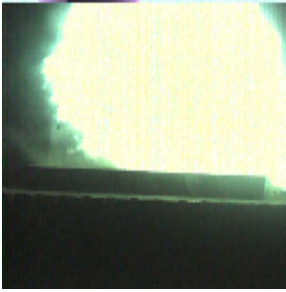


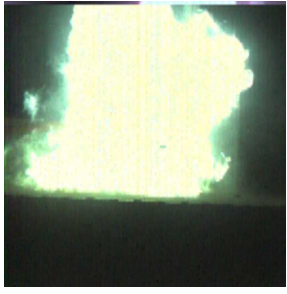
			
1 (Powder) 50% Mg/Al alloy 40% Barium nitrate 10% Potassium perchlorate	2 (Powder) 50% Mg/Al alloy 40% Barium nitrate 10% Potassium perchlorate	3 (Powder) 50% Mg/Al alloy 40% Barium nitrate 10% Potassium perchlorate	4 (Pellets) 50% Mg/Al alloy 40% Barium nitrate 10% Potassium perchlorate
			
5 (Pellets) 50% Mg/Al alloy 40% Barium nitrate 10% Potassium perchlorate	6 (Pellets) 50% Mg/Al alloy 40% Barium nitrate 10% Potassium perchlorate	10 (Powder) 50% Mg/Al alloy 35% Barium nitrate 15% Strontium nitrate	11 (Powder) 50% Mg/Al alloy 40% barium nitrate 10% Sodium nitrate
			
12 (Powder) 50% Mg/Al alloy 17.5% Barium nitrate 17.5% Potassium nitrate			

Figure 103; Trial 1, stills showing the frame with the largest output from a range of compositions.



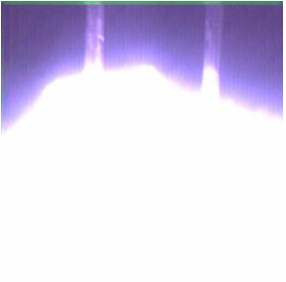
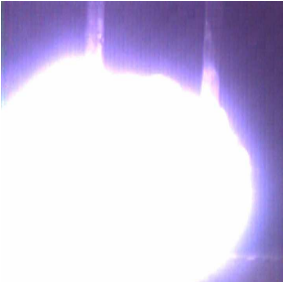


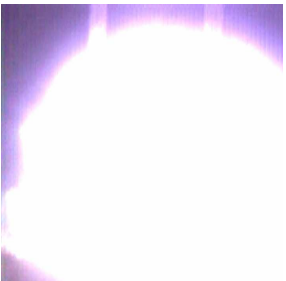





			
17 (Powder)	18 (Powder)	19 (Pellets)	20 (Pellets)

Figure 104; Trial 2, stills for gun firing of bullet containing 49% magnesium/aluminum alloy-49% potassium perchlorate and 2% calcium resinate.

			
16 (Powder) 50% Mg/Al alloy 35% Barium nitrate 15% Potassium sulfate	21 (Powder) 50% Mg/Al alloy 35% Barium nitrate 15% Strontium nitrate	22 (Powder) 50% Mg/Al alloy 50% Sodium nitrate	23 (Pellets) 50% Mg/Al alloy 50% Sodium nitrate
			
24 (Powder) 50% Mg/Al alloy 50% Potassium nitrate	25 (Pellets) 50% Mg/Al alloy 50% Potassium nitrate	26 (Powder) 50% Mg/Al alloy 50% Barium nitrate 15% Strontium sulfate	27 (Powder) 50% Mg/Al alloy 50% Potassium sulfate
			
28 (Powder) 50% Mg/Al alloy 50% Sodium sulfate	29 (Powder) 50% Mg/Al alloy 50% Strontium sulfate	30 (Powder) 50% Mg/Al alloy 35% Barium nitrate 15% Potassium nitrate	31 (Pellets) 50% Mg/Al alloy 35% Barium nitrate 15% Potassium nitrate









			
32 (Pellets) 50% Mg/Al alloy 35% Barium nitrate 15% Potassium nitrate	33 (Powder) 50% Magnesium 50% Sodium nitrate	34 (Powder) 49% Mg/Al alloy 49% Barium nitrate 2% PolyNIMMO	35 (Pellets) 49% Mg/Al alloy 49% Barium nitrate 2% PolyNIMMO
			
36 (Powder) 46% Mg/Al alloy 46% Barium nitrate 8% PolyNIMMO	37 (Pellets) 46% Mg/Al alloy 46% Barium nitrate 8% PolyNIMMO	38 (Powder) 45% Mg/Al alloy 45% Barium nitrate 10% PolyGlyN	39 (Pellets) 45% Mg/Al alloy 45% Barium nitrate 10% PolyGlyN

Figure 105; Trial 2, stills showing the frame with the largest output from a range of compositions.



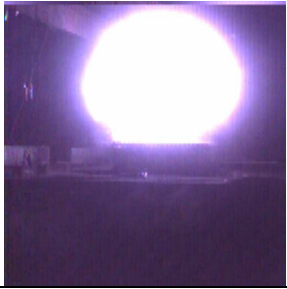
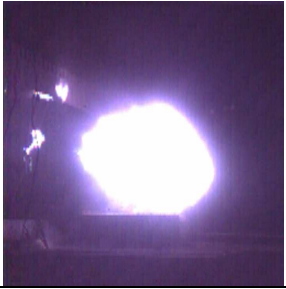


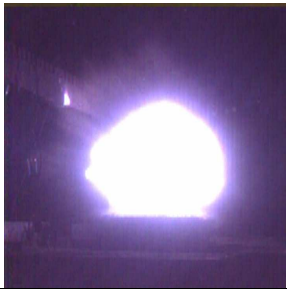




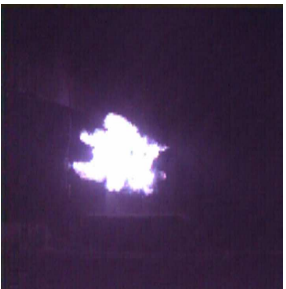




	
42 (Powder) 50% Mg/Al alloy 50% Barium nitrate	43 (Powder) 50% Mg/Al alloy 50% Barium nitrate

Figure 106; Trial 2, stills showing the frame with the largest output from a range of compositions Phantom camera on narrow field.

			
44 (Powder) 50% Mg/Al alloy 50% Strontium nitrate	45 (Powder) 50% Mg/Al alloy 50% Strontium nitrate	46 (Powder) 50% Mg/Al alloy 50% Calcium sulfate	47 (Powder) 50% Mg/Al alloy 35% Barium nitrate 15% Calcium sulfate
			
48 (Powder) 50% Mg/Al alloy 35% Barium nitrate 15% Sodium sulfate	49 (Powder) 50% Mg/Al alloy 35% Barium nitrate 15% Potassium sulfate	50 (Powder) 50% Magnesium 50% Sodium nitrate	51 (Powder) 50% Magnesium 50% Sodium nitrate
			
52 (Powder) 50% Magnesium 50% Strontium nitrate	53 (Powder) 50% Magnesium 50% Strontium sulfate	54 (Powder) 50% Magnesium 50% Potassium sulfate	55 (Powder) 50% Magnesium 50% Calcium sulfate
			
56(Powder) 50% Aluminum 50% Sodium nitrate	57 (Powder) 50% Aluminum 50% Strontium nitrate	58 (Powder) 50% Aluminum 50% Sodium sulfate	59 (Powder) 50% Aluminum 50% Barium sulfate

			
60 (Powder) 50% Aluminum 50% Strontium sulfate	61 (Powder) 50% Mg/Al alloy 35% Strontium nitrate 15% Sodium nitrate	62 (Powder) 50% Mg/Al alloy 35% Strontium nitrate 15% Potassium nitrate	63 (Powder) 49% Mg/Al alloy 49% Sodium nitrate 2% PolyGlyN
			
64 (Powder) 49% Mg/Al alloy 49% Sodium nitrate 2% PolyGlyN	65 (Powder) 49% Mg/Al alloy 49% Strontium nitrate 2% PolyNIMMO	66 (Powder) 49% Mg/Al alloy 49% Strontium nitrate 2% PolyNIMMO	67 (Powder) 50% Mg/Al alloy 40% Barium nitrate 10% Potassium perchlorate
			
68 (Powder) 50% Mg/Al alloy 40% Barium nitrate 10% Potassium perchlorate	69 (Powder) 49% Mg/Al alloy 49% Potassium perchlorate 2% Calcium resinate	70 (Powder) 19% Aluminum 81% Tungsten oxide	71 (Powder) 27% Mg/Al alloy 73% Ferric oxide (Fe ₂ O ₃)
			
72 (Powder) 27% Aluminum 73% Ferric oxide (Fe ₂ O ₃)	73 (Powder) 27% Al-B nano 43% Ferric oxide (Fe ₂ O ₃)		

Figure 107; Trial 3, stills showing the frame with the largest output from a range of compositions.

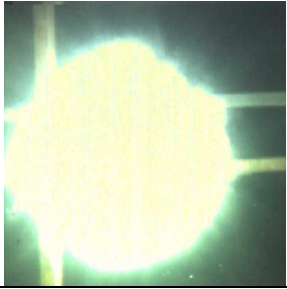
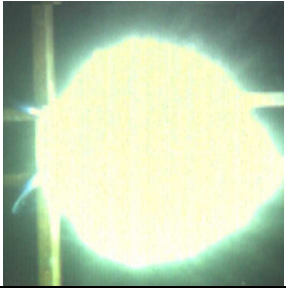
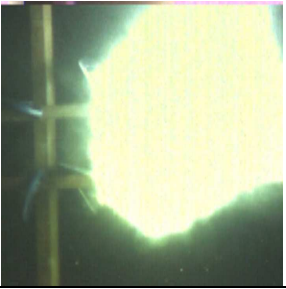
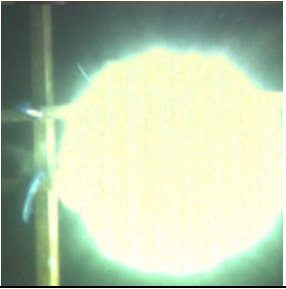
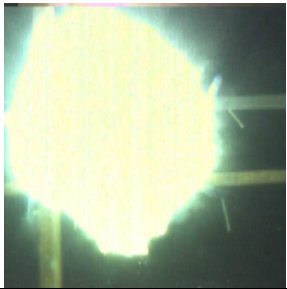
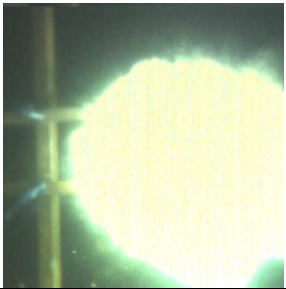
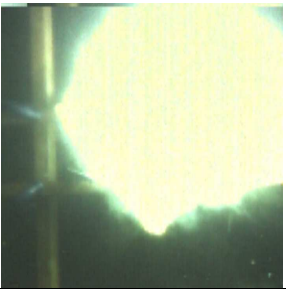
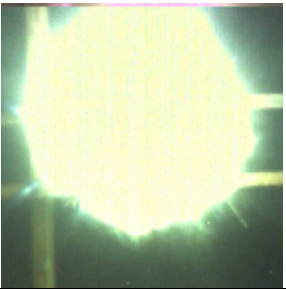
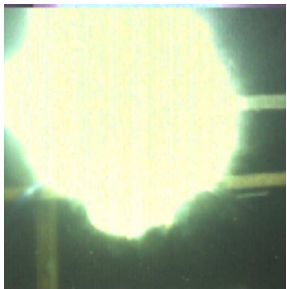
			
75 (Powder) 48% Mg/Al alloy 48% Sodium nitrate 4% Calcium resinate	76 (Powder) 49% Mg/Al alloy 49% Sodium nitrate 2% Boiled linseed oil	77 (Powder) 48% Mg/Al alloy 48% Sodium nitrate 4% Boiled linseed oil	78 (Powder) 49% Mg/Al alloy 49% Sodium nitrate 2% Lithographic varnish
			
79 (Powder) 48% Mg/Al alloy 48% Sodium nitrate 4% Lithographic varnish	80 (Powder) 49% Mg/Al alloy 49% Sodium nitrate 2% PVC powder	81 (Powder) 48% Mg/Al alloy 48% Sodium nitrate 4% PVC powder	82 (Powder) 49% Mg/Al alloy 49% Sodium nitrate 2% GAP
			
83 (Powder) 48% Mg/Al alloy 48% Sodium nitrate 4% GAP			

Figure 108; Trial 4, stills for gun firing of bullet containing magnesium/aluminum alloy-sodium nitrate and either 2% or 4% binder.

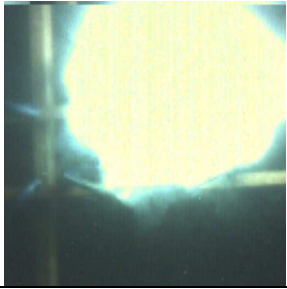
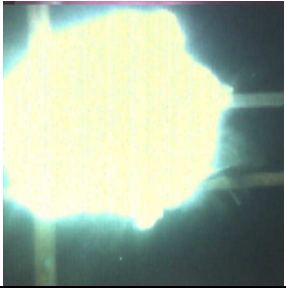
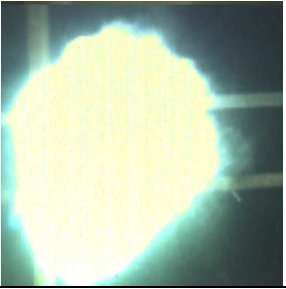
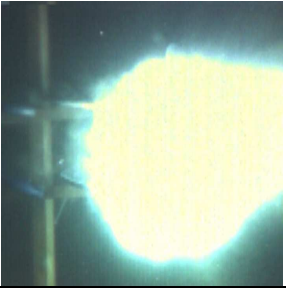
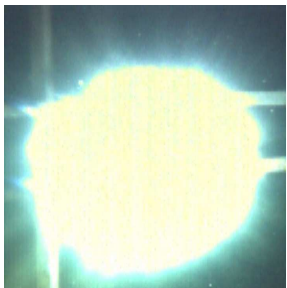
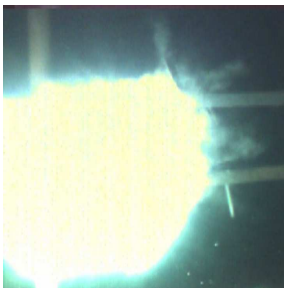
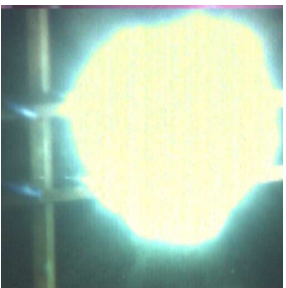
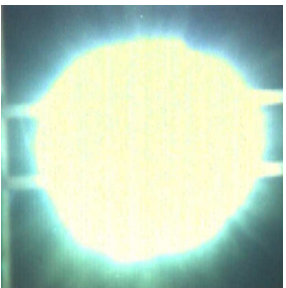
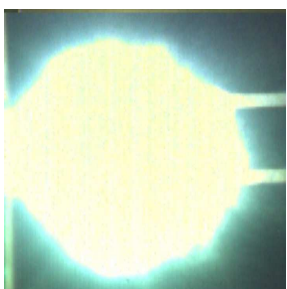

			
84 (Powder) 49% Mg/Al alloy 49% Potassium nitrate 2% Calcium resinate	85 (Powder) 48% Mg/Al alloy 48% Potassium nitrate 4% Calcium resinate	86 (Powder) 49% Mg/Al alloy 49% Potassium nitrate 2% Boiled linseed oil	87 (Powder) 48% Mg/Al alloy 48% Potassium nitrate 4% Boiled linseed oil
			
88 (Powder) 49% Mg/Al alloy 49% Potassium nitrate 2% Lithographic varnish	89 (Powder) 48% Mg/Al alloy 48% Potassium nitrate 4% Lithographic varnish	90 (Powder) 49% Mg/Al alloy 49% Potassium nitrate 2% PVC powder	91 (Powder) 48% Mg/Al alloy 48% Potassium nitrate 4% PVC powder
			
92 (Powder) 49% Mg/Al alloy 49% Potassium nitrate 2% GAP	93 (Powder) 48% Mg/Al alloy 48% Potassium nitrate 4% GAP		

Figure 109; Trial 4, stills for gun firing of bullet containing magnesium/aluminum alloy-potassium nitrate and either 2% or 4% binder.

			
94 (Powder) 49% Mg/Al alloy 49% Sodium nitrate 2% Calcium resinate	95 (Powder) 49% Mg/Al alloy 49% Sodium nitrate 2% Calcium resinate	96 (Powder) 49% Mg/Al alloy 49% Sodium nitrate 2% Calcium resinate	97 (Powder) 49% Mg/Al alloy 49% Sodium nitrate 2% Calcium resinate
			
98 (Powder) 48% Mg/Al alloy 48% Sodium nitrate 4% Calcium resinate	99 (Powder) 48% Mg/Al alloy 48% Sodium nitrate 4% Calcium resinate	100 (Powder) 48% Mg/Al alloy 48% Sodium nitrate 4% Calcium resinate	101 (Powder) 48% Mg/Al alloy 48% Sodium nitrate 4% Calcium resinate
			
102 (Powder) 50% Mg/Al alloy 40% Barium nitrate 10% Potassium perchlorate	103 (Powder) 50% Mg/Al alloy 40% Barium nitrate 10% Potassium perchlorate	104 (Powder) 49% Mg/Al alloy 49% Potassium perchlorate 2% Calcium resinate	105 (Powder) 49% Mg/Al alloy 49% Potassium perchlorate 2% Calcium resinate

Figure 110; Trial 5, stills for gun firing of bullet containing magnesium/aluminum alloy-potassium nitrate and either 2% or 4% calcium resinate or control compositions based on potassium perchlorate.

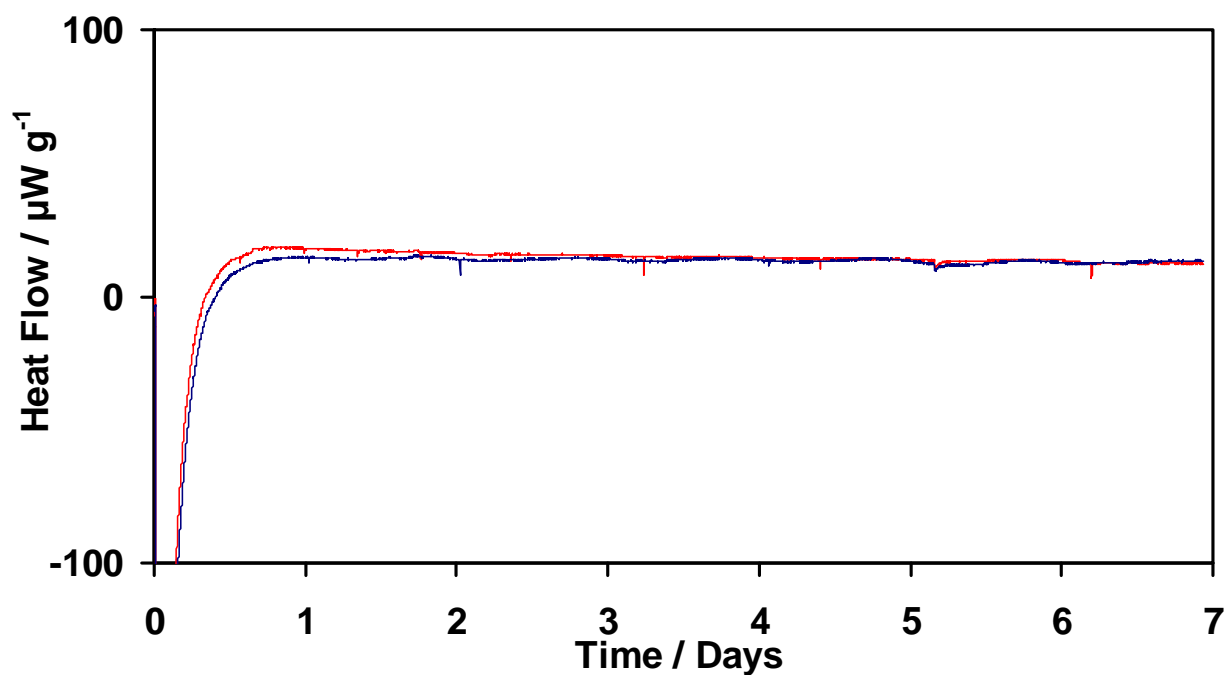


Figure 111; Microcalorimetry heat flow curves for magnesium/aluminum alloy.
(Sample mass, 100 mg; 50 °C, 65% RH; atmosphere, air)

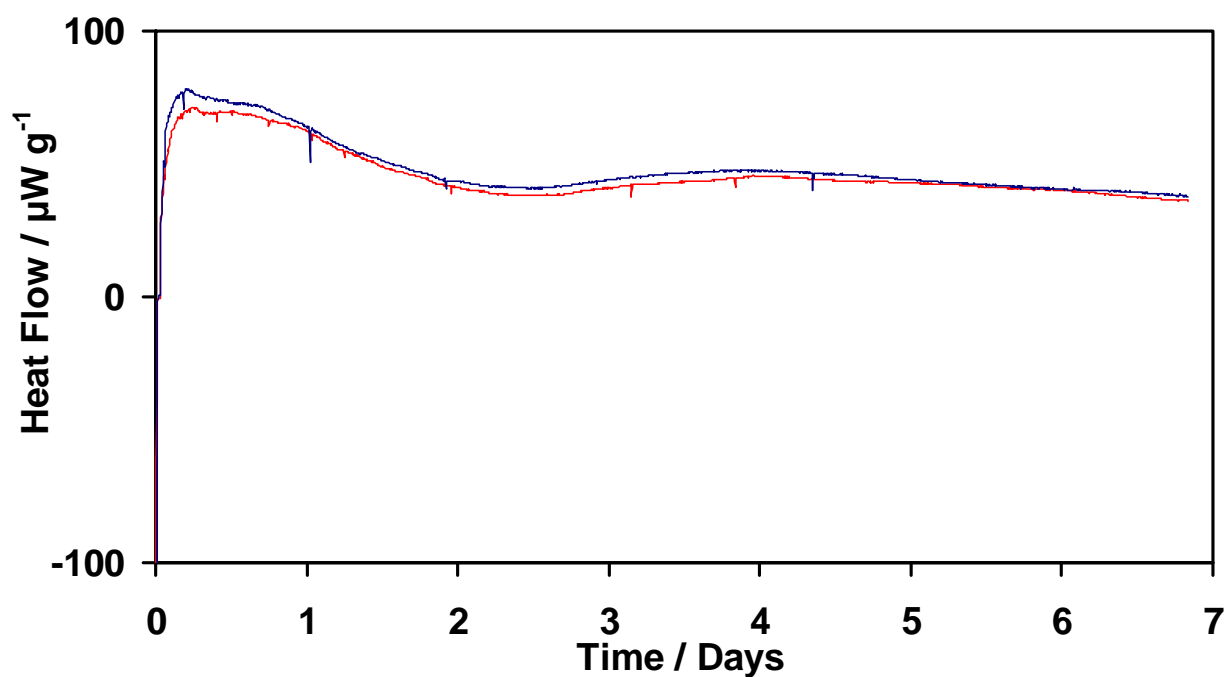


Figure 112; Microcalorimetry heat flow curves magnesium/aluminum alloy.
(Sample mass, 100 mg; 50 °C, 75% RH; atmosphere, air)

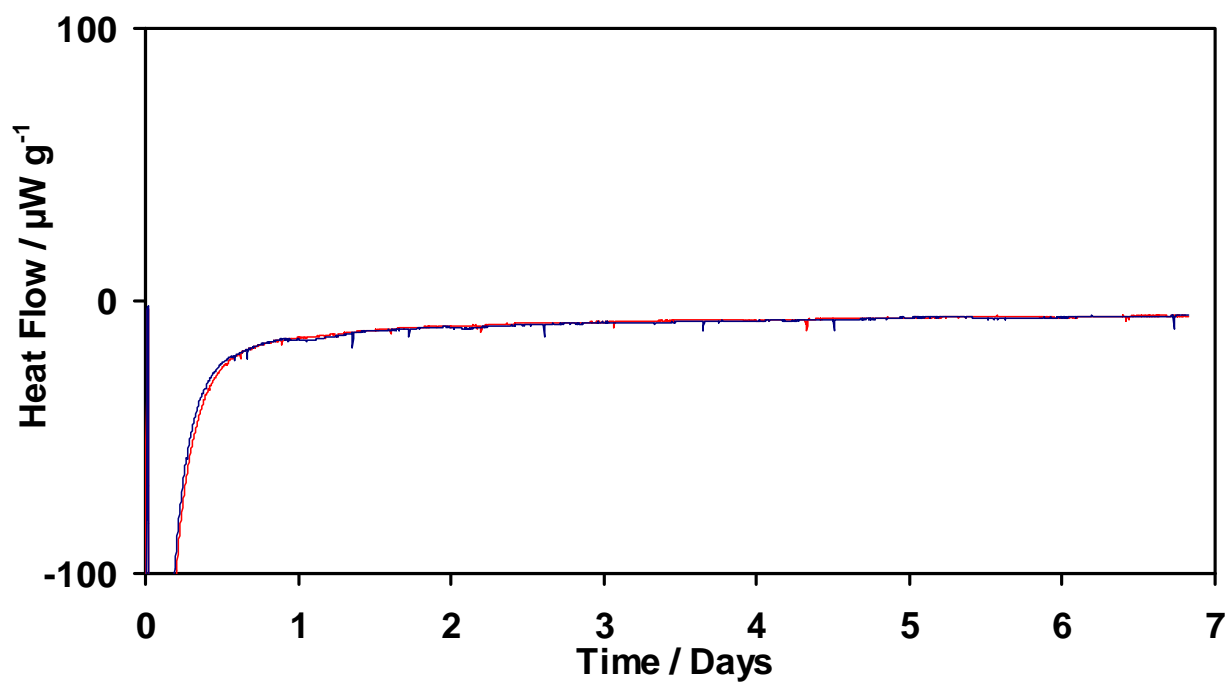


Figure 113; Microcalorimetry heat flow curves for potassium perchlorate.
(Sample mass, 100 mg; 50 °C, 65% RH; atmosphere, air)

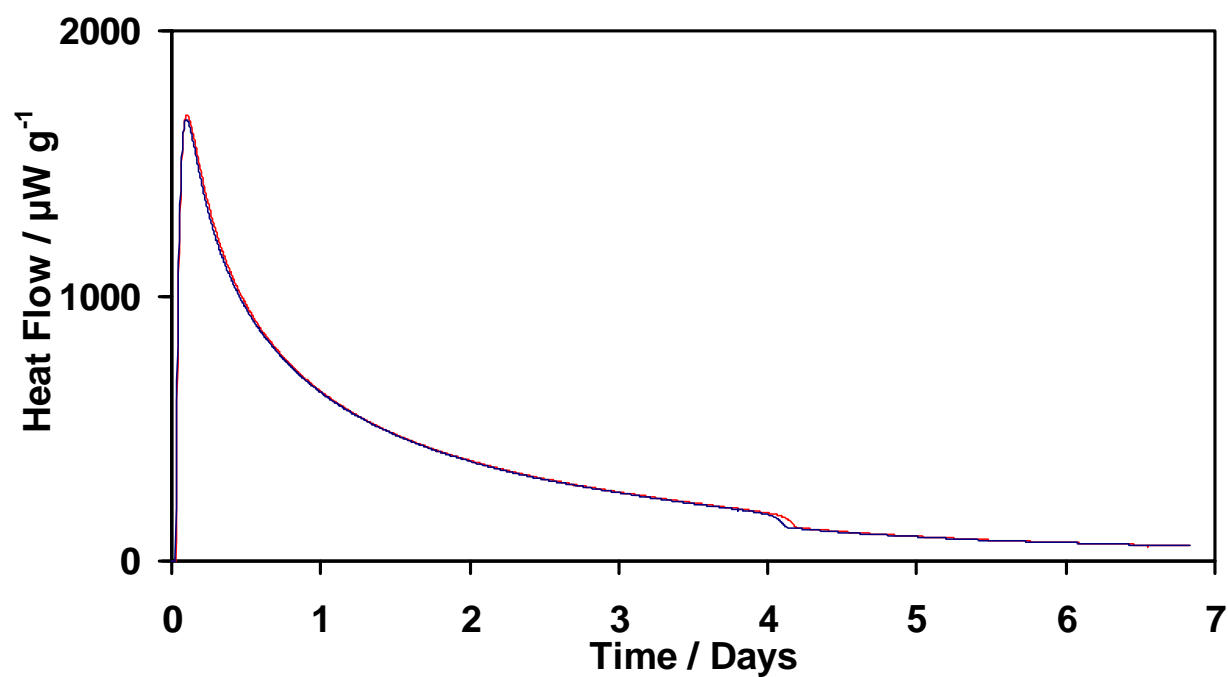


Figure 114; Microcalorimetry heat flow curves for calcium resinate.
(Sample mass, 100 mg; 50 °C, 65% RH; atmosphere, air)

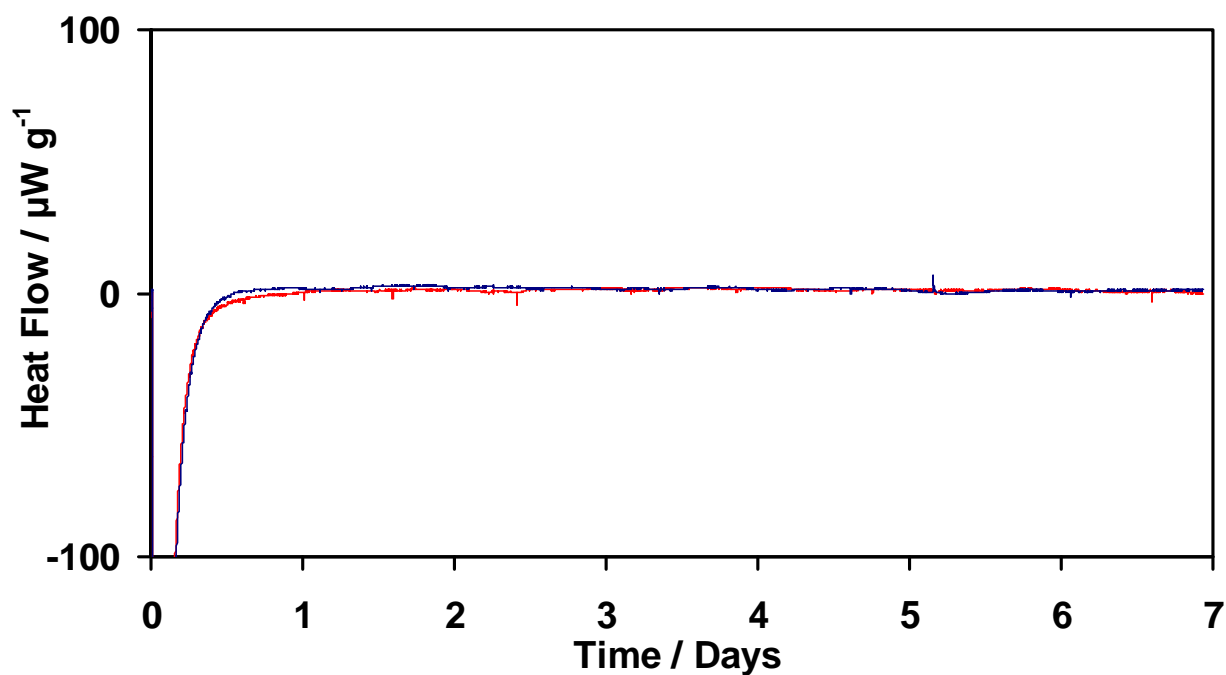


Figure 115; Microcalorimetry heat flow curves for a 50% magnesium/aluminum alloy-50% potassium perchlorate composition.
(Sample mass, 100 mg; 50 °C, 65% RH; atmosphere, air)

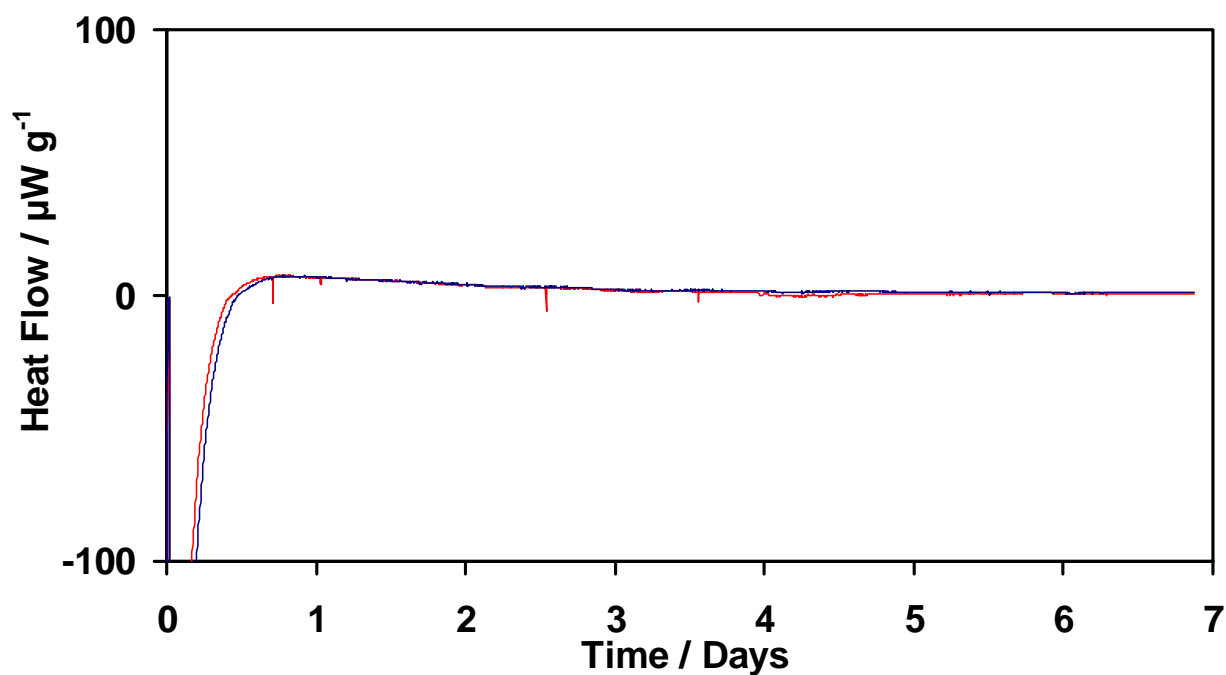


Figure 116; Microcalorimetry heat flow curves for a 49% magnesium/aluminum alloy-49% potassium perchlorate-2% calcium resinate composition.
(Sample mass, 100 mg; 50 °C, 65% RH; atmosphere, air)

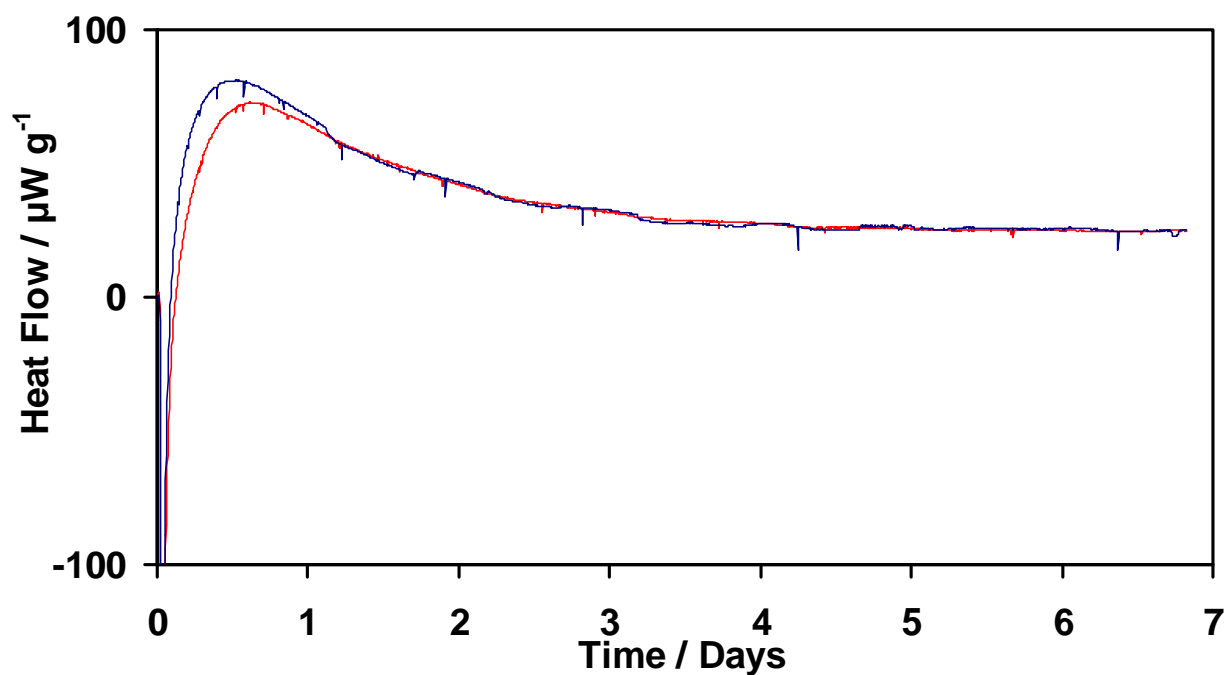


Figure 117; Microcalorimetry heat flow curves for a 44% magnesium/aluminum alloy-44% potassium perchlorate-12% calcium resinate composition.
(Sample mass, 100 mg; 50 °C, 65% RH; atmosphere, air)

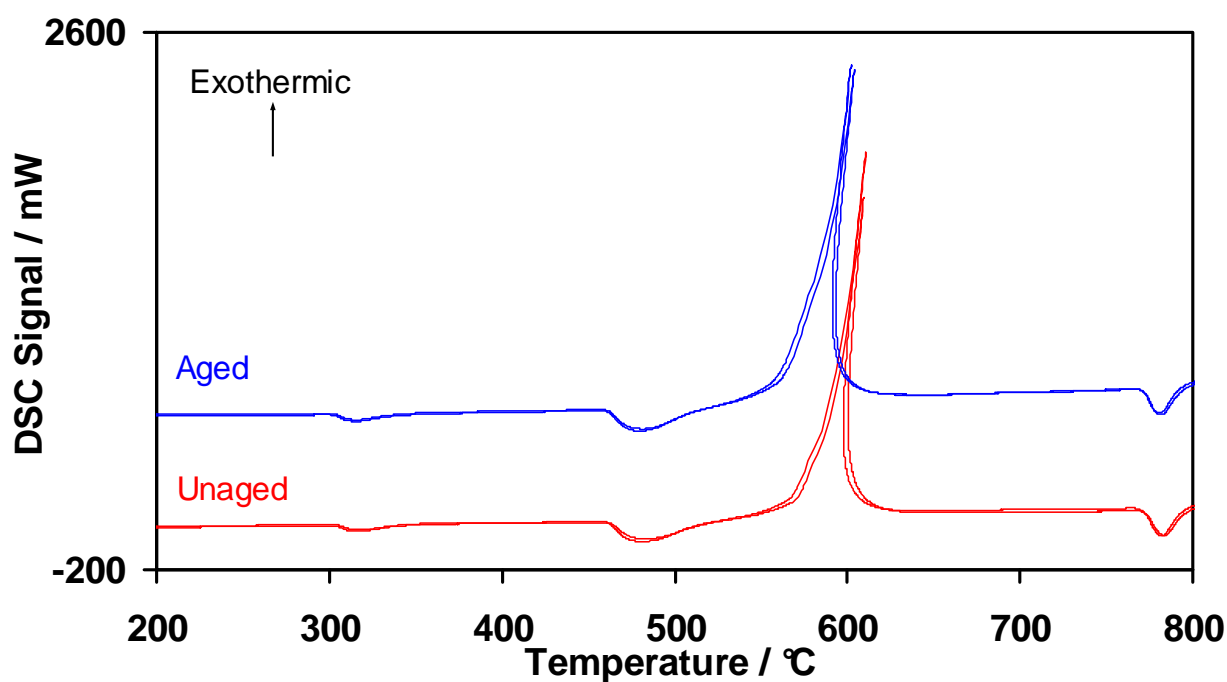


Figure 118; DSC curves for 50% magnesium/aluminum alloy-50% potassium perchlorate composition unaged and aged for 7 days at 50°C and 65% RH.
(Sample mass, 20 mg; heating rate, 50 °C min⁻¹; atmosphere, argon)

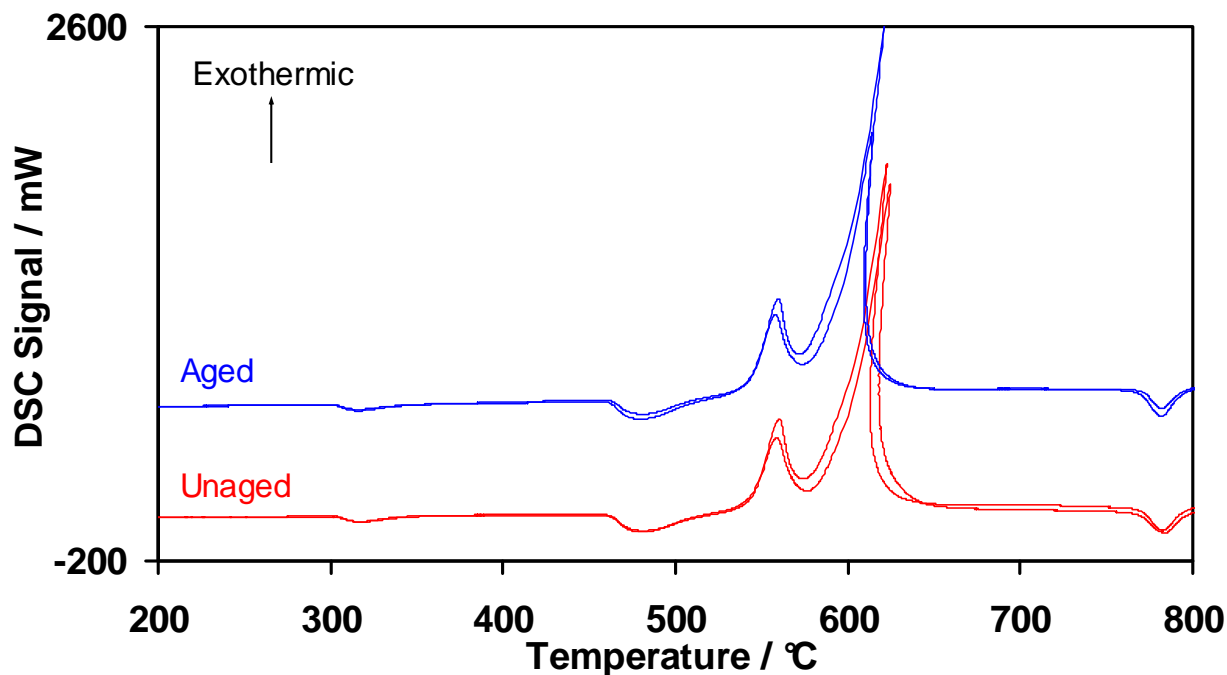


Figure 119; DSC curves for 49% magnesium/aluminum alloy-49% potassium perchlorate-2% calcium resinate composition unaged and aged for 7 days at 50°C and 65% RH. (Sample mass, 20 mg; heating rate, 50 °C min⁻¹; atmosphere, argon)

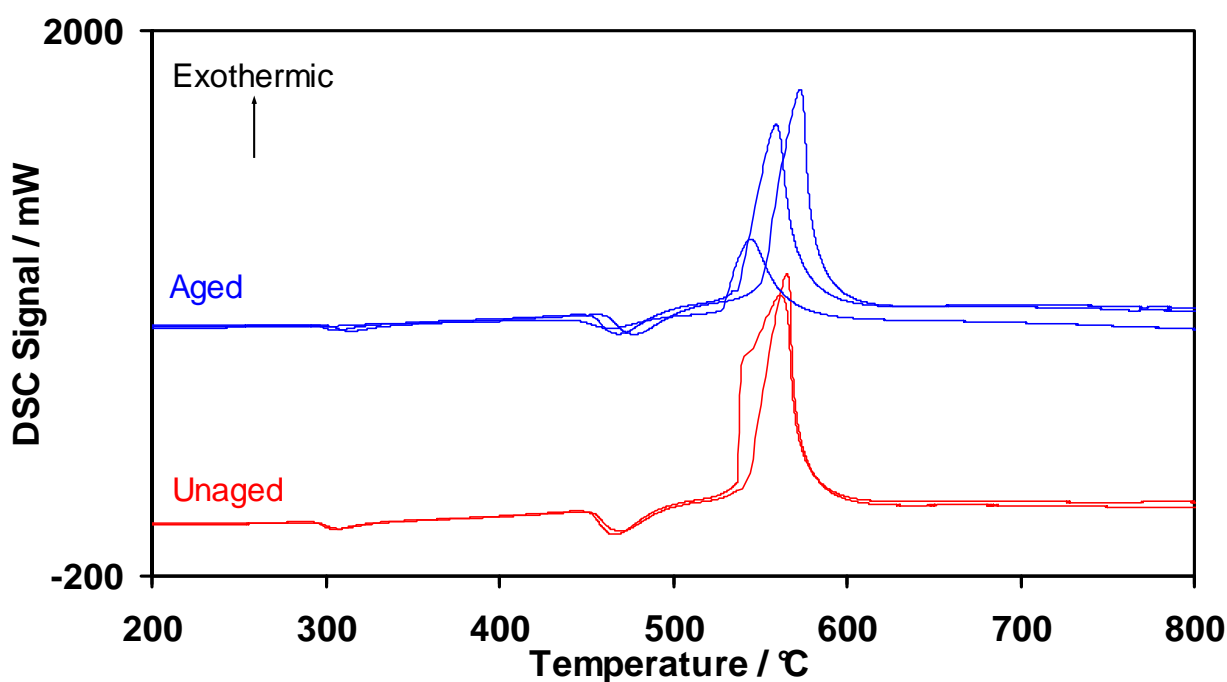


Figure 120; DSC curves for 44% magnesium/aluminum alloy-44% potassium perchlorate-12% calcium resinate composition unaged and aged for 7 days at 50°C and 65% RH. (Sample mass, 20 mg; heating rate, 50 °C min⁻¹; atmosphere, argon)

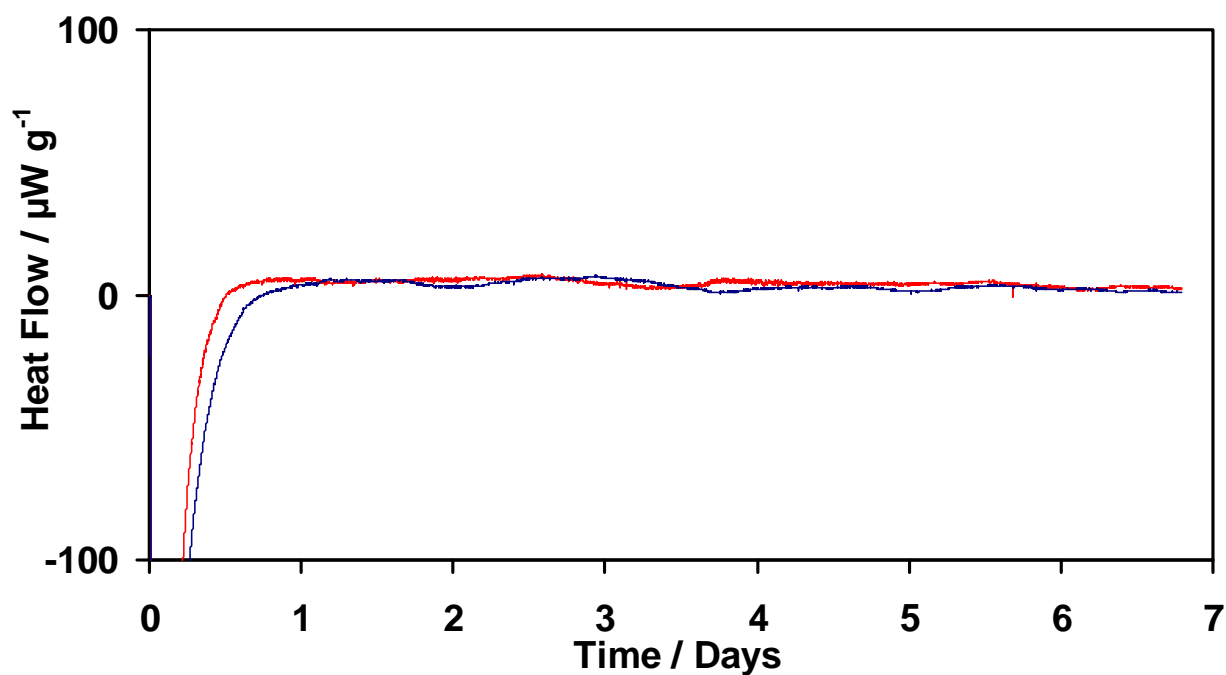


Figure 121; Microcalorimetry heat flow curves for a 50% magnesium/aluminum alloy-40% potassium perchlorate-10% potassium perchlorate composition.
(Sample mass, 100 mg; 50 °C, 65% RH; atmosphere, air)

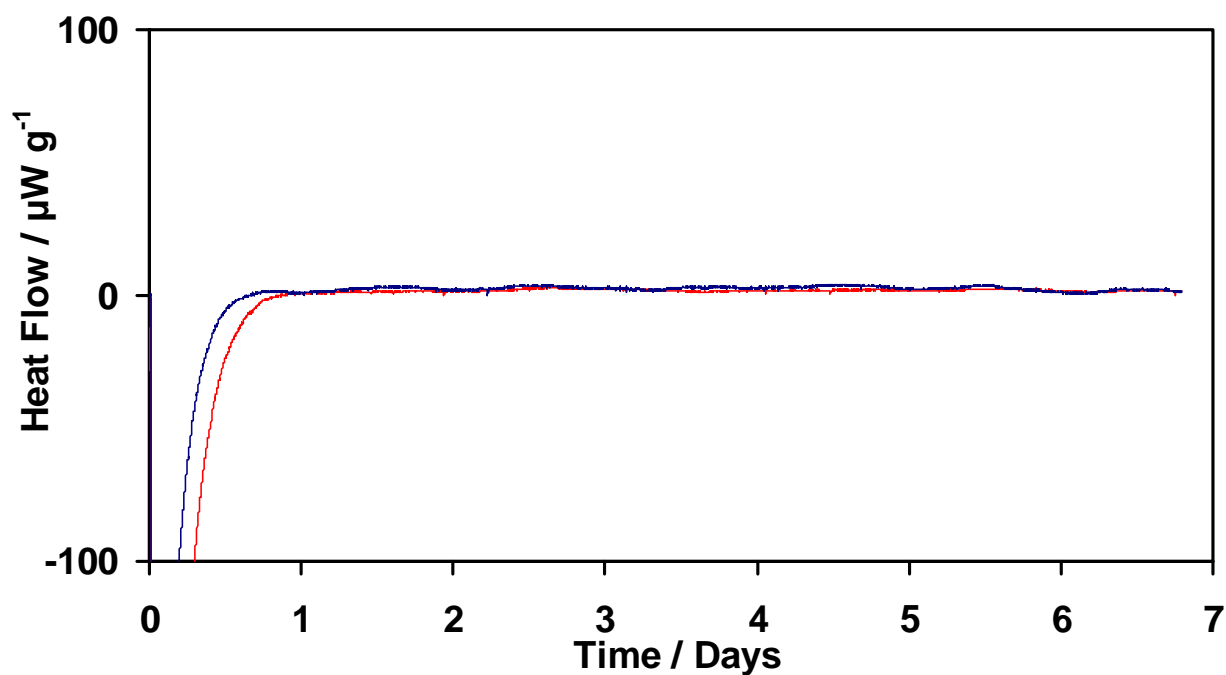


Figure 122; Microcalorimetry heat flow curves for a 50% magnesium/aluminum alloy-50% barium nitrate composition.
(Sample mass, 100 mg; 50 °C, 65% RH; atmosphere, air)

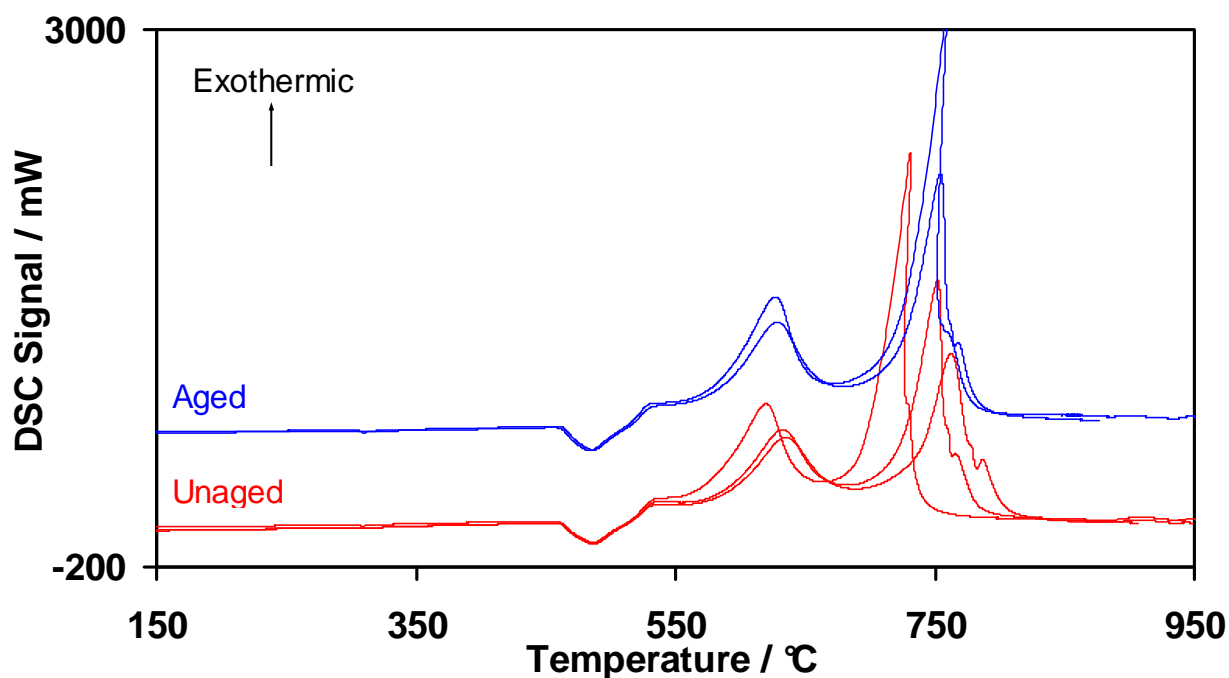


Figure 123; DSC curves for 50% magnesium/aluminum alloy-40% barium nitrate-10% potassium perchlorate composition unaged and aged for 7 days at 50°C and 65% RH. (Sample mass, 20 mg; heating rate, 50 °C min⁻¹; atmosphere, argon)

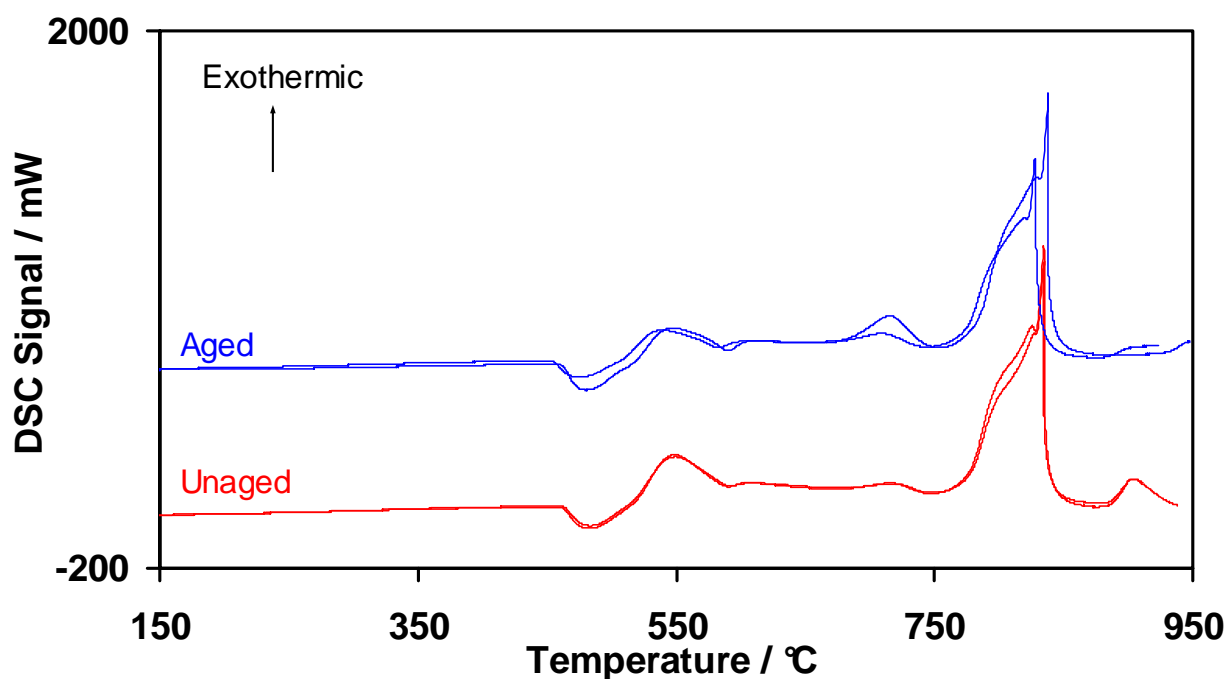


Figure 124; DSC curves for 50% magnesium/aluminum alloy-50% barium nitrate composition unaged and aged for 7 days at 50°C and 65% RH. (Sample mass, 20 mg; heating rate, 50 °C min⁻¹; atmosphere, argon)

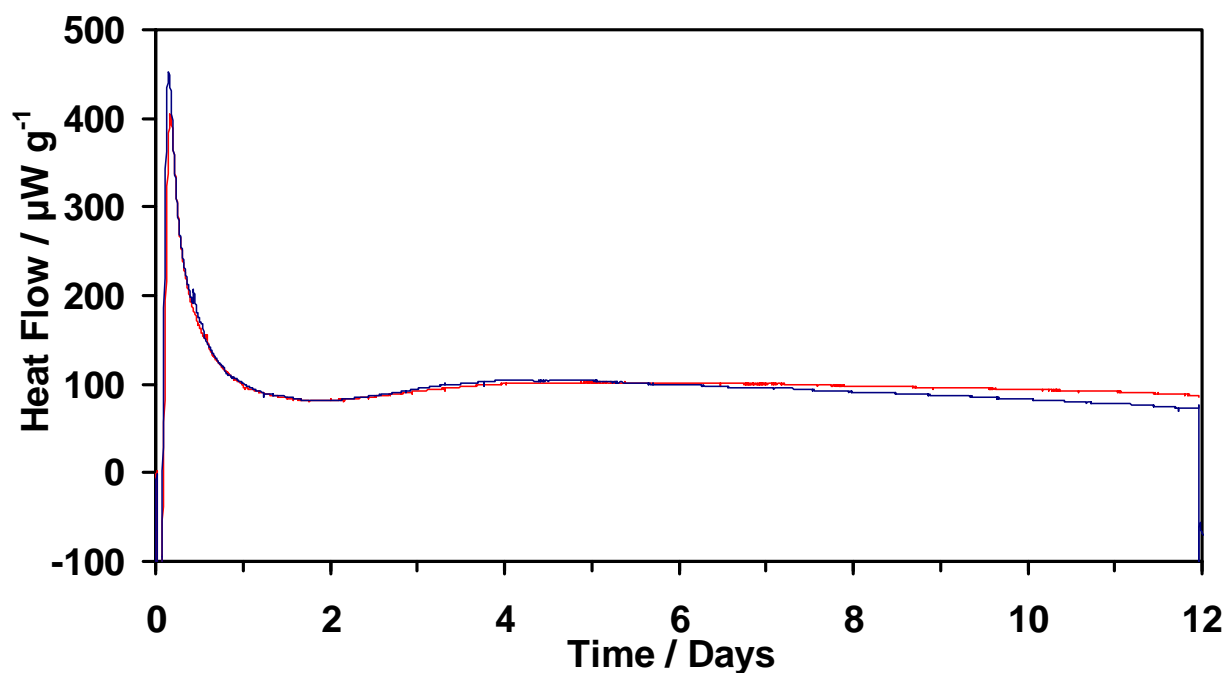


Figure 125; Microcalorimetry heat flow curves for a 50% magnesium/aluminum alloy-50% sodium nitrate composition.
(Sample mass, 100 mg; 50 °C, 65% RH; atmosphere, air)

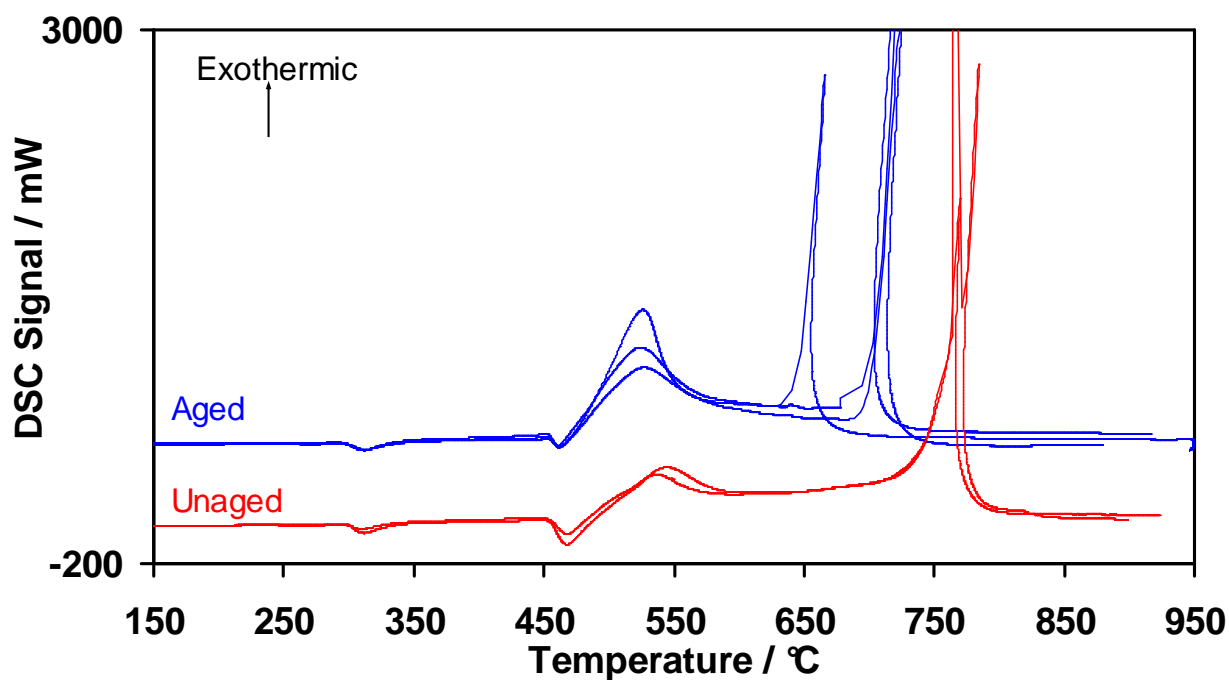


Figure 126; DSC curves for 50% magnesium/aluminum alloy-50% sodium nitrate composition unaged and aged for 7 days at 50°C and 65% RH.
(Sample mass, 20 mg; heating rate, 50 °C min⁻¹; atmosphere, argon)

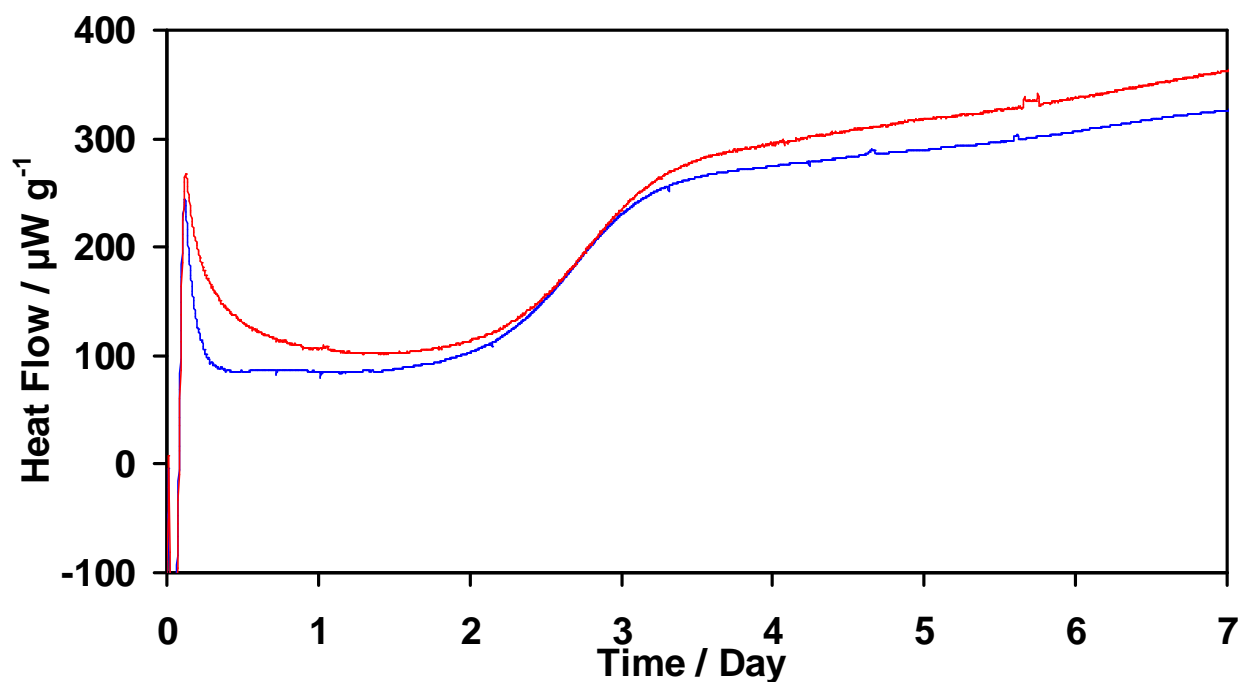


Figure 127; Microcalorimetry heat flow curves for a 50% magnesium/aluminum alloy-50% potassium nitrate composition.
(Sample mass, 100 mg; 50 °C, 65% RH; atmosphere, air)

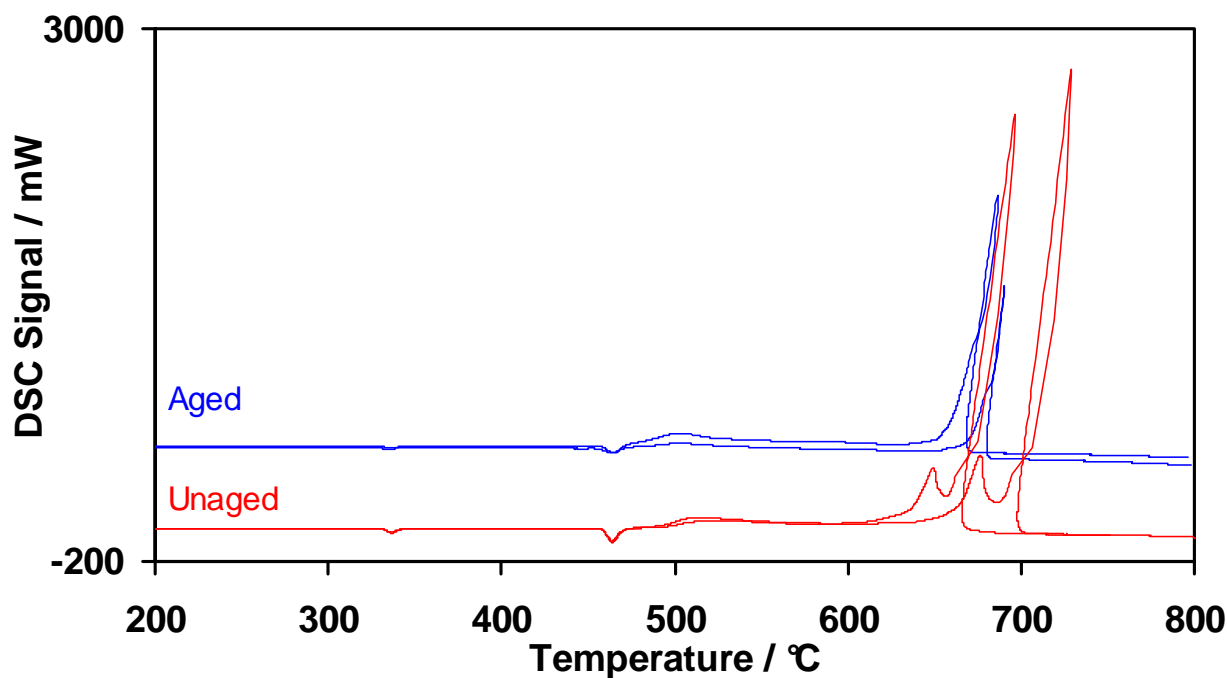


Figure 128; DSC curves for 50% magnesium/aluminum alloy-50% potassium nitrate composition unaged and aged for 7 days at 50°C and 65% RH.
(Sample mass, 20 mg; heating rate, 50 °C min⁻¹; atmosphere, argon)

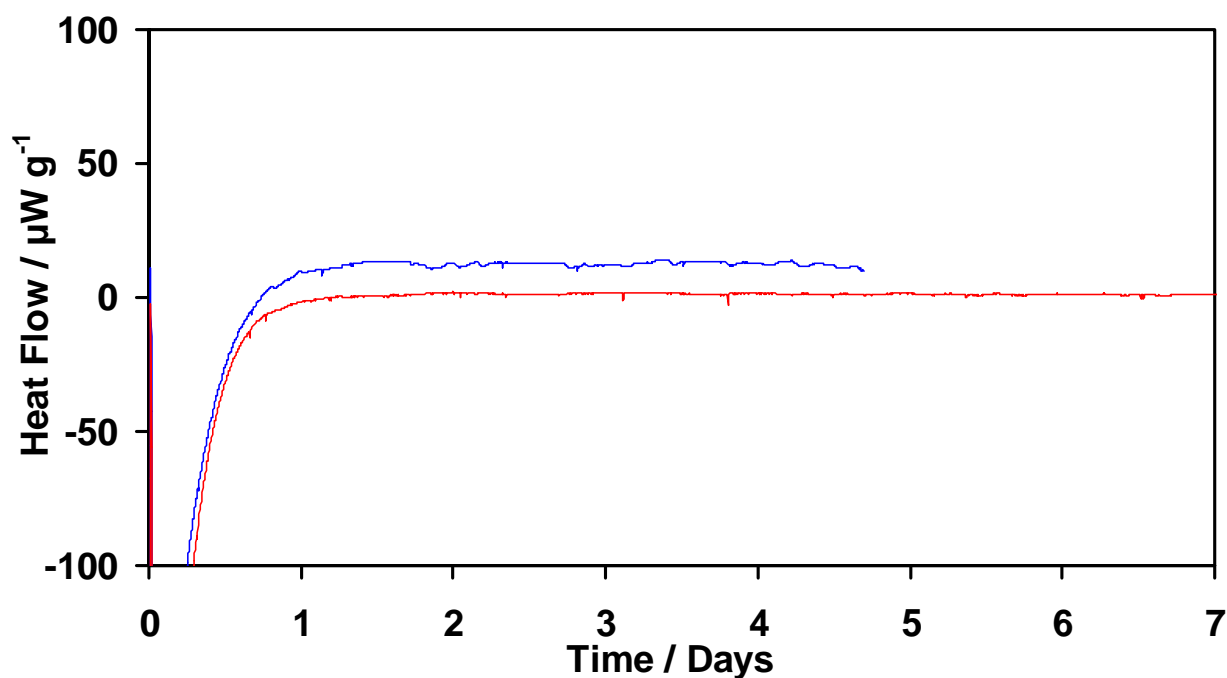


Figure 129; Microcalorimetry heat flow curves for 48% magnesium/aluminum alloy-48% sodium nitrate-4% calcium resinate composition.
(Sample mass, 100 mg; 50 °C, 65% RH; atmosphere, air)

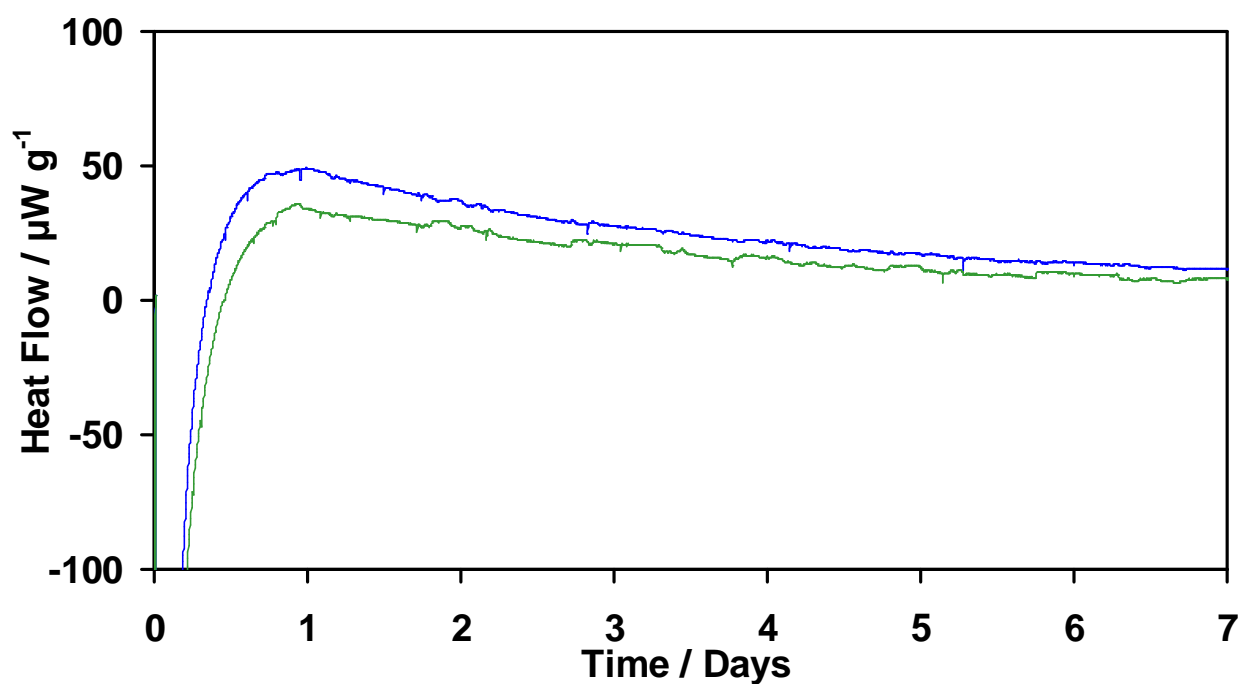


Figure 130; Microcalorimetry heat flow curves for 48% magnesium/aluminum alloy-48% sodium nitrate-4% lithographic varnish composition.
(Sample mass, 100 mg; 50 °C, 65% RH; atmosphere, air)

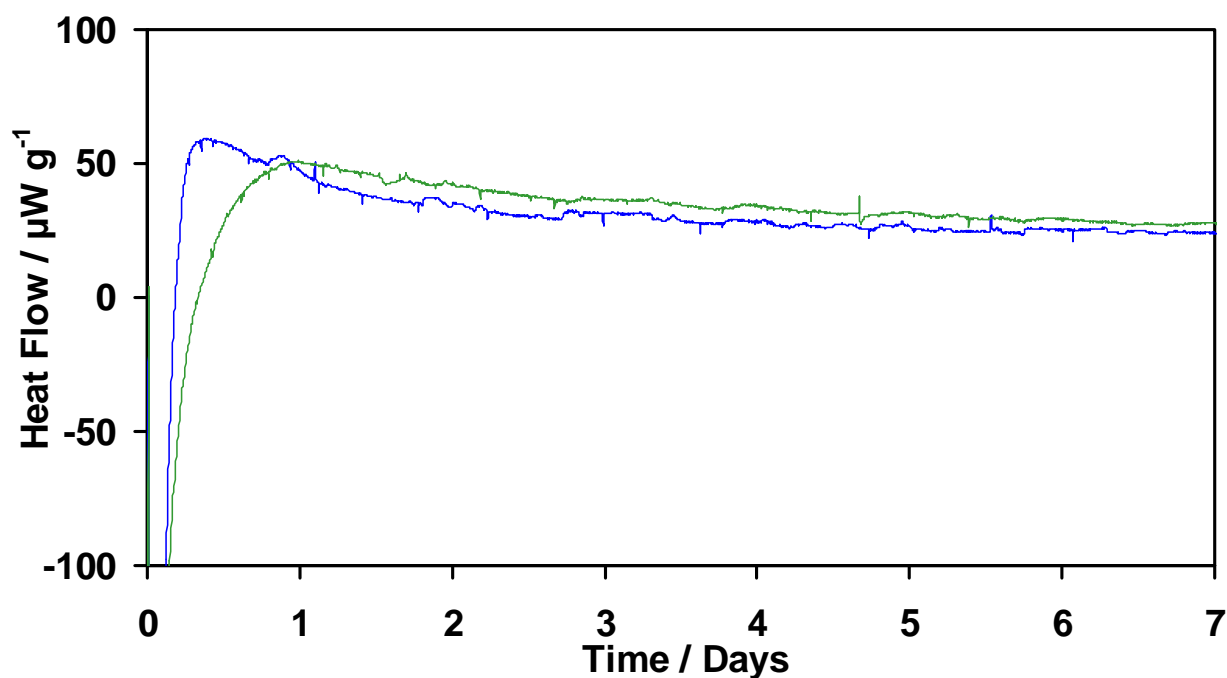


Figure 131; Microcalorimetry heat flow curves for 48% magnesium/aluminum alloy-48% sodium nitrate-4% GAP composition.
(Sample mass, 100 mg; 50 °C, 65% RH; atmosphere, air)

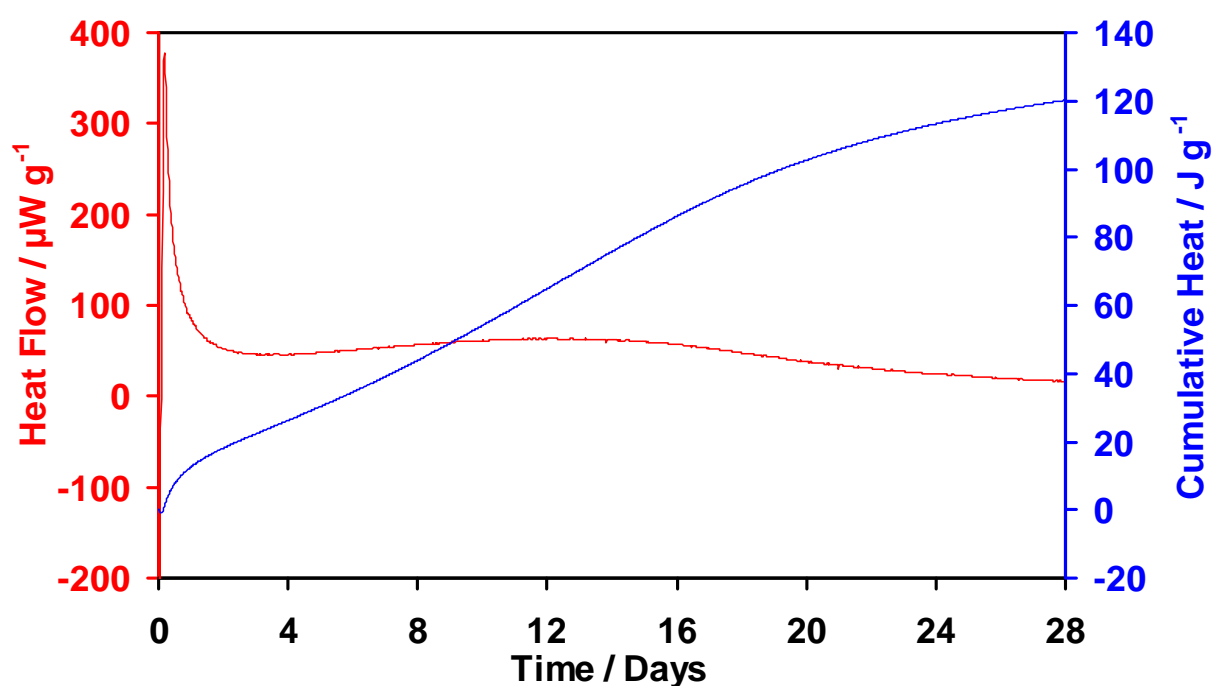


Figure 132; Microcalorimetry heat flow curves for a 50% magnesium/aluminum alloy-50% sodium nitrate composition.
(Sample mass, 100 mg; 50 °C, 65% RH; atmosphere, air)

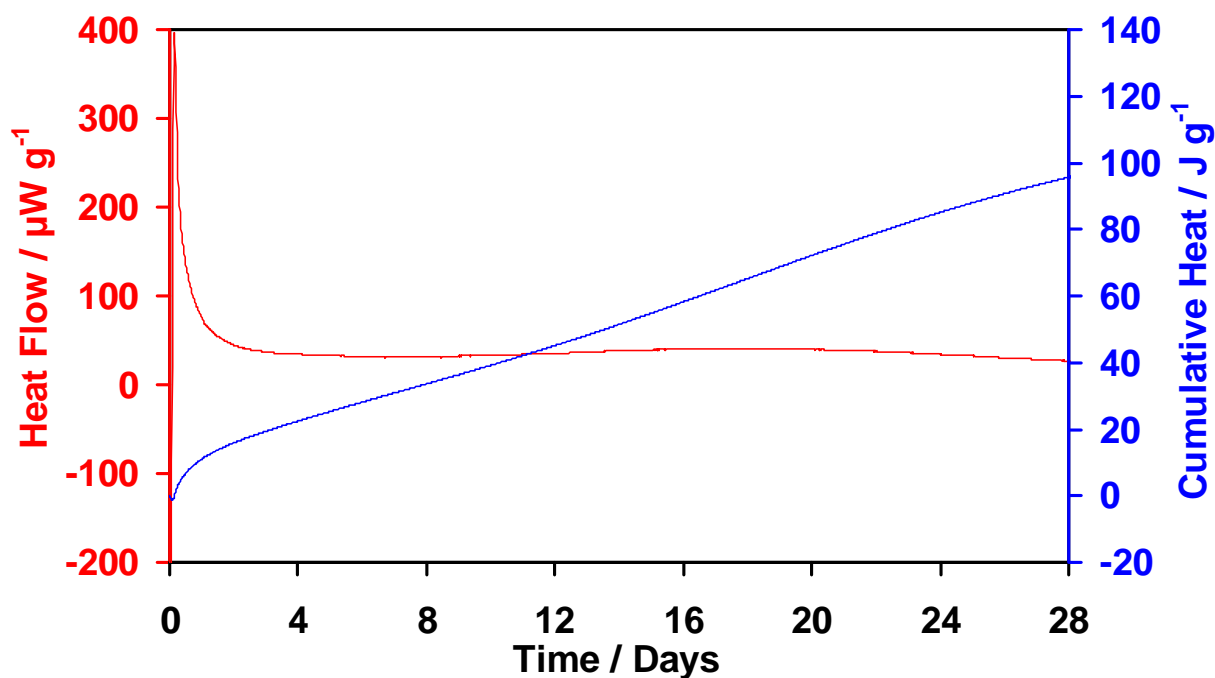


Figure 133; Microcalorimetry heat flow curves for a 50% magnesium/aluminum alloy-50% sodium nitrate composition.
(Sample mass, 100 mg; 50 °C, 65% RH; atmosphere, air)

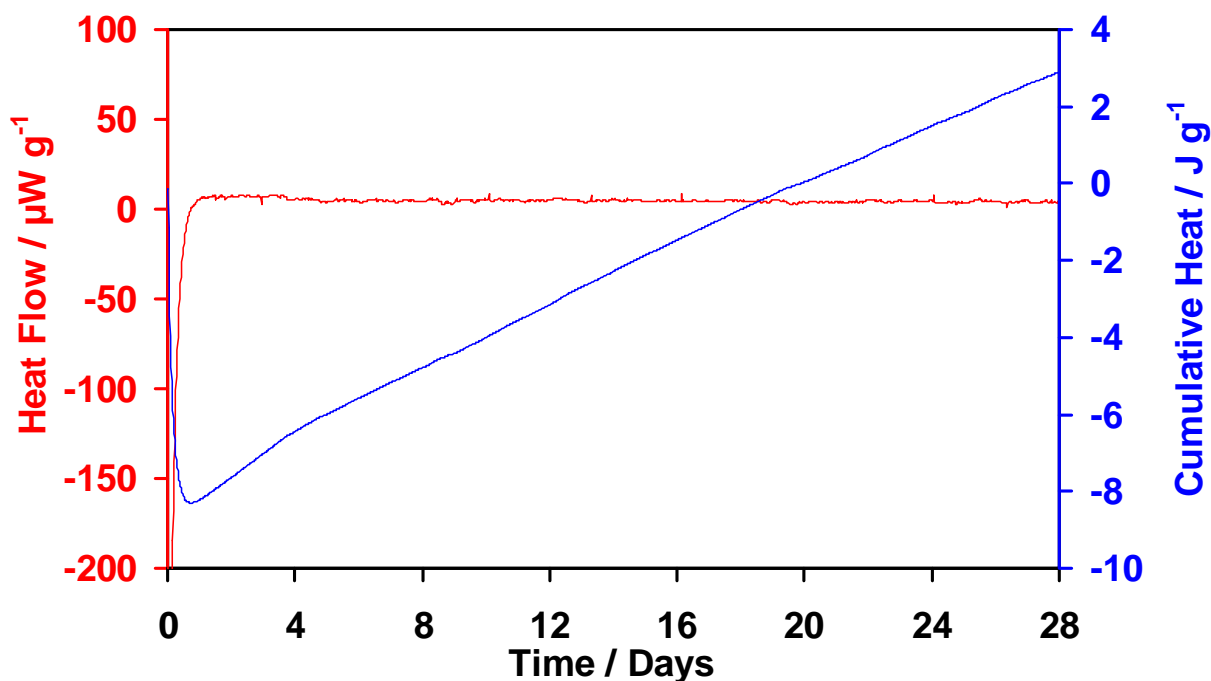


Figure 134; Microcalorimetry heat flow curves for 49% magnesium/aluminum alloy-49% sodium nitrate-2% calcium resinate composition.
(Sample mass, 100 mg; 50 °C, 65% RH; atmosphere, air)

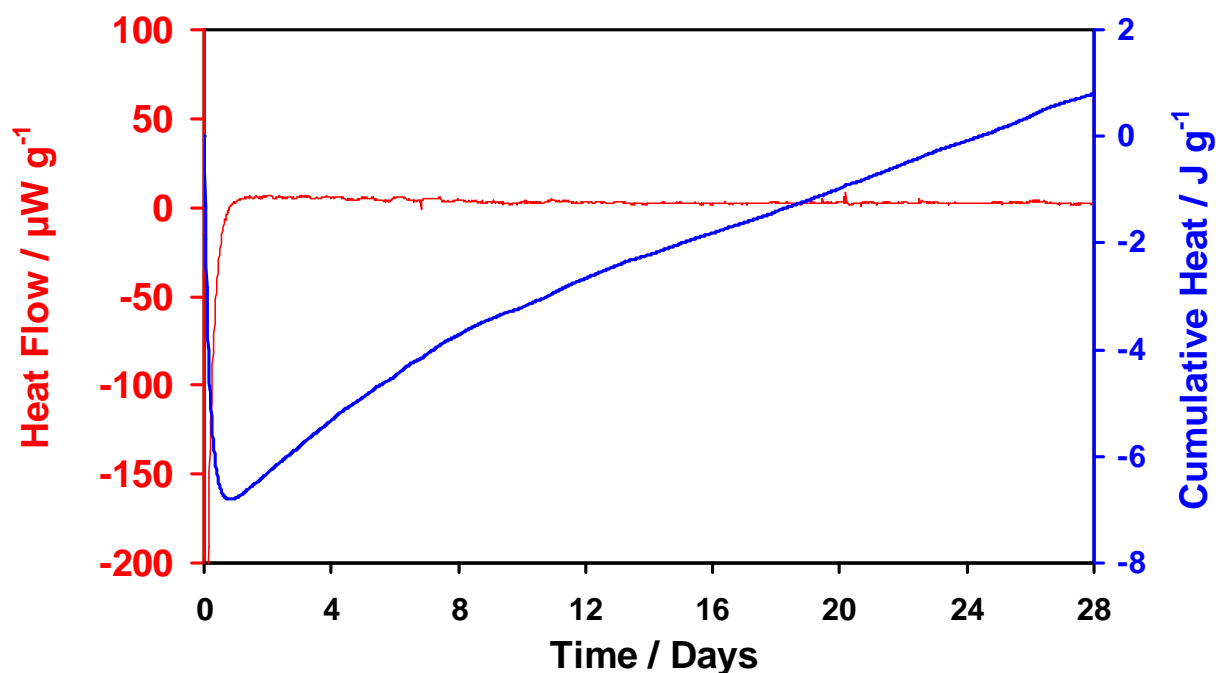


Figure 135; Microcalorimetry heat flow curves for 49% magnesium/aluminum alloy-49% sodium nitrate-2% calcium resinate composition.
(Sample mass, 100 mg; 50 °C, 65% RH; atmosphere, air)

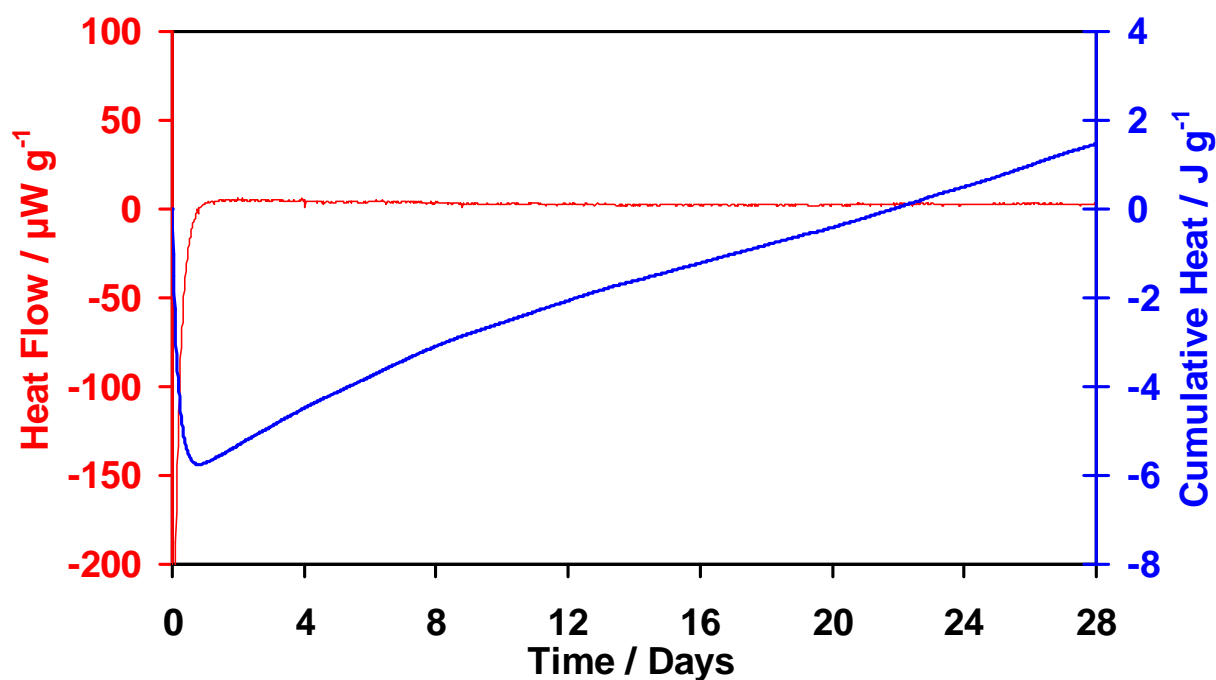


Figure 136; Microcalorimetry heat flow curves for 48% magnesium/aluminum alloy-48% sodium nitrate-4% calcium resinate composition.
(Sample mass, 100 mg; 50 °C, 65% RH; atmosphere, air)

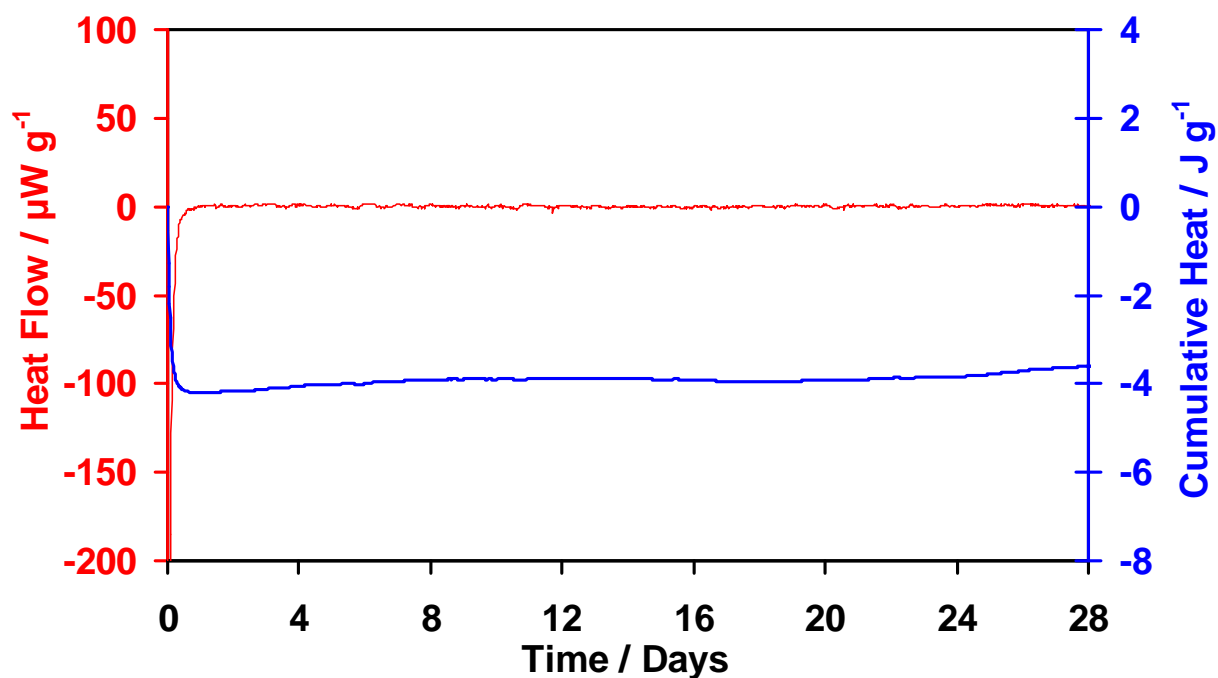


Figure 137; Microcalorimetry heat flow curves for 48% magnesium/aluminum alloy-48% sodium nitrate-4% calcium resinate composition.
(Sample mass, 100 mg; 50 °C, 65% RH; atmosphere, air)

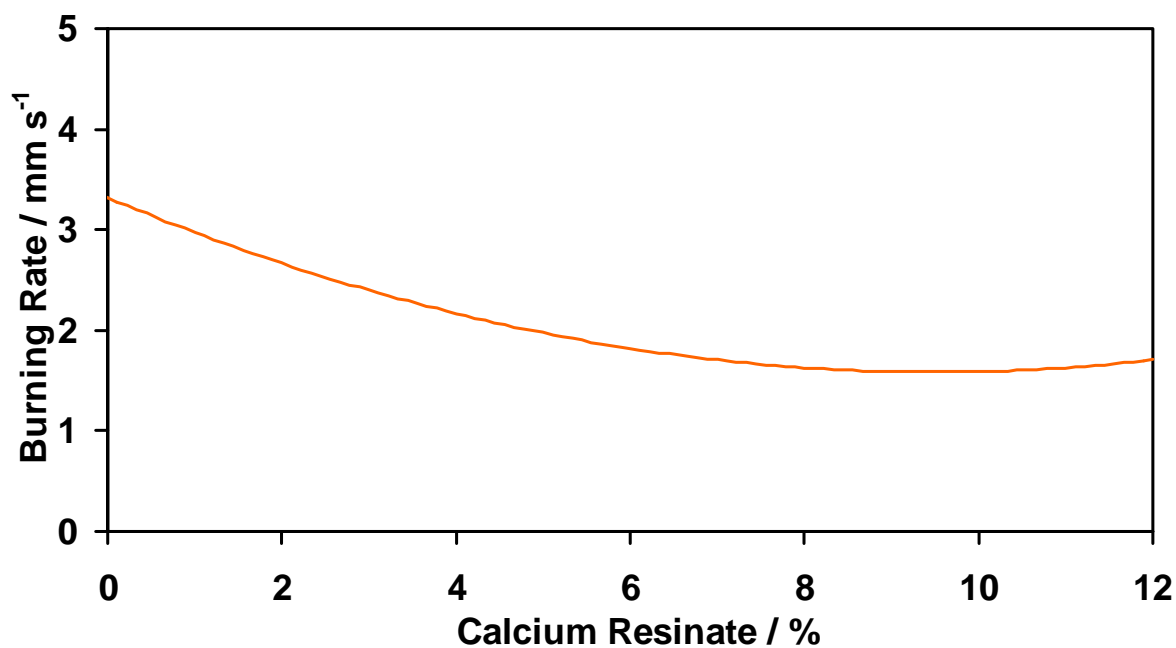


Figure 138; Burning rate curve for magnesium/aluminum alloy-sodium nitrate-calcium esinate.

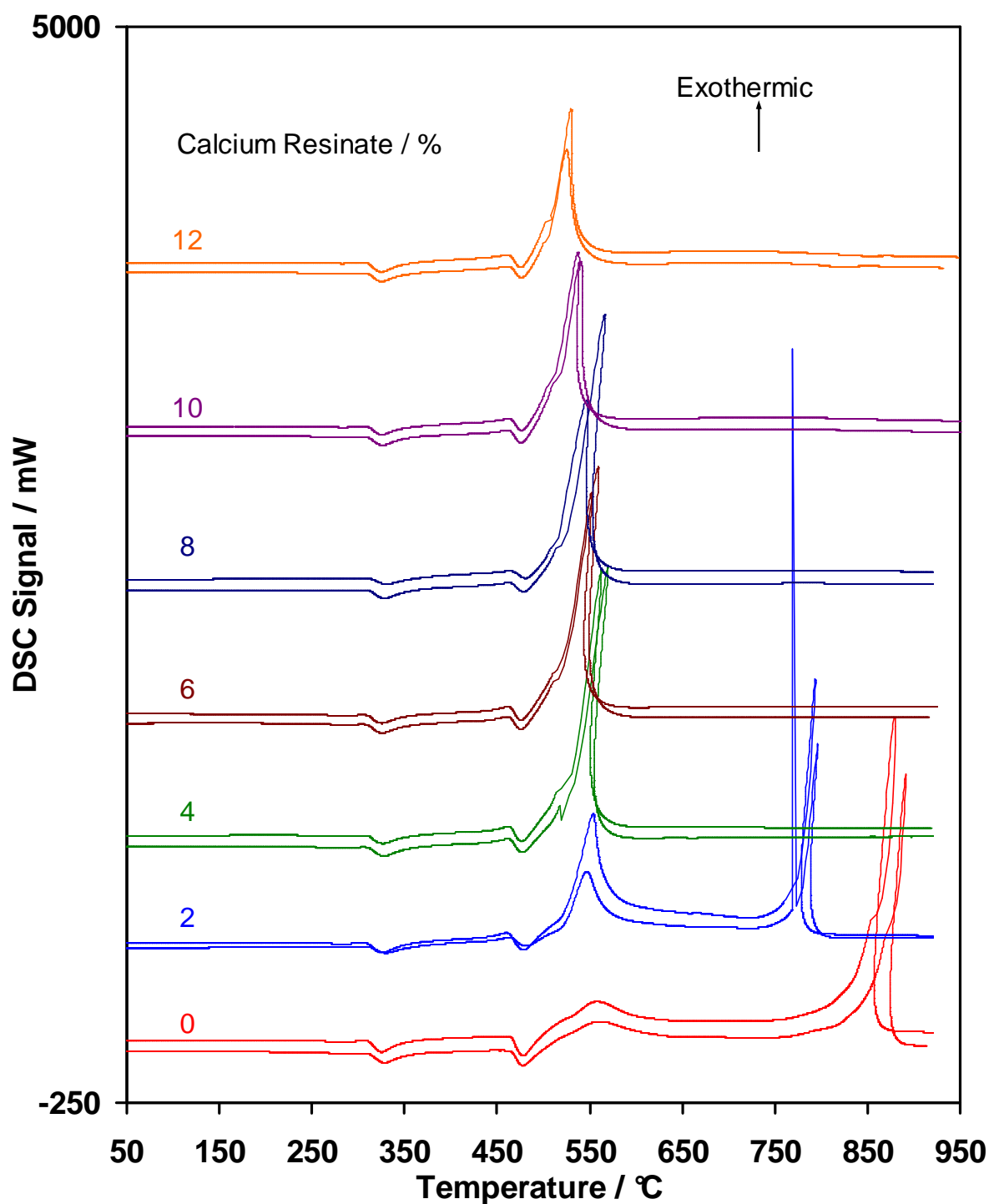


Figure 139; Ignition DSC curves for a range of magnesium/aluminum alloy-sodium nitrate-calcium resinate compositions.
(Sample mass, 20 mg; heating rate, 50 °C min⁻¹; atmosphere, argon)

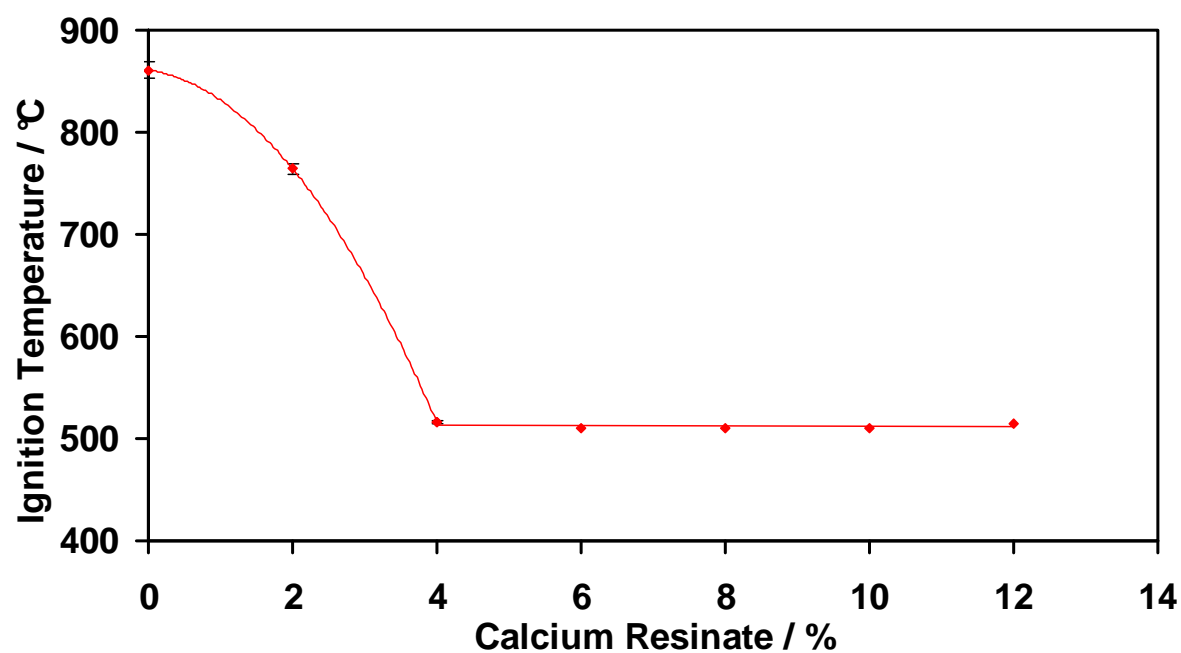


Figure 140; Plot of ignition temperature against calcium resinate content for a range of magnesium/aluminum alloy-sodium nitrate-calcium resinate compositions.

List of technical publications:

Technical reports

- [1] Screening level summary report 1: Barium nitrate, potassium dinitramide, nitrates and perchlorates, Centre for Ecology and Hydrology, February 2006.
- [2] Screening level summary report 2: magnesium, Magnesium/aluminum alloy, aluminum and boron, Centre for Ecology and Hydrology, February 2006.
- [3] Studies of Pyrotechnic Compositions containing magnesium/aluminum alloys, Huddersfield University, March 2006.
- [4] Screening level summary report 3: Polytetrafluoroethylene, tungsten oxide, molybdenum trioxide, copper oxide & manganese oxide, Centre for Ecology and Hydrology, March 2006.
- [5] Screening level summary report 4: Hexafluoropyropylene vinylidene fluoride polymer, polyGlyN, polyNIMMO, glycidyl axide polymer & polyvinyl chloride, Centre for Ecology and Hydrology, March 2006.
- [6] Screening level summary report 5: Calcium nitrate, strontium nitrate, strontium sulfate, sulfates and iron oxide, Centre for Ecology and Hydrology, April 2006.
- [7] Environmental assessment of pyrotechnic ingredients: Screening level summary report for parent compounds, Centre for Ecology and Hydrology, April 2006.
- [8] Studies of pyrotechnic compositions containing magnesium/aluminum alloys, Huddersfield University, September 2006.
- [9] QinetiQ/06/00593, Environmental assessment of pyrotechnic ingredients–screening level summary report, T T Griffiths and A Parker, December 2006.
- [10] Studies of pyrotechnic compositions, Huddersfield University, June 2007.
- [11] Studies of pyrotechnic compositions, Huddersfield University, December 2007.
- [12] Studies of pyrotechnic compositions, Huddersfield University, July 2008.
- [13] Studies of pyrotechnic compositions, Huddersfield University, January 2009.
- [14] Screening summary reports on antimony sulfide, hydrogen sulfide and the sulfides of calcium, potassium and sodium, Centre for Ecology and Hydrology, July 2007.
- [15] Screening summary reports on ammonia and calcium resinate, Centre for Ecology and Hydrology, September 2007.
- [16] Screening summary reports on magnesium, sulfur and sulfur dioxide, Centre for Ecology and Hydrology, October 2007.
- [17] Screening summary reports on the hydroxides of calcium, potassium and sodium, strontium hydroxide, aluminum nitride and sodium nitride, Centre for Ecology and Hydrology, November 2007.
- [18] Alternatives for perchlorate in incendiary and pyrotechnic formulations for projectiles-first annual report, T T Griffiths, A Parker, P D Howe, December 2006.
- [19] Alternatives for perchlorate in incendiary and pyrotechnic formulations for projectiles-second annual report, December 2007.

- [20] Environmental assessment of pyrotechnic ingredients-final report P D Howe, S Dobson, and H M Malcolm, Centre for Ecology and Hydrology, April 2008.

Conference/symposium proceedings

- [1] Preliminary investigation of pyrotechnic incendiary compositions, E.L.Charsley, H.M.Markham and J.J.Rooney, T.T.Griffiths, 33rd International Pyrotechnics Seminar, July 2006.
- [2] Elimination of perchlorate oxidizers from pyrotechnic incendiary compositions, G T Flegg, T T Griffiths, E L Charsley, H M Markham, J J Rooney and P D Howe, 38th International Annual conference of ICT, June 2007.
- [3] Environmental assessment of pyrotechnic ingredients, P D Howe, S Dobson, H M Malcolm, T T Griffiths and A Parker, 38th International Annual conference of ICT, June 2007.
- [4] Environmental assessment of pyrotechnic combustion products, P D Howe, S Dobson, H M Malcolm and T T Griffiths, 33rd International Pyrotechnics Seminar, July 2008.
- [5] Modelling of pyrotechnic combustion, T T Griffiths, 33rd International Pyrotechnics Seminar, July 2008.
- [6] New pyrotechnic compositions for incendiary ammunition applications, T T Griffiths, E L Charsley, J J Rooney, H M Markham, 33rd International Pyrotechnics Seminar, July 2008.

Published technical abstracts

- [1] Elimination of perchlorate oxidizers from incendiary compositions, T T Griffiths, E L Charsley, J J Rooney and H M Markham, Partners in Environmental Technology Technical Symposium and Workshop, December 2006.
- [2] Environmental assessment of pyrotechnic ingredients, P D Howe, T T Griffiths, S Dobson and H M Malcolm, Partners in Environmental Technology Technical Symposium and Workshop, December 2006.
- [3] Novel pyrotechnics for incendiary applications, T T Griffiths, E L Charsley, J J Rooney, H M Markham, P D Howe, Partners in Environmental Technology Technical Symposium and Workshop, December 2007.
- [4] Modeling of pyrotechnic combustion, T T Griffiths, Partners in Environmental Technology Technical Symposium and Workshop, December 2007.
- [5] Environmental assessment of pyrotechnic combustion products, P D Howe, S Dobson, H M Malcolm and T T Griffiths, December 2007.
- [6] Testing of novel pyrotechnic incendiary compositions by gun firing, T T Griffiths, Partners in Environmental Technology Technical Symposium and Workshop, December 2008.
- [7] Thermal analysis and combustion studies on novel pyrotechnic incendiary compositions, Partners in Environmental Technology Technical Symposium and Workshop, T T Griffiths, E L Charsley, J J Rooney, H M Markham, December 2008.

- [8] Environmental assessment of pyrotechnic ingredients and combustion products, Partners in Environmental Technology Technical Symposium and Workshop, P D. Howe, T T Griffiths, S Dobson and H M Malcolm, December 2008.